ISSN number 0971 - 9709

The Journal of Indian Geophysical Union

VOLUME 21, ISSUE 4 I JULY 2017

AN OPEN ACCESS BIMONTHLY JOURNAL OF IGU

EDITORIAL OFFICE

Indian Geophysical Union, NGRI Campus, Uppal Road, Hyderabad- 500 007
Telephone: +91 -40-27012799; 27012734; Telefax:+91-04-27171564
E. mail: jigu1963@gmail.com, website: www.j-igu.in

The Open Access Journal with six issues in a year publishes articles covering
Solid Earth Geosciences; Marine Geosciences; and Atmospheric, Space and Planetary Sciences.

Annual Subscription

Individual ₹ 1000 per issue and Institutional ₹ 5000 for six issues

Payments should be sent by DD drawn in favour of "The Treasurer, Indian Geophysical Union", payable at Hyderabad, Money Transfer/NEFT/RTGS (Inter-Bank Transfer), Treasurer, Indian Geophysical Union, State Bank of Hyderabad, Habsiguda Branch, Habsiguda, Uppal Road, Hyderabad- 500 007
A/C: 52191021424, IFSC Code: SBHY0020087, MICR Code: 500004020, SWIFT Code: SBHYINBB028.

For correspondence, please contact, Hon. Secretary, Indian Geophysical Union, NGRI Campus, Uppal Road, Hyderabad - 500 007, India; Email: igu123@gmail.com; Ph: 040 27012799

ISSN: 0257-7968 (Thomson Reuters)
ISSN: 0971-9709 (NISCAIR)

Approved as ESCI journal by Thomson Reuters
Cited in Indian Citation Index (ICI), New Delhi
Evaluated by NISCAIR, New Delhi

CONTENTS

Space Quotations

* “The contemplation of celestial things will make a man both speak and think more sublimely and magnificently when he descends to human affairs.”

- Marcus Tullius Cicero (106 - 43 BC) Rome’s greatest orators and prose stylists.

***

* “The sun, with all those planets revolving around it and dependent on it, can still ripen a bunch of grapes as if it had nothing else in the universe to do.”

- Galileo Galilei (1564-1642) an Italian polymath: astronomer, physicist, engineer, philosopher, and mathematician.

***

* “The Universe Is Full of Magical Things Patiently Waiting for Our Wits to Grow Sharper.”

- Eden Phillpotts (1862-1960) an English author, poet and dramatist.

***

* “Only two things are infinite, the universe and human stupidity, and I’m not sure about the former.”

- Albert Einstein (1879 – 1955) famous German-born theoretical physicist who developed the theory of relativity

* “To be able to rise from the earth;
to be able, from a station in outer space,
to see the relationship of the planet earth to other planets;
to be able to contemplate the billions of factors in precise and beautiful combination that make human existence possible; to be able to dwell on an encounter of the human brain and spirit with the universe; all this enlarges the human horizon.”

- Norman Cousins (1915-1990) American political journalist, and world peace advocate.

***

* “Just as Mars - a desert planet - gives us insights into global climate change on Earth, the promise awaits for bringing back to life portions of the Red Planet through the application of Earth Science to its similar chemistry, possibly reawakening its life-bearing potential.”

- Buzz Aldrin (1930--) an American engineer and former astronaut.

***

* “Look at the sky. We are not alone. The whole universe is friendly to us and conspires only to give the best to those who dream and work.”

- Abdul Kalam (1931-2015) Famous Space Scientist and Former President of Republic of India.

***

* “For me, it is far better to grasp the Universe as it really is than to persist in delusion, however satisfying and reassuring.”

- Carl Sagan (1934- 1986) an American astronomer, cosmologist, astrophysicist and astrobiologist.

***

* “The universe is not required to be in perfect harmony with human ambition.”

- Carl Sagan (1934-1986) an American astronomer, cosmologist, astrophysicist and astrobiologist.

***

* *“*The universe doesn’t give you what you ask for with your thoughts - it gives you what you demand with your actions.”

- Steve Maraboli (1975--) is a Behavioral Scientist.

Editorial

In the last four editorials importance was given to topics of interest to earth scientists. Since JIGU caters to the needs of earth system scientists I have selected for this issue a topic of importance to Space scientists/ cosmologists and astronomers. In a way this is in continuation of details given in the subsection "Space Science & Technology News" (Pages238-240 of News at a Glance of May, 2017 issue of JIGU). I believe that a time has come for scientists of all the branches of earth system to know more about cosmology and studies on the Universe.

*****Colonization of Planets and Exoplanets**

Man has been endowed with the extraordinary quality of exploring various unknowns, starting from the childhood. This quality can lead him to do knowingly and unknowingly both good and bad deeds that can alter the very evolutionary mechanism and life on earth.

Hardly 200 years back man could not develop a vessel that would help him to fly. Now we not only fly from one corner of the earth to the other in a few hours but also can go to Moon and also Mars in a few days. Significant efforts are made by different countries and especially NASA to colonize Moon followed by Mars overcoming number of hurdles. These efforts may yield in the next 100 years fruitful results. All these achievements by the man make us believe that we can conquer the Universe one day or the other; wild and intriguing imagination. Couple of decades back even many scientists were not familiar with the word Exoplanet (An exoplanet or extrasolar planet is a planet that orbits a star other than the Sun. The first scientific detection of an exoplanet was in 1988. However, the first confirmed detection came in 1992; since then, and as of 1 March 2017, there have been 3,586 exoplanets in 2,691 planetary systems and 603 multiple planetary systems confirmed). The Kepler space telescope really revolutionized the number of exoplanets that we know exist." (Kepler is credited with over 2,300 confirmed exoplanets, using a system to detect them called the transit method.)

But of all those, only a "handful" are potentially habitable, NASA confirmed. NASA also clearly stated that Humanity is not going to be visiting them anytime soon, though. Take, for example, to reach the nearest known exoplanet, Proxima Centauri B, which is about four light years away from here—(a light year being the distance that light can travel in 365 days) would take an astounding amount of time. If we send a probe there (for example Juno space probe, currently orbiting Jupiter at speeds in the neighbourhood of 150,000 miles per hour) to reach Proxima Centauri B, it would take an astounding 18,000 years. "So the technology really isn't there currently". (**Source:** https://en.wikipedia.org/wiki/Exoplanet & http://www.space.com/33844-proxima-b-exoplanet-interstellar-mission.html.).

Where are the exoplanets that have life?

The emergence, evolution, and survivability of extrasolar life, if any exists, involve enormous uncertainties. Despite remarkable progress toward producing life in the lab in recent years, the precise origin of life—the dramatic transformation from chemistry to biology—remains a mystery. Earth is blessed with a relatively large moon that has stabilized the climate. The asteroid belt, on one hand, may have helped to seed life and, on the other, may have been responsible for mass extinctions. Even the location of our solar system—within a minor spur off one of the two main arms of the galaxy, relatively far from the galactic center—has shielded it from the potentially sterilizing effects of gamma-ray bursts.

Given those uncertainties, scientists Mario Livio and Joseph Silk (2017) have reviewed potential life signatures and future plans to find them; to identify the most generic, remotely detectable signatures of an alien life, both simple and intelligent; and to examine the expected effectiveness of various search strategies. They have noted that searches for life focus on Sun-like and smaller stars because the vast majority of stars are smaller than the Sun: M dwarfs comprise some 70% of all stars in the Milky Way, and a large fraction of them harbour planets. Also, more massive stars have shorter lifetimes and emit intense UV radiation. Both factors make them less hospitable as energy sources for biochemical processes that may require billions of years to unfold and take effect. Stars more massive than about three times the mass of the Sun, for instance, will likely burn out before life has time to emerge and evolve. Ideally, therefore, researchers would like to find a star–planet system just like Sun–Earth—Earth 2.0 as it were— because at least we know without a doubt that life emerged here. A program to search for an Earth twin does not guarantee success in finding extrasolar life, but at least it should substantially increase the odds. Nevertheless, a recent comprehensive examination of the habitability of planets orbiting M dwarf stars concluded that some features of their stellar and planetary environments could confer advantages. For example, synchronous rotation could improve habitable conditions on planets orbiting at the inner edge of the habitable zone. Planets orbiting M dwarfs are also predicted to be more resistant to global glaciation. In the search for extra solar life, high priority targets are planets that are numerous and relatively easy to detect. The insistence on the existence of liquid water is again somewhat Earth-centric, but water does have a few special characteristics. It is an excellent solvent; it is less dense as a solid than as a liquid; it is amphoteric, which means it can become an acid or a base by donating or accepting a positive hydrogen ion; and it is abundant across the universe.

Some form of liquid solvent is undoubtedly necessary if chemicals are to be transported into and out of cells and if molecules are to come into contact with one another to form long-chained organic ingredients. A liquid environment would also protect those organic compounds from UV radiation. However, it is not entirely clear whether only water can play that role. To be detectable from a distance, life has to evolve to the point where it so dominates the planetary surface chemistry that it significantly alters the atmosphere. Only then will life give itself away through chemical bio-signatures that can in principle be detected remotely. Earth itself would probably not have been detectable as a life-bearing planet during the first billion or so years of its existence. Oxygen became an important atmospheric constituent due entirely to life processes but it built up slowly. Any oxygen produced by early organisms first went into oxidizing rocks. Only after the oxidizable rocks became saturated did free oxygen start to enrich the atmosphere. An excellent first step in the quest for extra-solar life in the relatively near future would be to search for planets with atmospheric oxygen in abundance. That could be achieved in principle with a next-generation European Extremely Large Telescope or other large, ground-based arrays of relatively low-cost flux collector telescopes.

One would ideally like to go beyond simple bio-signatures and seek the clearest sign of an alien technological civilization. That could be the unambiguous detection of an information-containing, non natural signal, most notably via radio transmission or optical/IR laser beaming. Such detection is the aim of Search for Extra Terrestrial Intelligence (SETI) and other similar programs. One interesting argument to make the search more efficient is that we should concentrate on those directions in which mini-eclipses of the Sun by transiting solar-system planets are detectable. Technological civilizations in those directions, the argument goes, are more likely to discover us and attempt communication.

However, the fraction of the Milky Way that has been reached by radio-communication signals from Earth was recently estimated to be only about 1%. To give ourselves better odds for success, we might want to reach about 50% of the suitable planets before expecting a return signal. That puts the more probable time for a reception of a radio signal from another galactic civilization, assuming it exists, some 1500 years into the future. Other potential signatures of technological civilizations that have been suggested, such as various forms of atmospheric industrial pollution and short-lived radioactive products, are necessarily transitory. Basically, we expect that aliens either learn how to clean up after themselves or they destroy themselves. Infrared emission, on the other hand, seems almost unavoidable. To end on a speculative and perhaps pessimistic note, biologically based intelligence may constitute only a very brief phase in the evolution of complexity. What follows could be what some futurists have dubbed the "singularity": the dominance of artificial, inorganic intelligence. If that is indeed the case, advanced species are likely not bound to a planet's surface, where gravity is helpful for the emergence of biological life but is otherwise a liability, but rather floating in space. Even with that imaginative conjecture, one can still argue that any surviving species must be near an energy supply, namely a star. But if such intelligent machines were to transmit a signal, it may well be unrecognizable and non-decodable to our relatively primitive, organic brains. The detection of potential signs of life with the upcoming generation of space telescopes, followed by the detection of high levels of oxygen from large ground-based telescopes and increasingly reliable detection of bio-signatures with the next generation of 10-m-class telescopes in space. Simultaneously, searches for electromagnetic signals from other galactic civilizations should continue, and searches for unusual IR emissions that could indicate energy consumption by remote species should be intensified.

Are we alone? The answer may affect nothing less than our claim for being special in the cosmos. Its importance cannot be overemphasized. Echoing what Giuseppe Cocconi and Philip Morrison said at the end of their seminal 1959 article on searching for extraterrestrials, **"We shall never know unless we search**!**"** (**Source:** http://physicstoday.scitation.org/doi/full/10.1063/PT.3.3494).

From the above exposition it is clear, as of now, it is beyond our capability to colonize habitable exoplanets and our focus should at first be confined to precisely identify those exoplanets that are habitable. Colonization follows much later, if at all possible. The following study addresses that in a precise manner.

Exoplanets atmosphere-the basic component to evaluate its habitability

While travelling to the probable habitable exoplanets is beyond our present technological efficiency, one has to first confirm the favourable habitability conditions of an exoplanet. The atmospheres of exoplanets can host bio-signature gases, so the path to finding possible signs of life on exoplanets most likely leads through their atmospheres. Indeed, the atmosphere is the window into all exoplanetary properties beyond mass, radius, and orbital dynamics. Moreover, exoplanetary atmospheres host a wide variety of fascinating physical processes, from intense infrared radiation and exotic chemistry, to super-sonic winds and electric currents. One of our best ways to probe the nature of these alien worlds is to measure the ultraviolet (UV), optical or infrared (IR) spectra of their atmospheres. We have also learned in the recent past that many exoplanets are strikingly different than the planets of our solar system. Most important, we now have dozens of alien atmospheres than are amenable to observations, so that we can measure their properties and begin to conduct comparative studies. The atmospheres of exoplanets reveal all their properties beyond mass, radius, and orbit. Based on bulk densities, we know that exoplanets larger than 1.5 Earth radii must have gaseous envelopes, hence atmospheres. There are contemporary techniques for characterization of exoplanetary atmospheres. The measurements are difficult, because - even in current favourable cases - the signals can be as small as 0.001% of the host star's flux. Consequently, some early results have been illusory, and not confirmed by subsequent investigations. Prominent illusions to date include polarized scattered light, temperature inversions, and the existence of carbon planets. The field moves from the first tentative and often incorrect conclusions, converging to the reality of exoplanetary atmospheres. That reality is revealed using transits for close-in exoplanets, and direct imaging for young or massive exoplanets in distant orbits. Several atomic and molecular constituents have now been robustly detected in exoplanets as small as Neptune. In our current observations, the effects of clouds and haze appear ubiquitous. Topics at the current frontier include the measurement of heavy element abundances in giant planets, detection of carbon-based molecules, measurement of atmospheric temperature profiles, definition of heat circulation efficiencies for tidally-locked planets, and the push to detect and characterize the atmospheres of super-Earths. Future observatories for this quest include the James Webb Space Telescope, and the new generation of Extremely Large Telescopes on the ground. On a more distant horizon, NASA's concepts for the HabEx and LUVOIR missions could extend the study of exoplanetary atmospheres to true twins of Earth. (**Source**: Illusion and Reality in the Atmospheres of Exoplanets; L. Drake Deming and Sara Seager. https://arxiv.org/ftp/arxiv/papers/1701/1701.00493.pdf).

Assuming that there is life on some exoplanets Man started planning to colonize them, an ambitious illusion. Before achieving it Man has to first colonize Space in general. This has become a necessity, as knowledgeable scientists have come to the conclusion that it would be difficult to sustain quality living on earth as we have considerably damaged our environment, polluted our life saving elements of nature and over consumed our non renewable natural resources and unable to ensure future demands of ever increasing population.

Space Colonization

Space colonization is permanent human habitation off the planet Earth. Many arguments have been made for and against space colonization. The two most common in favour of colonization are survival of human civilization and the biosphere in case of a planetary-scale disaster (natural or man-made), and the vast resources in space for expansion of human society. The most common objections to colonization

include concerns that the commoditisation of the cosmos may be likely to enhance the interests of the already powerful, including major economic and military institutions, and to exacerbate pre-existing detrimental processes such as wars, economic inequality, and environmental degradation.

No space colonies have been built so far. Currently, the building of a space colony would present a set of huge technological and economic challenges. Space settlements would have to provide for nearly all (or all) the material needs of hundreds or thousands of humans, in an environment out in space that is very hostile to human life. They would involve technologies, such as controlled ecological life support systems, that have yet to be developed in any meaningful way. They would also have to deal with the as-yet unknown issue of how humans would behave and thrive in such places long-term. Because of the present cost of sending anything from the surface of the Earth into orbit a space colony would currently be a massively expensive project. There are yet no solid plans for building space colonies by any large-scale organization, either government or private. However, many proposals, speculations, and designs for space settlements have been made through the years, and a considerable number of space colonization advocates and groups are active. Several famous scientists, such as Freeman Dyson, have come out in favour of space settlement. On the technological front, there is ongoing progress in making access to space cheaper. (**Source:** https://en.wikipedia.org/wiki/Space_colonization).

However, circumstances of the times stimulate the thought that space colonization offers large potential benefits and hopes to an increasingly enclosed and circumscribed humanity. Permanent communities can be built and inhabited off the Earth. Space colonization appears to be technically feasible, while the obstacles to further expansion of human frontiers in this way are principally philosophical, political, and social rather than technological. One of the space colonization systems developed by NASA focuses on a space habitat where 10,000 people work, raise families, and live out normal human lives. The people live in the ring-shaped tube, which is connected by six large access routes (spokes) to a central hub where incoming spacecraft dock. These spokes are 15 m (48 ft) in diameter and provide entry and exit to the living and agricultural areas in the tubular region. To simulate Earth's normal gravity the entire habitat rotates at one revolution per minute about the central hub. Much of the interior of the habitat is illuminated with natural sunshine. The Sun's rays in space are deflected by a large stationary mirror suspended directly over the hub. This mirror is inclined at 45 degrees to the axis of rotation and directs the light onto another set of mirrors which, in turn, reflect it into the interior of the habitat's tube through a set of louvered mirrors designed to admit light to the colony while acting as a baffle to stop cosmic radiation. With the help of abundant natural sunshine and controlled agriculture, the colonists are able to raise enough food for themselves on only 63 ha (156 acres). The large paddle-like structure below the hub is a radiator by which waste heat is carried away from the habitat. Abundant solar energy and large amounts of matter from the **Moon** are keys to successfully establishing a community in space. Not only does the sunshine foster agriculture of unusual productivity, but also it provides energy for industries needed by the colony. Using solar energy to generate electricity and to power solar furnaces the colonists refine aluminum, titanium, and silicon from lunar ores shipped inexpensively into space. With these materials they are able to manufacture satellite solar power stations and new colonies. The power stations are placed in orbit around the Earth to which they deliver copious and valuable electrical energy. The economic value of these power stations will go far to justify the existence of the colony and the construction of more colonies. The **colonization of the Moon** is proposed, as detailed above, by the establishment of permanent human communities or robotic industries on the Moon. Discovery of lunar water at the lunar poles by Chandrayaan-1 has renewed interest in the Moon. Polar colonies could also avoid the problem of long lunar nights – about 354 hours, a little more than two weeks – and take advantage of the Sun continuously, at least during the local summer. Perhaps mankind will make the purpose of the next century in space what Hermann Oberth proposed several decades ago: **"To make available for life every place where life is possible"**. (**Source**: https://settlement.arc.nasa.gov/75SummerStudy/Chapt.1.html&https://en.wikipedia.org/wiki/Colonization_of_the_Moon).

In the details given above, NASA suggested a colonization plan for Moon. Once colonization of moon is achieved earthlings can extend colonization to Mars. As in the case of Moon, Mars's polar regions are of special interest to both atmospheric scientists and geologists. The poles exhibit unique atmospheric processes that periodically spill over into the lower latitudes in the form of storms. The polar ice caps (and their extensions in the form of lower-latitude ground ice deposits) are geological deposits intimately connected to the atmosphere. They are also known records of climate variations. Thus, the polar ice caps, atmosphere, and climate are best interpreted as an ensemble. Scientists have identified a crater on Mars, possibly created by an asteroid that triggered 150 mtrs high tsunami waves when it plunged into an ocean on the red planet three billion years ago. It created a big 75 mile wide crater Lomonosov. Scientists think an ocean might once have filled the vast lowland region that occupied Mars`s northerly latitudes. Tsunami resultant water waves travelling 150 km inland substantiates that Martian surface at that time had a substantial amount of water in residence. This has likely implications for the total inventory of water on Mars, an encouraging component for colonization. (**Sources**: Smith,I.etal(2017),https://eos.org/meeting…/mars-polar-intrigue-spurs-multidisciplinary-collaboration,Eos,98, https://doi.org/10.1029/2017EO069599&http://www.techtimes.com/articles/203105/20170326/impact-crater-linked-to-powerful-tsunamis-on-mars-another-proof-of-an-ancient-ocean.htm).

Such Moon and Mars colonization initiatives are apt and needed but not those plans/ studies focusing on colonization of exoplanets. Irrespective of my predicament and apprehensions I do however continue to enjoy seeing the twinkle - twinkle little stars that glow like celestial angels, and not as distant gaseous hot glowing terrestrial bodies. I am fascinated by the quotation."**Looking at these stars suddenly dwarfed my own troubles and all the gravities of terrestrial life. I thought of their unfathomable distance, and the slow inevitable drift of their movements out of the unknown past into the unknown future**."— H. G. Wells, the Time Machine, 1895.

Search for Extraterrestrial Intelligence (SETI)

While we are trying to weigh our capabilities and limitations, in a realistic way the Search for Extraterrestrial Intelligence (SETI) has assumed a new dimension. This has enthused some and perturbed others. NASA has brought out a significantly important report, giving specifics of the initiatives made by man during the last 100 years, to contact aliens living in habitable exoplanets. Interested can go through the link given below to access this report. (**Source:** https://www.nasa.gov/sites/default/files/files/Archaeology_Anthropology_and_Interstellar_Communication_TAGGED.pdf.).

A team of scientists have revealed new research that seems to indicate intelligent aliens beyond planet Earth exist and are trying to communicate with others. A paper titled "Discovery

of peculiar periodic spectral modulations in a small fraction of solar type stars" doesn't necessarily sound like a stunning discovery to most people, but the research paper published in the journal Publications of the Astronomical Society of the Pacific may turn out to be the first step in the quest to establish the presence of intelligent life beyond our solar-system.

An analysis of 2.5 million stars that researchers have been watching has revealed 234 stars giving off "strange modulations" that suggest their origins are likely caused by an alien species, rather than natural causes." The fact that they are only found in a very small fraction of stars within a narrow spectral range centred near the spectral type of the sun is also in agreement with the ETI hypothesis," they add, referring to an "ETI" or "Extra Terrestrial Intelligent" hypothesis. Astronomers from a university in Quebec used a mathematical tool that hasn't really been studied in depth yet to analyze super quick light pulses of about less than a trillionth of a second to reach their conclusion. The scientists explored a series of other potential causes for the modulations, including instrument effects, rotation of molecules, rapid stellar pulsations and chemistry. "Breakthrough Listen", a project backed by Stephen Hawking and Mark Zuckerberg, will begin investigating the 234 star signals as well to see what can be determined. (**Source:** https://www.aol.com/article/news/2016/10/26/astronomers-signals-space-alien-lifeforms-communicate-earth/21592195/)

While many astronomers and cosmologists are fascinated by the above research findings, some highly intelligent and knowledgeable scientists strongly opposed the series of initiatives by NASA and others to contact intelligent aliens.

Stephen Hawking: Intelligent Aliens Could Destroy Humanity, But Let's Search Anyway

Famed astro physicist Stephen Hawking helped launch a major new effort to search for signs of intelligent alien life in the cosmos, even though he thinks it's likely that such creatures would try to destroy humanity. At the media event announcing the new project, he noted that human beings have a terrible history of mistreating, and even massacring, other human cultures that are less technologically advanced — why would an alien civilization be any different? And yet, it seems Hawking's desire to know if there is intelligent life elsewhere in the universe. He was part of a public announcement for a new initiative called "Breakthrough Listen", which organizers said will be the most powerful search ever initiated for signs of intelligent life elsewhere in the universe. Stephen Hawking said that intelligent aliens may be rapacious marauders, roaming the cosmos in search of resources to plunder and planets to conquer and colonize. He reiterates that one day, we might receive a signal from a planet, referring to a potentially habitable alien world known as Gliese 832c. "But we should be wary of answering back. Meeting an advanced civilization could be like Native Americans encountering Columbus. Some scientists believe that Stephen Hawking`s fears have no base as any alien civilization advanced enough to come to Earth would surely already know of humans' existence via the radio and TV signals that humanity has been sending out into space since 1900. (**Source:** http://www.space.com/29999-stephen-hawking-intelligent-alien-life-danger.html & http://www.space.com/34184-stephen-hawking-afraid-alien-civilizations.html).

What should be our immediate priority?

Recently Kasturi Rangan, former chief of ISRO stated that earthlings can colonize Moon. The scientific expeditions that help man to explore the Moon`s or Mars`s surface help us to have better insight into our earth`s origin and varied nature of earth`s atmosphere since 4.5 billion years till date. His prediction is strengthened by the colonization plan proposed by NASA (detailed above). While success of such colonization seems to be possible in about 100 years it needs to be planned meticulously to avoid conflicts in making it successful. I say so because of the following.

Man wishes to live in a normal way, without altering his basic way of living. To live on Moon or Mars that have varied morphology, atmosphere and internal structure and composition it is essential to forego his natural way of living and adapt to a way of life that is akin to that of a robot (as per NASA such a development can be avoided and man can lead a normal life). To ensure no setbacks due to presence of an entirely different environment there is every possibility that colonists will digress from their basic instincts. As man has strong likes and dislikes the migrants to Moon and Mars would slowly but steadily try to bring back their life styles on earth, there by destroying the adapted planets` natural resources and environment and polluting life saving water, air and food, as on Earth. This is evident when we see the way the serene environments of Antarctic and Arctic are degraded beyond limits in a matter of three decades. In spite of these questionable shortcomings it has become a necessity to explore the possibility of migrating and adapting to the local conditions on partly habitable planets like Moon and Mars to ensure survival of human race, amidst irreversible damage to mother Earth due to ever increasing needs of growing human population. Since colonization of large number of human beings is a significantly difficult proposition men belonging to developed and developing countries need to set aside the number of divisive and destructive factors and live like one unique race; as of now a difficult proposition, but not beyond our reach.

As mentioned above colonization of Moon is possible in the next 100 years. Colonization of exoplanets is different and difficult. When we look at the quality of life on Earth and probable deterioration in the next 100 to 200 years, let our scientific studies primarily focus on reduction of pollution and safety of all living creatures on Earth. As a right step let colonization of Moon is first achieved. Let also the exoplanet research continue to protect human race by liens.

Sometimes you have to go up really high in to space to understand how small you really are and then attempt to do such things that are within your reach to benefit the humanity, while curbing our urge to carry out such scientific activities that will unwittingly harm entire human race. I say so as some times intelligence and knowledge of highly capable scientists lead them to create monsters from mole hills due to lack of wisdom (for example creation of nuclear weapons).

*****In this issue**

It has nine research articles, an editorial and News at a glance. We are trying our best to make the journal a SCOPUS journal. Thomson Reuters are in principle happy with the quality of the content and our sincere effort to adhere to publication ethics. If not now it will definitely receive due recognition in the next 8 to 9 months. However, efforts have to be continued to maintain high standards and ensure publication of bi-monthly issues on time. This requires commitment and hard work by all those associated directly or indirectly with JIGU.

I solicit, on behalf of the editorial board, your continued support to JIGU.

P.R.Reddy

J. Ind. Geophys. Union (July 2017)
v.21, no.4, pp: 249-259

Geotechnical Studies using Geophysical Logs of Sravanapalli –II Dipside Block, Adilabad District, Telangana, India

K. Venkatesh*[1], V. Suman[1], K. A. V. L. Prasad[2], M. Shanmukha Rao[3] and A. Srinivasa Rao[4]

[1]Senior Geophysicist, Exploration Division, SCCL, Bellampalli, 504 251
[2]Superintending Geophysicist, Exploration Division, SCCL, Bellampalli, 504 251
[3]Superintending Geophysicist, Exploration Division, SCCL, Kothagudem, 507 101
[4]Deputy General Manager (Geophysics) Exploration Division, SCCL, Kothagudem, 507 101
*Corresponding Author: venky.geo@gmail.com

ABSTRACT

Strata control invariably depends upon precise understanding of geological and geotechnical characteristics of overburden strata of coals which helps in managing the risks associated with various forms of strata instability. Geophysical logs of exploratory boreholes, besides overcoming the inherent limitations of conventional methods address all the geotechnical characteristics of the surrounding strata so that geotechnical engineers can design mine openings, which differ according to the mine plan. The present study provides all the geological and geotechnical characteristics of Permian coals of Barakar Formation of Sravanapalli -II dipside block of North Godavari sub-basin, Telangana, India. The 200m thick coal-bearing Barakar is resolved into Lower and Upper sequences. The coals of Lower sequence have roof rocks varying from sandstones to shale in specific directions which are prone to wash out. The High strength massive sandstones having Uniaxial Compressive Strength (UCS) of 30 MPa to 50MPa constitute the overburden strata of lower set of coals. The coals of Upper sequence contain one metre to two metre thick beds of clays/shales along their roofs and medium strength sandstones of 10MPa to 20MPa. All these interburden strata of coals contain couple of one metre to two metre thick lenses of Very High to Extremely High strength sandstones of UCS of 60MPa to 200MPa. These overburden strata are also classified in terms of Geophysical Strata Rating (GSR) computed from suite of geophysical logs. Dynamic moduli of these sediments are even computed using density and sonic logs. These logs now give wider range and several options by providing petrophysical, elastic and mechanical properties of overburden strata to earth scientists involved in mine planning.

Key words: P-wave, UCS, CMRR, GSR, SS-80.

INTRODUCTION

Strata control is the most important aspect influencing both safety and productivity of coal mining. For underground mining, the most important of these geotechnical considerations are the roof support requirements and, if longwall mining is being practiced the caving behaviour of the strata. In open cast mines, wall stability and blasting/ digging requirements are major geotechnical concerns. Rock Quality Designation (RQD) and other strength parameters such as Unconfined/Uniaxial Compressive Strength (UCS), Young's Modulus (E), Coal Mines Roof Rating/Rock Mass Rating (CMRR/RMR) etc are usually determined at rock testing laboratories using the core samples obtained from exploratory boreholes.

Uday Bhaskar and Shanmukha Rao (2016a) reported that core samples subjected to core discing and poor core recoveries are not suitable to determine RQD and mechanical properties. Stress release during drilling also lowers UCS of core samples. Different laboratories produce different values of UCS of the same litho-units intersected in the same boreholes. Peng (2015) also concludes that laboratory determined rock/coal mechanical properties usually spread over a wide range and should not be averaged to avoid serious implications on overall design. Otherwise, the local falls would be considered as main fall as noticed by Uday Bhaskar and Shanmukha Rao (2016a) and Frith and Colwell (2008) recommend UCS as an index property rather than an absolute one. Hatherly et al., (2001) remarks that conventional methods of laboratory testing of cores are prone to sampling problems and misrepresentation of actual conditions insitu. The cost of coring and rock testing also makes it impractical to drill enough geotechnical holes to sample the full range of variability present within the rock mass. Hatherly, 2013; Hatherly et al., 2016 noticed that Australian coal industry therefore depends on a suite of borehole geophysical logs to acquire geological and geotechnical information (UCS) of the entire overburden strata of coals in a much reliable and accurate manner than from core samples. UCS is now routinely estimated from sonic logs. Geotechnical engineers use these two- and three-dimensional geological and geotechnical models obtained from geophysical logs to visualise and plan their mining operations. Using geophysical logs and Geophysical Strata Rating (GSR) methods, Medhurst et al., (2014) predicted caving of strata at various stages of high capacity longwall

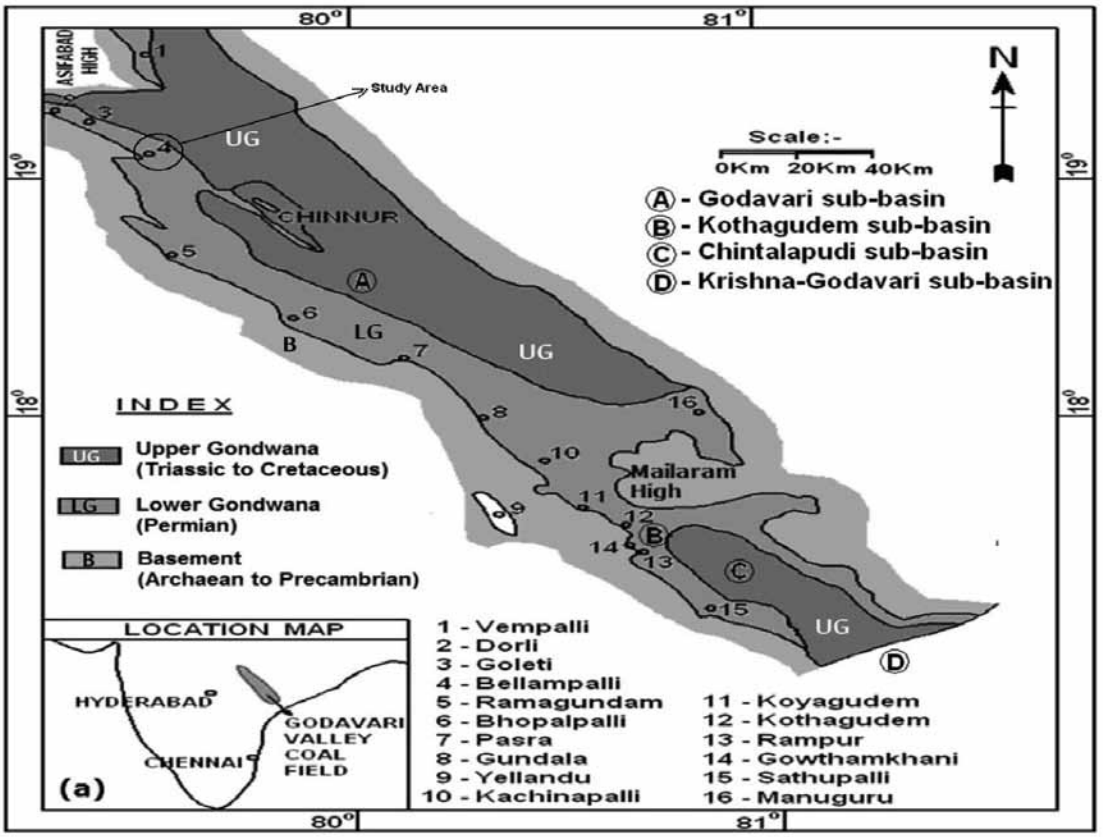

Figure 1. Outline of Pranhita-Godavari Valley.

mining in Australia. GSR introduced by Hatherly, 2013 and Hatherly et al., 2016 is considered the geophysical version of Coal Mines Roof Rating (CMRR) or Rock Mass Rating (RMR) proposed by Mark and Molinda (2003) and Bieniawski (1976) respectively.

Uday Bhaskar et al., (2015a, 2015b & 2016b); Shanmukha Rao and Uday Bhaskar (2015b); Uday Bhaskar and Shanmukha Rao (2016a); Shanmukha Rao et al., (2015a & 2015c) and Sharma et al., (2014 & 2016) of Singareni Collieries Company Limited (SCCL) situated in the state of Telangana, India carrying out detailed exploration and mining of Permian coals of Godavari Valley are the first in India to establish the usefulness of geophysical logging in coal exploration and mine planning programmes. Sharma et al., (2016); Chatterjee and Pal (2010) and Ghosh et al., (2016) computed ash and moisture contents of coal using geophysical logs from various coalfields of India. Similarly Sharma et al., (2014 & 2016); Singha and Chatterjee (2015) and Das and Chatterjee (2017) made use of geophysical logs to compute in-situ stress conditions and well bore stability. These geophysical logs now provide all the information related to geological, geochemical, geotechnical and mechanical properties of overburden of coals. The strength parameters are even empirically related to P wave velocities (Vp) obtained from sonic logs. These workers classified rock strength (UCS) proposed by (Larkin and Green, 2012) who classified rock strength by considering the Permian sediments alone but not the entire spectrum of rock types. The mechanical stratigraphy of the entire coal bearing Barakar Formation spread over a strike length of 350km is now well established from these geophysical studies. UCS and GSR maps prepared from geological and geophysical inputs provide an effective means to analyse the competency of immediate overburden strata of coals considered for underground mining and deep and large opencast mines. These maps now provide the basic inputs to construct geo-hazard maps. Uday Bhaskar and Shanmukha Rao (2016a) and Shanmukha Rao and Uday Bhaskar (2015b) demonstrated that geological and geotechnical data obtained from geophysical logs of non-cored wells allow planning and managing high capacity longwall mines of SCCL. Taking clues from these studies, an attempt is made to build up the geotechnical and geological characteristics of coal bearing Barakar Formation of Sravanapalli- II Dip side Block of North Godavari sub-basin (Figures 1 & 2).

Geological Setting

SCCL is a state owned public sector company exploring and extracting the coal deposits of Early Permian Barakar Formation along 350km long NNW-SSE trending Pranahitha Godavari Valley located in the state of

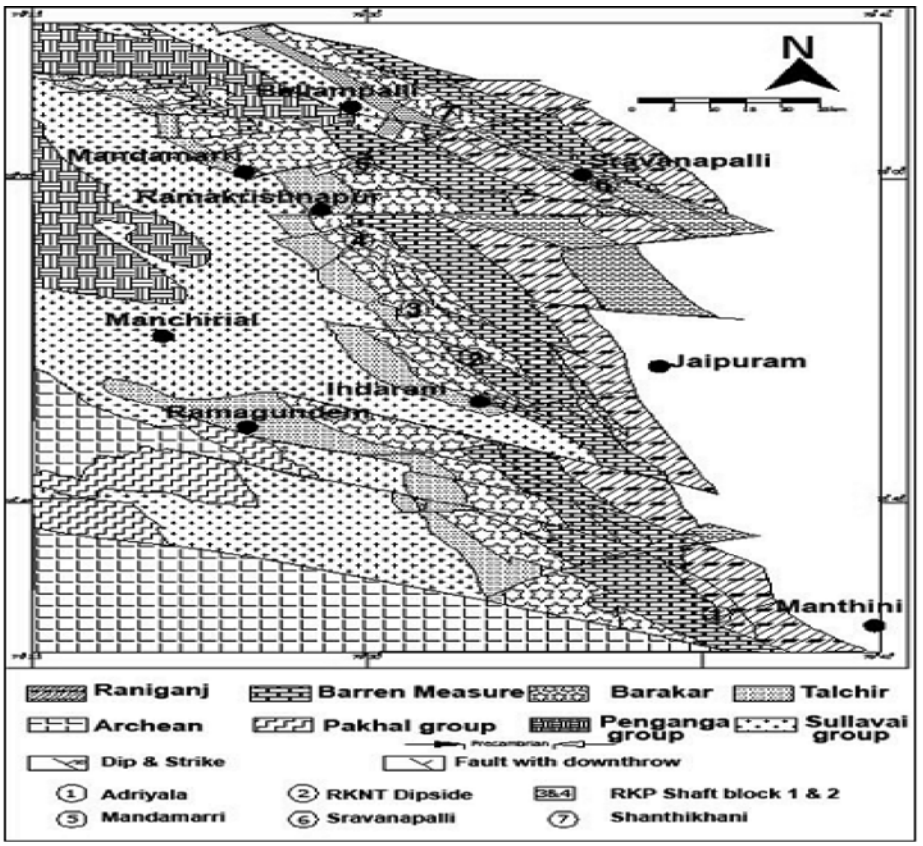

Figure 2. Geological Map of Sravanapalli-II Dipside Block and its Surrounding Areas.

Telangana, India (Figure 1). Based on geological and geophysical data, the valley is divided into four sub-basins by Ramana Murty and Parthasarathy (1988) from north to south as Godavari, Kothagudem, Chintalpudi and Krishna-Godavari sub-basins. The Early Permian Barakar Formation contains seven to ten correlatable coals of 1m to 22m thickness. The Late Permian Raniganj Formation contains intercalated carbonaceous horizons which are yet to be extracted. The Sravanapalli–II Dip side Block is located in the Northern part of the Godavari sub-basin (Figure 2). The block is bounded by Latitude: N18^0 58′ 58″ to 19^0 01′ 44″ and Longitude: E79^0 32′ 55″ to 79^0 35′ 03″of Survey of India Toposheet No: 56M/12 & 56N/09. The Sravanapalli–II Dip side Block covering an area of 7.13Sq. km (with strike length of about 5.1km and dip length of about 1.4km) is located on the almost extreme south eastern part of Dorli – Bellampalli coal belt. A few exposures of Barren Measure and Lower Kamthi (Raniganj) formations are present in the block. The area is mostly covered by soil followed by Late Permian Raniganj and Middle Permian Barren Measure formations. Figure 3 shows the location of boreholes drilled in the block.

The stratigraphic succession of the block worked out mostly from the subsurface data is furnished in Table 1. Coals are located between 300m and 700m depths below the surface. Figure 5 shows the core samples of Barakar Formation. In Sravanapalli Block –II Dip side, nine regionally persistent coal seams viz. IA, I, II, LB1, IIIB, IIIA, SJ (Top), SJ(Bot) and LB2 occur within the Early Permian Barakar Formation of 300m thickness, comprising white to greyish white, coarse to medium grained feldspathic sandstones interbedded with shale and coal horizons. The interburden strata of these coals are named SS-90, SS-80T, SS-80, SS-70, SS-65, SS-60, SS-50, SS-40, SS-40B and SS-30 in descending order (Figures 4, 5, 6a & 6b). The thickness of these coals ranges from one metre to six metres with Seam-II having maximum thickness of 6m. The 200m thick coal bearing Barakar Formation is overlain by 350m thick Barren Measure sediments comprising green to greenish grey, medium to very coarse grained feldspathic sandstones intercalated with shales and variegated clays. The Raniganj Formation of about 200m thickness in this block is made up of medium to coarse grained white to greenish grey white calcareous sandstone and buff to greenish grey clays. The Raniganj contains couple of uneconomic 0.60m to 2m thick correlatable coals, which are considered marker beds. Sondilla Seam is one such carbonaceous bed.

TABLE 1. Generalised Stratigraphic Succession Of Sravanapalli_II Dipside Block.

Age	Group	Formation	General Lithology	Thickness (m)
Recent			Soil cover/Alluvium	3.00
PERMIAN	LOWER GONDWANA	*Middle Kamthi*	Shale/clays with subordinate sandstone .	20.00+
		Raniganj (Lower Kamthi)	Sandstone with subordinate shale and coal seams	200
		Barren Measures	Coarse to pebbly feldspathic sand stones with variegated shales & clays	330.26+
		Barakar	Upper-Member: The sandstones are medium to coarse grained grey to greyish white in color with 10 correlatable coal seams.	200
			Lower Member : Predominantly fine to medium grained white sandstone with thin coal bands.	107.83+
		Talchir	Fine to medium grained greyish white to green colored sandstone and shale.	-

METHODOLOGY

Around 80 boreholes are drilled in the block to establish the lay out and disposition of coal seams (Figure 3). These boreholes were mostly non-cored and coring was limited to the coal seams and their roof and floor rocks. The Barren Measure and Raniganj formations are completely non-cored but for couple of boreholes. Similarly, the complete sequence of Barakar Formation was cored in a few boreholes. The core samples of sandstones are broken into pieces of different lengths (Figure 5). Most of these sandstone core lengths are between 10cm and 20cm while the core samples of coal are around 5cm to 10cm and clay samples are less than 5cm and often powdered. The soft and pliable nature of finer clastics and coals do not favour generating intact core samples. These core samples are broken along the same direction due to core discing and produce lower values of strength parameters as discussed by Uday Bhaskar and Shanmukha Rao (2016a). These core samples are therefore not suitable to determine RQD and mechanical properties since they mislead one to conclude massive sandstones as highly fractured/jointed rocks having low RQD. The geotechnical information of entire Barakar Formation might not possible from core samples and making it necessary to think of alternative methods to get these data. The geophysical logs of these boreholes therefore form the primary source of geological and geotechnical information. Figure 4 shows the geophysical logs along with interpreted lithologies, mechanical and elastic properties. The complete information of Barakar is possible and an easy affair from geophysical logs.

The geophysical logging was carried out using logging equipment of M/s. Robertson Geologging, Deganby, UK using SPRN, FDGS, HRAT and TRSS probes. SPRN probe contains single point resistance (SPR), short normal resistivity (SNR), self potential (SP), single detector of neutron and 241Am-Be radioactive source of 37GBq strength. FDGS probe contains far and near density detectors to compute bulk density (DENS), natural gamma (NGAM) and caliper (CALP) and 137Cs of 3.70GBq strength is the radioactivity source. HRAT is the high resolution acoustic televiewer imaging probe and TRSS is the tri-receiver monopole full waveform sonic probe. The interpretation of geophysical logs was carried out using the standard procedures and the various modules of WellCad software. The geophysical logs of nine boreholes located along the NNW-SSE strike direction are considered in the present study (locations in Figure 3). The interpretation of geophysical logs was also reviewed and correlated with the available core data.

Coals are identified by high resistance/resistivity, low density of 1.40 to 1.80g/cc, low neutron and natural gamma values of about 50cps and 30cps to 50 cps respectively (Figure 4) and Vp of coals are around 2300m/s. Coals and clays are characterised by the absence of propagation of shear waves (Vs) in the monopole sonic probe. Vp and Vs of very coarse to medium grained grey-white sandstones of Barakar are around 3000m/s to 3750m/s and 1500m/s to 2000m/s respectively and bulk density of 2.30g/cc to 2.50g/cc. Fine grained sandstones hard and compact and often silicified record high to very high resistance/resistivity, neutron (400cps to 700cps), density of 2.65g/cc to 2.80g/cc and Vp of 4500m/s to 6000m/s. Fine grained sandstones, sandy shales, shales and clays show low neutron (50cps to 125cps) and high gamma (200cps to 300cps) values and densities of 2.20g/cc to 2.50g/cc. Some of the clays and shales are prone to caving as observed from the increase in borehole diameter on caliper logs and are considered very weak beds. The neutron and Vp logs being easy to quantify give a basis to classify various lithounits on the basis of count rates and Vp values. The density and natural gamma values of coal increase with the increasing ash

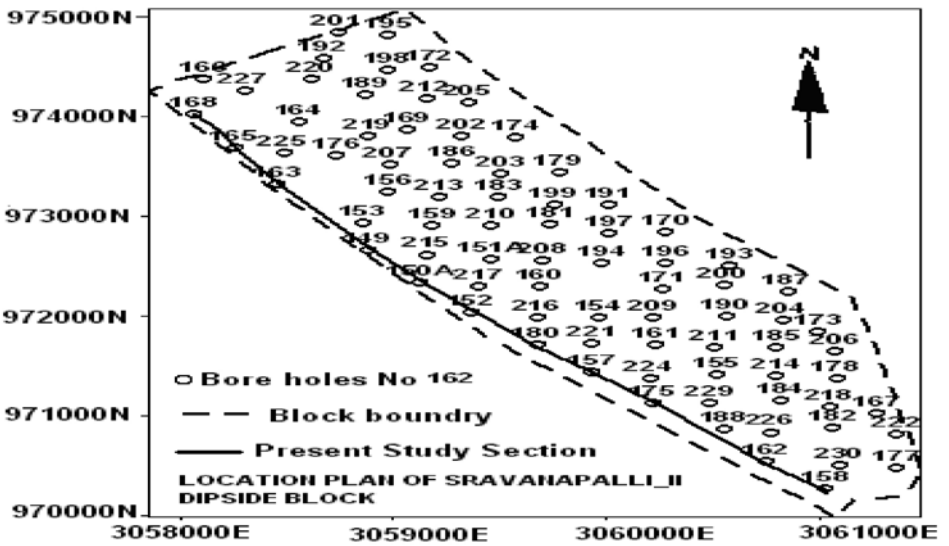

Figure 3. Location Plan of Sravanapalli –II Dipside Block.

content, while resistance and resistivity of coals decrease with ash contents.

The density and arrival times of P and S waves are used to calculate the dynamic modulus such as Bulk Modulus, Shear Modulus, Young's Modulus and Poisson's Ratio along with Vp/Vs to analyse the competency of various lithounits. The acoustic amplitude images indicate fine grained sandstones, shales and coals as high amplitude bright colour features and the medium to coarse grained sandstones as medium amplitude light brown colour features. The clay beds which are prone to easy caving appear as low amplitude dark shade features (Figure 4).

The sonic log being a function of rock elasticity can be empirically related to various rock strength parameters. Uday Bhaskar et al., (2015a, 2015b & 2016b), Shanmukha Rao and Uday Bhaskar (2015b), Uday Bhaskar and Shanmukha Rao (2016a), Shanmukha Rao et al., (2015a & 2015c) and Sharma et al., (2014 & 2016) estimated strength parameters of Permian sandstones of Godavari Valley from sonic logs. These studies also provide a clue to identify the uncertainties in the laboratory determinations of strength parameters of Permian sediments of Godavari Valley. Hanson et al., (2005) classified the sediments on the basis of Vp values rather than UCS values. Sonic logs provide reliable and accurate arrival times and wave velocities and are therefore considered to classify the rock strengths and even to compute UCS.

Empirical equation (1) developed by Uday Bhaskar and Shanmukha Rao (2016a) being comparable to the world-wide studies is considered to estimate UCS from Vp obtained from sonic logs.

$UCS = 10^{-5}\text{-}5Vp^2\text{-}0.0269Vp\text{-}122.73$ ($R^2=0.94$) (1)

UCS and Vp are in MPa and m/s respectively.

CMRR/RMR are usually preferred over UCS because the rocks of contrasting geological make up can still have similar and identical UCS values due to which the UCS on its own cannot ascertain the overall competency of the rock. CMRR/RMR though has the ability to define the overall competency of a rock is never determined during exploration stage in India. Mine plans are prepared only on the basis of much debated RQD and UCS values but not on the basis of CMRR/RMR in India. One has to wait for the opening to determine CMRR/RMR. GSR, the geophysical version of CMRR/RMR allows having first-hand information on competency of overburden strata of coals at the exploration stage itself. Medhurst et al., (2014) suggested a rating system based on GSR, wherein a range of approximately 15% for very poor quality rock to 100% for very good quality rock. The classification is in line with CMRR/RMR rating schemes which are based on core samples. GSR of the coal bearing Barakar Formation of Sravanapalli –II Dipside block has also been calculated by following the procedures of Hatherly et al., (2016).

A strike section along the NNW to SSE direction of about 5km length is constructed to analyse latero-vertical variations, UCS and GSR of the overburden strata of coals (Figure 4, 6a & 6b). The section extends from borehole SBS-168 in the NNW to borehole SBS-158 in SSE as shown in Figure 3

Discussion of Results

The coal bearing Barakar Formation can be resolved into Lower (70m) and Upper (80m) Sequences with the base of Seam-LB1 as the interface. The Lower Sequence comprises

Figure 4. Borehole Geophysical Logs along with Interpretation of Lithology, Mechanical and Elastic Properties, Borehole SBS-168.

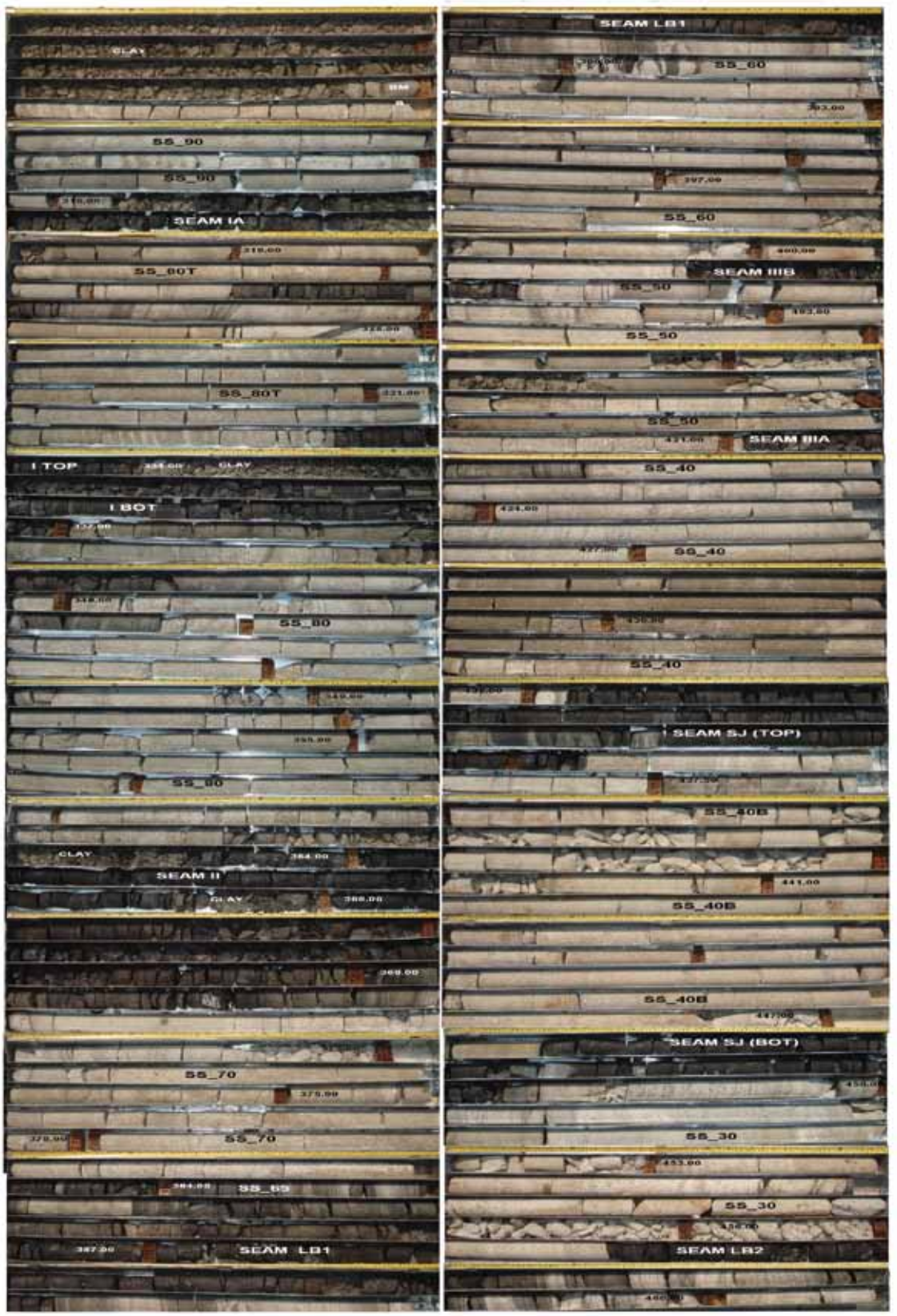

Figure 5. Core Samples of Barakar Formation, Borehole SBS-165. Core Samples are arranged in descending order. (Clay, Coal, Sandstone).

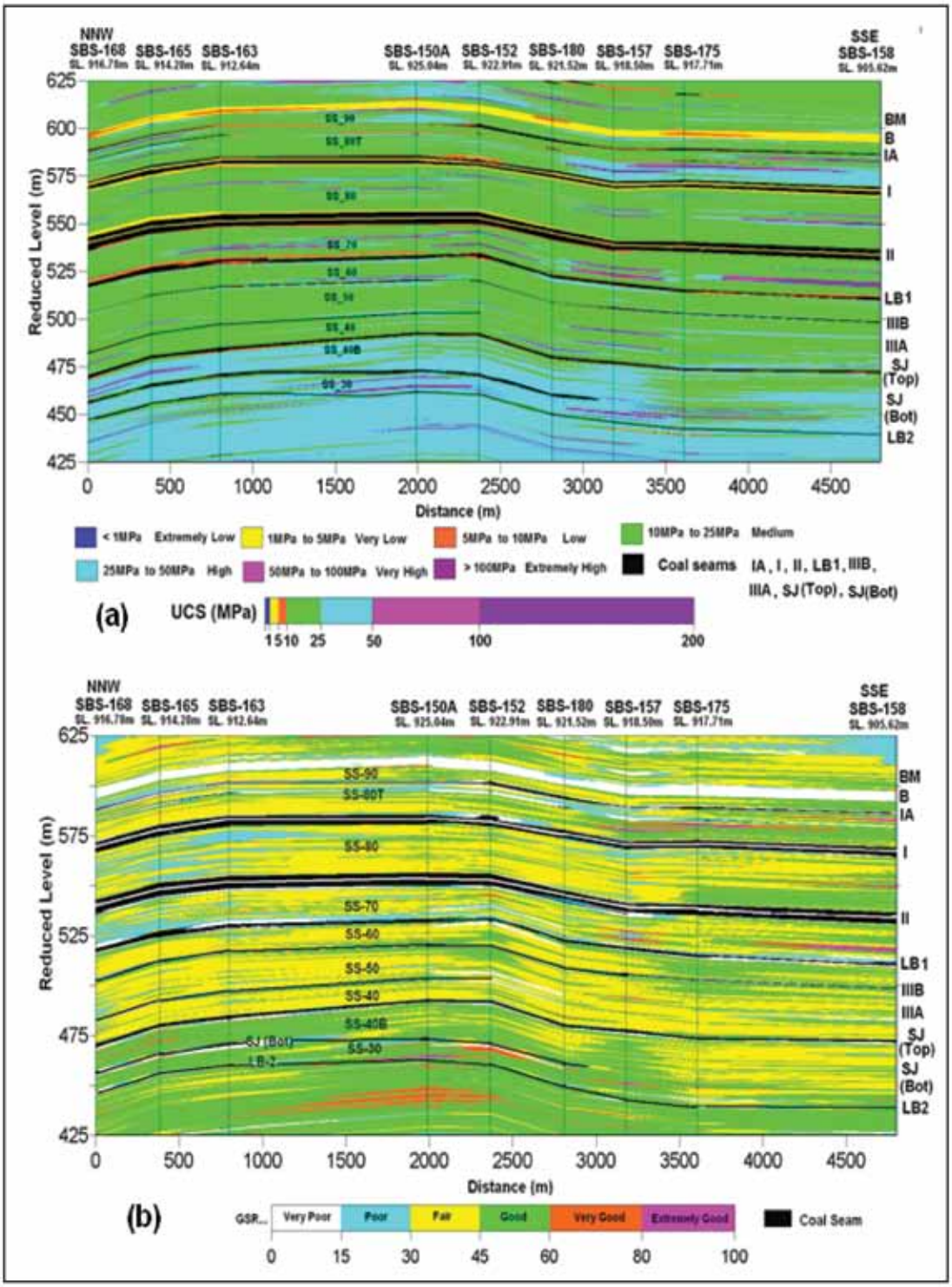

Figure 6. (a) UCS and (b) GSR Maps of Barakar Formation of Sravanapalli-II Dipside Block along Strike Section.

relatively compact and massive sandstones having Vp of 3500m/s to 4000m/s, UCS of 30MPa to 40MPa and GSR of 50% to 60% corresponding to a clasification as High Strength and Good rocks respectively. SS-30 and SS-40B show increasing trends towards SSE indicating that the channel was active along these portions of depositional sites. The wash out of coals LB2 and SJ (Bot) and their replacement by surrounding sandstones is a common phenomenon. Thus, these coals go through facies change from coals to sandstone through finer clastics. The net

increase in the thickness of Barakar from 146m in the NNW to 165m in the SSE is mostly due to the increase in the thickness of SS-30 and SS-40B. The sedimentation during the other various episodes is almost uniform indicating stable conditions of syn-sedimentary tectonic conditions. The thickness of Seam SJ (Bot) also displays decreasing thickness followed by washout along the SSE. The wash out of SJ (Bot) and LB2 at different parts indicates encroachment of coal swamps by active channels. The Seam SJ (Top) though having a better persistency shows variation in its thickness from 1.18m to 1.97m with a decreasing trend towards SSE. Similar to Seam LB2, the coals IIIA and IIIB are around 0.48m to 0.88m and 0.43 to 0.81m respectively. Seam IIIA is mostly washed out along the SSE direction. High Strength sandstones of about 30MPa to 40MPa (UCS) and GSR of 50% to 60% constituting the immediate roof rocks of these coals however grade to much weaker shale beds towards the zones of washout. Part of these coals could be replaced by shales and other finer clastics classified as poor to fair rocks by GSR. The floor rocks of these coals being deposited during in-active stages of channel are made up of one metre to two metres thick finer clastics of fine grained sandstones, sandy shales and shales. Thus, these coals have weak rocks as their immediate floor. The inter-tonguing and wedging of weak and strong rocks produces differential compaction and fracturing and jointing of rocks. These zones can be considered as geotechnical risks and appropriate measures should be taken to handle them.

The Upper Sequence extending from the base of LB1 to the BM/B contact of about 80m thickness shows near uniform thickness of overburden strata of various coals indicating uniform and stable conditions of deposition. The sandstones which are mostly medium to coarse grained are relatively less compact and less hard than those of sandstones of Lower Sequence. Vp and UCS of these sandstones are around 3000-3500m/s and 10MPa to 20MPa and can be classified as Medium strength rocks. GSR of these sandstones is around 30% to 45% and classified as Fair rocks. The coals LB1 (Bot), Seam-II, Seam-I and Seam-IA show uniform thickness while the thickness of Seam LB1 reduces to 0.80m at SSE. This is because of the replacement of coals by shales. LB1 (Top) is developed only in borehole SBS-152 located on this section. Clays, shales and other such weak beds form the immediate roof rocks of these coals of Upper Sequence thereby making it difficult to mine them. The less thickness (1.10m to 1.50m) of Seam-I and presence of 1.00m to 1.50m thick clay along the roof can make it difficult for mining of Seam-I. The Seam-LB1 (Bot) presents similar picture. The Seam-II of 6m thickness is one of the important coals which can be considered for mining by leaving coal along the roof. Uday Bhaskar et al., (2016b) indicated that the development of Seam-II of 6m thickness took place in coal swamp spread over the entire Godavari sub-basin. Inundation of coal swamps by flood basin produced higher amounts of ash of 25% to 40%. The 0.30m to 0.60m dirt band in the form clay, shale and carbonaceous shale resolves the Seam-II into Top and Bottom sections. Top section of Seam-II contains lesser amounts of ash of 25% to 30%. The bulk density as obtained from the density logs indicates that the Top and Bottom sections have a density of 1.50g/cc to 1.55g/cc and 1.55g/cc to 1.60g/cc respectively. The Seam-II can be mined by considering the experiences of Adriyala block as noticed by Uday Bhaskar and Shanmukha Rao (2016a).

The overburden strata of all these coals contain one metre to two metres thick fine grained to very fine sandstones, hard and compact and often silicified with their UCS varying from 60MPa to 200MPa and classified as Very High to Extremely High strength rocks. GSR of these beds range from 60% to 90%. Some of these beds persist over considerable extensions of hundreds of metres to one to two kilometers. The impact of these beds in terms of periodic weighing or differential compaction needs analysis using appropriate techniques.

The seam-wise overburden maps in terms of various mechanical, elastic and petrophysical properties gives further scope of taking up bed-wise analysis.

CONCLUSION

Geological investigations for coal mining should not be just about determining the thickness and quality of the seams to be mined. They should also address the geotechnical characteristics of the surrounding strata so that geotechnical engineers can design mine openings which differ according to the mine plan. The conventional methods often fall short of providing all these data. Geotechnical studies conducted in Sravanapalli-II dip side block using geophysical logs concludes that Geophysical logging of exploration boreholes provides a means for acquiring both geological and geotechnical information. The non-core drilling followed by geophysical logging should be considered as an additional advantage to bring down the exploration costs. To obtain these benefits, the main requirement is that the geophysical logging tools should be well calibrated. Mine companies should therefore properly supervise geophysical logging activities and ensure that logging contracts encourage delivery of high quality results. However, the human nature still continues to consider the bird in the hand in the form of a piece of core regarded much more highly than elusive birds in the bush in the form of 'esoteric' geophysical measurements. (Hatherly et al., 2016).

ACKNOWLEDGMENTS

Authors are grateful to the management of Singareni Collieries Company Limited for according permission to publish the paper. They are grateful to K. K. Sharma, GM (Exploration) for his encouragement and facilities provided to compile the paper. Opinions expressed in the paper are personal to the authors and do not represent the management of their company. The authors profusely thank Dr. Udaya Bhaskar and Prof. Rima Chatterjee for their critical comments and Dr. M.R.K. Prabhakara Rao for editing, which significantly helped to improve the quality of the manuscript. Thanks are due to Chief Editor for his kind support.

Compliance with Ethical Standards

The authors declare that they have no conflict of interest and adhere to copyright norms.

REFERENCES

Bieniawski, Z.T., 1976. Rock mass classifications in rock engineering, Exploration for Rock Engineering, v.1, pp: 97-106.

Chatterjee, R., and Pal, P.K., 2010. Estimation of stress magnitude and physical properties for coal seam of Rangamati area, Raniganj coalfield, India: International Journal of Coal Geology, v.81, pp: 25-36.

Das, B., and Chatterjee, R., 2017. Wellbore stability analysis and prediction of minimum mud weight for few wells in Krishna-Godavari Basin, India, International Journal of Rock Mechanics & Mining Sciences, v.93, pp: 30-37.

Frith, R., and Colwell, M., 2008. Geotechnical design at a mine site level–We have no choice, Underground Coal Operators Conference, http://ro.uow.edu.au/coal/8.

Ghosh, S., Chatterjee, R., and Shanker, P., 2016. Estimation of ash, moisture content and detection of coal lithofacies from well logs using regression and artificial neural network modelling, Fuel, v.177, pp: 279-287.

Hanson, C., Thomas, D., and Gallagher, B., 2005. The value of early geotechnical assessment in mine planning, Underground Coal Operators Conference, University of Wollongong, The Australasian Institute of Mining and Metallurgy & Mine Managers Association of Australia, http://ro.uow.edu.au/coal/65., pp: 17-30.

Hatherly, P., Medhurst, T., Zhou, B., and Guo, H., 2001. Geotechnical evaluation for mining – assessing rock mass conditions using geophysical logging, Final report, ACARP Project C8022b.

Hatherly, P., 2013. Overview on the application of geophysics in coal mining, International Journal of Coal Geology,. http://dx.doi.org/10.1016/j.coal.2013.02.006.

Hatherly, P., Medhurst, T., and Zhou, B., 2016. Geotechnical evaluation of coal deposits based on the Geophysical Strata Rating", International Journal of Coal Geology, v.163, pp: 72-86.

Larkin, B.J., and Green, D.R., 2012. Borehole data standard for Australian coal industry, ACARP Project C21003, (CoalLog Manual, version 1.1)., pp: 80-81.

Mark, C., and Molinda, G.M., 2003. The coal mine roof rating in mining engineering practice, Underground Coal Operators Conference, http://ro.uow.edu.au/coal/160., pp: 50-62.

Medhurst, T., Hatherly, P., and Hoyer, D., 2014. Investigation of the relationship between strata characteristics and longwall caving behaviour," 14th Coal Operators' Conference, University of Wollongong, The Australasian Institute of Mining and Metallurgy & Mine Managers Association of Australia, pp: 51-62.

Peng, S.S, 2015. Topical areas of research needs in ground control – A state of the art review on coal mine ground control, International Journal of Mining Science and Technology, v.25, pp: 1-6.

Ramana Murty, B.V., and Parthasarathy, E.V.R., 1988. On the evolution of the Godavari Gondwana graben based on LANDSAT imagery interpretation, Journal of Geological Society of India, v.32, no.5, pp: 417-425.

Shanmukha Rao, M., Uday Bhaskar, G., and Shiva Kumar, K., 2015a. Estimation of UCS of Coal Measures of Pranhita-Godavari Valley, India using Sonic Logs, 15th Coal Operators' Conference, University of Wollongong, The Australasian Institute of Mining and Metallurgy and Mine Managers Association of Australia, pp: 36-47.

Shanmukha Rao, M., and UdayBhaskar, G., 2015b. Geological and Geotechnical Characterisation using Geophysical Logs – An Example from Adriyala Longwall Project of Singareni Collieries, India, Journal of Indian Geophysical Union, v.19, no.3, pp: 270-281.

Shanmukha Rao, M., Prasad, K.A.V.L., and Uday Bhaskar, G., 2015c. Geological and Geotechnical Studies Using Geophysical Logs to Aid Pit Slope Stability, Examples from Koyagudem Blocks, Minetech, v.36, no.4, pp: 48-60.

Sharma, K.K., Uday Bhaskar, G., and Srinivasa Rao, A., 2014. Geological and geotechnical characterisation studies using geophysical logs-Experiences of Singareni Collieries, Telangana, Proceedings of All India Exploration Geologists Meet, organised by Mining Engineers Association of India, pp: 254-270.

Sharma, K.K., Uday Bhaskar, G., and Shanmukha Rao, M., 2016. Geophysical logging for coal exploration and mine planning at Singareni Collieries, Telangana, India, Minetech, v.37, no.2, pp: 30-40.

Singha, D.K., and Chatterjee, R., 2015, Geomechanical modeling using finite element method for prediction of in-situ Stress in Krishna-Godavari basin, India, International Journal of Rock Mechanics and Mining Sciences, v.73, pp: 15-27.

Uday Bhaskar, G., Srinivasa Rao, A., Prasad, G.V.S., and Shravan Kumar, B., 2015a. Geological and geotechnical characterisation of Ramagundam Opencast-II of Singareni Collieries using geophysical logs, Journal of Indian Geophysical Union, v.19, no.4, pp: 386-400.

Uday Bhaskar, G., Prasad, K.A.V.L., Suman, V., and Venkatesh, K., 2015b. Innovations in coal explortion techniques by Singareni Collieries using geophysical logs-An example from Ramakrishnapur Shaft Block-I, proceedings of international mining conference on technological innovations, interventions and colloborations for the development of mines and mineral industry, Hyderabad, 19-22 November, pp: 249-263.

Uday Bhaskar, G., and Shanmukha Rao, M., 2016a. Sub-surface Exploration Methodology for high capacity Longwall mining-Experiences of Singareni Collieries, Telangana, India, Journal of Geophysics, v.37, no.3, pp: 145-164.

Uday Bhaskar, G., Srinivasa Rao, A., Prasad, G.V.S., and Prasad, K.A.V.L., 2016b. Geomining conditions of Seam-I of Godavari sub-basin-A geophysical study, Journal of Indian Geophysical Union, v.20, no.2, pp: 178-190.

Received on: 12.1.17; Revised on: 11.2.17; Accepted on: 26.3.17

‘Super-deep’ diamonds- new information about Earth’s interior

Researchers at Tohoku University believe that it is possible for natural diamonds to form at the base of Earth’s mantle. The formation of such “super-deep” diamonds was simulated using high-pressure and high-temperature experiments by the Japanese research team, led by Fumiya Maeda.

Results of their experiment show that super-deep diamonds can form through the reaction of Mg-carbonate and silica minerals. The reaction may occur in cold plates which descend all the way to the base of the mantle.

Details of actual diamond formation in such a deep part of Earth has so far, never been reported. But researchers plan to combine their recent experimental model with observation and analysis, in the hopes of getting information from natural diamonds that would provide further knowledge about our planet.

Source: Fumiya Maeda et al., 2017. Diamond formation in the deep lower mantle: a high-pressure reaction of MgCO3 and SiO2. *Scientific Reports*, 2017; 7: 40602 DOI: 10.1038/srep40602

J. Ind. Geophys. Union (July 2017)
v.21, no.4, pp: 260-270

Assessment of Hydro-geochemical Evolution Mechanism and Suitability of Groundwater for Domestic and Irrigation Use in and Around Ludhiana city, Punjab, India

Sakambari Padhi[1], R. Rangarajan[*2], K. Rajeshwar[3], Sahebrao Sonkamble[2] and V. Venkatesam[4]

[1]Post-doctoral researcher, Department of Environment systems, Graduate school of Frontier Sciences, The University of Tokyo, Japan
[2]Scientist, Groundwater division, CSIR-NGRI, Hyderabad
[3]Scientist, Vimta Lab, Hyderabad
[4]Hydrogeologist, Central Groundwater Board, Central Region, Nagpur
*Corresponding Author: rangarajanngri@gmail.com

ABSTRACT

Groundwater and surface water samples in and around Punjab Agricultural University (PAU) Ludhiana were collected and analyzed for physico-chemical characteristics. The groundwater in the study area was found to be controlled by rock-water interaction, carbonate mineral (calcite and dolomite) weathering and ion exchange processes. The water facies were mainly of Ca-Mg-HCO_3 and Na-HCO_3 types, showing fresh water characteristics. All the groundwater samples were found to be with in the safe limits with respect to the dissolved solids, major cations, major anions and trace elements making it suitable for domestic use. However, the hardness may affect the acceptability of this groundwater for drinking. Most of the groundwater samples are suitable for irrigation, considering salinity hazard, sodicity hazard and bicarbonate hazard. However, magnesium hazard is found to persist in 63% of groundwater samples. The canal water is found to be of good quality for irrigation.

Key words: Hydro-geochemical evolution, Water quality, Domestic and Irrigation use, Salinity hazard, Sodicity hazard, Bicarbonate hazard, Magnesium hazard.

INTRODUCTION

In India, demand for fresh water is increasing rapidly due to population growth and intense agricultural activities. Water scarcity persists even in large parts of the Indo-Gangetic alluvial plains of north and northwest India. These alluvial formations have been extensively exploited for large-scale water supplies for industrial, irrigation and urban uses. A steady and large-scale groundwater loss in the northern India was reported by Tiwari et al., (2009). In Punjab, more than 83% of land is under agriculture. Traditionally, the farmers follow the maize-wheat or sugarcane-maize-wheat cropping pattern. During the last three to four decades, they have shifted to wheat-rice cropping pattern, thereby leading to an increased demand for irrigation water. Groundwater has been the main source of irrigation in these Indo-Gangetic alluvial plains of Punjab region, basically from tube wells. Presently, there are more than one million tube wells in Punjab (Gupta, 2010).

Central Pollution Control Board (CPCB, 2007) reported that groundwater quality of Ludhiana city is good for irrigation and drinking. Apart from CPCB, previous studies on groundwater quality in Ludhiana were mostly focused on heavy metal pollution around Buddha nullah (Garg et al., 2015). High concentration of heavy metals in groundwater were reported, e.g., chromium and cyanide (Chaudhary et al., 2001), and arsenic (Garg et al., 2015; Jain and Kumar, 2007).

The objective of this study is to understand the hydro-geochemistry of the study area and to examine groundwater suitability for domestic and irrigation purposes based on physico-chemical parameters, such as, pH and Electrical Conductivity (EC); major cations such as sodium (Na^+), calcium (Ca^{2+}), magnesium (Mg^{2+}) and potassium (K^+); major anions such as chloride (Cl^-), sulfate (SO_4^{2-}), carbonate (CO_3^{2-}), bicarbonate (HCO_3^-), nitrate (NO_3^-) and fluoride (F^-); total hardness (TH), and trace elements including copper (Cu), iron (Fe), manganese (Mn), zinc (Zn), arsenic (As), selenium (Se), and chromium, (Cr). The suitability of groundwater and surface water for irrigation purpose based on parameters such as EC, Sodium percentage (Na^+ %), Sodium adsorption ratio (SAR), Residual sodium carbonate (RSC), Permeability index (PI), Kelly's Ratio (KR) and Magnesium hazard (MH) is also investigated.

Study Area

The study area in and around the PAU campus is located in the central part of Punjab region (Figure 1a-b). It lies between latitudes of 30° 45′ to 31° and longitudes of 75° 45′ to 76°.

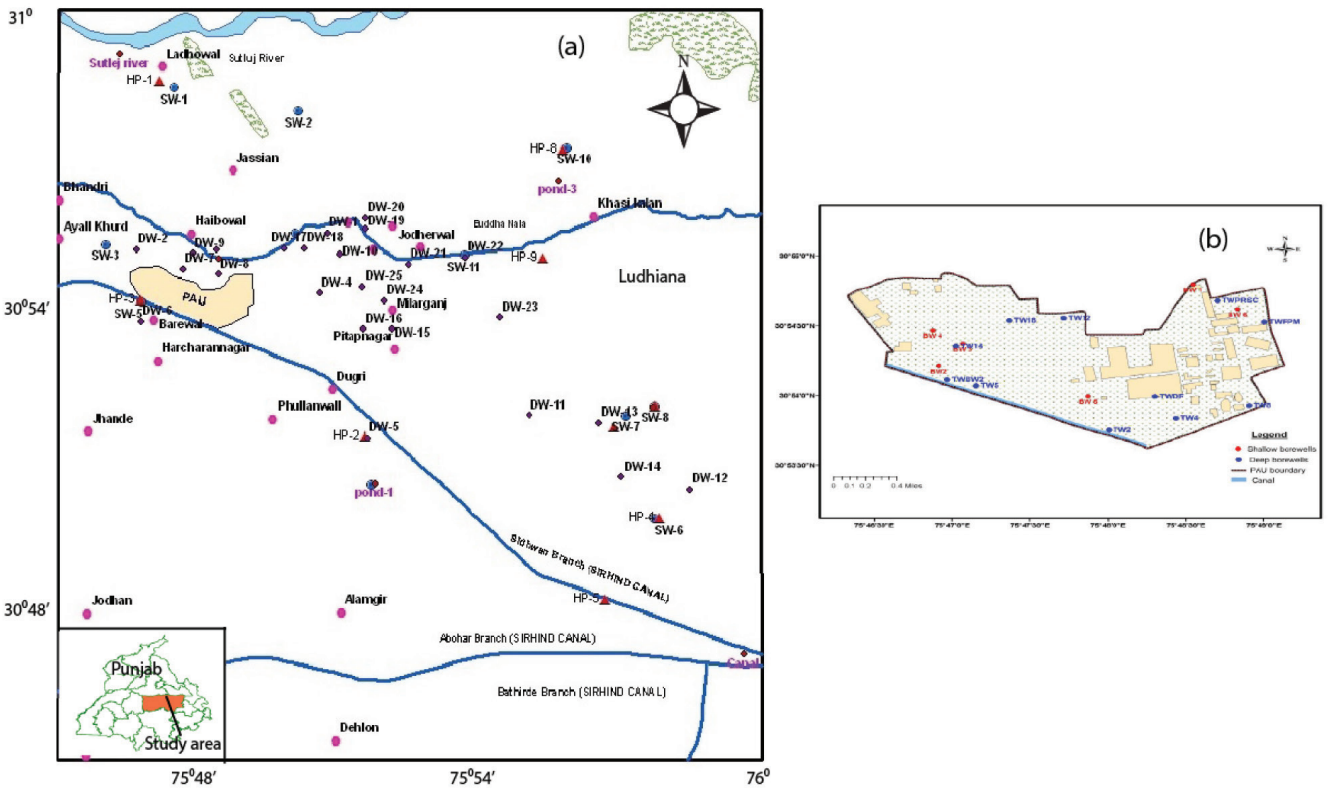

Figure 1. Location of sampling points (a) around PAU campus, Ludhiana city, Punjab, (b) inside the PAU campus.

PAU is located in the south western part of Ludhiana city and is situated at an elevation of 247m above mean sea level. Most part of the area is under anthropogenic activities for the last 30 to 35 years including intensive agriculture and poultry farming (Thind and Kansal, 2002). Irrigation, mainly by tube wells, is supported by canal water in some parts of the area. The EW flowing Sutlej River lies on the northern part of the study area. The Buddha nullah (stream) between Sutlej River and PAU campus runs parallel to the Sutlej River for a fairly large section of its course in the district and ultimately joins the river in the northwestern corner of the district. The stream water witnessed pollution after entering the Ludhiana city due to the city sewerage discharges. The Buddha nullah is reported to be extremely polluted because of the untreated industrial discharge (Singh et al., 2013). Bhalla et al., (2011) reported high concentration of Cr, Fe and Pb in the nullah. The Sirhind canal passes on the south, adjoining the campus.

Geology and Hydrogeology

Ludhiana district is occupied by Indo-Gangatic alluvium of Quaternary age. The subsurface geological formations of the area comprise of sand, silt, clay and kankar in various proportions. The litholog data of bore wells drilled to a depth of 400m by Central Ground Water Board (CGWB) and state government indicate the presence of many sand beds (5 prominent sand horizons) forming the principal aquifers separated by clay beds at various depths. The first aquifer generally occurs between 10 and 30m, the second between 50 and 120m, third between 150-175m, fourth between 200-250m and the fifth between 300-400m. The combined aquifer discharge rate lies between 3-52 lps with 4.3×10^{-4} to 6.98×10^{-4} storativity and transmissivity in the range of 628 to 1120 m^2/day. The sand content of the aquifer in the district varies from 50 to 80%. Clay beds, though thick at places, occur mostly as lenses and pinch out laterally. The granular material becomes coarser with depth. The aquifer at deeper levels acts as semi-confined to confined conditions (CGWB, 2007).

In the study area, groundwater is being pumped from moderate and deep wells (300-400 feet depth) mainly for agricultural purposes. There are about 40 deep wells within the university campus area and innumerable number of agricultural wells with approximate discharge rate of about 50-60 m^3/h. The first aquifer occurring within the depths of 10 and 30m is completely desaturated. The static water level in the shallow observation wells (150-200 feet) in the university campus area varies from 20-26m below ground level.

Materials and Methods

A total of 17 ground water samples from inside the PAU campus and 15 ground water samples from outside the

Table 1. Location of sampling sites and depth of groundwater samples.

Inside PAU campus			Outside PAU campus		
S. No.	Name	Well depth (m bgl)	S. No.	Name	Well depth (m bgl)
1	BW1	150-200	18	HP3	75-100
2	BW2	-do-	19	HP5	-do-
3	BW3	-do-	20	HP6	-do-
4	BW4	-do-	21	HP8	-do-
5	BW5	-do-	22	SW3	250-300
6	BW6	-do-	23	SW4	-do-
7	TW12	250-300	24	SW7	-do-
8	TWFPM	-do-	25	SW9	-do-
9	TWDF	-do-	26	SW10	-do-
10	TWBW2	-do-	27	DW1	350-400
11	TWPRSC	-do-	28	DW5	-do-
12	TW2	350-400	29	DW8	-do-
13	TW4	-do-	30	DW14	-do-
14	TW5	-do-	31	DW23	-do-
15	TW8	-do-	32	DW24	-do-
16	TW14	-do-	33	pond	-do-
17	TW18	-do-	34	canal	-do-

campus and two surface water samples (from the canal and pond) were collected from different depths during March 2009, before the onset of monsoon. The sampling locations are shown in Figure 1a (wells outside campus) and Figure 1b (wells inside campus), and are listed in Table 1. The results of analyses (range and mean value with standard deviation) for groundwater and surface water from inside and outside campus along with World Health Organization (WHO 1996, 2011) guidelines for maximum permissible limit (MPL) and BIS (2003) guidelines for MPL and desirable limit (DL) are presented in Table 2.

The irrigation water quality parameters, such as SAR, % Na^+, RSC, PI, KR and MH are computed from the chemical analytical data of groundwater sample.

RESULTS AND DISCUSSION

Mechanisms controlling groundwater chemistry

Hydro-chemical facies, the Gibb's diagram, and thermodynamic approach were used to understand the geochemical mechanisms that control the groundwater chemistry in the study area.

Gibb's diagram

The groundwater chemistry in an aquifer depends upon the chemical composition of the infiltrating (precipitation/surface) water, rate of evaporation, and chemical composition of rocks present in the aquifer (Gibbs, 1970). In order to assess the groundwater evolution mechanism in and around the PAU campus, the Gibbs ratio I: $Na^+/(Na^+ + Ca^{2+})$ for cations and the Gibb's ratio II: $Cl^-/(Cl^- + HCO_3^-)$ for anions were plotted with respect to TDS in Figure 2a and 2b respectively. The data on the Gibbs diagram suggest that groundwater chemistry is mainly controlled by water-rock interactions, irrespective of well depth, both inside and outside the PAU campus.

Hydro-chemical facies

Piper diagrams (Piper, 1944 and 1953) are used to understand the hydro-chemical patterns and water type, which help in hydro-geochemical classification (Back and Hanshaw, 1965). The piper diagrams for this study, obtained with the Geochemist Workbench software (Bethke and Yeakel, 2012) (Figure 3), is classified in to six hydro-chemical facies based on the dominance of different cations and anions, such as: facies 1: Na^+-Cl^- type (saline), facies 2: Ca^{2+}- HCO_3^- type (temporary hardness), facies 3: Na^+-Ca^{2+}- HCO_3^- type, facies 4: Ca^{2+}-Mg^{2+}- Cl^- type, facies 5: Ca^{2+}- Cl^- type (permanent hardness), and facies 6: Na^+-HCO_3^- type (alkali carbonate). In the study area, most of the samples are Ca-HCO_3 type where the alkaline earth elements ($Ca^{2+}$and Mg^{2+}) exceed the alkalis (Na^+ and K^+), and weak acids (CO_3^{2-} and HCO_3^-) exceed strong acids (Cl^- and SO_4^{2-}).

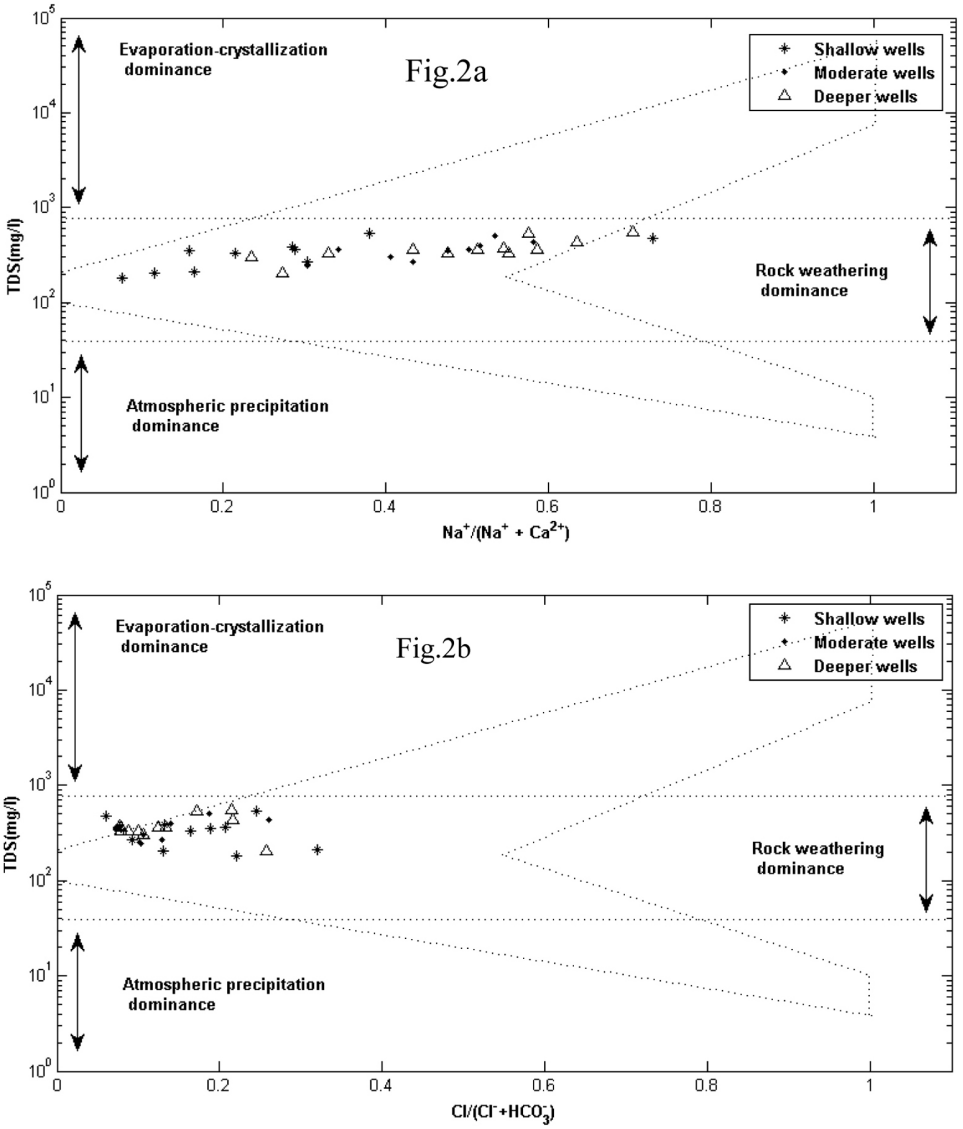

Figure 2. (a) Gibb's diagram1 and (b) Gibb's diagram 2.

Geochemical equilibrium and reactions

The groundwater chemistry of the study area is further investigated by adopting equilibrium thermodynamic approach. $Ca^{2+}$and Mg^{2+} in groundwater are most likely to be supplied by the dissolution of various minerals, such as dolomite, gypsum, calcite, or weathering of silicate minerals (Freeze and Cherry, 1979). Also, if certain minerals, e.g., calcite and dolomite are in equilibrium with groundwater, it is assumed that these minerals can control the groundwater chemical composition (Rajmohan and Elango, 2004; Sonkamble et al., 2013). In this study, Saturation Indices (SI) of calcite, dolomite, and halite were calculated with the help of the GWB software, using the default thermodynamic database to determine the chemical equilibrium in the mineral-water system. The SIs are approximate indicators of equilibrium because of uncertainty in the analytical measurements and the thermodynamic constants used to calculate the equilibrium constants. Deutsch et al., (1982) suggested an SI of ± 5% of the logarithm of the solubility product (log K) of the solid for the probable range of saturation; while, Paces (1972) suggested a broad range of SI of ± 0.5 units from zero for equilibrium or for saturation. With the exception of few samples, all groundwater samples inside and outside campus, irrespective of depth, are super saturated with respect to both calcite and dolomite, and all the samples are under saturated with respect to halite (Table 3). These findings suggest that the carbonate mineral phases are extensively present in the corresponding host rock and the incongruent dissolution of these carbonate minerals

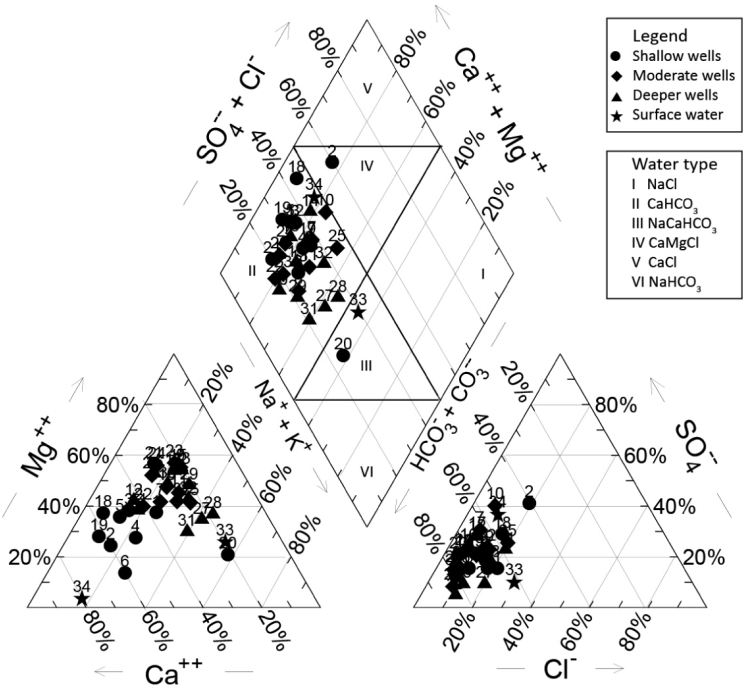

Figure 3. Piper diagram showing water types for samples in the study area.

is among the major controlling process of groundwater chemical constituents in the study area. In addition, because, Ca^{2+} and Mg^{2+} are the dominant cations in the groundwater, this can be explained by the weathering of calcite and dolomite, as expressed by the following reactions:

Calcite : $CaCO_3 + H_2O + CO_2 \leftrightarrow Ca^{2+} + 2\ HCO_3^-$ (1)

Dolomite : $CaMg(CO_3)_2 + 2H_2O + 2\ CO_2 \leftrightarrow Ca^{2+} + Mg^{2+} + 4\ HCO_3^-$ (2)

The relationship between Ca^{2+} and HCO_3^- concentrations is shown in Figure 4. Most of the data points are distributed around the line of calcite and dolomite weathering, which suggests that the weathering reactions for calcite and dolomite mainly account for the Ca^{2+} concentration of the groundwater in the study area.

Ion Exchange

Another significant factor that affects the groundwater chemical constituents is ion exchange (Appelo and Postma 2005). The chloro-alkaline indices CAI-I and CAI-II (hereafter referred as Schoeller indices), can be used to study ion exchange processes (Schoeller 1965, 1967). When there is an exchange of Ca^{2+} or Mg^{2+} in groundwater with Na^+or K^+ in aquifer matrix, both CAI-I and CAI-II are negative, and if there is a reverse ion exchange, both indices are positive. The Schoeller indices are calculated as:

$$CAI - I = \frac{Cl^- - (Na^+ + K^+)}{Cl^-} \quad (3)$$

$$CAI - II = \frac{Cl^- - (Na^+ + K^+)}{HCO_3^- + SO_4^{2-} + CO_3^{2-} + NO_3^-} \quad (4)$$

where all ions are expressed in meq/l.

The calculated values of CAI-I and CAI-II for groundwater samples are presented in Table 3. The results show that all the samples, except two shallow wells (BW2 inside the campus and HP3 outside the campus) have negative Schoeller index values suggesting the possibility of ion exchange of Ca^{2+} or Mg^{2+} in groundwater with Na^+ or K^+ in the aquifer matrix. The calculated Schoeller indices strongly suggest the occurrence of ion exchange process and potentially explain Na^+ and K^+ concentration in the groundwater of the study area.

Groundwater quality evaluation for drinking

The water quality standard for drinking has been specified by WHO and BIS, based on the dissolved ions and toxic trace elements. The behavior of major ions and important physico-chemical parameters and the suitability of groundwater for drinking in the study area are discussed below.

Groundwater of all wells with different depths in our study area showed alkaline nature and could be classified as fresh water as per TDS measurement (TDS <1,000; Freeze and Cherry (1979)) (Table 4). Considering total hardness, groundwater samples are within the safe limit of usage (Table 4).

Table 2. Summary statistics of groundwater and surface water chemical constituents. The WHO (WHO, 1996, 2011) standards for drinking with maximum permissible limit (MPL), and BIS (BIS, 2003) standard for Desirable limit (DL) and MPL are also shown.

Parameter	Groundwater Range	*Mean	Surface water Canal	Pond	WHO MPL	DL	BIS MPL
pH	7.2-8.1	7.7±0.1	7.5	7.4	9.2	6.5-8.5	9.2
Ec (μS/cm)	284-863	550.3±151.7	246	1400	1400	500	1000
TDS (mg/l)	182-552	352.2±97	157	896	1000	-	-
Na^+ (mg/l)	3-98	31.3±21.9	8	116	200	-	-
K^+ (mg/l)	3-9	4.5±1.4	3	105	-	-	-
Ca^{2+} (mg/l)	24-72	35.1±11.8	40	56	200	75	200
Mg^{2+} (mg/l)	10-53	28.1±10.5	1	44	150	30	100
HCO_3^- (mg/l)	73-270	187.6±51.5	70	426	-	-	-
Cl^- (mg/l)	10-50	18.7±11.1	8	120	600	250	1000
SO_4^{2-} (mg/l)	11-75	43.2±16.6	38	54	400	200	400
F^- (mg/l)	0.03-0.94	0.3±0.1	0.12	0.45	1.5	1.0	1.5
NO_3^- (mg/l)	0-17.5	3.7±4.4	0.3	11.5	45	45	45
Cu (mg/l)	0.003-0.017	0.02±0.04	0.004	0.02	2.0	0.05	1.5
Fe (mg/l)	0.07-0.7	0.22±0.16	0.1	0.3	0.3	0.3	1.0
Mn (mg/l)	0-0.1	0.01±0.02	0.01	0.2	0.4	0.1	0.3
Se (mg/l)	0-0.025	0.006±0.006	0	0.004	0.01	0.01	0.01
As (mg/l)	0.001-0.01	0.002±0.002	0.002	0.004	0.01	0.05	0.05
Zn (mg/l)	0.005-1.0	0.12±0.25	0.01	0.03	3	5	15
Cr (mg/l)	0.001-0.007	0.004±0.001	0.002	0.01	0.05	0.05	0.05
Hardness (mg/l $CaCO_3$)	132-320	204±44.5	104	320	500	300	600

*Mean values with standard deviation

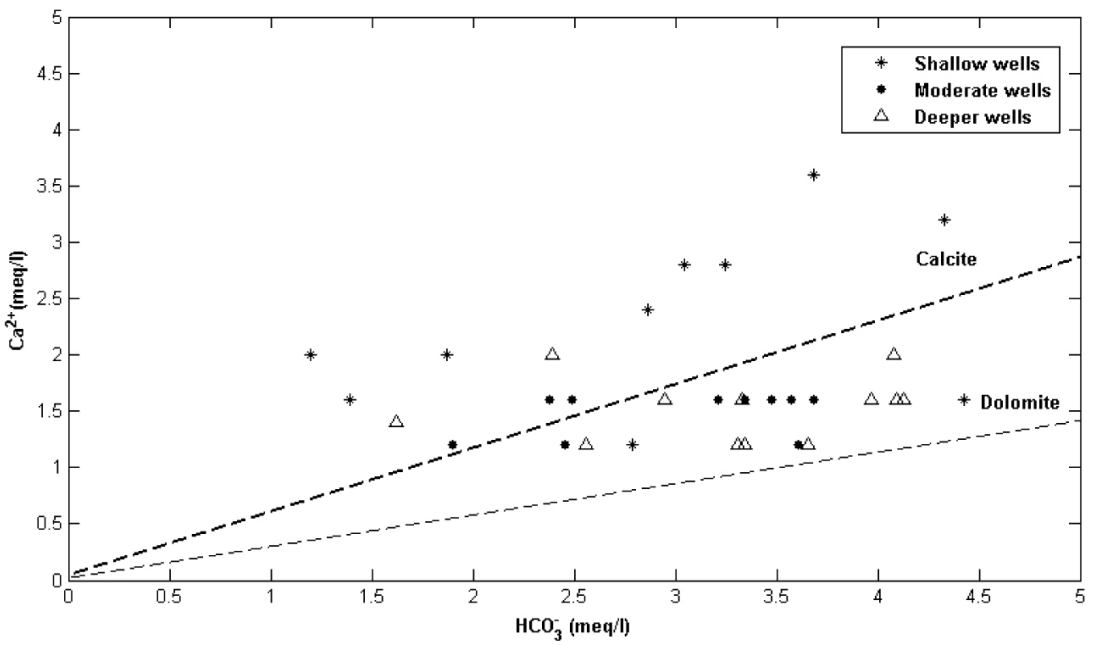

Figure 4. The Ca^{2+} versus HCO_3^- concentration of groundwater for all samples inside and outside campus.

Table 3. Saturation indices of minerals and Schoeller indices for groundwater samples from inside and outside campus.

Mineral	Range of Saturation Indices
Calcite	-0.319 – 0.393
Dolomite	-0.1 – 2.1
Aragonite	-0.48 – 1.5
Halite	-8.4 – -7.0
Schoeller indices	
CAI-I	-14.4 – 0.4
CAI-II	-0.7 – 0.08

Table 4. Suitability of groundwater for drinking based on Total hardness (TH) and dissolved solids (TDS).

Parameter	Remarks	% of groundwater samples
Total hardness (mg/l) as $CaCO_3$ (Sawyer and McCarty 1967)		
< 75	Soft	0
75-150	Moderately Hard	18
150-300	Hard	75
>300	Very Hard	7
TDS (mg/l)		
< 200	Excellent	4
200-500	Good	84
500-1500	Fair	12
>1500	Unsuitable	0

Considering major ions, the dominant ions in the groundwater of the study area are in the order of Ca^{2+}, $Mg^{2+} > Na^{+} > K^{+}$ for cations and $HCO_3^{-} > SO_4^{2-} > Cl^{-}$ for anions. All the samples are well within the drinking water limits considering major ions, except for the well near the dairy farm (TWDF), where the Mg^{2+} was higher than that of the safe drinking water limit.

Nitrate (NO_3^{-}) and Fluoride (F^{-})

While NO_3^{-} is a common nitrogenous compound due to natural processes of the nitrogen cycle, anthropogenic sources have greatly increased the nitrate concentration, particularly in groundwater. Nitrate concentration of groundwater in the study area falls within the safe drinking water range. The highest NO_3^{-} concentration inside campus is found to be 15.5 mg/l for the well near the dairy farm (well no. 9, Table 1 and Figure 1b), which could be due to anthropogenic input from the dairy farm. Our results are consistent with that of Thind and Kansal (2002), who also reported NO_3^{-} concentration in groundwater to be the maximum near the dairy farm inside the campus and minimum near the canal owing to seepage from the canal. Thind and Kansal, (2002) also reported NO_3^{-} concentrations of the deeper wells inside the campus to be less as compared to the shallow wells. However, in this study, no clear distribution of NO_3^{-} is observed for shallow and deeper wells.

All the water samples in the study area exhibit F^{-} within the safe drinking water limit (Table 2).

Trace elements

Bhalla et al., (2011) reported high concentration of trace elements including Cr, Fe and Se in groundwater of Punjab. Also, Singh (1994) reported Cr and CN concentrations exceeding the permissible limit in groundwater of Ludhiana. However, from the present study all the groundwater samples from inside and outside campus are found to be within the safe limit of BIS (2003) with respect to Cu, Fe, Mn, Se, As, Zn and Cr.

Water quality evaluation for irrigation

Quality of irrigation water is an important factor for crop production. Irrespective of the sources of irrigation water, soluble salts are always present, which are mostly Na^{+}, Ca^{2+}, $Mg^{2+}$and sometimes K^{+} as cations, and Cl^{-}, F^{-}, CO_3^{2-}, HCO_3^{-}, and NO_3^{-} as anions. The suitability of ground water for irrigation is generally assessed from its chemical composition along with other factors such

Table 5. Summary statistics of groundwater and surface water for irrigation quality parameters.

Parameter	Groundwater		Surface water	
	Range	*Mean	Canal	Pond
SAR	0.1-3.3	0.94±0.67	0.3	2.8
%Na	7.2-58.0	25.8±11.6	13.9	35.6
KR	0.04-1.34	0.33±0.2	0.1	0.8
SSP (%)	4.6-57.4	22.9.1±11.0	14.3	44.0
PI (%)	42.8-85.7	56.1±8.9	58.4	67.0
RSC (meq/l)	-2.2-1.26	-0.99±0.67	-0.9	0.5
MH	3.9-73.2	55.8±14.0	3.9	56.6
Ca^{2+}/Mg^{2+}	0.3-4.3	0.97±0.8	24.2	0.8

*Mean values with standard deviation

as: type of soil, type of crop, climate and drainage type. The various hazardous categories used for irrigation water quality evaluation in this study are: salinity hazard, sodicity (alkali) hazard and bi-carbonate hazard. KR and MH are also used as criteria to evaluate irrigation water quality. The range with mean and standard deviation calculated for these parameters are presented in Table 5.

Salinity Hazard

Salinity hazard is associated with high soluble salts in water and is measured in terms of TDS or EC. Based on TDS, all the groundwater samples and samples from surface water bodies are suitable for irrigation (TDS < 1500 mg/l)..

Sodicity (alkali) hazard

Irrigation water containing large amounts of Na^+ is of special concern, because increase of Na^+ concentration in irrigation water deteriorates soil quality norms by reducing permeability (Kelley 1951). Sodium hazard is usually expressed in terms of sodium adsorption ratio (SAR), % Na^+ and soluble sodium percent (SSP).

Sodium adsorption ratio (SAR)

The average SAR calculated for the groundwater samples of the study area is 0.9 (Table 5), and it evaluates the sodium hazard in relation to Ca^{2+} and Mg^{2+} concentrations. Water quality is described as excellent for irrigation when the SAR value is less than 10 and termed as unsuitable with a SAR value greater than 26. Accordingly, all the samples including the surface waters are classified as suitable for irrigation.

The United States of Salinity diagram (USSL 1954) can be used for a detailed analysis for suitability of water for irrigation, which uses EC as salinity hazard and SAR as alkalinity hazard. The USSL diagram (Richards 1954) for water samples is presented in Figure 5, which shows that all samples fall in the C2S1 and C3S1 categories. This indicates that all the groundwater and surface water samples are of medium salinity and low sodium. As such, both ground and surface waters can be used in all types of soil for irrigation without the risk of exchangeable Na^+. Thus, the USSL diagram classifies the groundwater and surface water in the study area as good quality for irrigation.

Percent Sodium (% Na^+)

Sodium in irrigation water is generally expressed as % Na^+ and is calculated with respect to the relative proportion of cations present in water as:

$$\% Na^+ = \frac{Na^+ + K^+}{Ca^{2+} + Mg^{2+} + Na^+ + K^+} \times 100 \quad (5)$$

where the quantities of all cations are expressed in meq/l. According to BIS (2003), the maximum Na^+ recommended in irrigation water is 60%. In reference to % Na^+, 37% of groundwater samples are of excellent quality; 53% are of good quality for irrigation, and 10% of groundwater samples are of fair quality. The canal water is also of excellent quality for irrigation based on % Na^+ calculation.

Wilcox (1955) classified groundwater based on % Na^+ and EC for irrigation use. The Wilcox diagram for all the samples is shown in Figure 6. Following the Wilcox diagram, all the water samples are classified as good for irrigation.

Soluble sodium percent (SSP)

SSP is another parameter used to assess suitability of water for irrigation. SSP can be expressed as:

$$SSP = \frac{Na^+}{Ca^{2+} + Mg^{2+} + Na^+} \times 100 \quad (6)$$

where the quantities of all cations are expressed in meq/l. Water with a SSP greater than 50% is unsafe for irrigation (USDA 1954); which may result in sodium accumulation that will cause a breakdown in the soil's physical properties. Based on SSP, all the samples are good quality waters for irrigation, except one shallow groundwater sample from outside campus (well no. 20), which is found to have a SSP of 57%.

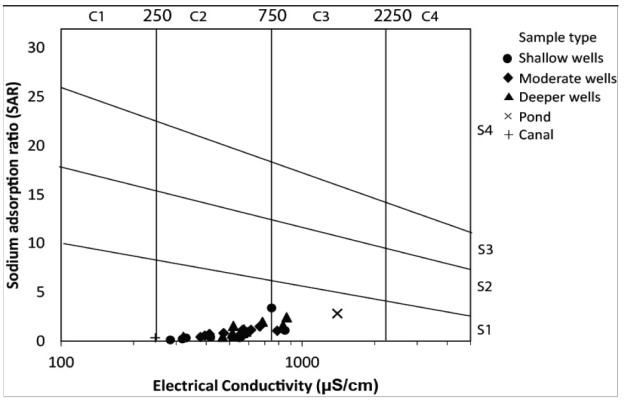

Figure 5. Water classification based on USSL diagram.

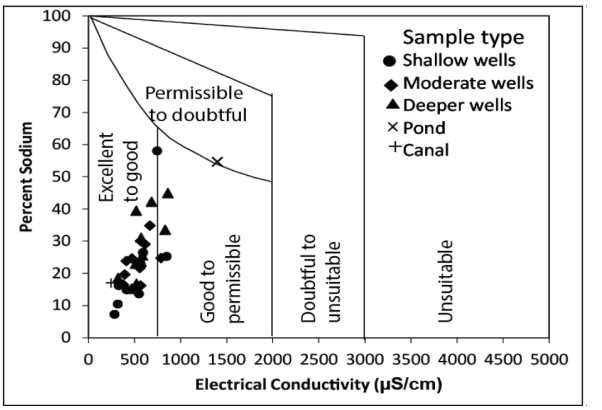

Figure 6. Suitability of groundwater and surface water for irrigation as per the Wilcox diagram.

Bi-carbonate hazard

Water having excess carbonate and bicarbonate over the alkaline earths, mainly calcium and magnesium, affects agriculture unfavorably (Eaton 1950; Richards 1954). RSC is an indirect expression for CO_3^{2-} and HCO_3^- of Na^+ in groundwater, which can be expressed as:

$$RSC = \left(HCO_3^- + CO_3^{2-}\right) - \left(Ca^{2+} + Mg^{2+}\right) \quad (7)$$

where the quantities of all cations and anions are expressed in meq/l.

Water with RSC <1.25 are considered to be safe for irrigation, whereas water with RSC >2.5 are considered unsuitable for irrigation. The negative RSC values (Table 5) indicate that the alkaline earths (Ca^{2+} and Mg^{2+}) are in excess and Na^+ buildup in the soil is unlikely, if irrigated with this water. RSC values for all the water samples studied are less than 1.25, which suggests that water in the entire study area is safe for irrigation.

Permeability Index (PI)

The permeability of soil is affected by the long term use of irrigation water as it is influenced by Na^+, Ca^{2+}, Mg^{2+} and HCO_3^- content of the soil (Ramesh and Elango 2012). Doneen (1966) proposed a criterion for evaluating the suitability of groundwater based on permeability index (PI), which can be evaluated as (Ragunath 1987):

$$PI = \frac{Na^+ + \sqrt{HCO_3^-}}{Ca^{2+} + Mg^{2+} + Na^+} \times 100 \quad (8)$$

where the quantities of all cations and anions are expressed in meq/l.

Based on PI, water is classified as excellent (PI >75%), good (PI in the range of 25-75%) and unsuitable (PI <25%) for irrigation. In the study area, all the samples, except well no. 20 fall in the class II category (PI value of 25-75%) in the Doneen chart (Domenico and Schwartz 1990), which suggests the suitability of groundwater and canal water for irrigation.

Kelley's Ratio (KR)

The sodium problem in water for irrigation can be expressed in terms of KR, which can be calculated as (Kelley 1940; Paliwal 1967):

$$KR = \frac{Na^+}{Ca^{2+} + Mg^{2+}} \quad (9)$$

where the cations are in meq/l.

KR values of less than 1 are found to be suitable for irrigation, whereas, KR of more than 1 indicates an excess of Na^+ in water, and hence are unsuitable for irrigation. In the study area, all the samples, except well no. 20, are safe for irrigation according to the values of KR.

Magnesium Hazard (MH)

Excess of magnesium affects the quality of soil, which is the cause for poor yield of crops. MH value for irrigation water can be expressed as (Szabolcs and Darab1964):

$$MH = \frac{Mg^{2+}}{\left(Ca^{2+} + Mg^{2+}\right)} \times 100 \quad (10)$$

where all the cations are in meq/l.

Water with MH values > 50% are unsuitable for irrigation. In the study area, MH for the groundwater samples ranges from 3.9 to 73.2 with an average of 55.8 (Table 5). 37% of groundwater samples and the canal water in the study area are found to be safe for irrigation (MH < 50); whereas, 63% of groundwater samples and the pond water are unsuitable for irrigation (MH >50). Groundwater samples with MH >50% are mostly from moderate to deeper level (Tables 1 and 5). Irrigating with water having MH > 50% may cause adverse effect on the agricultural yield. However, with an average MH of nearly 50% may indicate moderate quality water for irrigation. High magnesium concentration observed in the study area could be from anthropogenic sources.

In order to further evaluate the magnesium hazard for irrigation water, the ratio of Ca^{2+}/Mg^{2+} can be considered as a criterion (Ayers and Westcot, 1985). When the ratio Ca^{2+}/Mg^{2+} is < 1 in the irrigation water, the potential

effect of Na^+ may be slightly increased. The suitability of groundwater and surface water in the study area based on Ca^{2+}/Mg^{2+} ratio exhibits the same behavior as that of MH (Table 5).

CONCLUSION

The suitability of groundwater for domestic and agricultural uses is evaluated inside the PAU campus and surrounding area, based on the physico-chemical properties of groundwater. Concentration of major ions, both inside and outside the PAU campus are in the order of Ca^{2+}, $Mg^{2+} > Na^+ > K^+$ for cations and $HCO_3^- > SO_4^{2-} > Cl^-$ for anions. Water rock interaction is the dominant mechanism controlling the groundwater chemistry. Calcite and dolomite are found to be saturated in groundwater, whereas halite and gypsum are unsaturated. Mineral weathering along with ion exchange, control the groundwater chemistry of the study area. Based on major ion and trace element concentrations, groundwater samples fall within the permissible limit of WHO and BIS, and are found to be safe for drinking and domestic applications. In terms of irrigation water quality parameters, such as dissolved solids, SAR, % Na^+, RSC, PI, and KR, all the groundwater samples except one shallow well (well no. 20), are found suitable for irrigation for most of the soil types. Considering magnesium hazard, however, 63% of the groundwater samples have a MH value of >50%, which may restrict the use of this water for irrigation. The canal water is found to be of excellent quality for irrigation based on all the irrigation quality parameters.

ACKNOWLEDGEMENTS

We are thankful to Director, CSIR-National Geophysical Research Institute, Hyderabad, India for giving permission to publish the paper. The first author sincerely acknowledges Prof. T. Tokunaga for hosting the PhD, and The University of Tokyo for providing TODAI Fellowship. Thanks are due to valuable suggestions made by the two reviewers; Prof. B. Venkateswara Rao and Dr. M.R.K. Prabhakara Rao. We express our gratitude to Chief Editor Dr. P.R. Reddy for his encouragement and apt editing.

REFERENCES

Appelo, C.A.J., and Postma, D., 2005. Geochemistry, groundwater and pollution (2nd ed.), A.A Balkema, Amsterdam.

Ayers, R.S., and Westcot, D.W., 1985. Water quality for agriculture. FAO Irrigation and Drainage, U.N. Food and Agriculture Organization, Rome, v.29, no.1.

Back, W., and Hanshaw, B.B., 1965. Chemical geohydrology (Chow VT ed.). Advances in hydroscience, 2, Academic Press, New York.

Bethke, C.M., and Yeakel, S., 2012. Geochemist workbench, Version 9.0. Essentials guide, Aqueous Solutions, LLC, Champaign, Illinois.

Bhalla, A., Singh, G., Kumar, S., Shahil, J.S., and Mehta, D., 2011. Elemental analysis of ground water from different regions of Punjab state (India) using EDXRF technique and the sources of water contamination. International Conference on Environmental and Computer Science, v.19.

BIS., 2003. Bureau of Indian Standards Specification for drinking water. IS: 10500:91. Revised 2003, Bureau of Indian Standards, New Delhi.

CGWB, 2007. Groundwater information booklet. Ludhiana district, Punjab.

Chaudhary, V., Singh, K.P., Jacks, G., and Bhattacharya, P., 2001. Groundwater contamination at Ludhiana, Punjab, India. Journal of Indian Works Association, l, XXXIII, 3, pp: 251-261.

CPCB, 2007. Status of groundwater quality in India- Part-I. Groundwater quality series: GWQS/ 09/2006-2007.

Deutsch, W.J., Jenne, E.A., and Krupka, K.M., 1982. Solubility equilibria in basalt aquifers: The Columbia Plateau, eastern Washington, U.S.A. Chem. Geol., v.36, pp: 15-34.

Domenico, P.A., and Schwartz, F.W., 1990. Physical and chemical hydrogeology. New York, Wiley.

Doneen, L.D., 1966. Water quality requirement for agriculture. Proceedings of The National Symposium on Quality Standards for Natural Waters, University of Michigan, Ann Arbor, pp: 213-218.

Eaton, F.M., 1950. Significance of carbonate in irrigation waters. Soil Sci., v.69, pp: 123-133.

Freeze, R.A., and Cherry, J.A., 1979. Groundwater. Englewood Cliffs: Prentice Hall.

Garg, S., Singla, C., and Aggarwal, R., 2015. Evaluation of groundwater quality using contamination index in Ludhiana, Punjab (India). Jour. Ind. Pollut. Cont., v.31, no.1, pp: 33-39.

Gibbs, R.J., 1970. Mechanisms controlling world water chemistry. Science, v.170, pp: 1088-1090.

Gupta, S., 2010. Ground Water Management in Alluvial Areas. CGWB, New Delhi, India.

Jain, A.K., and Kumar, R., 2007. Water management issues – Punjab, North-West India. Indo-US Workshop on Innovative E-technologies for Distance Education and Extension/ Outreach for Efficient Water Management, Patancheru / Hyderabad, Andhra Pradesh, India.

Kelley, W.P., 1951. Alkali Soils: their formation properties and reclamations. Reinhold, New York.

Kelley, W.P., 1940. Permissible composition and concentration of irrigation water. Proceedings of American Society of Civil Engineers, v.66, pp: 607-613.

Paces, T., 1972. Chemical characteristics and equilibrium in natural water-felsic rock-CO_2 systems. Geochem. Cosmochim. Acta., v.36, pp: 217-240.

Paliwal, K.V., 1967. Effect of gypsum application on the quality of irrigation waters. The Madras Agricultural Journal., v.59, pp: 646-647.

Piper, A.M., 1944. A graphic procedure in the geochemical interpretation of water analyses. Transactions, American Geophysical Union, v.25, no.6, pp: 914-928.

Piper, A.M., 1953. A graphic procedure in the chemical interpretation of water analysis. US Geological Survey, Groundwater Note 12.

Ragunath, H.M., 1987. Groundwater. Wiley Eastern, New Delhi.

Rajmohan, N., and Elango, L., 2004. Identification and evolution of hydrogeochemical processes in the groundwater environment in an area of the Palar and Cheyyar River Basins, Southern India. Environ. Geol., v.46, pp: 47-61.

Ramesh, K., and Elango, L., 2012. Groundwater quality and its suitability for domestic and agricultural use in Tondiar river basin, Tamil Nadu, India. Environ. Monit. Assess., v.184, pp: 3887-3899.

Richards, L.A., 1954. Diagnosis and improvement of saline alkali soils. US Department of Agriculture, Hand Book, 60.

Schoeller, H., 1965. Qualitative evaluation of groundwater resources. Methods and techniques of ground-water investigations and development, UNESCO, pp: 54-83.

Schoeller, H., 1967. Geochemistry of groundwater. An international guide for research and practice, UNESCO, v.15, pp: 1-18.

Singh, G., Singh, D.D., and Sharma, S.K., 2013. Effect of polluted surface water on groundwater: A case study of Budha Nullah. IOSR Jour. Mechanical. Civil. Eng. v.5, no.5, pp: 1-8.

Singh, K.P., 1994. Temporal changes in the chemical quality of groundwater in Ludhiana area, Punjab, India. Curr. Sci., v.66, no.5, pp: 375-378.

Sonkamble, S., Chandra, S., Ahmed, S., and Rangarajan, R., 2013. Source speciation resolving hydrochemical complexity of coastal aquifers – a case study near Cuddalore, Tamil Nadu, India. Marine Pollution Bulletin, M.S. MPB-D-13-00728.

Szabolcs, I., and Darab, C., 1964. The influence of irrigation water of high sodium carbonate content of soils. Proceed. 8th Int. Cong. of ISSS, Trans, II, pp: 803-812.

Thind, H.S., and Kansal, B.D., 2002. Nitrate contamination of groundwater under different anthropogenic activities. 17th WCSS, Thailand.

Tiwari, V.M., Wahr, J., and Swenson, S., 2009. Dwindling groundwater resources in northern India, from satellite gravity observations, Geophys. Res. Lett., doi:10.1029/2009GL039401., v.36.

USDA, 1954. Diagnosis and improvement of saline and alkali soils. U.S. Salinity laboratory staff, Govt. Printing office, Washington DC.

USSL, 1954. Diagnosis and improvement of saline and alkali soils. USDA Agriculture Handbook, 60, Washington DC.

WHO, 1996. Guidelines to drinking water quality. World Health Organization, Geneva 2:989.

WHO, (World Health Organization) 2011. Guidelines for drinking water quality: Fourth edition. ISBN 978 92 4 154815 1.

Wilcox, L.V., 1955. Classification and use of irrigation waters. USDA Circular, 696, Washington DC.

Received on: 17.2.17; Revised on: 17.4.17; Accepted on 18.4.17

*"I didn't like to stop playing for a second to bother with eating or going to the bathroom. I was a really skinny kid, and I remember my mother always telling people, 'I don't know how she's alive. I think she gets all of her nutrients from air pollution."- Tig Notaro -An American Actress

***

*"Carpooling is important for urban density, air pollution and other reasons, but carpooling is not the kind of thing that actually changes the energy equation."- Clay Shirky - American writer, consultant and teacher

***

* "The Chinese have figured out that they have a giant environmental problem. Folks in Beijing, some days, literally can't breathe. Over a million Chinese die prematurely every year because of air pollution".- Joe Biden- 47th Vice President of the United States

***

*"Sooner or later, we will have to recognise that the Earth has rights, too, to live without pollution. What mankind must know is that human beings cannot live without Mother Earth, but the planet can live without humans." - Evo Morales - Bolivian politician and 80th President of Bolivia

***

*"I'd never felt afraid of pollution before and never wore a mask no matter where. But when you carry a life in you, what she breathes eats and drinks are all your responsibility; then you feel the fear." - Chai Jing - Chinese journalist and environmental activist.

***

*"We already have the statistics for the future: the growth percentages of pollution, overpopulation, desertification. The future is already in place."- Gunter Grass- German novelist and recipient of the 1999 Nobel Prize in Literature

J. Ind. Geophys. Union (July 2017)
v.21, no.4, pp: 271-276

A Hybrid Prediction Algorithm using Naive Bayes Classifier for Improving Accuracy in Classifying LISS III Data

Kalyan Netti*[1] and Y.Radhika[2]

[1]CSIR-National Geophysical Research Institute, Uppal Road, Hyderabad
[2]Associate Professor, CSE Dept., GITAM University, Visakhapatnam
*Corresponding Author: nettikalyan@gmail.com

ABSTRACT

We propose a hybrid model for improving the accuracy in classifying LISS III Data using Naïve Bayes Classifier. The assumption of Conditional Independence among the predictors is one of the main reasons for loss of accuracy in Naïve Bayes Classifier. The effect of conditional independence on the accuracy varies on the data chosen for analysis. As there are cases where the predictor-outcome has become null, ignoring such results is not advisable as the outcome may affect the accuracy. In this paper, remote sensing data for Land use/Land cover is used as an input to the algorithm for classification. The Linear Imaging Self Scanning Sensor (LISS-III) data of Resourcesat-2 satellite has been used for this study. The Naive Bayes algorithm has been applied to the data, and the results are compared with the standard classification methods such as Maximum likelihood classifier and Mahalanobis classifier. The result of the study shows Naive Bayes classification performs better compared to conventional classifiers such as Maximum likelihood classifier and Mahalanobis classifier.

Key words: Hybrid prediction algorithm**,** Naive Bayes Classifier, Conditional Independence, Supervised Classification, Maximum likelihood classifier, Mahalanobis classifier.

INTRODUCTION

In Data Mining, classification is one of the best techniques available to predict outcomes in data sets. Naïve Bayes Classifier, a traditional supervised classification method, is one such classification techniques used to predict outcomes. In general, Naïve Bayes Classifier performs well when compared to other classifiers due to its simplicity, less computational complexity, less memory requirement and good prediction accuracy (Han et al., 2011; Wang et al., 2014). The better performance of Naive Bayes Classifier is attributed to the assumption of independence among predictors. This hypothesis sometimes leads to loss of accuracy in NBC. This loss can be more when data sets for classification has strong inter-relation among attributes. Thus, improving Naive Bayes classifier with the assumption of Independence among predictors is a challenging task (Wilson et al., 2009; Xi-Zhao et al., 2014). The primary goal of a Classifier is to predict the class value accurately for each instance in a given data set (Han et al., 2011; Haleem et al., 2014). In this paper the authors present a model using Naïve Bayes Classifier to estimate accuracy in LIS-III data for estimating accuracy of various factors associated with Forest cover, area specific water body dynamics, Wasteland status with time, Vegetation cover, Fallow and Built-up land particulars. The main aim of this paper is to show that the accuracy estimation using Naïve Bayes Classifier is better compared to Maximum Likelihood Classifier and Mahalanobis Classifier.

Many researchers have demonstrated that supervised classification is a proven technique for automatic generation of land cover maps (Richards, 1993; Benediktsson et al., 1990; Bruzzone et al., 1999; Bruzzone and Fernández Prieto 1999; Bruzzone, 2000). In supervised classification, analyst supervises the pixel categorization process by specifying the various land cover types present in a scene to the computer algorithm. Supervised classification procedures require substantial interaction with the analyst, who must guide the computer by identifying areas in the image that are known prior to the classification, which belongs to particular land use land cover classes. These areas are referred as training sites. The training sites are known identities, which are used to classify pixels of unknown. The locations of the training site pixels must stem from ground truth or higher quality maps or data sets. The computer uses the spectral characteristics of the training pixels to identify other unknown pixels in the image with similar characteristics (Richards, 1993). The quality of these training pixels decides mostly the success of supervised classification method. Parallelepiped, Maximum Likelihood, Minimum Distance and Mahalanobis Distance are the important classifier methods used widely (Khalid and Shakil, 2014; Zhu et al., 2006).

Maximum Likelihood classification assumes that Statistics for each Class belonging to each band is distributed normally and calculates the probability whether a given pixel belongs to a particular class or not. Each pixel is assigned to the class that has the highest probability. If

the highest probability is less than a threshold, the pixel remains unclassified. (Bruzzone, 2000)

The Mahalanobis distance classification is a direction-sensitive distance classifier that uses statistics of each class. It is similar to the maximum likelihood classification. However,as it assumes that all class covariances are equal it is realistically classified as a faster method. All pixels are classified to the closest Region of Interest (ROI) class unless distance threshold is not specified.In such cases, some pixels may be unclassified as they do not meet the threshold.

Specific study particulars, results and conclusions are structured in the manuscript as per section wise details. Section-II explains Naïve Bayes Classifier, Section –III presents Implementation and Section-IV explains Data considered in this paper. Results are presented in Section-V and Section-VI offers conclusions.

Naive Bayes Classifier

Naïve Bayes Classifier, a supervised classification technique based on Bayes' Theorem, is used to predict the class from the attributes of a data set (Han et al., 2011; Dunham, 2006). Bayesian Classifier is stated at (1)

$$P(C|X) = \frac{P(X|C)P(C)}{P(X)} \quad (1)$$

Where, the posterior probability, *P(C/X)* (the probability of a attribute value X belonging to a class C), is calculated using Class Prior Probability *P(C)* (probability of class), Predictor Prior Probability *P(X)* (probability of attribute value) and Likelihood *P(X/C)* (probability of attribute value X given class C).

In Naïve Bayes Classifier, the assumption that the probabilities of each attribute with respect to a class are independent of all other attribute values is found to be apt. This assumption is made to basically simplify the calculation of probabilities. This assumption is called as Conditional Independence (Srisuan and Hanskunatai 2014; Domingos and Pazzani, 1996). It is explained, in this scenario as: the predictor (X) value of class (C) has little effect on the predictor's values of the other.This inturn leads to the loss of accuracy.

The proposed new method considers numerical attributes as input, and the values are Gaussian distributed. For Gaussian distribution mean and standard deviation need to be computed; the Gaussian distribution function is stated at (2).

$$P(X_j|C = c_i) = \frac{1}{\sqrt{2\pi}\sigma_{ji}} exp\left(-\frac{(X_j - \mu_{ji})^2}{2\sigma_{ji}^2}\right) \quad (2)$$

μ_{ji} : Mean (average) of feature values x_j of examples for which $c=c_i$

σ_{ji} : Standard deviation of feature values x_j of examples for which $c=c_i$

Accuracy Assessment

The accuracy assessment of classification technique was carried out using confusion matrix. The confusion matrix was plotted with respect to the reference and predicted classes of three classifications. The confusion matrix compares the pixel classified by the classification method against the same site in the field. In confusion matrix, diagonals represent sites that are classified correctly according to the reference data. Off-diagonals are misclassified. The result of the confusion matrix provides the overall accuracy of the each class map. The overall accuracy of the classification is the ratio of the sum of correctly classified pixel to the total number of pixel (Overall Accuracy= No. of Correct Plots / Total No.of plots). However, the problem with overall accuracy is that it does not reveal if (any) error was evenly distributed among classes or not. For example,if some classes are null and others are excellent, the performance of a classification method is measured based on user and producer accuracy.

The producer's accuracy is derived by dividing the number of correct pixels in a particular class divided by the total number of pixels as derived from reference data. It means, the producer's accuracy measure for a given class in reference plots is based on how many pixels on the map are labeled correctly. It includes the error of omission, which refers to the proportion of observed features on the ground that is not classified in the map.

User accuracy measures for a given class are defined based on how many of the pixels on the map are rightly classified. The user's accuracy measures the commission error and indicates the probability that a pixel classified into a given category represents that group on ground.

Producer's Accuracy (%) = 100% - error of omission (%)
User's accuracy (%) = 100% - error of commission (%)

For a given class in reference plots, how many of the pixels on the map are labeled correctly

DATA

Study Area

The study area covers Nagpur and surrounding region (Maharashtra; India) centered at 21°22'N/78°59'E.The study area is one of the worst drought affected areas.

Resourcesat-2 LISS III

ResourceSat-2 carries three electro-optical cameras such as LISS-III, LISS-IV, and AWiFS. Resourcesat-2 provides continuity and increases the observation timeliness (repetitive) in tandem with ResourceSat-1. The Resourcesat data is very useful for agricultural crop discrimination and monitoring, crop acreage/yield estimation, precision farming, water resources, forest mapping, rural infrastructure development, disaster management. In the present study, we have used LISS III data. The Linear Imaging Self Scanning Sensor (LISS-III) is a multi-spectral camera operating in four spectral bands, three in the visible and near to infrared and one in the SWIR region, as in the case of IRS-1C/1D. LISS III sensor has the following configuration (Table 1) with resolution of 24m.

Table 1. LISS III sensor configuration.

Bands	Wavelength (μm)
B2 - Green	0.52 - 0.59
B3 - Red	0.62 - 0.68
B4 - NIR	0.77 - 0.86
B5 - SWIR	1.55 - 1.70

Conversion of Radiance from Digital number

The image acquired is recorded as digital numbers. To convert back to the original object reflectance values, the DN values are processed using Equation-1. It needs the maximum and minimum radiance value for each band, which is unique for each sensor. This information is provided with the header file of the image.

$$L_{rad} = (DN / MaxGray) * (L_{max} - L_{min}) + L_{min} \quad (3)$$

L_{rad}: Radiance for a given DN value (Table 2), DN: Digital count, MaxGray: 255
L_{min} / L_{max}: Minimum/ Maximum radiance value for a given band available in the header file of the image

Table 2. Conversion table for DN to radiance for LISS-III.

Satellite Image	Band	L_{min}	L_{max}
IRS – 1C	band1 band1 band1	1.76 1.54 1.09	14.4500 17.0300 17.1900

RESULTS AND DISCUSSION

The results of the three classifiers, the proposed model using Naive Bayes, MXL, Mahanoblis are shown in Tables 3, 4, 5. Figure 1 shows the data used for the study i.e., Resoursesat-2 LISS III & figures 2, 3, 4 show the output when classified using Naive Bayes, MXL and Mahanoblis. The proposed model using Naive Bayes classifier produces output with the user accuracy of 0.91,1.0, 0.80, 0.81, 0.82, 0.77 for Forest,Water body, Wasteland, Vegetation,

Table 3. Confusion matrix of Naive Bayes classification.

Naive Bayes	Forest	Water body	Waste land	Vegetation	Fallow	Built-up	Total	User accuracy
Forest	1217	0	0	106	0	2	1325	0.918
Water body	0	169	0	0	0	0	169	1
Wasteland	0	0	179	23	0	21	223	0.802
Vegetation	314	0	0	1452	7	6	1779	0.816
Fallow	1	2	3	34	640	97	777	0.823
Built-up	0	0	25	2	153	612	792	0.772
	1532	171	207	1617	800	738	5065	
Producer accuracy	0.794	0.988	0.864	0.897	0.8	0.82		

Table 4. Confusion matrix of MXL Classification.

MXL	Forest	Water body	Waste land	Vegetation	Fallow	Built-up	Total	User accuracy
Forest	1169	0	0	263	0	0	1432	0.816
Water body	0	171	0	0	5	8	184	0.929
Wasteland	20	0	168	51	3	21	263	0.638
Vegetation	341	0	0	1194	3	3	1541	0.774
Fallow	2	0	2	104	625	67	800	0.781
Built-up	0	0	37	5	164	639	845	0.756
	1532	171	207	1617	800	738	5065	
Producer accuracy	0.763	1	0.811	0.738	0.781	0.86		

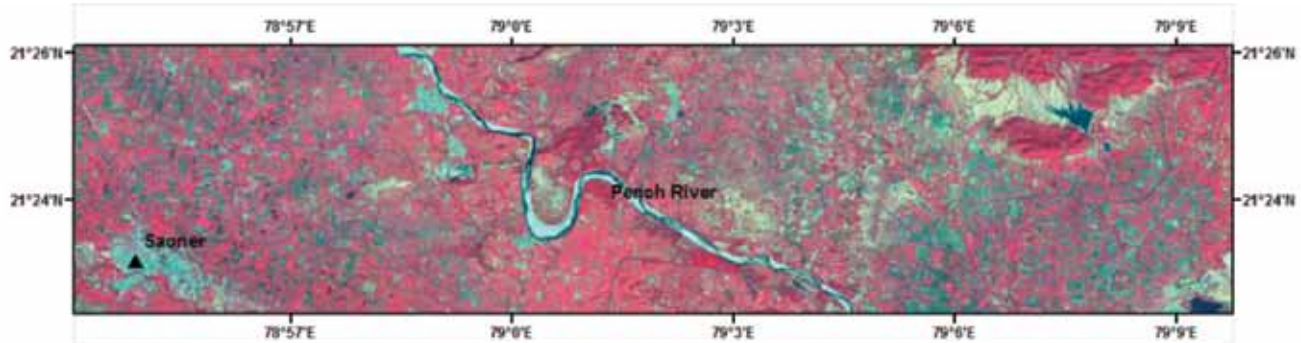

Figure 1. Resoursesat-2 LISS III data.

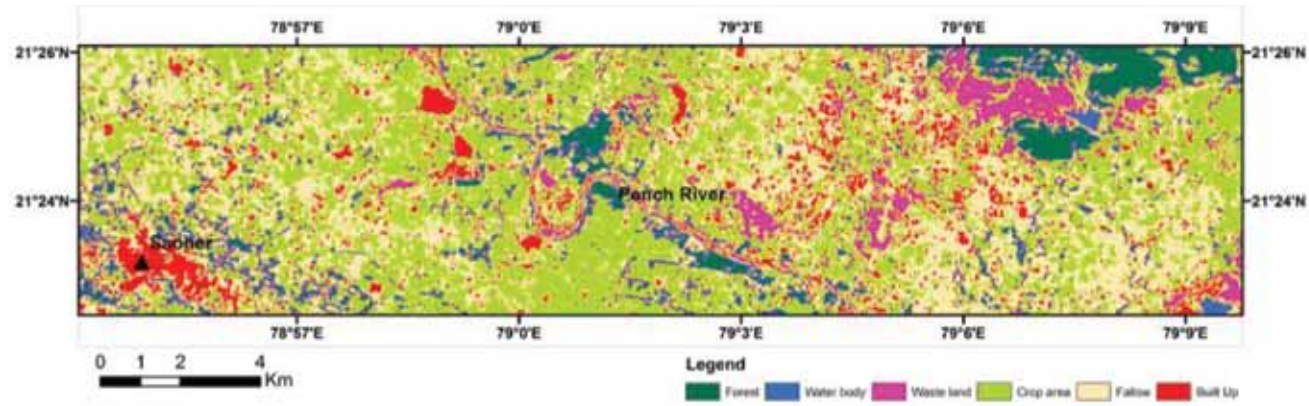

Figure 2. Propsed model using Naïve Bayes Classifier Output.

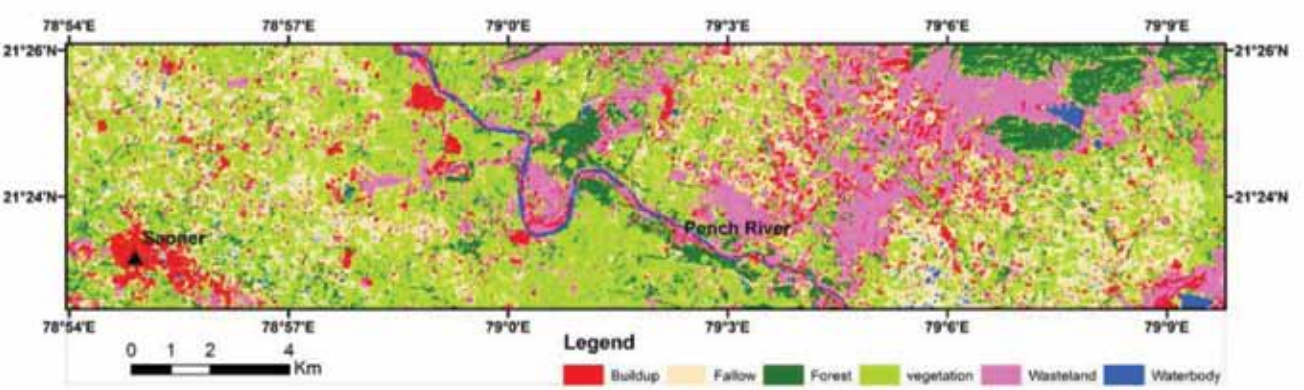

Figure 3. MXL classification Output.

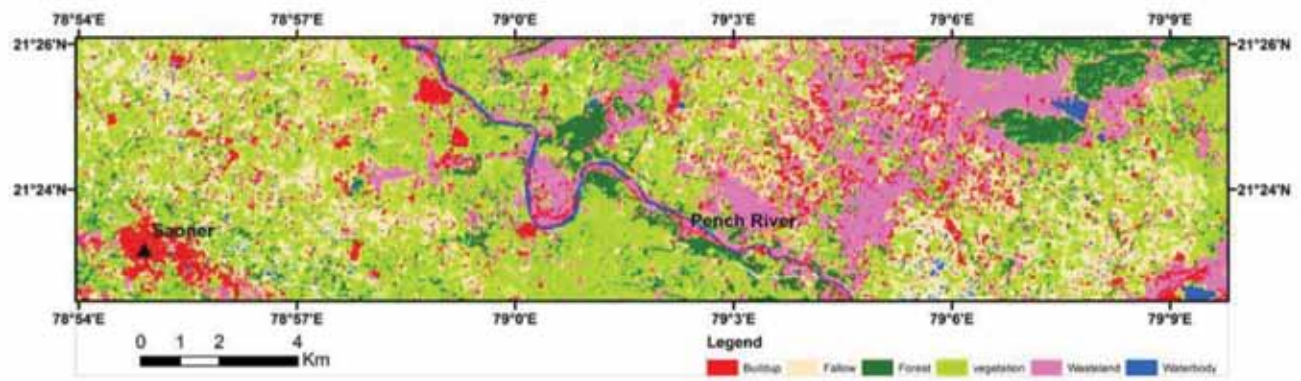

Figure 4. Mahalanobis classification Output.

Table 5. Confusion matrix of Mahanoblis Classification.

Mahanoblis	Forest	Water body	Waste land	Vegetation	Fallow	Built-up	Total	User accuracy
Forest	1169	0	0	250	0	0	1419	0.823
Water body	0	171	0	0	5	6	182	0.939
Wasteland	21	0	166	51	3	19	260	0.638
Vegetation	340	0	0	1198	7	3	1548	0.773
Fallow	2	0	2	113	624	62	803	0.777
Built-up	0	0	39	5	161	648	853	0.759
	1532	171	207	1617	800	738	5065	
Producer accuracy	0.76	1	0.801	0.740	0.78	0.87		

Table 6. User accuracy comparison.

	Proposed Algorithm using NBC	Mahanoblis	MXL
Forest	0.918	0.823	0.816
Water body	1	0.939	0.929
Wasteland	0.802	0.638	0.638
Vegetation	0.816	0.773	0.774
Fallow	0.823	0.777	0.781
Built-up	0.772	0.759	0.756

Fallow and Built-up area, respectively. For the same class, producer accuracy of Naive Bayes is 0.79, 0.98, 0.86, 0.89, 0.80 & 0.82 (Table 3). The user and producer accuracy of MXL classifier are 0.81, 0.92, 0.63, 0.77, 0.78, 0.75 & 0.76, 1.0, 0.81, 0.73, 0.78, 0.86 for Forest, Water body, Wasteland, Vegetation, Fallow, Built-up area, respectively (Table 4). The user and producer accuracy of Mahanoblis are almost same as the MXL (Table 5). The comparison of the three classifiers shows (Table 6) that the accuracy of the proposed algorithm is better when compared with the accuracies of MXL and Mahanoblis (Table 6). For example the user accuracy of Wasteland is 0.802 using the proposed algorithm, whereas the user accuracy is 0.638 for MXL and Mahanoblis. The accuracies for Forest, Water body, Fallow, Vegetation, Built-up area are also better for the proposed algorithm (Table 6). The results indicates that the accuracy has significantly improved by using NBC even with the assumption of Conditional Independence.

CONCLUSION

One of the reasons for loss of accuracy in Naïve Bayes Classifier is Conditional Independence. The Hybrid model proposed in this paper has better accuracy with the assumption of Conditional Independence when applied on LISIII data. The results show that the method used in this article has the highest prediction accuracy when compared with standard classification methods such as Maximum likelihood classifier, Mahalanobis classifier. The conclusion, based on the experimental results is that accuracy of Naïve Bayes classifier can be improved even with the assumption of Conditional Independence. Based on the experimental results, we can assert that addressing the loss of accuracy in Naïve Bayes Classifier due to Conditional Independence proved advantageous for better analysis of data.The proposed model has improved the accuracy when applied on a complex data with more number of attributes in a given data. Our future work includes observing the impact of the complex data on the performance of the proposed model and exploring the possibility of cleaning the data before applying Naïve Bayes Classifier for further improvement of accuracy.

ACKNOWLEDGEMENTS

Authors want to sincerely thank Director, CSIR-NGRI for permitting them to carry out this study and allowing its publication in JIGU. Our thanks are due to Prof.A.D.Sarma for critically evaluating the manuscript and for useful suggestions. We are grateful to Chief editor for his support to our research endeavours and for apt editing.

Compliance with Ethical Standards

The authors declare that they have no conflict of interest and adhere to copyright norms.

REFERENCES

Benediktsson, J.A., Swain, P.H., and Ersoy, O.K., 1990. Neural Networks:Approaches versus statistical methods in classification of multisource remote sensing data,IEEE Trans. Geosci. Remote Sensing, v.28, pp: 540-552.

Bruzzone, L., 2000. An approach to feature selection and classification of remote sensing images based on the Bayes rule for minimum cost. IEEE Trans. Geosci. Remote Sensing, v.38, pp: 429-438.

Bruzzone, L., and Fernández Prieto, D., 1999. A Technique for the selection of kernel function parameters in RBF neural networks for classification of remote-sensing images, IEEE Trans. Geosci. Remote Sensing, v.37, pp: 1179-1184.

Bruzzone, L., Fernández Prieto, D., and Serpico, S.B., 1999. A neural statistical approach to multi-temporal and multisource remotesensing image classification. IEEE Trans. Geosci. Remote Sensing, v.37, pp: 1350-1359.

Domingos, P., and Pazzani, M., 1996. Beyond Independence: Conditions for the Optimality of the Simple Bayesian Classifier. Proceedings of International Conference of Machine Learning, pp: 105-112.

Dunham, M.H., 2006. Data Mining: Introductory and advanced topics. Pearson Education India.

Haleem, H., Sharma, P.K., and Sufyan Beg, M.M., 2014. Novel frequent sequential patterns based probabilistic model for effective classification of web documents. In Computer and Communication Technology (ICCCT), 2014 International Conference on IEEE., pp: 361-371.

Han, J., Kamber, M., and Pei, J., 2011. Data mining: concepts and techniques. Elsevier.

Khalid Omar Murtaza, and Shakil A. Romshoo, 2014. Determining the Suitability and Accuracy of Various statistical Algorithms for Satellite Data Classification. International journal of geomatics and geosciences, pp: 585-599.

Richards, J.A., 1993. Remote Sensing Digital Image Analysis, 2nd ed. New York: Springer-Verlag.

Srisuan, J., and Hanskunatai, A., 2014. The Ensemble of Naïve Bayes classifiers for hotel searching. In Computer Science and Engineering Conference (ICSEC), 2014 International, IEEE., pp: 168-173.

Wang, X.Z., He, Y.L., and Wang, D.D., 2014. Non-naive Bayesian classifiers for classification problems with continuous attributes.Cybernetics, IEEE Transactions on, v.44, no.1, pp: 21-39.

Wilson, M.L., 2009. Exploring heterogeneous datasets from different searcher perspectives.

Xi-Zhao Wang,Yu-Lin He and Debby D.Wang., 2014. Non-Naïve Bayesian Classifiers for Classification Problems with Continous Attributes. IEEE Transactions on Cybernetics, v.44.

Zhu, G.B., Liu, X.L., and Jia, Z.G., 2006. A multi-resolution hierarchy classification study compared with conservative methods, ISPRS Workshop on Multiple representation and interoperability of spatial data, pp: 79-84.

Received on: 9.1.17; Revised on: 10.2.17; Re-revised on: 24.3.17; Accepted on: 26.3.17

*“Twenty years from now,
You will be more disappointed
By the things you didn’t do,
Than by the ones you did
So
Throw off the bowlines,
Sail away from the safe harbour,
Catch the tradewinds in your sails,
DREAM
EXPLORE
DISCOVER”
Scott J. Fitzgerald – one of the greatest American writers of the 20th century.

J. Ind. Geophys. Union (July 2017)
v.21, no.4, pp: 277-284

A complete chaotic analysis on daily mean surface air temperature and humidity data of Chennai

A. Antony suresh* and R. Samuel Selvaraj
Department of Physics, Presidency College, Chennai, Tamil Nadu, India
*Corresponding Author: antony.suresh4@gmail.com

ABSTRACT
In this article are presented results from analysis of daily mean surface air temperature and humidity data applying nonlinear techniques. The data are collected for Chennai, India during January 1988–December 2013. The phase space, which illustrates the progress of the behavior of a nonlinear dynamical system, is reconstructed by Takens delay embedding theorem. The delay time and embedding dimension are estimated using average mutual information (AMI) and false nearest neighbor (FNN) algorithm respectively. Based on these embedding parameters (delay time τ and embedding dimension m) the correlation dimension for various embedding dimension and largest lyapunov exponent are estimated. Finally, the phase space reconstruction algorithm is employed to make a short-term prediction of the chaotic time series, whose governing equations of the system are unknown. The predicted values are in good agreement with the observed ones within 7 days, but they appear much less accurate beyond that limit (7 days). These results indicate that chaotic characteristics clearly exist in the air temperature and humidity data; techniques based on nonlinear dynamics can therefore be used to analyze and predict the air temperature.

Key words: Chaos, Phase space reconstruction, Hurst exponent, Lyapunov exponent and Poincare map.

INTRODUCTION

Atmospheric processes, such as air temperature and humidity, are usually nonlinear and complex (Selvam, 2012). The underlying complexity with in temperature and humidity makes the investigation as one of the indefinable tasks. The advancement in chaos theory offers new ways to draw the hidden information in random-like data. However, the methods originally branches from nonlinear dynamics and chaos theory, are now used to identify pure deterministic nonlinear mechanisms. Chaotic mechanisms are also used to identify deterministic elements which are mixed with other stochastic elements in the data. Although, chaotic time series illustrates the characteristic of dynamical systems as random, in the embedding phase space they represent deterministic behavior (Zhang and Man, 1998). Over the past two decades, distinguishing deterministic chaos and noise has become an important problem in many diverse fields, e.g., weather forecast (Lorenz, 1993), sunspot prediction (Park et al., 1996), hydrology (Sivakumar, 2000 and 2004; Rodriguez et al., 1989; Elshorbagy et al., 2002), traffic flow (Nair et al., 2001), foreign exchange rate (Das and Das, 2007), economics (Chen, 1998), etc., this is due to the availability of numerical algorithms for quantifying chaos using experimental time series.

The concept Phase-space reconstruction, embedding of a single-dimensional time series in a multi-dimensional phase-space to characterize the underlying dynamics, could be an useful methodology for forecasting. In recent time Phase-space reconstruction has found its applications in various fields such as lake volume (Abarbanel and Lali, 1996), rainfall (Berndtsson et al., 1994; Rodriguez et al., 1989), rainfall-runoff (Sivakumar et al., 2001b), etc. In this paper, we use nonlinear time series techniques to analyze the temperature and humidity data of Chennai, India. The results indicate that chaotic characteristics obviously exist in the temperature and humidity data; a technique which is based on phase space dynamics, can be used to analyze and predict the temperature and humidity.

Analysis of Nonlinear Time Series

Reconstruction of phase space

The fundamental idea of the phase space reconstruction is that, a time series contains the information about unobserved state variables, which can be used in the prediction of the present state. For a scalar time series x_t, where t = 1, 2, 3, . . ., may be used to construct a vector time series that is equivalent to the original dynamics from a topological point of view. The phase space can be reconstructed using the method of delays (Cao, 1997; Abarbanel et al., 1990; Frede, and Mazzega, 1999; Fraser and Swinney1986; Takens, 1981). The state space needs to form a coordinate system to confine the structure of orbits in phase space, this can be made by using lagged variable; $x_{t+\tau}$, where τ is the delay.

$$Y_t = \{x_t, x_{t+\tau}, x_{t+2\tau}, \ldots\ldots, x_{t+(m-1)\tau}\} \quad (1)$$

Where τ, m is referred to as the delay time and embedding dimension respectively.

Determining Time-Delay and embedding dimension

Time–delay embedding is the best empirical method for analyzing a dynamical system (Packard et al., 1980). It has been shown that under reasonable conditions, a time delay embedding preserves the quantities of the dynamical system in which we are interested (Takens, 1981; Whitney, 1936; Andrew and Harry 1986).

The proper choice of the time delay τ, is needed for reconstructing the trajectory in phase space from the chaotic scalar time series data. In order to characterize the chaotic systems and to obtain the quantities such as lyapunov exponent and other generalised entropies for a measured scalar time series, which is generated by a chaotic system, an appropriate state vector needs to be constructed with suitable time delay τ. For an infinite noise free data set the value of the delay time τ is in principle almost arbitrary (Takens, 1981), however for finite amount of data the choice of τ determines the quality of reconstructed trajectory in phase space and thereby one obtains for the generalized entropies, exponents and dimensions. The problem of proper choice of τ has been tackled by Fraser and Swinney (Andrew and Harry, 1986; Liebert and Schuster, 1989). Mutual information is a tool to measures of independence between data samples, the value of τ that produces the first local minimum of mutual information be used for phase space construction (Shaw, 1985), the first minimum of the mutual information can be selected as time delay. Average mutual information (AMI) is a theoretic method to connect two sets of measurements with each other criterion. The average mutual information between x(t) and x(t+ τ) can be calculated by

$$I(\tau) = \sum_{x(t),x(t+\tau)} \Pr(x(t), x(t+\tau) \log_2 \left[\frac{\Pr(x(t), x(t+\tau)}{\Pr((x(t)) \Pr(x(t+\tau))} \right] \quad (2)$$

I(τ) determines the average amount of information shared by two values in the time series. When the value of T increases, x(t) and x(t+τ) becomes independent and I(t) will tends to zero (Abarbanel and Lali, 1996).

Similarly, determining an optimum embedding is a significant process, the precision of τ and m is directly related with the accuracy of invariables of the described characteristics of the strange attractors in phase space reconstruction. Time series which is reconstructed in minimal embedding dimension m, and the reconstructed attractor is a one-to-one image of the attractor in the original phase space. As the embedding dimension increases, the attractor unfolds; the same points on the attractor will not cross itself. The attractor would be completely unfolded in dimension (Embedding Dimension), where number of nearest neighbours arising through projection is zero. If time series is reconstructed to a smaller embedding dimension than minimum embedding dimension, then the state space trajectories projection of the points might appear as near neighbourhoods of other points which they are not neighbours in actual. The benefit of these neighbours, among other things, is that they allow the information on how phase space neighbourhoods evolve to be used to generate equations for the precise prediction of the time evolution of new points on or near the attractor (Abarbanel et al., 1990; Whitney, 1936; Farmer and Sidorowich,1987). The lowest dimension, in which none of the orbits in the attractor overlaps, is called the embedding dimension of that attractor. False nearest neighbour is an appropriate method for estimation of the optimum embedding dimensions, because this algorithm eliminates the incorrect neighbours. The points which are close to each other in one dimension, due to projection the points will be separated in higher embedding dimensions. The distance between two neighbor points amplify when going from dimension d to d+1 and it is a criterion for casting the embedding errors. This criterion is called false nearest neighbour, and should satisfy the following equation:

$$\left[\frac{R_{d+1}^2(t,r) - R_d^2(t,r)}{R_d^2(t,r)} \right]^{0.5} = \frac{|x(t+\tau) - x(t_r+\tau)|}{R_d(t,r)} > R_{tot} \quad (3)$$

Where t and t_r are the times corresponding to neighbour point and the origin point, respectively. R_d is the distance in the phase space with embedding dimension d. R_{tot} is the tolerance threshold (Abarbanel et al., 1990).

Hurst exponent

Harold Edwin Hurst is known for introducing the Hurst exponent as a measure for the predictability of a time series (Hurst, 1951; Harris et al., 1987). Hurst exponent is not only used as a measure of long-term memory but also correlate the fractal dimension of the time series, and it has been used in many fields.

The Hurst exponent is determined using R/S analysis.

$$(R/S)_n \approx cn^H \quad (4a)$$

$$\log(R/S)_n = \log c + H \log n \quad (4b)$$

Where H is the Hurst exponent

Hurst exponent can change between 0 and 1. The Hurst exponent of 0.5 shows a true random walk. A value between 0 and 0.5 indicates non-persistent behavior, meaning that the data is not random but the current trend is unlikely to continue. A Hurst exponent between 0.5 and 1 proves that the data are more persistent and the current direction is likely to continue. Hurst exponent value is 0 means that the time series changes direction with every sample. A constant time series with non-zero gradient will result in a Hurst value of 1 (Edman, 1996).

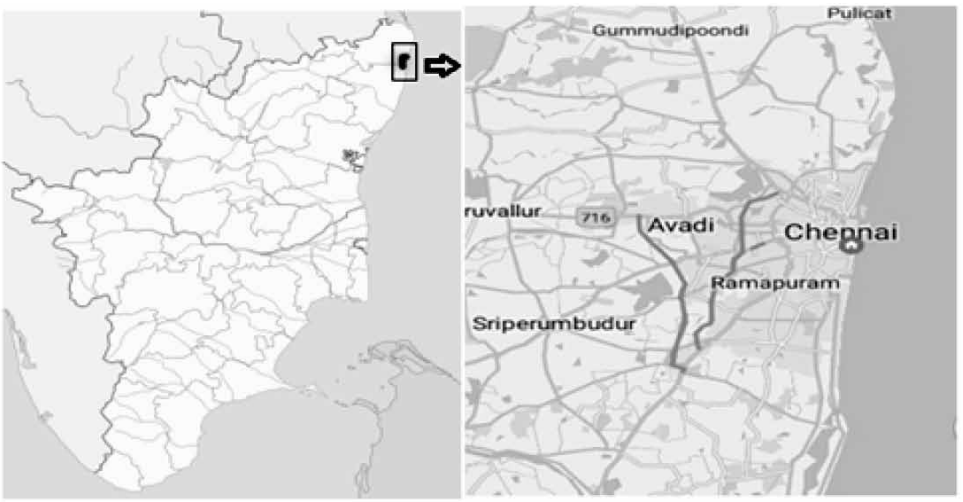

Figure 1. Map showing the location of study area.

Poincaré map

The Poincaré map is a tool to observe the response of a nonlinear system. Analyzing high dimensional dynamical flow of the nonlinear system in the corresponding phase space is an important task. Typically, rather than analyzing the continuous flow in the $(d)^{th}$ dimension phase space, we observe the dynamics induced by the flow on a particular section of the phase space called Poincaré section (Basu, 2007). A Poincaré section is a hypersurface in the phase space, which is transverse to the flow of a given dynamic system. The intersection induces a set of points in $(d-1)^{th}$ dimension space. The projection of a Poincaré section on the X(T)-Y(T) plane is referred to as the Poincaré map of the dynamic system, where T is driving force. For chaotic motion, the return points in the Poincaré map form a geometrically fractal structure.

Largest Lyapunov Exponent

Lyapunov exponent is an appreciable quantitative measure of chaotic dynamics and in many cases it is the only evidence for chaos, Exponential divergence of nearby orbits in phase space is accepted as the hallmark of chaotic behaviour (Drazin, 1994; Ramasubramanian and Sriram, 2002). A system with at least one positive lyapunov exponent is defined to be chaotic. The magnitude of the exponent confirms the time scale, beyond which the system dynamics become unpredictable, that can be determined (Shaw, 1981). Lyapunov exponents are the average exponential rates of divergence or convergence of nearby orbits in phase space. Since nearby orbits correspond to nearly identical states, exponential orbital divergence means that the separation between the two orbits in that system will also be a function of time, whose initial difference will soon behave quite differently, so predictability is rapidly vanished. The mean exponential rate of divergence of two initially close orbits was described by

$$\lambda = \lim_{t\to\infty} \frac{1}{t} \ln \frac{|\Delta x(X_0, t)|}{|\Delta X_0|} \quad (5)$$

This number, called the largest lyapunov exponent (λ) is used for distinguishing among the various types of orbits and provides a measure of the rate of this divergence (Froyland, 1992), the exponents measure the rate at which system processes create or destroy information (Shaw, 1981).

Chaos is basically deterministic; it is unpredictable beyond certain short intervals. In fact, the accurate prediction of a chaotic dynamical system is a function of the largest Lyapunov exponent (Abarbanel and Lali, 1996).

$$\Delta t_{max} = \frac{1}{\lambda_{max}}. \quad (6)$$

Study Area

Chennai is spread roughly from 12°50′ N to 13°17′ N latitude, and from 79°59′ E to 80°20′ E longitude. This area is one of the most highly populated urban sites and the fourth largest metropolis in India and 36^{th} largest urban area in the world, encompassing a total area of roughly $426km^2$ (Figure 1). It is located on the south-eastern coast of India in north-eastern part of Tamil Nadu on a flat coastal plain known as the eastern coastal plains, with the Bay of Bengal to its east. For most part of the year, the weather is hot and humid.

Time series of daily mean temperature and humidity data of Chennai, were obtained from IMD. The 26-year period from 1988 to 2013, with 9055 data points is used in the study. Various researches over the past two decades have made a significant progress in the methods to identify chaos in a time series (Abarbanel and Lali, 1996; Berndtsson et al.,1994; Li and Liu, 2000) are used in this studies.

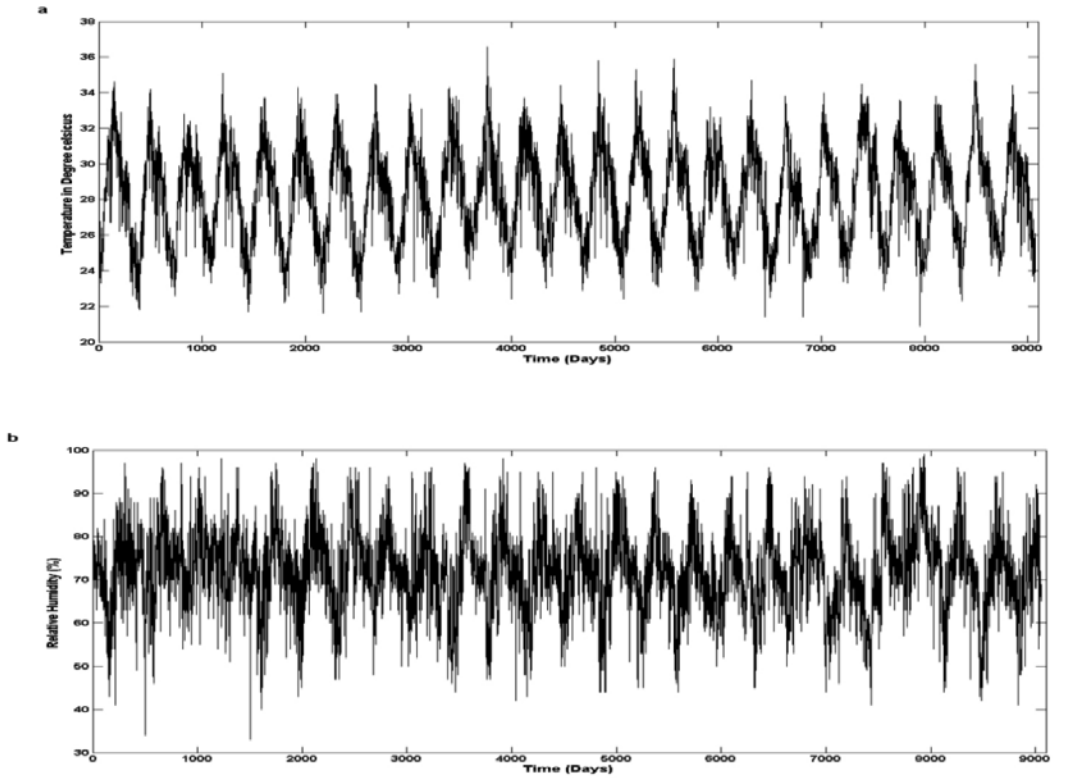

Figure 2(a, b): Time series plot of mean temperature and humidity.

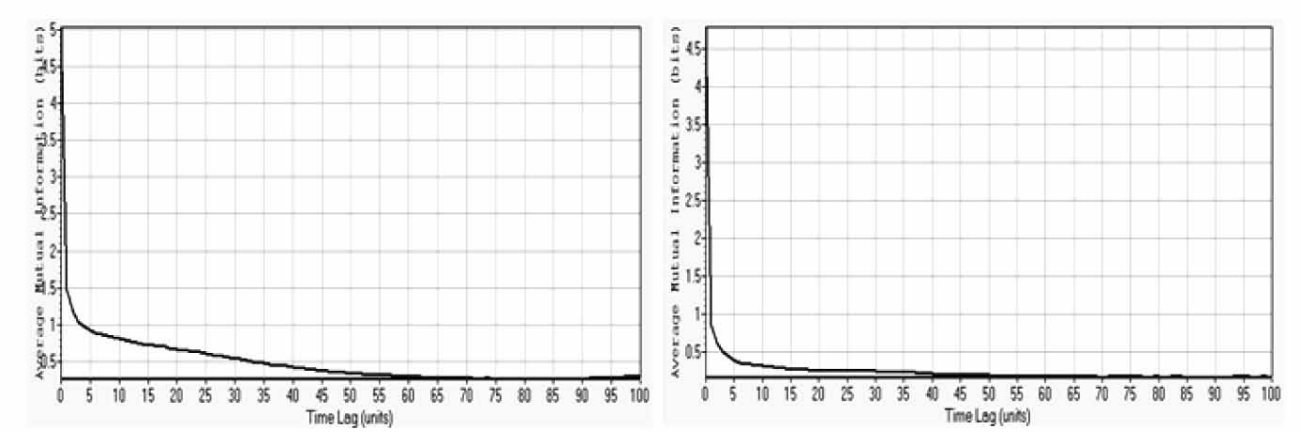

Figure 3. AMI bits Vs Time Lag for daily mean Air temperature and humidity.

Analysis and results

The time series of the daily mean temperature and humidity, collected over a period of about 26 years at chennai, India is shown in the Figure 2 (a,b).

Determination of reconstruction parameters

In order to reconstruct the original phase space, we need to calculate approximate reconstruction parameters, the delay time (τ) and embedding dimension (m). For both daily temperature and humidity time series, first minima time lag is calculated by AMI. The results (Figure 3) expose first minima at time lag 50 days and 7 days and for temperature and humidity time series respectively.

Calculating the percentage of false nearest-neighbors for the time series is the method used for the determination of the sufficient embedding dimension. The method shows that the estimation value of embedding dimension is 20 for both temperature and humidity data which is illustrated in the Figure 4. Both AMI and embedding dimension are estimated using Visual Recurrence Analysis (VRA) software.

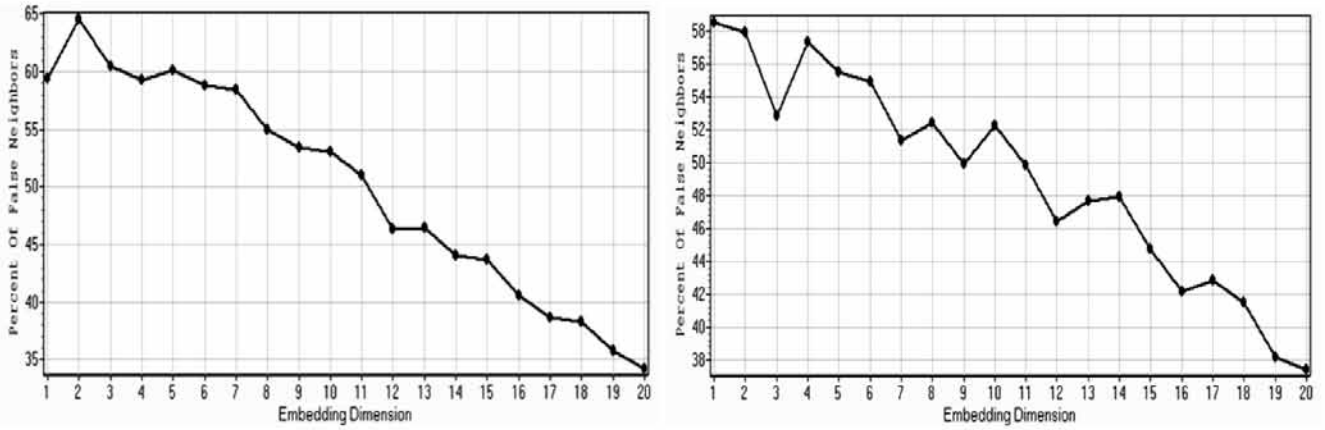

Figure 4. Embedding dimension Vs False neighbors for daily mean Air temperature and humidity.

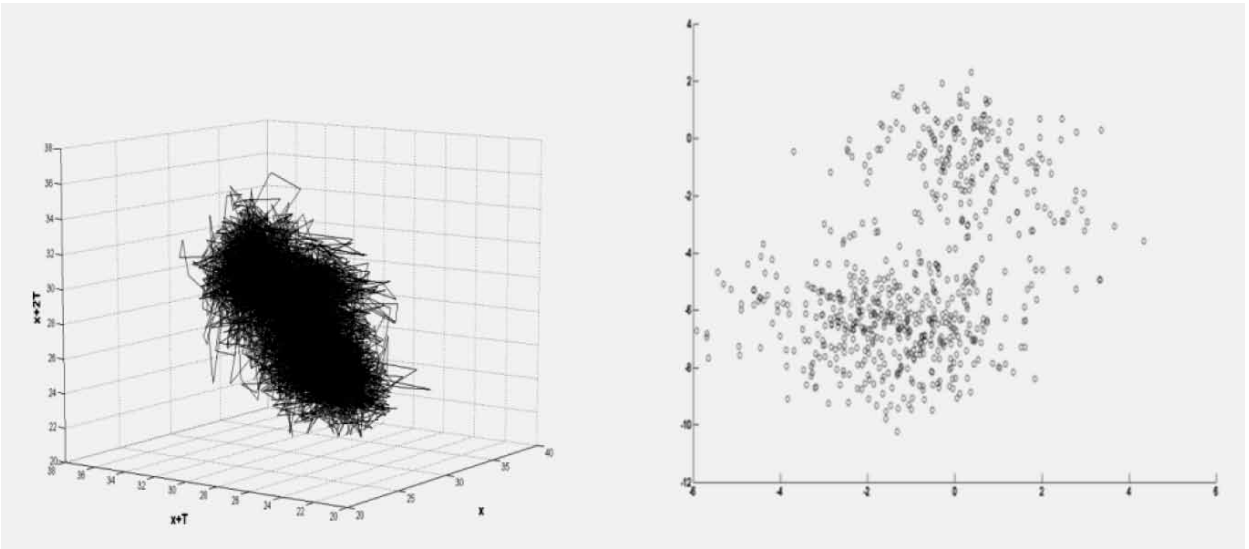

Figure 5 (a). Shows three- dimensional phase portraits and Poincaré map of the daily mean air temperature time series.

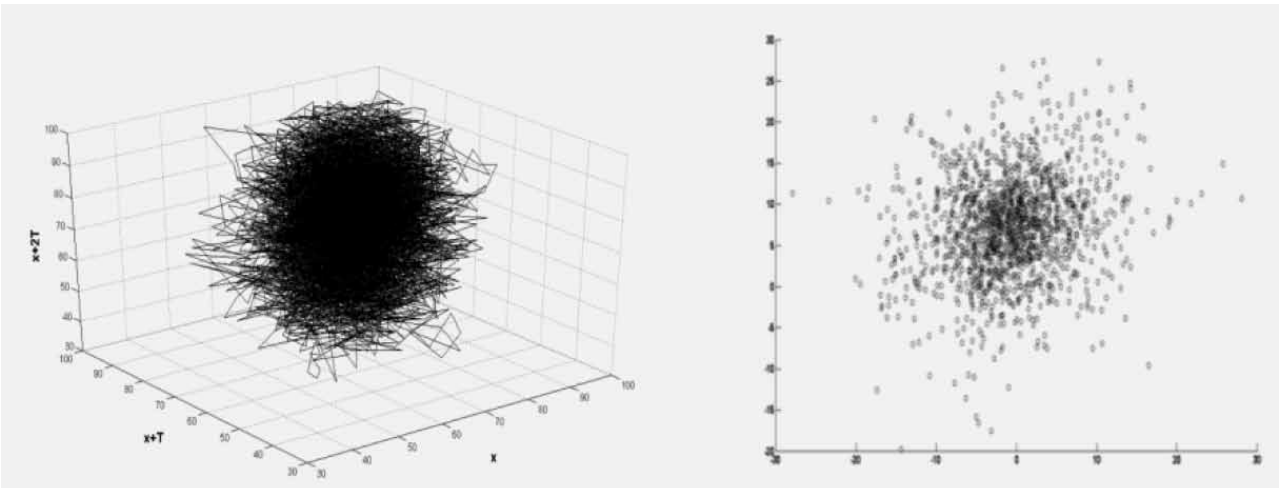

Figure 5 (b). Shows three- dimensional phase portraits and Poincaré map of the daily mean relative humidity time series.

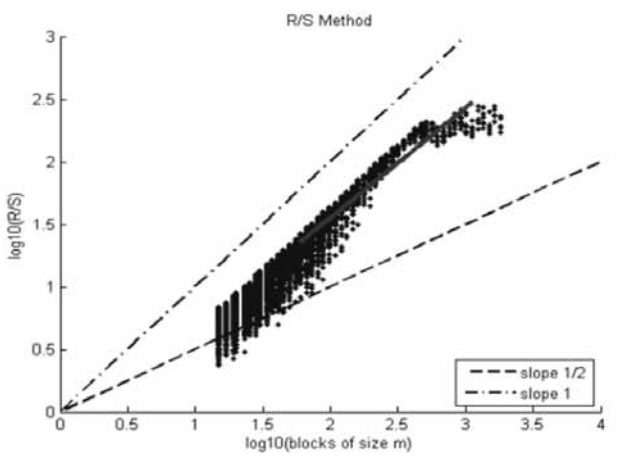

Figure 6(a). Hurst exponent plot for temperature data.

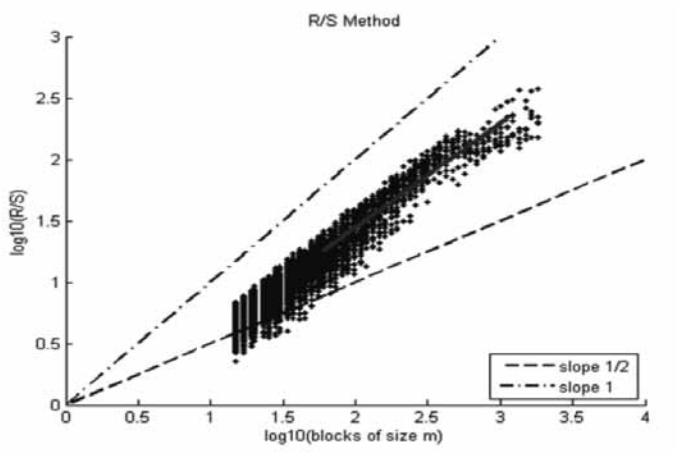

Figure 6(b). Hurst exponent plot for humidity data.

Table 1. complete analysis of time series data.

Period	Data type	Time delay (τ)	Embedding Dimension (m)	Hurst exponent (H)	Lyapunov exponent (λ)	Correlation coefficient between temperature and humidity data
1988-1993	Temperature	13	17	0.9826	0.084	-0.54
	Humidity	8	17	0.8953	0.528	
1994-1999	Temperature	13	17	0.9920	0.185	-0.65
	Humidity	11	17	0.9431	0.485	
2000-2005	Temperature	7	20	0.9775	0.266	-0.70
	Humidity	7	18	0.9617	0.335	
2007-2013	Temperature	16	20	0.9741	0.383	-0.65
	Humidity	10	19	0.9699	0.358	

Phase Space Representation

Phase space is a representer of a dynamical system where each point on that phase space represents a particular state of the system at a particular time. Phase space representation is versatile tool in time series analysis. Due to the fact that, phase space determines all the states of a dynamical system, analysis of that system can be achieved in both identifying the system and predicting the future states via Phase space representation. Figure 5(a, b): Shows three dimensional phase portraits of the reconstructed attractor for the daily mean air temperature time series reconstructed for $\tau=50$ and reconstructed at $\tau=7$ for relative humidity time series. Poincaré map is geometrically fractal structure, which confirms the chaos in the time series.

Estimation of Hurst exponent

Hurst exponent is derived using R/S analysis (MATLAB). Hurst exponent values calculated from Figure 6a and Figure 6b for temperature and humidity time series data are 0.8762 and 0.8495 respectively. The results show that both the time series data exhibit persistence nature.

Forecasting daily surface air temperature by Phase Space Reconstruction approach

Phase-space is a useful tool for characterizing dynamical systems. Firstly, in 1980, Packard, Crutchfiled, Farmer and Shaw suggested the theory of generating a reconstruction space from a single time series to characterize nonlinear dynamical system, and the theory was completed by F.Takens in 1981. Reconstruction of a single dimensional time series in a multi-dimensional phase-space explores the underlying phenomena. In that embedded phase space, the phase space analysis can be applied, because it owns the geometric properties as the state space. This fact arises from the fact that the attractor in reconstructed phase space is one to one image of the attractor in state space. Takens phase space reconstruction is the most popular method, using the past history and an appropriate time delay.

Math code for the phase-space reconstruction (PSR) approach is written, and forecasting is carried out in MATLAB.

The prediction for the daily mean temperature time series in Chennai is shown in Figure 7. The difference between the actual value and predicted data is negligible,

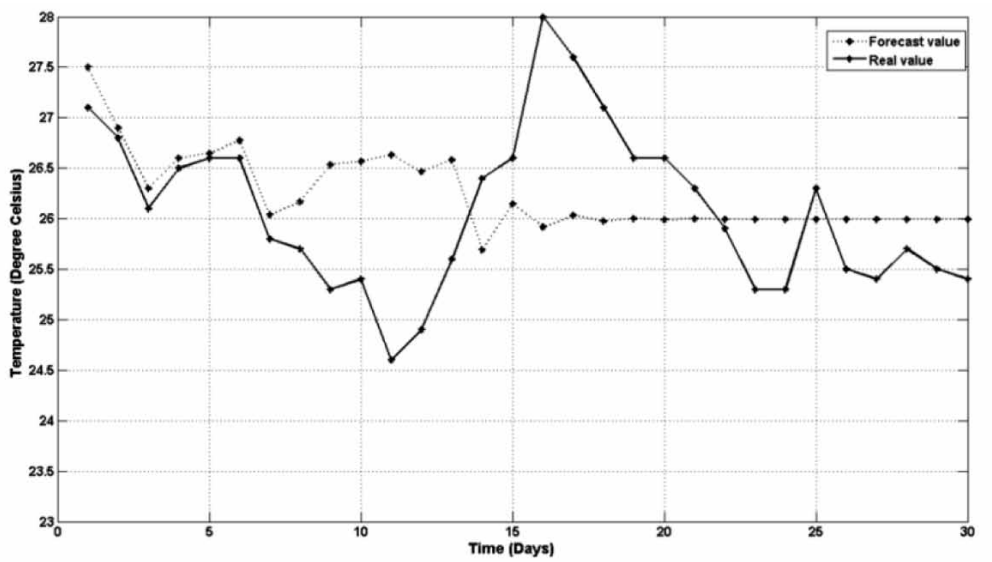

Figure 7. Comparison of observed and predicted daily mean air temperature in Chennai.

for 7 days, and it doesn't hold well beyond that. In fact, the largest Lyapunov exponent, from Eq. (5), suggests that the maximum window for accurate predictions of daily mean temperature data is about 2-3 days. The sensitivity to initial condition limits the predictive ability of a chaotic dynamical system. As Sugihara suggested, it is expected that chaos decreases the correlation between observed and predicted values as prediction time stretches (Sugihara and May, 1990). Also, the prediction results firmly develop the fact that information is contained in the data, so it is very effective for short term predictions only.

CONCLUSION

In this paper an attempt was made to study on the probable use of the concept of Phase-space reconstruction for understanding nonlinear dynamics behavior and to predict meteorological parameters like Air temperature and humidity data. Series of techniques were used to investigate chaotic behaviors in the temperature and humidity time series data. We have analyzed the time series observed over 26 years (January 1988 – December 2013) in Chennai, using Phase space reconstruction techniques. The results have shown that chaotic features evidently exist in the temperature and humidity data from the positive largest Lyapunov exponent and from the Poincaré map. The Largest Lyapunov tells us the maximum length of an accurate prediction is 3 days. These techniques can be further applied to other meteorological chaotic time series data.

ACKNOWLEDGEMENTS

Authors are thankful to Dr. V. Jothiprakash for constructive review and suggestions. They also thank Prof. B. V. S. Murty for editing the manuscript. We thank the Chief Editor for the support and guidance.

Compliance with ethical Standards

The author declares that they have no conflict of interest and adhere to copyright norms.

REFERENCES

Abarbanel, H.D.I., and Lali, U., 1996. Nonlinear dynamics of the Great Salt Lake: system identification and perdition. Climate Dyn., v.12, pp: 287-297.

Abarbanel, Henry, D.I., Brown, R., and Kartke, J.B., 1990. Prediction in chaotic nonlinear systems: methods for time series with broadband Fourier spectra. Phys. Rev., A., v.41, pp: 1782–1807.

Andrew M. Fraser., and Harry L. Swinney., 1986. Independent coordinates for strange attractors from mutual information. Phys. Rev. A., v.33, pp: 1134.

Berndtsson, R., Jinno, K., Kawamura, A., Olsson, J., and Xu, S., 1994. Dynamic system theory applied to long-term temperature and precipitation time series. Trends Hydrol., v.1, pp: 291-297.

Basu, A., 2007. Project in School of Electric and computer Engineering Georgia Institute of Technology Atlanta, GA.

Cao, L., 1997. Practical method for determining the minimum embedding dimension of a scalar time series. Physica, D., v.110, pp: 43-50.

Chen, P., 1998. Empirical and theoretical evidence of economic chaos. Syst Dynam Rev., v.4, no.1-2, pp: 11-38.

Das, A., and Das, P., 2007. Chaotic analysis of the foreign exchange rates, Applied Mathematics and Computation, v.185, pp: 388-396.

Drazin, P.G., 1994. Nonlinear systems. New York: Cambridge University Press.

Edman, A.N., 1996. Time Series Prediction Using Supervised Learning and Tools from Chaos Theory. PhD Thesis, University of Luton.

Elshorbagy, A., Simonovic, S.P., and Panu, U.S., 2002. Estimation of missing stream flow data using principles of chaos theory. J Hydrol., v.255, pp: 123–133.

Farmer, J.D., and Sidorowich, J.J., 1987. Predicting chaotic time series. Phys. Rev., Lett., v.59, no.8, pp: 845-848.

Fraser, A.M., and Swinney H.L., 1986. Independent coordinates for strange attractors from mutual information. Phys. Rev., A., v.87, pp: 1134-1140.

Frede, V., and Mazzega, P., 1999. Detectibility of deterministic nonlinear processes in earth rotation time series I. Embedding. Geophys. J. Int., v.137, pp: 551-564.

Froyland, J., 1992. Chaos and Coherence, Institute of Physics Publications.

Harris, C.M., Todd, R.W., Bungard, S.J., Lovitt, R.W., Morris, J.G., and Kell, D.B., 1987. The dielectric permittivity of microbial suspensions at radio-frequencies: a novel method for the estimation of microbial biomass. Enzyme Microbial Technology, v.9, no.3, pp: 181-186.

Hurst, H.E., 1951. Long term storage capacity of reservoirs. Transactions of the American Society of Civil Engineers., v.116, pp: 770-799.

Li, T.Y., and Liu, Z.F., 2000. The chaotic property of power load and its forecasting. Proc CSEE v.20, no.11, pp: 36-40.

Liebert, W., and Schuster, H.G., 1989. Proper choice of the time delay for the analysis of chaotic time series, Phys. lett. A., v.142, no.2-3, pp: 107-111.

Lorenz, E.N., 1993. The Essence of Chaos, University of Washington Press, Seattle.

Nair, A.S., Liu, J.C., Rilett, L., and Gupta, S., 2001. Non-linear analysis of traffic flow, In: Proceedings of the IEEE Intelligent Transportation Systems Conference, Oakland, pp: 25-29.

Packard, N.H., Crutchfield, J.P., Farmer, J.D., and Shaw, R.S., 1980. Geometry from a time series. Physical Review Letters, v.45, no.9, pp: 712-716.

Park, Y.R., Murray, T.J., and Chen, C., 1996. Predicting sun spots using alayered perceptron neural network, IEEE Transactions on Neural Networks1(2)., pp: 501-505.

Ramasubramanian, K., and Sriram, M.S., 2002. A comparative study of computation of Lyapunov spectra with different algorithms.

Rodriguez-Iturbe, I., De Power, F.B., Sharifi, M.B., and Geograkakos, K.P., 1989. Chaos in rainfall. Water Resour. Res., v.25, no.7, pp: 1667-1675.

Selvam, A.M., 2012. Nonlinear Dynamics and Chaos: Applications in Atmospheric Sciences Journal of Advanced Mathematics and Applications, v.1, no.2, pp: 181-205 (25).

Shaw, R.S., 1985. The Dripping Faucet as a model chaotic system (Aerial Press, Santa Cruz, CA.

Shaw, R., 1981. Strange Attractors, Chaotic Behaviour, and Information Flow, Z. Naturforsch. 36A 80.

Sivakumar, B., 2004. Chaos theory in geophysics: past, present and future. Chaos, Solitons & Fractals., v.19, no.2, pp: 441-462.

Sivakumar, B., 2000. Chaos theory in hydrology: important issues and interpretations. J Hydrol; v.227, pp: 1-20.

Sivakumar, B., Berndtsson, R., Olsson, J., and Jinno, K., 2001b. Evidence of chaos in the rainfall- runoff process. Hydrol. Sci.J., v.46, no.1, pp: 131-145.

Sugihara, G., and May, R.M., 1990. Nonlinear forecasting as a way of distinguishing chaos from measurement error in time series. Nature, v.344, pp: 734-741.

Takens, F., 1981. Detecting strange attractors in turbulence, in dynamic systems and turbulence, Lecture Notes in Mathematics, Springer Verlag, Berlin, pp: 366-381.

Whitney, H., 1936. Differentiable manifolds. Annals of Mathematics, v.37, pp: 645-680.

Zhang, J., and Man, K.F., 1998. Time series prediction using recurrent neural network in multi-dimension embedding phase space, IEEE International Conference on Systems, Man, and Cybernetics2, pp: 11-14.

Received on: 7.9.16; Revised on: 10.2.17; Accepted on: 28.2.17

"Even as global warming increases the frequency of El Nino and the Atlantic event, their effects are being amplified by the annual loss of an area of rain forest the size of New Jersey. Less rain falls, and the water runs into the rivers instead of being sucked up by the fungus filaments and tree roots." Alex Shoumatoff (1946--) is an American writer known for literary journalism, nature and environmental writing.

J. Ind. Geophys. Union (July 2017)
v.21, no.4, pp: 285-291

Monsoon Could Trigger the Global Abrupt Climate Changes: New Evidence from the Bay of Bengal

Pothuri Divakar Naidu*[1] and Pawan Govil[2]

[1]National Institute of Oceanography, Dona Paula 403 004, Goa, India
[2]Birbal Sahni Institute of Palaeosciences, 53 University Road, Lucknow – 226 007, India
*Corresponding Author: divakar@nio.org

ABSTRACT

In recent years evidence has been pouring in mainly from marine records, supporting the hypotheses that temperature changes in the Arctic and Greenland steer the intensity of the Asian Monsoon (Schulz et al., 1998; Kudrass et al., 2001; Gupta et al., 2003; Wang et al., 2001). However, the physical link between the high latitude climate and monsoons are still elusive. Here we use oxygen isotopes and Mg/Ca data of planktonic foraminifera species (Globigerinoides ruber) from a sediment core in the Bay of Bengal to reconstruct sea surface temperature (SST) and surface water oxygen isotopic values. We find that oxygen isotopic values (monsoon signal) and SST of the Bay of Bengal (BOB) lead the Dansgaard-Oeschger (D-O) events. We, therefore suggest that the monsoon could kick the start of millennial scale abrupt climate changes through the shifts of the Intertropical Convergence Zone (ITCZ) and associated convection, water vapor supply to the tropical troposphere and latent heat penetration.

Key words: Monsoon, climate change, oxygen isotopes, planktonic foraminifera species, sea surface temperature, Dansgaard-Oeschger (D-O) events, Intertropical Convergence Zone (ITCZ).

INTRODUCTION

The Indian monsoon is an important component of global climate transporting heat and moisture from the warmest part of the tropical ocean across the equator and to higher latitudes. Seasonal reversals of monsoon winds and associated monsoon rainfall over Asia have a direct effect on the socio-economic and agricultural development in the densely populated Asian region. Monsoon reconstructions based on proxies such as Globigerina bulloides abundances (Gupta et al., 2003), total organic carbon records (Schulz et al., 1998) from marine sediment cores from the Arabian Sea and oxygen isotopic ratios of speleothem deposits from Oman (Fleitman et al., 2003) and China (Wang et al., 2001) have demonstrated that abrupt changes in monsoon intensity coincide with temperature changes indicated in the Greenland GISP2 ice core record. Such kind of coherent changes between monsoon and high latitude climate records prompted to link the monsoon changes to the North Atlantic and/or Greenland temperature changes (Schulz et al., 1998; Kudrass et al., 2001; Gupta et al., 2003). Similarly, synchronous occurrences of Dansgaard-Oeschger (D-O) events in the tropical Atlantic Ocean and South America (Jennerjahn et al., 2004; Wang et al., 2004) and in the equatorial Pacific (Kienast et al., 2006) were documented.

Martin et al., (1981) have indicated that the four major rivers Irrawaddy, Brahmaputra, Ganges and Godavari discharge annually approximately $1.5x10^{12}m^3$ of fresh water into the Bay of Bengal (BOB). In addition annual rainfall over the bay varies between 1 m off the east coast of India to more than 3 m in the Andaman (Baumgartner and Reichel, 1975). The peak discharge of rivers and rainfall over the bay occurs during the SW monsoon season, which leads to a strongly stratified near-surface layer. Therefore, the salinity variations and oxygen isotopic values of surface water ($\delta^{18}O_{SW}$) of the BOB on interannual and longer time scales are strongly controlled by SW monsoon rainfall. Therefore, we investigate the SST and $\delta^{18}O_{SW}$ changes of the BOB at the millennial time scale for the last 33 kyr to determine: i) the past variability of the local salinity to infer changes in the monsoon precipitation ii) how variability of the fresh water flux and ocean dynamics of the Bay of Bengal was related to the high latitude climate changes.

Material and Methods

Core SK-218/1 was collected at a water depth of 3307 m from the BOB (14°02′06″ N; 82°00′12″ E), this location experiences more than 2000 mm of annual rainfall, primarily during the summer monsoon season. The site location is characterized by moderate rates of sediment accumulation throughout over last 60 kyr. The age model for the last 37 kyr is based on the AMS carbon 14 dates determined on the species Globigerinoides ruber. The measured ^{14}C ages were converted to sediment ages using the online CalPal version quickcal 2005 ver1.4 (Weninger et al., 2006) routine with a marine reservoir correction of 400 years. The chronology is extended further by correlating $\delta^{18}O$ of G. ruber to the low latitude isotopic

stack chronology of Martinson et al., (1987). The time scale was constructed assuming constant sedimentation rates between radiocarbon dates and isotope tie points. On the basis of this model, the average sample spacing is 500 years. The sediment accumulation rate varies significantly from 6 to 18 cm/kyr between the Holocene and the glacial period.

For determination of Mg/Ca, for each sample 30 to 40 individuals of Globigerinoides ruber (white variety) with a size range of 250 to 350μm were picked. The picked specimens were then cleaned following the procedure of Barker et al., (2003). Splits of the cleaned samples were digested in diluted HNO_3 and analyzed for Mg and Ca on a ThermoFinnigan Element2 sector field inductively coupled plasma mass spectrometer. Elemental concentrations were derived from the isotopes ^{25}Mg and ^{43}Ca; ^{89}Y served as internal standard. The analytical errors for the Mg and Ca concentrations were better than 0.7% relative standard deviation (RSD). 40 sample solutions were measured in replicate, and the repeatability for Mg/Ca was routinely better than -0.1 mmol/mol. This translates to an uncertainty of about ±0.2 °C in the reconstructed SST.

For $\delta^{18}O$ of calcite a split of the cleaned foraminifers were loaded in a stainless steel boat, an automated sample carousel, for sequential acidification online. The CO_2 evolved in the reaction was transferred to the inlet of a gas ratios table isotope mass spectrometer using cryogenically routine procedures and the sample gas was compared to an internal standard gas sequentially 10 times. The difference in the $^{18}O/^{16}O$ of the sample and the internal standard is reported in the delta ($\delta^{18}O$) notation relative to the PDB standard. Our routine precision of $\delta^{18}O$ for standards run in conjunction with samples averaged ~0.10‰ over the course of the present study. By subtracting the Mg/Ca-derived temperature component from $\delta^{18}Oc$, we obtained $\delta^{18}O_{SW}$. $\delta^{18}O_{sw}$, in turn, is linearly correlated with salinity; the modern slope for the Bay of Bengal is 0.18 ‰ per psu (Delaygue et al., 2001). Further, $\delta^{18}O_{SW}$ and SST at this site show an insignificant relationship (r=-0.32).This also suggests that dilution plays a major role in controlling the salinity variation. After the removal of global $\delta^{18}O_{SW}$ linked to ice volume and sea level changes (Shackleton, 2000), the fluctuation in $\delta^{18}Osw$ of the BOB essentially serves as a proxy of rainfall and river runoff, both are strongly coupled to the summer monsoon. Hence we will interpret changes in $\delta^{18}Osw$ in the BOB core solely as a monsoon signal.

RESULTS AND DISCUSSION

Synchronous $\delta^{18}O_C$ Changes

For the time period from 12 to 65 kyr the foraminiferal $\delta^{18}O$ record from the BOB shows striking similarities with the GISP2 ice core $\delta^{18}O$ record, which essentially represents changes of air temperature in the high latitudes of the northern hemisphere (Dansgaard et al., 1993). However, from 12 kyr to present day the BOB $\delta^{18}O_C$ record is more variable compared to the Globigerinoides ruber (GISP2) $\delta^{18}O$ record (Figure 1). The BOB $\delta^{18}O_C$ record exhibits minima corresponding to the Dansgaard-Oeschger (D-O) events 1,3,5,6,7,8,9,10,12,14,15 and 16, suggesting that whenever the temperatures were warmer (interstadials) in Greenland, the BOB was less saline. This observation is in line with several other studies from the Arabian Sea (Schulz et al., 1998) and the Bay of Bengal (Kudrass et al., 2001) and speleothem records from Hulu Cave, China (Wang et al., 2001). However, two factors can contribute to the lighter $\delta^{18}O$ values in foraminifera; warm calcification temperatures as well as lower $\delta^{18}O_{sw}$.

The SK-218/1 $\delta^{18}Oc$ record does exhibit a few differences compared to the GISP2 record: the D-O events 2 and 4 and the Younger Dryas event lead by 1 kyr. To isolate precipitation and river-run off, which are strongly associated with monsoon rainfall in this region (i. e. monsoon signal), we have compared $\delta^{18}Osw$ with the D-O events documented in the GISP2 record for the period where we have a good control on the chronology of the BOB core and GISP2 record.

The mean $\delta^{18}Oc$ difference between the Holocene and last glacial maximum is about 2.1‰ after removing the global ice volume effect of 1.2‰. The remaining 0.86‰ reflects temperature and salinity changes. The 2°C temperature change between Last Glacial Maximum (LGM) and Holocene (Figure 1) accounts for 0.48‰, remaining 0.38‰ indicates that salinity was ~2 psu higher in the Bay of Bengal during the LGM, with more evaporation and less precipitation. Although the NE monsoon activity was stronger during the LGM (Duplessy, 1982), this did not lower the salinity considerably in the BOB. However, one could see the difference in salinity gradient between the Arabian Sea and BOB during LGM which is attributable to the cause of NE monsoon during LGM.

δ^{18}Osw, SST and D-O Events:

The $\delta^{18}Osw$ in the BOB shows D-O events 1, 2, 3 and 4 very prominently with shifts of 0.54‰, 0.31‰, 0.37‰ and 0.55‰ respectively, but the timings of the $\delta^{18}O_{SW}$ shifts (events) differ as compared to the GISP2 data set, all four events in the BOB record lead the D-O events as recorded in the GIPS2 core (Figure 2). Similarly, BOB SST changes in particular at Heinrich Events, during deglaciation and at D-O events 1, 2, 3, and 4 lead the GISP2 $\delta^{18}O$ record (Figure 2). More strikingly, the deglacial warming in the BOB started between 17 to 18 kyr (Figure 3), leading the warming of the high latitudes by 2-3 kyr. Similarly, other well-dated cores from the Arabian Sea show an early deglacial warming (Sirocko et al., 1993; Peeters et al., 1999). We realize that the robustness of the

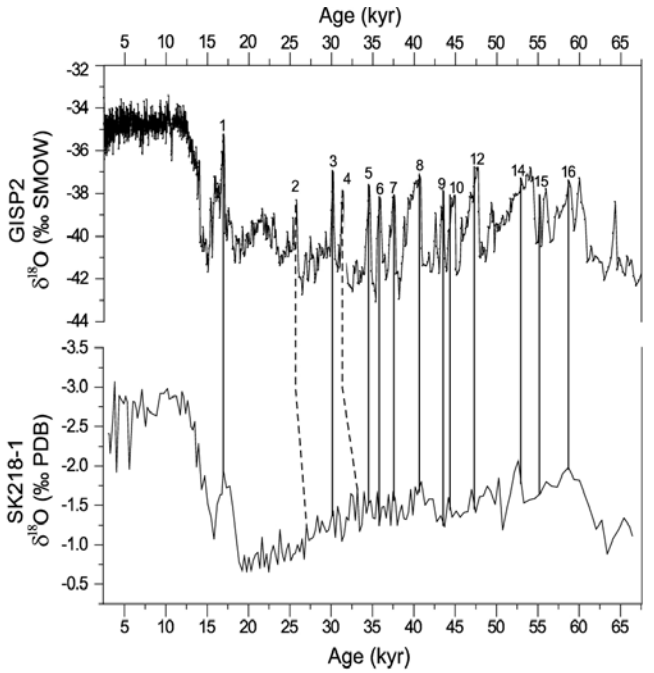

Figure 1. Oxygen isotopic values of Globigerinoides ruber ($\delta^{18}O_C$) from a SK-218/1 sediment core from the Bay of Bengal and GISP2 $\delta^{18}O$ record data plotted as a function of age. The chronologies of SK218-1 and GISP2 are independent. The vertical dotted lines represent synchronous changes in oxygen isotopic values during Dansgaard-Oeschger (D-O) cycles between these two records.

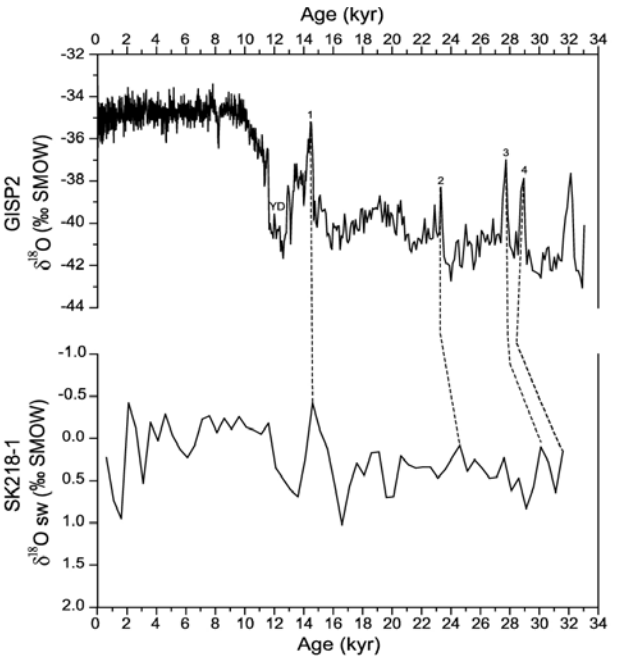

Figure 2. Oxygen isotopic values of waters ($\delta^{18}O_{SW}$) from the Bay of Bengal and oxygen isotopic values of GISP2 ice core plotted as a function of age. The abrupt changes in $\delta^{18}O_{SW}$ at YD, D-O Event 1, 2, 3, and 4 lead the similar changes in GISP2 Ice core. YD: Younger Dryas.

comparison of the BOB $\delta^{18}O_{SW}$ and SST records with the GISP2 $\delta^{18}O$ record depend on the synchronization of age scales. The age model of the BOB core (SK218/1) does not have sub-millennial precision. However, the lead of SST and $\delta^{18}O_{sw}$ versus air temperature by 600 to 1000 years is persistent throughout the record. It is this persistence that gives us the confidence to interpret the lead as true environmental signal and not as artifact or random result due to limitations of the age model.

Our record of $\delta^{18}O_{SW}$, which is a more reliable proxy of monsoon rainfall than the other marine proxies used so far in the northern Indian Ocean (Schulz et al., 1998; Kudrass et al., 2001) show an apparent lead over the D1, D2, D3 and D4 of the GISP2 $\delta^{18}O$ record. Not only the $\delta^{18}O_{SW}$ but also the SST shows a clear lead over the GISP2 $\delta^{18}O$ record. Similarly, equatorial Pacific (Lea et al., 2000), Sulu Sea (Rosenthal et al., 2000) and equatorial Indian Ocean SST records (Saraswat et al., 2005) also show a lead over the global ice volume curve. Accordingly, the lead of tropical Pacific and Indian Ocean temperatures appears to be a robust feature. Therefore, we suggest that abrupt climate shifts such as the D-O events have first occurred in the monsoon-influenced regions and later in the northern hemisphere high latitudes.

Role of monsoon in triggering D-O events

It was proposed that fresh water input to the North Atlantic would initiate thermohaline circulation changes responsible for abrupt climate shifts during the last glaciation (Clark et al., 2001). Nevertheless, model simulations do not provide compelling proof to support the role of thermohaline circulation changes in governing the abrupt climate shifts on the global scale (Broecker, 2003). Accordingly, the mechanism by which thermohaline circulation changes of the North Atlantic will propagate the abrupt climate changes to the tropics in general, and monsoon changes, in particular, are not clear yet. We, therefore, invoke a role of the monsoon, which could propagate the signal from the tropics to high latitudes through tropical convection.

During Boreal Summer, the ITCZ migrates northward across the Indian Ocean and the Indian subcontinent, bringing with it summer monsoon rainfall (Gadgil, 2003). The Asian monsoon plays a dominant role in the tropical climate because it transports heat and moisture from the warmest part of the tropical ocean across the equator and to the high latitudes. The addition of water vapor to the atmosphere affects temperature both as a greenhouse gas and as a mechanism of latent heat transport from the

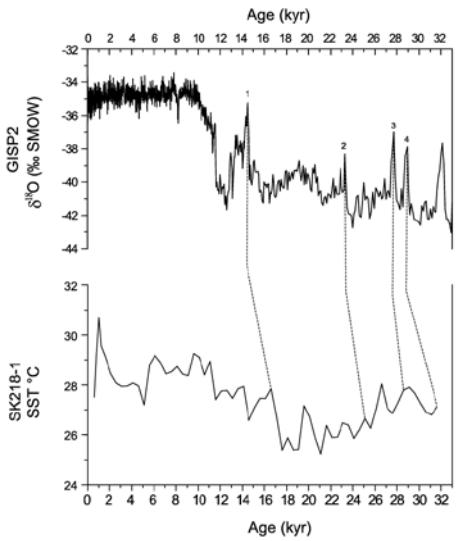

Figure 3. Sea surface temperatures variations in Bay of Bengal and oxygen isotopic variations of GISP2 ice core plotted as a function of age. Sea surface temperatures in the Bay of Bengal (calculated from Mg/Ca) lead the Greenland air temperatures indicated by ice $\delta^{18}O$.

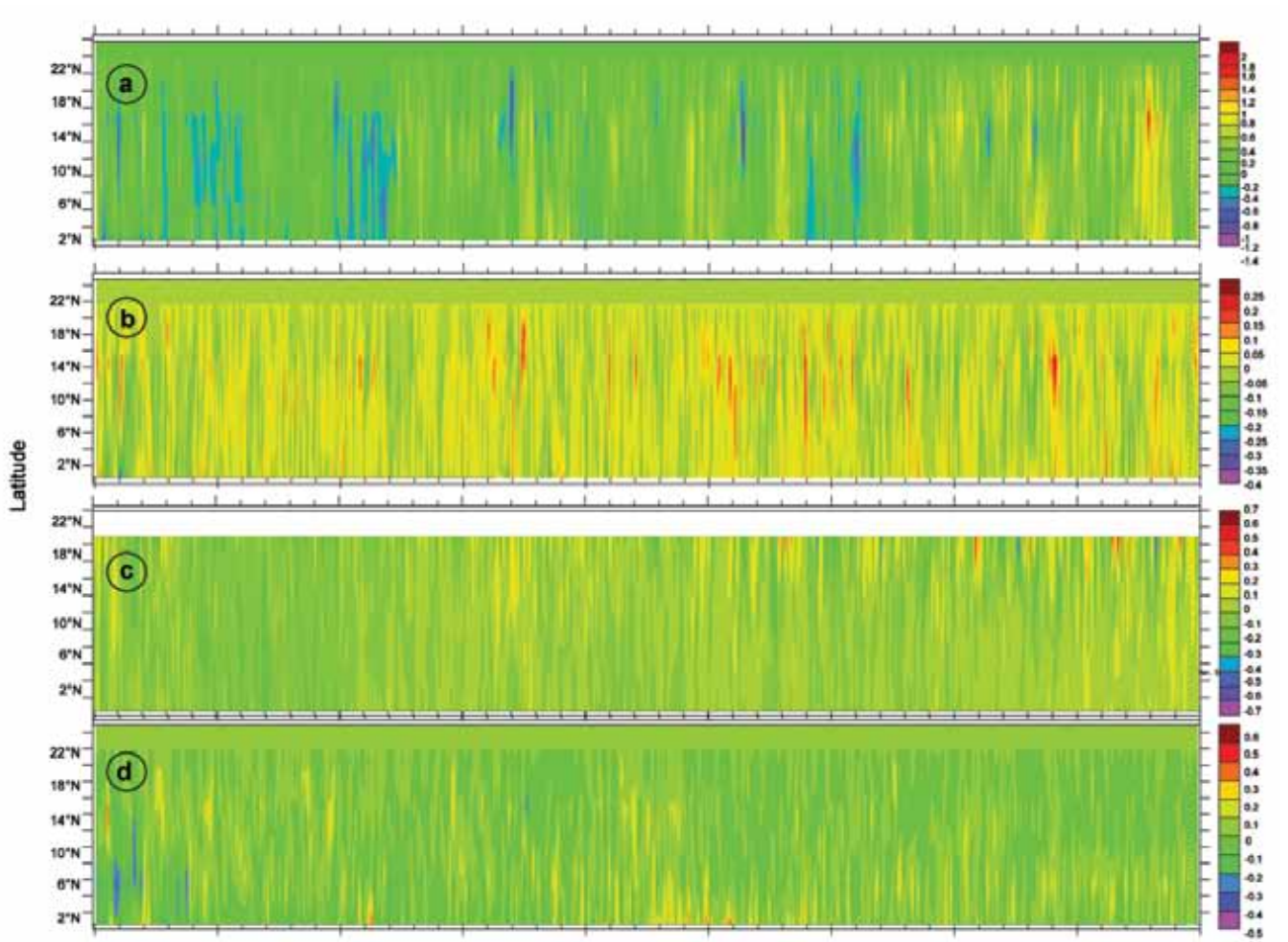

Figure 4. Instrumental data set obtained from Wooodruff et al., (1987), for the years from 1945 to 1985, anomalies of (a) SST, (b) cloudiness (ITCZ), (c) evaporation (latent heat) and (d) rainfall.

Table 1. Chronological tie points with reference to depth in the Core SK 218-/1 from the Bay of Bengal. 0 to 66 cm sediment contains slumped material from the slope indicated by an age reversal. Below 68 cm the sediment is undisturbed.

Depth (cm)	C^{14} Ages (in years)	Calendar Age (in kyr BP)
68	1055+60	0.62
266	10400+60	11.51
322	13940+90	16.81
638	33060+90	37.10
742	3.3 event	50.51*
794	4/5 boundary	58.96*

tropics to high latitudes. During interstadials (D-O events 1, 2, 3 and 4) the ITCZ had moved further north which increases the tropical convection, resulting in an increase in overall tropical humidity and consequently an increase in the temperature of the tropics. As a consequence of air temperature rise in the Asian region ice melts on the Tibet Plateau, decreases the albedo in the region, increasing the pressure gradient between the Indian Ocean and the Tibet Plateau. This kind of set-up accelerates the monsoon circulation and precipitation over the Indian subcontinent. As the position of the ITCZ shifts away from the equator during the monsoon season the mass energy transport carried by the Hadley cell intensifies (Lindzen and Hou, 1988). Such intensification enhances the water vapor supply to the tropical troposphere, which affects the mean tropical SST (Seager et al., 1988). Tropics in general and the Indo-Pacific warm pool in particular are the main regions from which water vapors are supplied to the atmosphere. As the water vapor is one of the main greenhouse gases, its substantial variation in the atmosphere directly affects the SST in the region.

The global atmosphere is very sensitive to changes in tropical SST (Pierrehumbert, 2000) and SST changes in the tropics must initiate feedbacks that alter the energy budget of the planet, which in turn affect climate over much of the globe through changes in the stationary wave pattern (Trenberth et al., 1998). Further, tropical convection could reorganize in a way to shift the ITCZ, either through autonomous variability of the coupled atmosphere-ocean system or in response to orbital changes in the insolation pattern. The propensity for convection increases with SST, and there is a threshold value of SST of about 27.5°C for the Indian Ocean, above which convection increases (Gadgil, 2003). Thus, if the SST of the BOB exceeds 27.5 °C, as a result, the co-variation between SST and precipitation in the tropical Indian Ocean increases. A contraction and expansion of the tropical convection region can decrease and increase temperature, respectively in the tropics (Pierrehumbert, 2000). Further, a decrease in Asian monsoon activity during stadials was related to less convective activity in the monsoon regions (Wang et al., 2001), which supports the concept that tropical convection and monsoon strength are related

In this contexts, we have analyzed SST, cloudiness (ITCZ), evaporation (latent heat) and rainfall for the years from 1945 to 1985. During the active monsoon years, 1961, 1970, 1975, 1983 and 1988 a strong coupling among the ITCZ propagation and rate of evaporation and precipitation is found (Figure 4). Thus, high energy of the tropics and the associated hydrological cycle of the monsoon system itself have a scope for reorganization that could lead to rapid climate transitions. Therefore, SST and $\delta^{18}O_{SW}$ changes in the BOB lead the D-O events in the high-latitude North Atlantic during the past 30 kyr.

It was pointed out earlier that the tropical Pacific is actively involved in forcing global climate change because the tropical Pacific serves as a heat engine for earth's climate and as a vapor source of its hydrological cycle (Lea et al., 2001; Clement et al., 1999; Visser et al., 2003). On the other hand, it is now evident that the Indian Ocean plays an active role in controlling the SST in other parts of the tropics including the Pacific (Cobb and Charles, 2001). Further, Indian Ocean SST anomalies peak 2-3 years prior to those in the Pacific and maximum Indian Ocean anomalies occur at a time when the external forcing from tropical Pacific SST is minimum (Cobb and Charles, 2001). Thus, monsoonal processes in the Indian Ocean should exert considerable influence over the climate variability of both the tropical and mid-latitudes.

A teleconnection mechanism through the Pacific El Niño system was invoked to explain synchronous changes between monsoon records from the Arabian Sea and northern hemisphere high latitude records (Sirocko et al., 1996). However, linking the monsoon changes to El Niño is rather complex, because during the ENSO initiation phase (June – August), for example, Arabian Sea summer monsoon winds are weakened while those in the South China Sea are strengthened. In contrast, during the mature phase of ENSO (December- February) South China Sea winter monsoon winds are significantly weakened while the Arabian Sea winter monsoon winds are only slightly weakened (Wang et al., 2003).

Long-term rainfall variations in China (Wang et al., 2005) and Oman (Neff et al., 2001) appear to follow summer insolation changes. Similarly, temperature changes in the North Atlantic also show a similarity with solar insolation changes (Bond et al., 2001). Such kind of synchronous shifts in high latitude climate and tropical monsoon, and their overall trends matching solar insolation changes suggest that the foot-print of solar impact on climate extended from polar to tropical latitudes. In the tropics the solar insolation is predominantly tied to the precession cycle of the Earth's orbit (Berger and Loutre, 1991), the monsoon changes occurred in close association with the harmonic tones of Earth's precessional cycle (23 kyr) (Sirocko et al., 1996). Hence, the precession cycle of variation in solar insolation, water vapor, convection, ITCZ movement in the tropics and the strong tropical ocean-atmosphere feedbacks (Wang et al., 2001; Ivancho et al., 2006) could initiate and enforce the millennial-scale abrupt climate changes on the global scale.

CONCLUSION

The primary implication of this study lies in monsoon and associated water vapor of the tropics. It is evident that the linkage between monsoon and associated water vapor of the tropics has a strong bearing on the tropical SST and convection. Both monsoon changes and tropical convection can be forced by the solar insolation changes caused by the precession cycle, which would trigger the abrupt climate changes noticed in the northern hemisphere high latitudes. As such, primary lead of monsoon signal over the northern hemisphere high latitude climate strongly supports the notion that the tropics are actively involved in forcing abrupt climate changes on the global scale, but such kind of tropical forcing mediated through monsoons.

ACKNOWLEDGEMENTS

The lead author acknowledges the close association and positive support received from Chief Editor of JIGU through personal interaction spanning over two decades. Thanks are also due to him for useful suggestions and apt editing.

Compliance with Ethical Standards

The authors declare that they have no conflict of interest and adhere to copyright norms.

REFERENCES

Barker, S., Greaves, M., and Elderfield, H., 2003. A study of cleaning procedures used for foraminiferal Mg/Ca paleothermometry. Geochem. Geophys. Geosyst., 8407 doi:10.1029/2003GC000559., v.4, no.9.

Baumgartner, A., and Reichel, E., 1975. The World Water Balance: Annual Global, Continental and Maritime Precipitation, evaporation and Runoff. Elsevier Sci., New York, 31 charts, pp: 197.

Berger, A., and Loutre, M.F., 1991. Insolation values for the climate of the last 10 million years. Quaternary Science Reviews., v.10, no.4, pp: 297-317.

Bond, G., Kromer, B., Beer, J., Muscheler, R., Evans, M.N., Showers, W., Hoffmann, S., Lotti-Bond, R., Hajdas, I., and Bonani, G., 2001. Persistent solar influence on north Atlantic climate during the Holocene. Science., v.294, no.5549, pp: 2130-2136.

Broecker, W.S., 2003. Does the trigger for abrupt climate change reside in the ocean or in the atmosphere? Science., v.300, no.5625, pp: 1519-1522.

Clark, P.U., Marshall, S.J., Clarke, G.K.C., Hostetler, S.W., Licciardi, J.M., and Teller, J.T., 2001. Freshwater forcing of abrupt climate change during the last glaciation. Science., v.293, no.5528, pp: 283-287.

Clement, A.C., Seager, R., and Cane, M.A., 1999. Orbital controls on the El Nino/Southern Oscillation and the tropical climate. Paleoceanography., v.14, no.4, pp: 441-456.

Cobb, K.M., and Charles, C.D., 2001. A central tropical Pacific coral demonstrates Pacific, Indian, and Atlantic decadal climate connections. Geophysical Research Letters., v.28, no.11, pp: 2209-2212.

Dansgaard, W., Johnsen, S.J., Clausen, H.B., Dahl-Jensen, D., Gundestrup, N.S., Hammer, C.U., Hvidberg, C.S., Steffensen, J.P., Sveinbjörnsdottir, A.E., Jouzel, J., and Bond, G., 1993. Evidence for general instability of past climate from a 250- kyr ice-core record. Nature., v.364, pp: 218-220.

Delaygue, G., Bard, E., Rollion, C., Jouzel, J., Stievenard., M., Duplessy, J.C., and Ganssen G., 2001. Oxygen isotope/salinity relationship in the northern Indian Ocean. J. Geophys. Res., v.106, no.C3, pp: 4565-4574.

Duplessy, J.C., 1982. Glacial to interglacial contrast in the northern Indian Ocean. Nature., v.295, pp: 494-498.

Fleitmann, D., Burns, S.J., Mudelsee, M., Neff, U., Kramers, J., Mangini, A., and Matter, A., 2003. Holocene Forcing of the Indian Monsoon Recorded in a Stalagmite from Southern Oman. Science., v.300, no.5626, pp: 1737-1739.

Gadgil, S., 2003. The Indian Monsoon and its variability. Annual Review Earth and Planetary Science., v.31, pp: 429-467.

Gupta, A.K., Anderson, D.M., and Overpeck, J.T., 2003. Abrupt changes in the Asian southwest monsoon during the Holocene and their links to the North Atlantic Ocean. Nature., v.421, pp: 354-356.

Ivancho, T.S., Ganeshram, R.S., Brummer, G.A., Ganssen, G., Jung, S.J.A., Morton, S.G., and Kroon, D., 2006. Variation in tropical convection as an amplifier of global climate change at the millennial scale. Earth and Planetary Science Letters., v.235, pp: 302-314.

Jennerjahn, T., Ittekot, V., Arz, H.W., Behling, H., Patzold, J., and Wefer, G., 2004. Asynchrony of preserved terrestrial and marine signals of climate change in the tropics during the Heinrich events. Science., v.306, no.5705, pp: 2236-2239.

Kienast, M., Kienast, S.S., Calvert, S.E., Eglinton, T.I., Mollenhauer, G., Francois, R., and Mix, A.C., 2006. Eastern Pacific cooling and Atlantic overturning circulation during the last deglaciation. Nature., v.443, pp: 846-849.

Kudrass, H.R., Hofmann, A., Doose, H., Emeis, K., and Erlenkeuser, H., 2001. Modulation and amplification of climatic changes in the northern hemisphere by the Indian summer monsoon during the past 80 k.y. Geology., v.29, no.1, pp: 63-66.

Lea, D.W., Park, D.K., and Spero, H.G., 2000. Climate impact of late Quaternary equatorial Pacific sea surface temperature variations. Science., v.289, no.5485, pp: 1719-1724.

Lea, D.W., 2001. Paleoclimate: Ice ages, the California current, and Devils Hole. Science., v.293, no.5527, pp: 59-60.

Lindzen, R.S., and Hou, A.Y.J., 1988. Hadley circulations for zonally averaged heating centered off the equator. Atmos. Science., v.45, no.17, pp: 2416-2427.

Martin, J.M., Burton, J.D., and Eisma, D., 1981. River inputs to Ocean systems, United Nations Press, Geneva, Switzerland, pp: 384.

Martinson, D.G., Pisias, N.G., Hays, J.D., Imbrie, J., Moore, T.C., and Shacleton, N.J., 1987. Age dating and the orbital theory of the ice ages: development of a high resolution 0 to 300,000-year chronostratigraphy. Quaternary Research., v.27, no.1, pp: 1-29.

Neff, U., Burns, S.J., Mangini, A., Mudelsee, M., Fleitmann, D., and Matter, A., 2001. Strong coherence between solar variability and the monsoon in Oman between 9 and 6 kyr ago. Nature., v.411, pp: 290-293.

Peeters, F., Ivanova, E., Conan, S., Brummer, G.J., Ganssen, G., Troelstra, S., and Van Hinte, J., 1999. A size analyses of planktonic foraminifera from the Arabian Sea. Marine Micropaleontology., v.36, no.1, pp: 31-63.

Pierrehumbert, R.T., 2000. Climate change and the tropical Pacific: The sleeping dragon wakes. Proceedings of National Academy of sciences., v.97, no.4, pp: 1355-1358.

Rosenthal, Y., Lohman, G.P., Lohman, K.C., and Sherell, R.M., 2000. Incorporation and preservation of Mg in Globigerinoides sacculifer: Implications for reconstructing the temperature and $^{18}O/^{16}O$ of sea water. Paleoceanography., v.15, no.1, pp: 135-145.

Saraswat, R., Nigam, R., Weldeab, S., Mackensen, A., and Naidu, P.D., 2005. A first look at past sea surface temperatures in the equatorial Indian Ocean from Mg/Ca in foraminifera. Geophysical Research Letters., L24605, v.32.

Schulz, H.S., Von Rad, U., and Erlenkeuser, H., 1998. Correlation between Arabian Sea and Greenland climate oscillations of the past 110, 000 years. Nature., v.393, pp: 54-57.

Seager, R., Zebiak, S.E., and Cane, M.A., 1988. A model of the tropical Pacific sea surface temperature climatology. J. Geophys. Res., v.93, no.C2, pp: 1265-1280.

Shackleton, N.J., 2000. A 100,000 year ice-age cycle identified and found to lag temperature, carbon-dioxide, and orbital eccentricity. Science., v.289, no.5486, pp: 1897-1902.

Sirocko, F., Sarnthein, M., Erlenkeuser, H., Lange, H., Arnold, M., and Duplessy, J.C., 1993. Century scale events in monsoon climate over the past 24,000 years. Nature., v.364, pp: 322-324.

Sirocko, F., Garbe-Schonberg, D., McIntyre, A., and Molfino, B., 1996. Teleconnection between the subtropical monsoon and high latitude climates during the last deglaciation. Science., v.272, no.5261, pp: 526-529.

Trenberth, K., Branstator, G., Karoly, D., Kumar, A., Lau, N.C., and Ropelewski, C., 1998. Progress during TOGA in understanding and modeling global teleconnections associated with tropical sea surface temperatures. J. Geophys. Res., v.103, no.C7, pp: 14291-14324.

Visser, K., Thunell, R., and Stott, L., 2003. Magnitude and timing of temperature change in the Indo_pacific warm pool during deglaciation. Nature., v.421, pp: 152-155.

Wang, Y., Cheng, H., Edwards, R.L., An, Z.S., Wu, J.Y., Shen, C.-C., and Dorale, J.A., 2001. A high-resolution absolute-dated late Pleistocene monsoon record from Hulu Cave, China. Science., v.294, no.5550, pp: 2345-2348.

Wang, B., Clemens, S., and Liu, P., 2003. Contrasting the Indian and East Asian monsoons implications on geological time scale. Marine Geology., v.201, pp: 5-21.

Wang, Z., Hu, R., Mysac L. A., Blanchet, J-P., and Feng, J., 2004. A parameterization of solar energy disposition in the climate system. Atmosphere-Ocean., v.42, no.2, pp: 113-125.

Wang, Y., Cheng, H., Edwards, R.L., He, Y., Kong, X., An, Z., Wu, J., Kelly, M.J., Dykoski, C.A., and Li, X., 2005. The Holocene Asian Monsoon Links to solar changes and north Atlantic climate. Science., v.308, no.5723, pp: 854-857.

Weninger, B., Jöris, O., and Danzeglocke, U., 2006. Calpal-Cologne Radiocarbon Calibration and Paleoclimate Research Package, Universität zu Köln, Institut für Ur-und Frühgeschichte Radiocarbon Laboratory. http : //www.calpal.de/

Woodruff, S.D., Slutz, R.J., Jenne, R.L., and Steurer, P.M.A., 1987. Comprehensive ocean-atmosphere data set. Bull. Amer. Meteor. Soc., v.68, pp: 1239-1250.

Received on: 24.3.17; Revised on: 10.4.17; Accepted on: 12.4.17

J. Ind. Geophys. Union (July 2017)
v.21, no.4, pp: 292-297

Resorbed forsterite in the carbonatite from the Cretaceous Sung Valley Complex, Meghalaya, NE India – Implications for crystal-melt interaction from textural studies

V.V.Sesha Sai*[1] and Shyamal Kumar Sengupta[2]

[1]Geological Survey of India, Southern Region, Hyderabad - 500068
[2]Director (Retd.) CPL, Geological Survey of India, Central Headquarters Kolkata – 700016
*Corresponding Author: seshu1967@gmail.com

ABSTRACT

Through this paper, we present the significance of textural studies and discuss on the petrogenetic implications of resorbed forsterite from the Sung valley carbonatite, Meghalaya, NE India. Petrographic studies revealed the presence of resorbed olivine, exhibiting conspicuous reaction rim with the surrounding carbonate in the Sung carbonatite. Studies reveal the presence of calcite as dominant mineral phase, with subordinate apatite and accessory magnetite, ilmenite and perovskite. Olivine is noticed as a conspicuous silicate phase in the carbonatite. EPMA studies indicated high Mg nature of the olivine i.e. $Fo_{97.3}$. The SiO_2 content in the forsterite olivine range from 40.95 to 41.60% and MgO content from 54.43 to 56.31%. In the Fe_2 / (Fe_2+Mg) / (Mg/(Fe_2+Mg) mineral chemistry plot, the resorbed olivine from the Sung valley carbonatite falls close to the vicinity of the forsterite end member. We present the succinct details on petrographic and mineral chemistry and discuss on the petrogenetic significance of the forsterite olivine in the Sung carbonatite. Presence of Mg rich foresterite exhibiting spectacular resorbed texture in the carbonatite of Sung Valley Complex indicate early crystallization of olivine and subsequent crystal-melt interaction between the early formed silicate and carbonate melt.

Key words: Forsterite, carbonatite, Sung valley, Meghalaya.

INTRODUCTION

The Sung valley ultramafic-alkaline-carbonatite complex (SACC) occurs as an intrusive suite within the Shillong Group metasediments around Sung area in parts of East Khasi Hills and Jaintia Hills of Meghalaya (Yusuf and Saraswat, 1977; Chattopadhyay, 1979; Chattopadhyay and Hashmi, 1983; Krishnamurthy, 1985; Srivastava and Sinha, 2004; Srivastava et al., 2005; Melluso et al., 2010; Ranjith and Sadiq, 2013). The NNW-SSE trending oval shaped SACC has a partial ring structure with a central serpentinite surrounded by pyroxenite (Figure 1). It is about 4 km in width and extends over a stretch of 7.2 km in NNW-SSE direction from Umkehn nala in north to Byrthar in south. Presences of carbonatites, ultramafic and alkaline rocks were established in Sung Valley Complex during mapping (Gogoi, 1973; Chattopadhyay, 1979). The first major account of Sung valley carbonatite was given by Yusuf and Saraswat (1977). The dominant rock type of the complex includes (i) peridotite, (ii) serpentinite, (iii) pyroxenite, (iv) uncomphagrite (v) alkaline rocks, (vi) biotite – alkali feldspar, and (vii) carbonatite (Figure 1). Apatite-magnetite rock is also present in significant amount in southern part of SACC. Krishnamurthy (1985) carried out petrological studies of Sung valley carbonatites. Viladkar et al., (1994) carried out the mineralogical and geochemical studies of Sung carbonatite complex. A narrow zone of fenite and a brecciated zone of mixed fenite and quartzite have developed at places particularly along the border (Chakraborty and Thapliyal, 2000). In one of the earlier works on geochronology, a $^{206}Pb/^{204}Pb$–$^{207}Pb/^{204}Pb$ age of 134 ± 20 Ma with a model μ_1 of 8.19 ± 0.02 has been obtained for the carbonatite from Sung Valley, Meghalaya, placing their time of emplacement very close to the time assigned for the break-up of Gondwana (Veena et al., 1998). Rb–Sr isochron of the Sung Valley carbonatites, pyroxenite and a phlogopite from a carbonatite yielded an age of 106±11 Ma (Jyotiranjan Ray et al., 2000). An age of 115.1 ± 5.1 Ma was reported by U–Pb dating of perovskite from the ijolite of Sung Valley (Srivastava et al., 2005). However, a precise ^{40}Ar-^{39}Ar age of 107.2 ± 0.8 Ma was reported for the Sung Valley carbonatite alkaline complex (Ray and Pandey, 2001). In a significant contribution, the mineral compositions from the Ultramafic and alkaline rocks and carbonatite from the Sung Complex have been studied by Melluso et al., (2010). Recently, eleven carbonatites were delineated during mapping by GSI (Ranjith and Sadiq, 2013), while Sadiq et al., (2014), reported uraninite, xenotime and REE bearing minerals in Sung carbonatite.

Significance of Magnesium Rich Olivine

Forsterite is a Mg rich end-member of the olivine isomorphous solid solution series involving forsterite

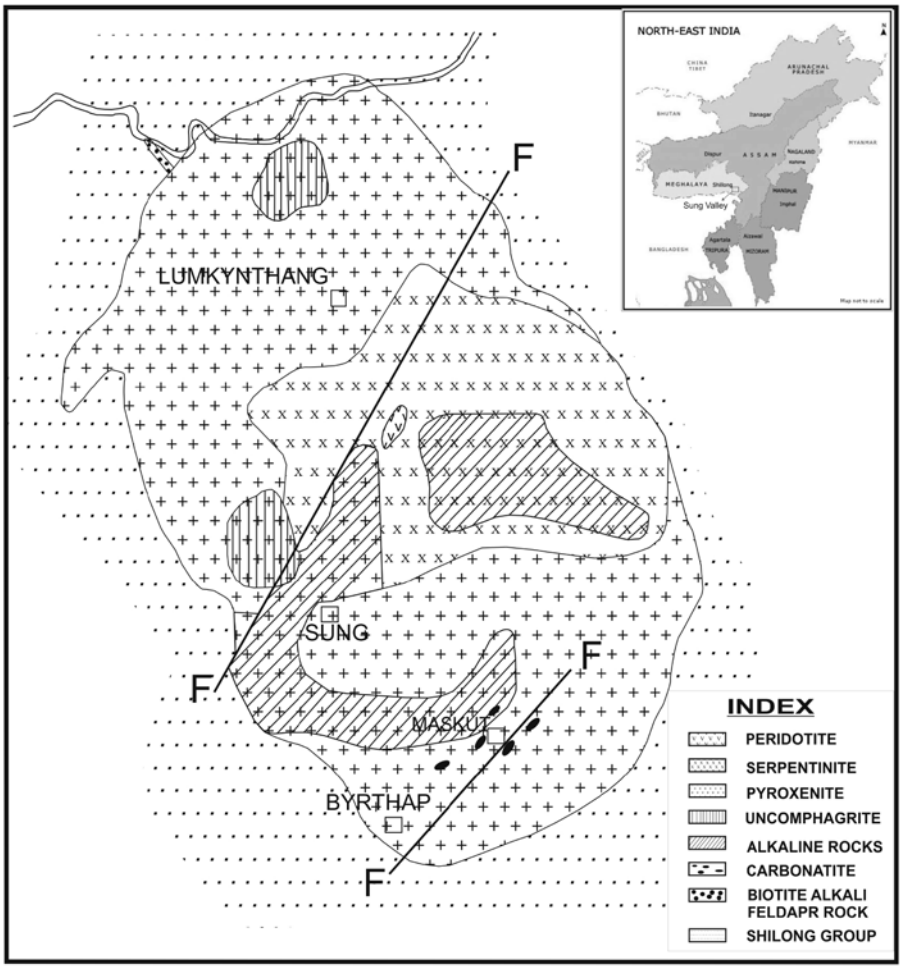

Figure 1. Geological Map of Sung Valley Alkaline-Ultramafic Complex, Meghalaya. (Modified after Chattopadyay and Hashimi, G.S.I. 1984). Inset: Location of Sung Complex in Meghalaya, NE India.

(Mg_2SiO_4) and fayalite [(Fe_2SiO_4), (Deer et al., 1992)]. Forsterite olivine can occur in high Mg ultramafic rocks, kimberlites, lamproites and carbonatites; mantle derived rocks of igneous origin. Among these, carbonatites are rare carbonate rich magmatic rocks; generally confined to the intracontinental rift association. High pressure experimental studies involving (i) olivine-basalt system and (ii) olivine carbonatite system in conditions corresponding to upper mantle, indicated that 'Mg-carbonatite melt has higher conductivity than basaltic melt' (Yoshina et al., 2010). Irrespective of immiscible or residual origin, the carbonatitic melts are rich in alkalis and evolve to alkali-rich compositions (Lee and Wyllie, 1997). This observation is supported by the abundance of Na–K–Ca and Na–Mg carbonate daughter minerals in the inclusions within the forsterite olivine from Kovdor carbonatites (Vekslar et al., 1998). Forsterite can also occur during the process of silicification involving contact thermal metamorphism of Mg rich sediments like dolomite (eg. Ferry et al., 2011). In one of the most significant contributions, presence of forsterite olivine (Fo_{83}) has been observed in interplanetary dust particle (Scott Messenger et al., 2005). Hence, the genesis of the Mg rich olivine in rocks and particles of terrestrial and extra-terrestrial origin indicate a specific petrogenetic process. The present study provides detailed petrographic and mineral chemistry studies of the high Mg forsterite olivine from the Sung valley carbonatite and highlights the textural significance of the resorbed forsterite.

Field Disposition

The oval shaped SACC of Meghalaya plateau in NE India has an areal extent of 26 sq. km (Chattopadhyay and Hashmi, 1983; Ranjith and Sadiq, 2013). The carbonatite occurs as plugs within a highly weathered terrain of mainly pyroxenite and alkaline country rocks around Maskut area, in the southern part of the Cretaceous Sung Complex. Carbonatite, carbonate-apatite rich rocks and magnetite apatite rocks are located in the vicinity of a NE-SW trending fault (Figure 1, Chattopadhyay and Hashmi, 1984).

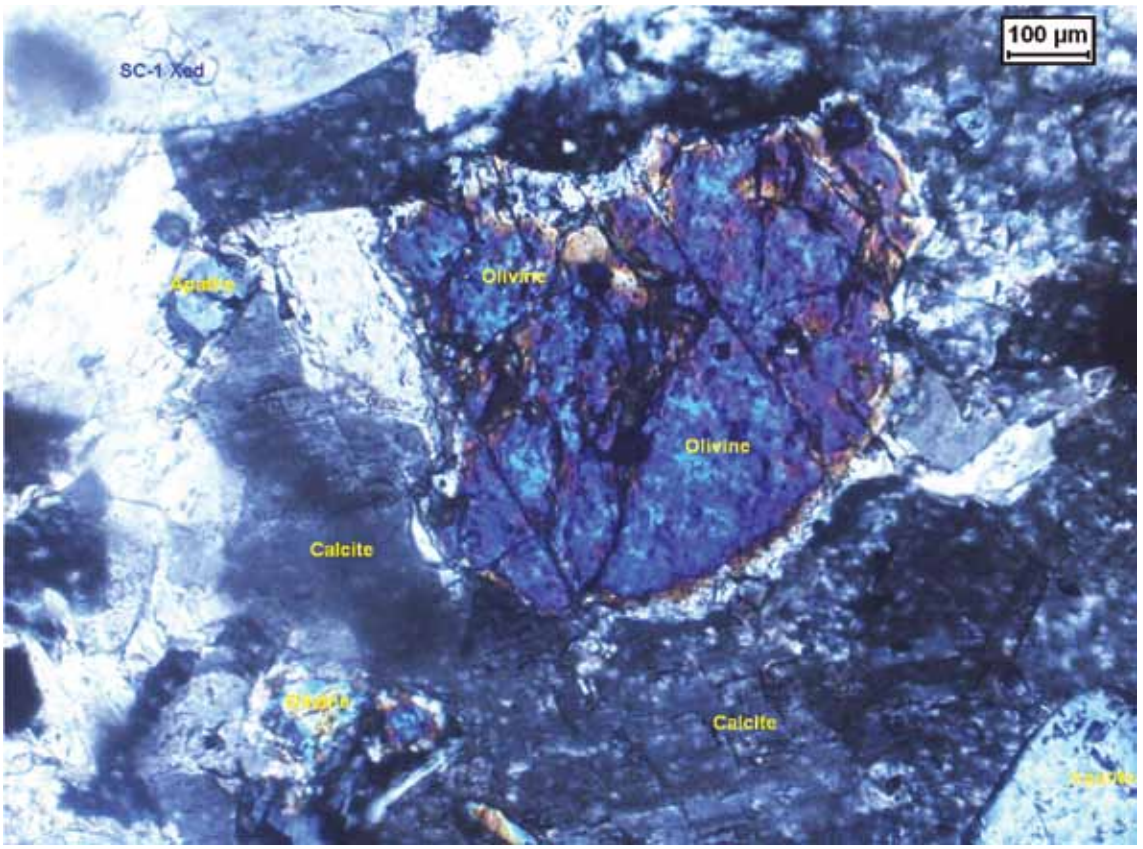

Figure 2. Photomicrograph under crossed Nichols showing the resorbed nature of the olivine at the interface of forsterite and carbonate in Sung valley carbonatite. Note the reaction rim all around the olivine.

Ijolitic rocks occur as small lenses along with carbonate-apatite rich lenses and apatite-magnetite rocks that analyses phosphate content upto 31.36% P_2O_5 was analysed in the around Maskut area (Chattopadhyay and Hashmi, 1983). The carbonatite of the Sung Complex occurs in the form of isolated oval shaped bodies, minor dykes and veins that vary in length from 20 to 125 m with a maximum width of 40 m (Ranjith and Sadiq, 2013; Sadiq et al., 2014).

Petrography and Mineral Chemistry

Petrographic studies of the carbonatite rock from SACC indicate that the rock is coarse grained with crystalline texture and essentially constituting coarse grained crystals of calcite. The size of the calcite crystals ranges from ~ 4 to 5.2 mm. Euhedral to subhedral apatite is conspicuous and is more or less uniformly distributed throughout the carbonatite. Opaque oxides are represented by magnetite and ilmenite, while the conspicuous silicate phase is olivine. In the carbonatites, the non-carbonate component is apatite, olivine, or magnetite (Chakhmouradian et al., 2016). Pervoskite occurs as minute euhedral grains ranging in size from 0.05 to 0.1 mm. Metamict grains after pyrochlore are also noticed in the carbonatite.

Electron Probe Micro Analyses (EPMA) was carried out at Central Petrological Laboratory, GSI, Kolkata by CAMECA Sx 100. Analyses conditions: Accelerating voltage: 15 kV, current: 12 nA. Beam size: 1 μ. All natural standards have been used except for Mn and Ti for which synthetic standards have been used.

Modal abundance of the carbonate minerals in the carbonatite ranges between 65 to 80%. Most of the carbonate grains show rhombohedral cleavage and twinning characteristic of calcite. Consertal relationship in the form of embayed contact is often noticed along the grain boundaries of the carbonate grains. Olivine is noticed as euhedral to subhedral inclusions (0.05 mm size) within the calcite and often a sharp reaction rim is noticed along the interface of olivine and carbonate (Figure 2). Occurrence of pyrochlore associated with calcite and apatite is reported along with bastnasite and other REE minerals recently (Sadiq et al., 2014).

Mineral chemistry studies indicated that the SiO_2 content in the forsterite olivine range from 40.95 to 41.60%, MgO content vary from 54.43 to 56.31%, MnO content of 0.24 to 0.40%, FeO^T content of 1.51 to 2.75 % and Cr_2O_3 content upto 0.05%. CaO is negligible; upto 0.09% EPMA analyses of the forsterite olivine are furnished in Table-1. The Mg # varies for the olivine analyses

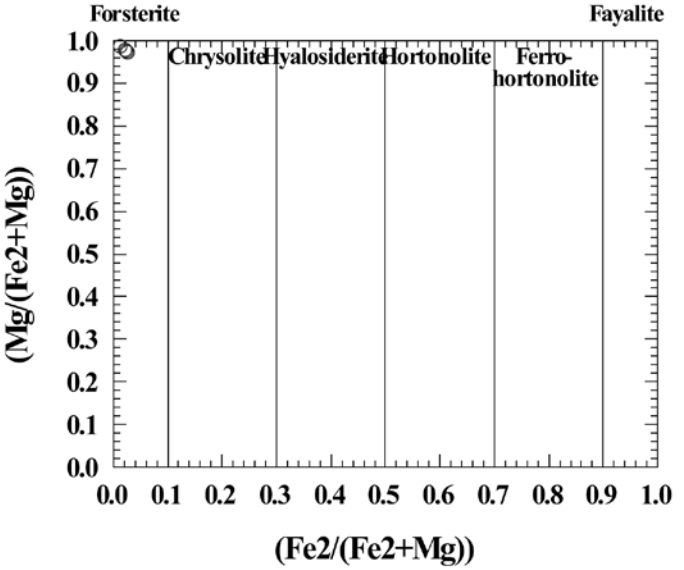

Figure 3. Fe_2/ (Fe_2+Mg)/(Mg/(Fe_2+Mg) plot showing the position of Forsterite from the carbonatite of Sung valley, Meghalaya, NE India.

Table 1. Mineral chemistry of olivine (shown in Figure 2) from the carbonatite of Sung Valley Alkaline-Ultramafic- Carbonatite Complex, Meghalaya.

Oxide	**SA-1/1**	**SA-1/2**	**SA-1/3**	**SA-1/4**	**SA-1/5**	**SA-1/6**
SiO_2	40.95	41.31	41.09	41.60	41.42	41.00
Al_2O_3	0.00	0.05	0.00	0.02	0.00	0.03
TiO_2	0.03	0.00	0.00	0.00	0.03	0.00
MnO	0.39	0.33	0.40	0.24	0.30	0.36
MgO	55.52	55.59	56.31	54.43	55.51	55.92
FeO^T	2.60	2.54	1.51	2.75	2.54	2.41
Na_2O	0.10	0.06	0.06	0.08	0.05	0.06
K_2O	0.02	0.02	0.04	0.01	0.02	0.01
CaO	0.05	0.09	0.00	0.07	0.05	0.02
Cr_2O_3	0.04	0.00	0.05	0.00	0.02	0.00
P_2O_5	0.10	0.00	0.36	0.00	0.00	0.28
BaO	0.00	0.00	0.00	0.00	0.13	0.00
Total	99.79	100.00	99.82	99.19	100.10	100.10
Mg #	95.52	95.63	97.38	95.19	95.62	95.86
Cation						
Si	0.977	0.983	0.975	0.996	0.985	0.973
Al	0.000	0.000	0.000	0.001	0.000	0.001
Ti	0.000	0.000	0.000	0.000	0.001	0.000
Mn	0.008	0.008	0.008	0.005	0.007	0.007
Mg	1.975	1.971	1.991	1.943	1.968	1.979
Fe	0.052	0.051	0.030	0.055	0.050	0.048
Na	0.005	0.003	0.003	0.004	0.002	0.006
K	0.001	0.001	0.001	0.000	0.001	0.001
Ca	0.001	0.000	0.000	0.002	0.001	0.000
Cr	0.001	0.001	0.001	0.000	0.000	0.000
P	0.002	0.001	0.007	0.000	0.000	0.006
Ba	0.000	0.000	0.000	0.000	0.001	0.000
Mineral	Forsterite	Forsterite	Forsterite	Forsterite	Forsterite	Forsterite

indicated in Table-1 is > 95; ranging from 95.19 to 97.38. In Fe_2/ (Fe_2+Mg)/(Mg/(Fe_2+Mg) plot the olivine falls close to forsterite end member (Figure 3). Based on the average of the six point analyses (Table-1), the calculated structural formula for the olivine is $(Mg_{1.97}\ Fe_{0.047}\ Mn_{0.007}\ Ca_{0.0006})_{2.0}$ $(Si_{0.98}\ Al_{0.00})_{0.98}\ O_4$. End member in terms of Forsterite and Fayalite are $Fo_{97.3}$ and $Fe_{2.3}$ respectively; indicating the presence of a very high Mg olivine as a silicate phase in Sung carbonatite.

DISCUSSION

Several occurrences of forsterite in carbonatites have been reported in the world (eg Veksler et al., 1998; Woolley, 2001; Lee et al., 2005). Experimental studies demonstrated that carbonatitic melts percolate in olivine (Hammouda and Laporte, 2011). It is observed that in the reactions involving percolation of carbonate melt in olivine are accompanied by the reprecipitation of the forsterite in the carbonatite reservoir. Melluso et al., (2010) identified the presence of olivine during the mineral composition study of the Sung Valley carbonatite. The threshold abundance of the carbonate minerals in the mantle derived magmatic carbonatites is 50% (Le Maitre 2002). However, by mode the carbonate can exceed 90% in some of the cumulus carbonatites (e.g., Xu et al., 2007). Modal abundance of the carbonate minerals in the carbonatite ranges between 65 to 80%. Forsterite-bearing calcite carbonatite is also reported from the Kovdor complex of Kola Peninsula (Veksler et al., 1998). Co_2 enriched volatile magmas may result due to the phenomenon of crystallization and fractionation of early high-magnesium minerals (Panina and Motorina, 2008). One of the possibilities of the generation of carbonatite melts can be due to fractional crystallisation of CO_2-rich alkaline silicate magma. Experimental studies demonstrated that liquid immiscibility does occur between the silicates and carbonate melts (Hamilton and Ian 979). Sen, (1999), observed that Mg rich peridotite and pyroxenite of SACC were initially fractionated from the parental melilitic magma; resulting in enrichment of calcium and generation of carbonatite melt by the process of liquid immiscibility. However, Melluso et al., (2010), observed that the genesis of the Sung valley carbonatites (with very high Mg minerals), is not related to the mafic and felsic rocks in the Complex. Melluso et al., (2010), further indicated that the rocks of Sung complex evolved independently in batches from a primitive magma. The present study highlights the presence of high Mg olivine as a conspicuous silicate phase in the Sung valley carbonatite from Maskut area. Olivine is noticed as euhedral to subhedral grains (0.05 mm size) within the calcite and often a sharp reaction rim is noticed along the interface of olivine and carbonate (Figure 2). Mineral chemistry by EPMA indicates high MgO (54.43 to 55.92%) and low Cr_2O_3 content (upto 0.05) in the resorbed forsterite from the Sung carbonatite.

CONCLUSION

Presence of olivine exhibiting resorbed texture in the carbonatite of Sung Valley Complex indicates early crystallization of olivine (Figure 2). The high Mg nature of the olivine (average composition of $Fo_{97.3}$ based on EPMA analyses of the resorbed olivine) and its conspicuous reaction rim with the surrounding carbonate is a significant petrographic textural feature, indicating crystal-melt interaction between an early formed silicate and carbonate melt in the mantle originated Sung carbonatite. We observe that further analyses, involving mineral inclusion studies of the olivine from Sung carbonatite will help to understand the evolution of carbonatite melts of the SACC.

ACKNOWLEDGEMENTS

First author VVSS thankfully acknowledges Shri. Sudipta Lahiri and Late Shri. Jitendranath Ray, Deputy Directors General (Retd.), GSI and Shri. Jayapaul D, Director (Retd.) GSI, for their valuable support. Shri. Sandip Nandy, Geologist, Central Petrological Laboratory, GSI, Kolkata, is thankfully acknowledged for EPMA analyses. Dr. T.R.K. Chetty and an anonymous reviewer are thankfully acknowledged for their constructive review. We also gratefully acknowledge Dr. P.R. Reddy, Chief Editor for his support and editorial handling.

Compliance with Ethical Standards

The authors declare that they have no conflict of interest and adhere to copyright norms.

REFERENCES

Chakhmouradian, A.R., Ekaterina, R.P., and Zaitsev, A.N., 2016. Calcite and dolomite in intrusive carbonatites. Textural variations. Miner Petrol., v.110, pp: 333-360.

Chakraborty, S.K., and Thapliyal, A.P., 2000. Petrology and geochemistry of the Sung valley Alkaline-Ultramafic-Carbonatite Complex, Meghalaya. Unpub. Prog. Rep. G.S.I. FS 1996-1998.

Chattopadhyay, N., 1979. Report on the Sung Valley Alkaline-Ultramafic-Carbonatite Complex, Khasi and Jaintia Hills districts, Meghalaya. Unpub. Prog. Rep. G.S.I. FS 1976-1977.

Chattopadhyay, N., and Hashimi, S., 1983. Report on the investigation of the phosphate mineralisation in the Sung Valley Alkaline-Ultramafic-Carbonatite Complex, Meghalaya. Unpub. Prog. Rep. G.S.I. FS 1980-1981.

Chattopadhyay, N., and Hashimi, S., 1984. The Sung Valley alkaline-ultramafic-carbonatite, East Khasi and Jaintia Hills districts, Meghalaya. Rec. Geol. Surv. India, v.113, pp: 24-33.

Deer, W.A., Howie, R.A., and Zussman, J., 1992. An introduction to the rock-forming minerals (2nd ed.). Harlow: Longman ISBN 0-582-30094-0.

Ferry John, M., Ushikubo Takayuki and John W. Valley., 2011. Formation of Forsterite by Silicification of Dolomite during Contact Metamorphism. Journal of Petrology., v.52. no.9, pp: 1619-1640.

Gogoi, K., 1973. Geological mapping of parts of Khasi and Jaintia Hills, Meghalaya. Unpub. Prog. Rep. G.S.I. FS 1972-1973.

Hamilton, D.L., and Ian, C., 1979. Freestone, Dawson J. Barry and Donaldson, H. Colin., Origin of carbonatites by liquid immiscibility. Nature 279, pp: 52-54.

Hammouda, T., and Laporte, D., 2000. Ultrafast mantle impregnation by carbonatite melts. Geology., v.28, no.3, pp: 283-285.

Jyotiranjan Ray, S., Trivedi, J.R., and Dayal, A.M., 2000. Strontium isotope systematics of Amba Dongar and Sung Valley carbonatite-alkaline complexes, India: evidence for liquid immiscibility, crustal contamination and long-lived Rb/Sr enriched mantle sources. Jour. of Asian Earth Sciences., v.18, no.5, pp: 585-594.

Krishnamurthy, P., 1985. Petrology of the carbonatites and associated rocks of Sung Valley, Jaintia hills district, Meghalaya, India. J. Geol. Soc. India, v.26, pp: 361-379.

Le Maitre, R.W., 2002. Igneous rocks: a classification and glossary of terms: recommendations of International Union of Geological Sciences Subcommission on the Systematics of Igneous Rocks. Cambridge University Press, pp: 236.

Lee, M.J., Lee, J.I., Garcia, D., Moutte, J., Williams, T.C., Wall, F., and Kim, Y., 2005. Pyrochlore chemistry from the Sokli phoscorite-carbonatite complex, Finland: Implications for the genesis of phoscorite and carbonatite association. Geochemical Journal, v.40, pp: 1-13.

Lee, W., and Wyllie, P.J., 1997. Liquid Immiscibility in the Join NaAlSiO_4-NaAlSi_3O_8-CaCO_3 at 1 GPa: Implications for Crustal Carbonatites. Journal of Petrology, v.38, no.9, pp: 1113-1135.

Melluso, L., Srivastava, R.K., Guarino, V., Zanetti, A., and Sinha, A.K., 2010. Mineral compositions and petrogenetic evolution of the Ultramafic-Alkaline-Carbonatite complex of Sung Valley, Northeastern India. Can. Mineral., v.48, pp: 205-229.

Panina, L.I., and Motorina, U.V., 2008. Liquid immiscibility in deep-seated magmas and the generation of carbonatite melts. Geochemistry International, v.46, no.5 pp: 448-464.

Ranjith, A., and Sadiq, M., 2013. Preliminary search for REE in the peripheral part of Sung ultramafic-alkaline carbonatite complex, East Khasi Hills and Jaintia Hills district, Meghalaya (G4 Stage). Rec. Geol. Surv. India, Pt. 145–146, pp: 22-28.

Ray, J.S., and Pandey, K., 2001. ^{40}Ar- ^{39}Ar age of carbonatite-alkaline magmatism in Sung Valley, Meghalaya, Journal of Earth System Science, v.110, no.3, pp: 185-190.

Sadiq, M., Ranjith, A., and Ravi Kumar Umrao., 2014. REE mineralization in the carbonatites of the Sung valley ultramafic-alkaline-carbonatite complex, Meghalaya, India. Central European Journal of Geosciences, v.6, no.4, pp: 457-475.

Scott Messenger, Lindsay P. Keller, and Dante S. Lauretta., 2005. "Supernova olivine from cometary dust". Science., v.309, no.5735, pp: 737-741.

Sen, A.K., 1999. Origin of the Sung Valley Carbonatite Complex, Meghalaya, India: Major Element Geochemistry Constraints. Jour. Geol. Soc. Ind., v.53, no.3, pp: 285-297.

Srivastava, R.K., and Sinha, A.K., 2004. Early Cretaceous Sung Valley ultramafic-alkaline-carbonatite complex, Shillong Plateau, Northeastern India: petrological and genetic significance. Min. and Pet., v.80, no.3, pp: 241-263.

Srivastava, R.K., Heaman, L.M., Sinha, A.K., and Shihua, S., 2005. Emplacement age and isotope geochemistry of Sung Valley alkaline - carbonatite complex, Shillong Plateau, northeastern India: implications for primary carbonate melt and genesis of the associated silicate rocks. Lithos, v.81, pp: 33-54.

Veena, K., Pandey, B.K., Krishnamurthy, P., and Gupta, J.N., 1998. Pb, Sr and Nd Isotopic Systematics of the Carbonatites of Sung Valley, Meghalaya, Northeast India: Implications for Contemporary Plume-Related Mantle Source Characteristics. Jour. of Pet., v.39, no.11-12, pp: 1875-1884.

Veksler, I.V., Nielsen, T.F.D., and Sokolov, S.V., 1998. Mineralogy of Crystallized Melt Inclusions from Gardiner and Kovdor Ultramafic Alkaline Complexes: Implications for Carbonatite Genesis. Journal of Petrology., v.39, no.11-12, pp: 2015-2031.

Viladkar, S.G., Schleicher, H., and Pawaskar, P., 1994. Mineralogy and geochemistry of the Sung Valley carbonatite complex, Shillong, Meghalaya, India. NJb Mineral, MhH11, pp: 499-517.

Woolley, A.R., 2001. Alkaline rocks and carbonatites of the world: Africa (Pt.3) The Geological Society Spl. Pub. ISBN 10: 1862390835.

Xu, C., Campbell, I.H., Allen, C.M., Huang, Z., Qi, L., Zhang, H., and Zhang, G., 2007. Flat rare earth element patterns as an indicator of cumulate processes in the Lesser Qinling carbonatites, China. Lithos., v.95, pp: 267-278.

Yoshino Takashi, Micka¨el Laumonier, Elizabeth Mcisaac, and Tomoo Katsura., 2010. Electrical conductivity of basaltic and carbonatite melt-bearing peridotites at high pressures: Implications for melt distribution and melt fraction in the upper mantle. Earth and Planetary Science Letters, v.295, no.3-4, pp: 593-602.

Yusuf, S., and Saraswat, A.C., 1977. A preliminary note of carbonatite in Sung valley of Jaintia Hills district, Meghalaya. Current Science, v.46, no.20, pp: 703-704.

Received on: 21.2.17; Revised on: 4.4.17; Accepted on: 6.4.17

J. Ind. Geophys. Union (July 2017)
v.21, no.4, pp: 298-308

Intraseasonal Variability of Rainfall, Wind and Temperature during summer monsoon at an Indian tropical west coast station, Goa– Role of synoptic systems

B. S. Murthy* and R. Latha

Indian Institute of Tropical Meteorology, Dr Homi Bhabha Road, NCL Post, Pune-411008, India

*Corresponding Author: murthy@tropmet.res.in

ABSTRACT

Rain gauge data of daily rainfall and in-situ high frequency (10 Hz) measurements of turbulent wind and air temperature at Goa (15.5^{0}N, 73.8^{0}E), located on the west coast of India, are subjected to wavelet analysis to understand dominant periods of oscillations during the summer monsoon. Heavy (subdued) rainfall spells over the west coast of India at Goa are associated with intense phase of 3-7 day (10-20 day) mode of Monsoon Rainfall Oscillation (MRO) as revealed by wavelet analysis of daily rainfall. This is unlike that over the monsoon core region where active or weak monsoon is associated with the strong phase of 10-20 day or 30-60 day mode of oscillations, respectively. Intense or weak rainfall spells are found to be coincident with positive or negative wind anomalies at 850 hPa over the Arabian Sea off Goa coast. Maxima or minima in the relative contribution of 3-7 day mode to total variance are mostly coincident with active or feeble/no 'offshore trough' or Somali Jet positive or negative wind anomalies indicating that 'offshore trough' and 'Somali Jet' oscillations could apparently be responsible for dominance of 3-7 day mode over other modes. Oscillations of wind and temperature reveal that 3-7 day and 10-20 day modes are in opposite phase, especially during July and August. When the convection associated with the lows/depressions in the Bay of Bengal extends up to the west coast, the 3-7 day mode of rainfall and wind are 'in phase' and they are in 'opposite phase' when the 'offshore trough' is prominent.

Key words: Monsoon rainfall oscillation, West coast of India, 3-7 day mode, offshore trough.

INTRODUCTION

Intra-seasonal and inter-annual variability in Indian Summer Monsoon Rainfall (ISMR) has been studied by several researchers (Krishnan et al., 2000; De and Mukhopdhyay, 2002; Bhatla et al., 2004; Gadgil and Joseph 2003 and others) and this topic continues to be of interest from the perspective of prediction at various space and time scales. Inter-annual variability depends on intra-seasonal variability (Ferranti et al., 1997; Krishnamurthy and Shukla 2000; Goswami and Mohan, 2001; Lawrence and Webster 2001), which in turn depends on frequency of occurrence of lows, depressions, cyclones and their movement across the Indian landmass as well as the seas on either side of India. The conceptual model of Krishnamurthy and Shukla (2000) suggests that the "active" and "break" phases are fluctuations about seasonally persisting components that vary on inter-annual time scale. If the seasonally persisting components make a relatively large contribution to the seasonal mean rainfall and are related to slowly varying boundary forcing or other low frequency global circulations, the seasonal rainfall anomaly over India may be more predictable.

ISMR exhibits various dominant modes of oscillations or quasi periodicities like 3-7 day, 10-20 day and 30-60 day. While the latter two modes are associated with "active/break" cycle and large-scale circulation features (Kulkarni et al., 2011), the former mode is linked to waves, depressions and storms with a lifetime of 2-7 days that arise from instability induced by horizontal and vertical wind shear and convection (Krishnamurti and Sanjay, 2003). These high-frequency (2 to 7 day) time scales are a major source of energy for the 30-60 day Madden- Julian Oscillation (MJO) (Sheng and Hayashi, 1990 a, b). The above results are the outcome of the analyses of large data of a few decades to 100 years of seasonal rainfall and based mainly on the variability of rainfall over central and north-west India, known as monsoon core region. The west coast of India experiences heavy rainfall (> 10 cm/day) mostly when offshore trough over the Arabian Sea parallel to the peninsular India is prominent and it is usually well-marked during active monsoon conditions. Meso-scale vortices that develop in the offshore trough are responsible for heavy rainfall events over the coast (George, 1956). Field experiments like MONEX-1979 and ARMEX-2002 (Sikka, 2003; Francis and Gadgil, 2006) had been conducted to investigate the organization of strong offshore convection along the west coast of India. Maintenance of offshore convection is attributed to upstream convergence aided by frictional convergence as the monsoon flow approaches the west coast (Grosman and Durran, 1984) and also the dynamics of air-sea fluxes, latent heat release and

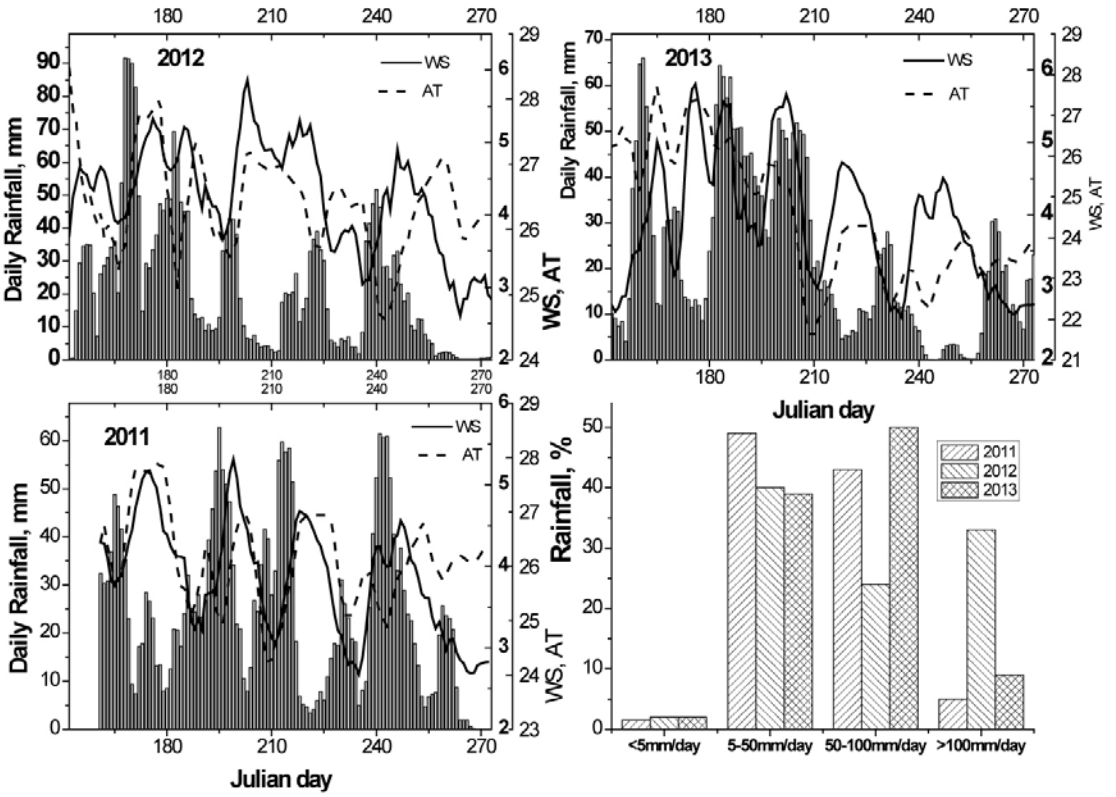

Figure 1. Rainfall (bars), wind speed (solid curve) and air temperature (dashed curve) during monsoon (June to September) (lower left) 2011, (top left) 2012 and (top right) 2013. Wind speed in ms^{-1}, air temperature in deg Celsius. Time series of daily mean are 5-point adjacent averaged to get clarity of oscillations; (lower right) Contribution of rainfall events in three categories (< 5mm; 5-50 mm; 50-100 mm and > 100 mm per day) to seasonal rainfall.

topography of the Western Ghats (Ogura and Yoshizaki, 1988).

Monsoon Rainfall Oscillation (MRO) over the west coast could be different from the central India since it is influenced more by the quasi-stationary mid-tropospheric disturbances and topography-related off-shore vortices while low pressure systems (LPS) over Bay of Bengal contribute little to heavy rainfall (Krishnamurthy and Shukla, 2005). Goa is chosen for the MRO study over the west coast as it is proximate to the Somali Jet and continuous in-situ observations are available. Although satellite and reanalysis estimates of rainfall are available for many years, they suffer from several uncertainties. As reported by Singh and Singh (2013), Quantitative Precipitation Estimates (QPE) derived from Kalpana-1 Satellite and Tropical Rainfall Measuring Mission (TRMM) rainfall did not have good agreement with observed gridded rainfall over six representative regions of India during southwest monsoons 2009 and 2010, though good correlation coefficients existed between the satellite precipitation estimates and actual rainfall. The objective of this study is to understand intraseasonal variability of in-situ observed rainfall, wind and temperature during summer monsoon over the west coast and probable controlling factors.

DATA AND METHODOLOGY

Wind and air temperature were measured at 10 Hz sampling at a height of 25 m using a sonic anemometer (Gill) during the monsoon season (June-September) of 2011, 2012 and 2013 at Saligao, Goa. These data were filtered to remove spikes, if any, and averaged over 30 minutes to prepare half-hourly and then daily time series. Very few missing half-hourly values were filled by linear interpolation. Time series of daily precipitation were obtained from rain gauge measurements. Goa experiences about 3000 mm of rainfall in the season as it is located towards north of the monsoon westerly low level jet core (850 hPa). These daily time series of Rainfall (RF), Wind Speed (WS) and Air Temperature (AT) were subjected to wavelet analysis in order to delineate the dominant modes of oscillations/periodicities and their occurrence as well as duration during the monsoon season. Morlet wavelet and the MATLAB program were used here for computing the power at various time scales and also the global spectrum (time averaged). Details of the technique are available elsewhere (Torrence and Compo, 1998; Foufoula-Georgiou and Kumar, 1995). The relative contribution of various modes of oscillations to the total variance (from all time

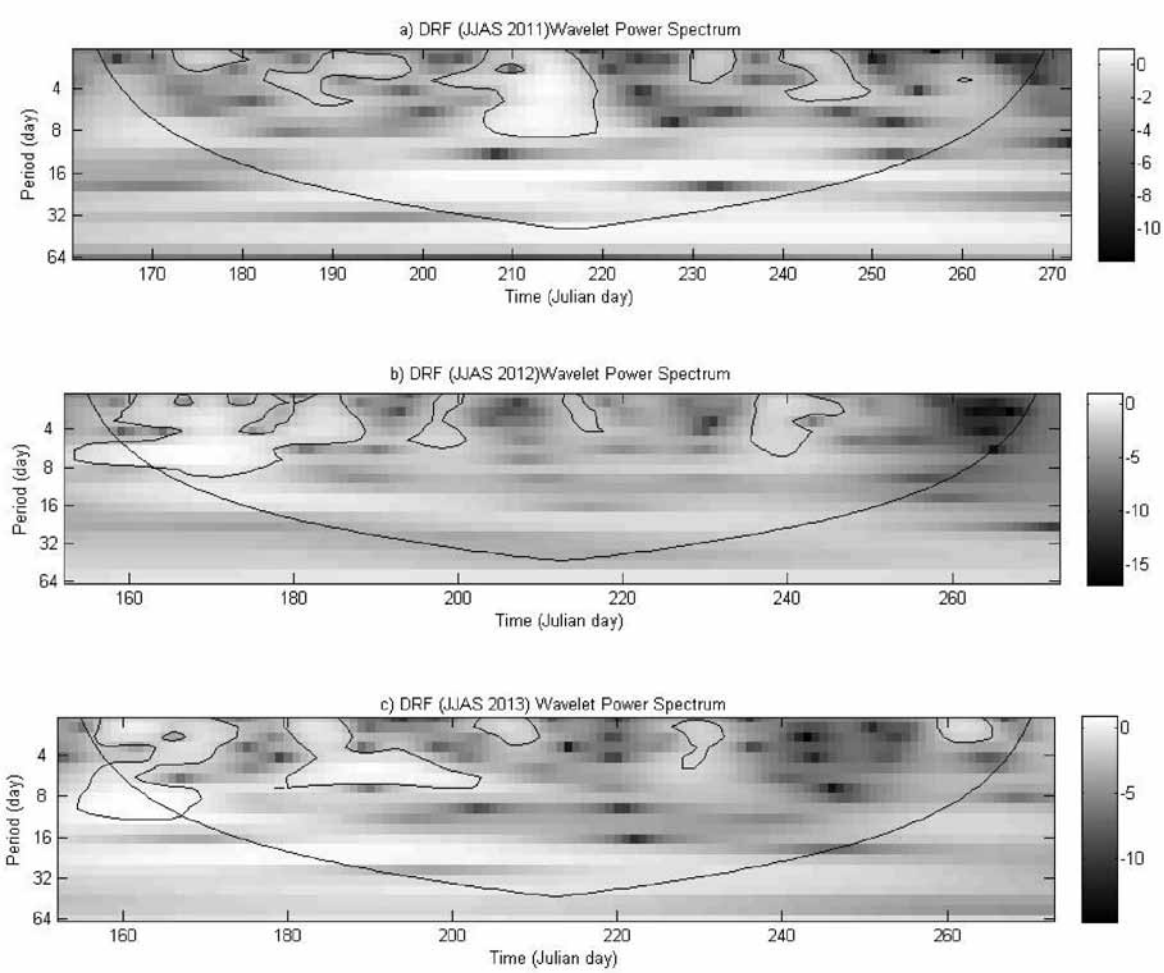

Figure 2. Wavelet power spectra of Daily Rainfall (DRF) for monsoons 2011, 2012 and 2013. Contours indicate power at 95% significance. Thick solid curve indicates 'cone of influence' below which values are dubious. Julian day ranges from 161 to 272 in 2011 (scaling is different) while it is from 152-273 in 2012 and 2013.

scales) was derived by integrating wavelet power (variance) in time scale bands (like 3-7 day; 10-20 day and 30-60 day) and normalizing it with total variance. Thus time series of percentage contributions of various modes to the total variance were compared to know their "active" and "weak" phases during the monsoon season.

Analysis

Time series of daily mean parameters are smoothed by 5 day adjacent averaging to illustrate coherent, "active"/"weak" spells of rainfall during the monsoon season without high frequency fluctuations. Figures 1a-c show time series of RF, WS and AT for 2011, 2012 and 2013. From these figures it can be inferred that there are about 3 to 4 spells of intense rainfall interspersed by approximately 10 or 20 days of subdued or little rainfall. These active phases are uniformly distributed in 2011 whereas they are dominant in June 2012 and in July 2013. Peaks in RF are associated with depressions/minima in WS while AT peaks in between the active spells of RF. ISMR was 102%, 93% and 106% of its Long Period Average (LPA) (www.imd.gov.in IMD monsoon reports) in 2011, 2012 and 2013 respectively and are considered as 'normal' monsoons. Rainfall sorted into 4 categories of < 5 mm/day, 5-50 mm/day, 50-100 m/day and > 100 mm/day indicates that maximum contribution to ISMR is from 5-50 mm/day events in 2011and 2012 while 50-100 mm/day events dominate in 2013 (Figure 1d). Very heavy rainfall (> 100 mm/day) events contributed $\sim 32\%$ in 2012, the year that had relatively less seasonal rainfall. Time lags of a few days were observed among RF, WS and AT on some occasions of intense/moderate RF events in all the years. Wind maxima followed intense rainfall events. The AT is expected to rise during the lull period between the heavy rainfall events. This could explain observed time lags among RF, AT and WS.

Wavelet power spectra of the daily RF for 2011, 2012 and 2013 (Figure 2) are depicted as Julian day-wave period

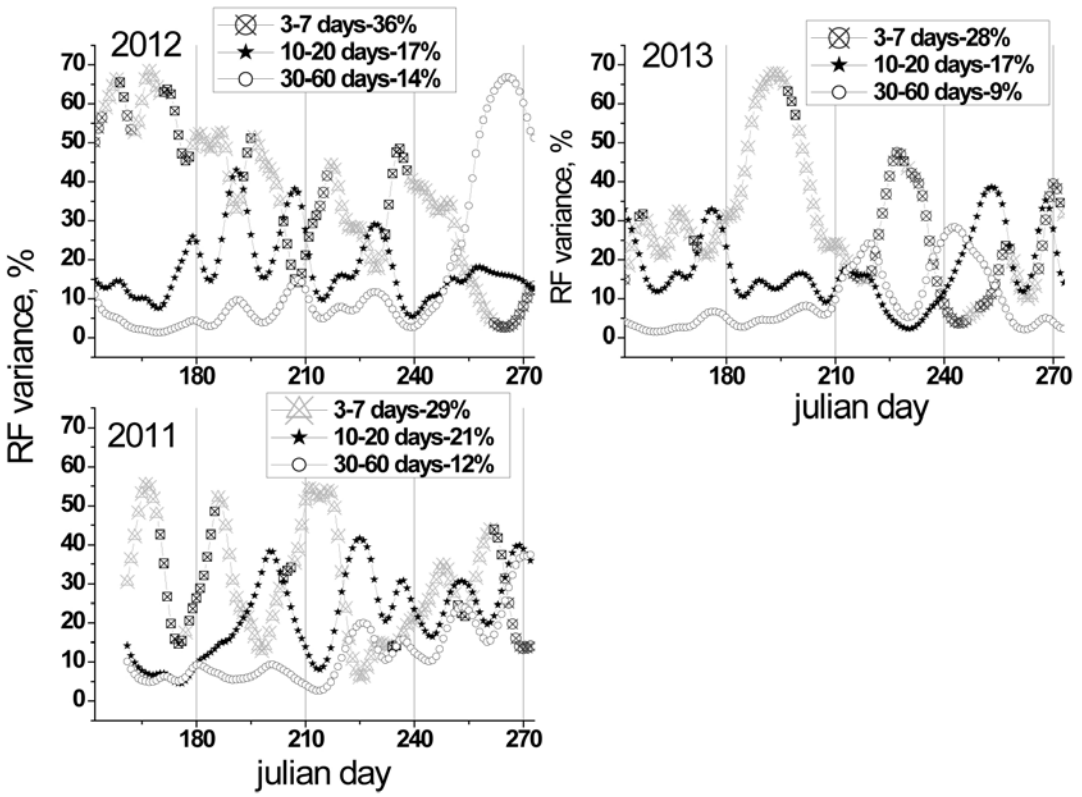

Figure 3. Relative contribution of various modes of Intraseasonal Oscillation (ISO) viz. 3-7 day; 10-20 day and 30-60 day modes, to total variance of rainfall for monsoon (lower left) 2011, (top left) 2012 and (top right) 2013. In the 3-7 day ISO curve, 'Triangle' represents 'active offshore trough'; 'square' and 'circle' indicate 'feeble' and 'No' offshore trough respectively as reported in IMD's annual monsoon reports. It may be noted that maxima in 3-7 day mode curve (active phase of 3-7 day ISO) are in general coincident with 'active' offshore trough while the minima (weak phase of 3-7 day ISO) are associated with 'feeble or 'no' offshore trough.

cross-section of power. It may be noted that less than 8 day periodicities are conspicuous.They occur with a gap of about 20 days in between them and correspond to active spells of RF. In 2011 they are distributed more or less uniformly while in 2012 and 2013 they are prevalent in the first half of the season as compared to the second half.

In order to quantify the relative contribution of various modes of monsoon rainfall oscillations to total variance through the season, percentage variance of 3-7 day, 10-20 day and 30-60 day modes are computed for 2011, 2012 and 2013 and are depicted in Figure 3. The 3 modes contribute 29%, 21% and 12% respectively to total variance indicating the dominance of 3-7 day mode over the other two modes. The peaks in 3-7 day mode roughly correspond to intense spells of RF in time series (Figure 1) indicating that 3-7 days mode are mainly responsible for intense RF spells over the west coast. Time series of 3-7 day mode curve has points of different shapes that represent the status of the 'offshore trough' through the season. 'Triangle' indicates active trough, 'square' corresponds to feeble trough while 'circle' represents 'absence of trough'. Thus the peaks with > 50% contribution are mostly associated with an active offshore trough. The 10-20 day mode is in the opposite phase of 3-7 day mode, especially in July and August; i.e., in general, while the 3-7 day mode is associated with intense rainfall, the 10-20 day mode is related to subdued rainfall. The 30-60 day mode becomes prominent during second half (August and September) and is in phase with the 10-20 day mode. Similar analyses of WS and AT (given in 'supplementary material as SFigure 1, 'SFig' referes to supplementary material) also indicates approximately an opposite phase relationship between 3-7 day and 10-20 day modes for both WS and AT, particularly in July and August. In 2012, the 3-7 day mode contributes on an average 36% to the total variance, which is twice of that by 10-20 day mode (Figure 3). Similar to 2011, generally the peaks in 3-7 day mode are associated with persistence of offshore trough ('Triangle' dots) while the minima are coincident with feeble or absence of offshore trough. The two modes (3-7 day and 10-20 day) are in opposite phase during July and August. The 30-60 day mode is in phase with 10-20 day mode. As shown in SFigure 2, WS and AT depicting

Table 1. Correlations between various modes of RF oscillations and comparison of Goa RF with TRMM rainfall over the west coast and the central India.

Correlation between parameters	Correlation, R		
	2011	2012	2013
Goa RF (Rain gauge) and West coast TRMM RF	0.54	0.21	0.20
Goa TRIMM RF and West coast TRMM RF	0.62	-	-
Goa TRIMM RF and Central India TRMM RF	0.04	-	-
Time series of Goa RF and 3-7 days mode variance of RF	0.31	0.66	0.55
RF modes: 3-7 days & 10-20 days	-0.61	-0.25	-0.38
RF modes: 3-7 days & 30-60 days	-0.46	-0.80	-0.51
RF modes: 10-20 days & 30-60 days	+0.71	-0.01	+0.06
Parameter	Value		
3-7 days mode variance contribution to total variance of RF	29 %	36 %	28 %
RF > 100 mm/day contribution to total RF	5 %	35 %	10 %
5 <RF<100 mm/day contribution to total RF	90 %	65 %	87 %

Note: R-Correlation; RF-Rainfall; TRMM RF (0.25 x 0.25 deg): Goa (lat 15.00, lon 73.25, lat 18.00, lon 74.10); West coast (72.42, 11.09, 75.94, 20.23); Central India (24.00, 78.00, 26.00, 80.00)

the percentage variance contribution through the season for the three modes supports the opposite phase relationship between the 3-7 day and 10-20 day modes in July and August. In 2013, the peaks in 3-7 day mode in June and July are associated with an active offshore trough leading to intense RF spells (Figure 3). In August, RF spell is not associated with an active offshore trough as indicated by absence of trough (Circle dots) suggesting the role of other systems. The 3-7 day and 10-20 day modes are roughly in opposite phase as observed in 2011 and 2012. Time series of variance of WS and AT in 2013 also show that 3-7 day and 10-20 day modes are mostly in opposite phase (SFigure 3).

DISCUSSION

Role of synoptic systems in rainfall variability

Time series of RF, WS and AT reveal that monsoon rain occurs in multiple spells with "active" and "weak/break" periods along with associated wind and temperature variations (Figure 1). An overview of these figures indicates that the peaks in WS follow (lagging) the peaks in RF while AT rises during "weak/break" periods of RF. The west coast of India, in general, is affected by the systems/ processes in the Arabian Sea rather than those in the Bay of Bengal due to the presence of the Western Ghats. Since the study location, Goa is situated towards the north of the semi-permanent 'Somali Jet' in the Arabian Sea, it is significantly influenced by shear vorticity of the jet that results in cyclonic circulation and convection leading to intense rainfall. Thus the fluctuations in Somali jet speed and the position of its core with respect to Goa determines the intensity of rainfall as well as wind speed. It appears that intense rainfall occurs (with less wind over Goa) and wind speed increases after the rainfall subsides. Anomalies of wind speed over the Arabian Sea off Goa coast are discussed below. Relatively clear skies and more sensible heat flux causes temperature to rise during the intervening period of active RF spells.

Our analyses find that 3-7 day mode of oscillation in RF dominates over the other two modes during active rainfall spells over the west coast, which is different from that over the monsoon core region or central India where the intense phases of 10-20 day mode and 30-60 day modes are related to "active/break" cycles respectively of monsoon (Kulkarni et al., 2011). Another contrasting feature is that 10-20 day and 30-60 day are in opposite phase over central India (Kulkarini et al., 2011) while the 3-7 day and 10-20 day are in opposite phase over the west coast. This implies that the intense phase of 10-20 day mode is related to subdued rainfall over the west coast while the same is related to active/intense rainfall over central/rest of India. According to Kulkarni et al., (2011) the intense phase is associated with anti-cyclonic circulation over the Indian Ocean, easterly flow over the equatorial Pacific Ocean resembling the normal or cold phase (La Nina) of El Nino Southern Oscillation (ENSO) phenomenon, and weakening of the north Pacific Sub-tropical High. It may be noted that in their paper Figure 1 indicates negative anomalies of rainfall over the west coast for strong phases of both 10-20 day and 30-60 day modes suggesting that the physical mechanism influencing the west coast could be different from that of central India. Our analysis of rainfall during the monsoons of 2011, 2012 and 2013, brings out the fact that good rainfall spells over Goa, representative of the west coast are associated with intense phase of 3-7 day mode, not the 10-20 day mode as over the rest of India.

Rainfall over Goa is compared to that over the west coast as well as the central India, obtained from Tropical Rainfall Measuring Mission, TRMM (Geovanni). Correlations between various modes of oscillations and rainfall are provided in Table 1. For 2011, TRMM rainfall (0.25 x 0.25 deg) over the west coast of India and Goa rainfall (Rain gauge) has a correlation (R) of 0.54 while it has R = 0.62 with Goa TRMM rainfall. For 2012 and 2013, the correlation between Goa RF and West coast TRMM RF is 0.21 and 0.20, respectively. In 2011 rainfall over Goa is uniformly distributed through the monsoon season with heavy rain events (> 100 mm/day) contributing ~ 5% to seasonal RF. In 2012 and 2013, heavy rain events contributed ~ 35% and 10%, respectively. It appears that when RF is moderate (RF between 5 and 100 mm/day contributes ~ 90%) and intense RF events are meager, TRMM RF over the west coast and Goa RF match reasonably well (in 2011) but they mismatch if intense rain events are significant (with 35% and 10% contribution to total RF) as in 2012 and 2013. No correlation is observed between the west coast and the central India RF as obtained from TRMM. Time series of Goa RF and 3-7 day mode variance of RF have R=0.31, 0.66, 0.55 in 2011, 2012 and 2013, respectively suggesting that if there are significant intense rainfall events then active RF spells are relatively better associated with 3-7 day mode of oscillation. Correlations among 3-7 day, 10-20 day and 30-60 day modes of RF oscillations indicate that reasonably better relationship is observed in 2011 (with a few heavy RF events) as compared to 2012 and 2013 (Table 1). Comparison of TRMM and Goa RF, thus indicates that Goa represents the west coast in RF variability reasonably well in 2011 but not so in 2012 and 2013. No relationship is observed between the west coast RF and the Central India RF, which may be indicating that different physical mechanism or same mechanism with different degrees of influence are in operation at these two locations. Central India (Monsoon core region) is prone to monsoon trough oscillations, "active/break" cycles, LPS in Bay of Bengal (BOB), Somali jet, etc. while the west coast is very much influenced by offshore trough, Somali jet, the Western Ghats and to some extent by LPS in Bay of Bengal (BOB) and the Arabian Sea. In addition to these synoptic scale systems that transport moisture leading to moisture convergence over land, inland terrestrial ecosystems pump in much moisture into the atmosphere through evapo-transpiration. Thus, it is quite difficult to explain from observations alone, which process dominates at what time to induce precipitation.

In addition to 'Somali jet' and 'offshore trough' over the Arabian Sea, there are several other synoptic systems (like low pressure systems and depressions and cyclonic circulations) that may also contribute partially to rainfall over the west coast in spite of the presence of the Western Ghats. There are 10 LPSs in 2011 out of which 5 formed over land, 4 over the BOB and 1 over the Arabian Sea. Depression over BOB during June 16-23 and the same over land during July 22-23 are coincident with strong and moderate phases of 3-7 day mode of RF. The one during September 22-24 also coincides with intense phase. In 2012 there are 10 LPS (2 in July; 5 in August; 3 in September) and no depressions. The monsoon trough was in its normal position during July 20 – August 16 giving wide spread rainfall. During the same period the 3-7 days mode shows weak and intense phases consecutively. There are no LPS in June but in the 3rd week intense rainfall of 90 mm/day occured over the west coast, which is related to positive wind anomalies of 'Somali jet'.

As shown in Figure 3, majority of the peaks in 3-7 day mode variance through the season are associated with active 'offshore trough'. But there are some exceptions like that in August 2013 (Figure 3c) that show 'absence of offshore trough' (Circle dots) but 3-7 day mode is in intense phase as well as rainfall (Figure 1c). IMD's monsoon report for 2013 mentioned that there were one depression over land and 5 low pressure systems of short duration in BOB in August. In July there are 3 LPSs and 1 depression in BOB and one LPS over land and intense and continuous rainfall is noticed in July 2013. From the perspective of the influence of lows and depressions and monsoon trough position on rainfall, it may be inferred that although the rainfall over the west coast shows dominance of 3-7 day mode, its intense phase (coincident with intense rainfall spell) cannot be attributed to a single one system like 'offshore trough' or 'low/depression' or 'monsoon trough oscillation'. At times there may be contributions from other systems like a sub-tropical westerly jet, Mascarene High, etc. However, most of the intense spells of rainfall (associated with peaks in 3-7 day mode variance) are found to be associated with an active 'offshore trough' as evident from Figure 3.

OLR from NOAA/ESRL weekly averaged plots (not shown here) indicate propagation/spread of convective cores over BOB to the peninsular India and the west coast in July and August 2013. There are 4 and 3 LPS in June and September, respectively in 2013. Thus the synoptic systems in BOB also influence the rainfall over the west coast to some extent since low OLR values indicate thick clouds that may or may not confirm precipitation always.

Oscillations in wind and temperature along with rainfall in terms of percentage variance in 3-7 day mode is depicted in SFigure 4 to understand the similarities in their modes of oscillations through the season. In 2011 there is one active RF spell in June, July and August and 2 spells in September as indicated by peaks in 3-7 day mode. In July and August the intense phase in RF is coincident with the weak phase of WS and vice versa while they are in same phase in June. In September some lag is observed between RF and WS phases. In 2012 also RF and WS are mostly

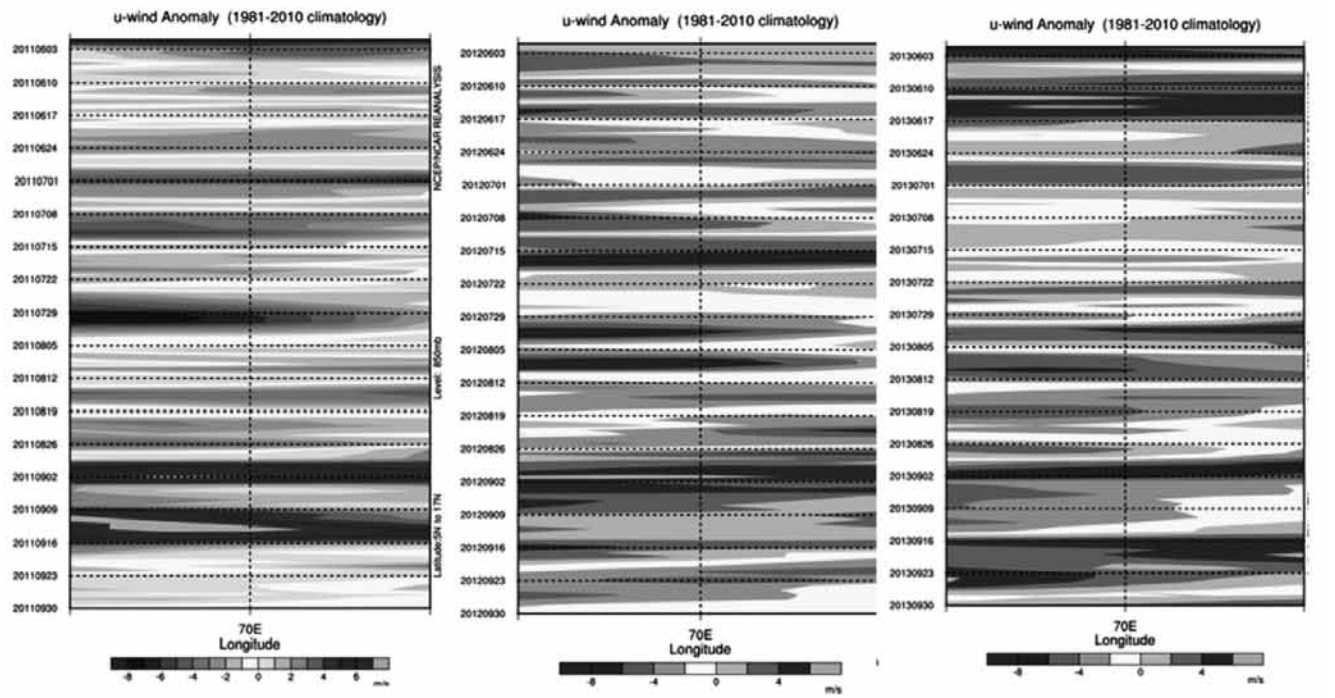

Figure 4. Time-longitude (65^{0}E to 75^{0}E) section of U-wind anomaly averaged between 5^{0}N to 17^{0}N to illustrate variability of 'Somali jet' strength during the summer monsoon a) 2011, b) 2012 and c) 2013 (left to right) respectively. Time axis starts from top to bottom (i.e. from June to September). Images have been obtained from NCEP/NCAR Reanalysis visualization website.

in opposite phase except during the last week of August. In 2013 during July (influenced by synoptic systems) RF, WS and AT are in phase while during August (with LPS of short duration) RF and WS are in opposite phase. No specific phase relationship is discernable between RF and AT for the 3-7 day mode of oscillation.

Objective analysis of synoptic systems and rainfall

Oscillations of monsoon rainfall are quite complex with interactions of various waves of different periodicities like the 3-7 day, 10-20 day and 30-60 day modes. The 10-20 day and 30-60 day modes are, in general, associated with "active/break" cycles of monsoon and MJO, respectively (Madden and Julian, 1972; Kulkarni et al., 2011 and several references therein), The 3-7 day mode is related to monsoon trough oscillations (Tyagi et al., 2012). Surface fluxes of momentum and moisture (thus wind and convection/rainfall) are observed to be amplified as the waves in MJO time scales interact with synoptic scales of 2-7 days (Krishnamurti et al., 2003). RF, WS and AT are in phase (SFigure 4) during the active spell of rain throughout July 2013 when synoptic activity is very strong (3 LPS in BOB; one over land) while RF and WS are roughly in opposite phase in August 2013 when synoptic systems are relatively weak with LPS of short duration. It appears that RF and WS are in opposite phase when offshore trough is prominent and in phase when lows/depressions are dominant in BOB with convective clouds extending up to the west coast (as inferred from OLR plots). 'Somali jet' being one of the major characteristic features of the summer monsoon influencing moisture transport over the Indian land mass (Joseph and Sijikumar, 2004), its effect on the west coast (especially over Goa as it crosses the coast at Goa latitude) is expected to be much more. Time-longitude cross-section of wind anomalies at 850 hPa (averaged between latitudes 5^0 N and 17^0 N) over the Arabian Sea off Goa coast (65^{0}E to 75^{0}E) is illustrated in Figure 4 for 2011, 2012 and 2013, respectively (Image provided by the NOAA/ESRL Physical Sciences Division, Boulder Colorado from their Web site at http://www.esrl.noaa.gov/psd/). It may be noted that in general positive (negative) anomalies of U-wind are associated with intense (weak) rainfall spells (Figure 4a and Figure 1a). Similar feature (correspondence between wind anomalies and rainfall spells) is exhibited during the 2012 (Figure 4b and Figure 1b) as well as in 2013 (Figure 4c and Figure 1c). Intense rainfall during August 29 – September 15 in 2011 (Figure 1a) is associated with positive wind anomalies (Figure 4a) while the weak rainfall spell during July 25 – August 3 relates to negative wind anomalies. Similarly, heavy or subdued rainfall (Figure 1b) during August 26 – September 15 in 2012 (August 1 – 19) corresponds to positive or negative wind anomalies (Figure 4b). However, intense spell during June 15-22 (Figure 1b)

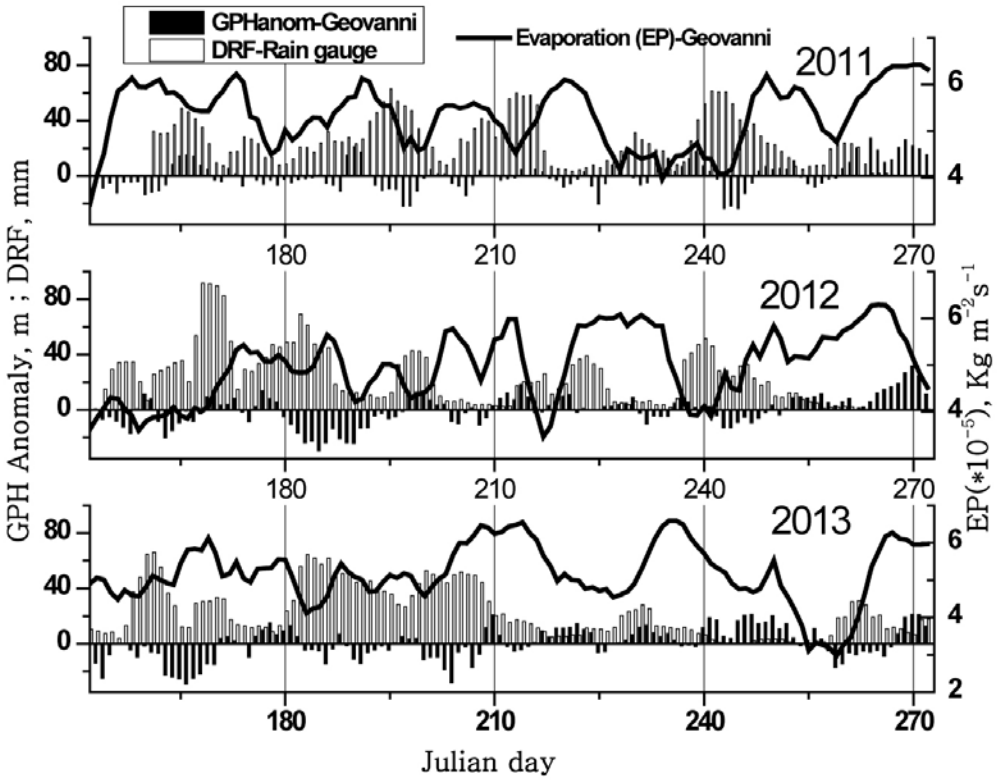

Figure 5. Time series of Daily rainfall (DRF), Geopotential height anomaly (GPH anom) and Evaporation rate (EP).

is not associated with positive wind anomalies, but near to 75^{0}E there are positive wind anomalies. In 2013 no rainfall is observed during September 1-15 (Figure 1c) and it coincides with strong negative wind anomalies (Figure 4c). It appears that in general positive wind anomalies over the Arabian Sea tend to produce intense rainfall over the coast.

In order to understand the role of LPS or depressions, Somali jet wind anomalies and offshore trough in causing intense rain spells, we have tabulated the presence of these systems during each one of the rain spells in 2011, 2012 and 2013 (Table 2). There are 4 active rain spells in 2011, 5 spells each in 2012 and 2013. To be more precise about the offshore trough, we have obtained geopotential height at 850 hPa from Geovanni – Atmospheric InfraRed Sounder (AIRX3STD_006_GPHeight_A/D, 1.0 x 1.0 deg) over the west coast (area-averaged over Lon 65-75; Lat 5-17deg). As shown in Figure 5, there are inconsistencies between rain spells, offshore trough, Offshore Trough (OST) (negative geopotential height) and wind anomalies and they are provided in Table 2 along with LPS/depressions. It may be noted that different systems prevailed during different spells. Though there are several LPS in BoB in 2011, 2012 and 2013, most of them are not coincident with active rain spells over Goa. Only 2 LPS/depressions formed over land are coincident with intense rainfall over Goa (i.e., Aug 12-14, 2012 and Aug 20-22, 2013) when offshore trough is absent as well as –ve wind anomalies are present. On two occasions (Aug 1-7, 2011 and June 15-22, 2012) no system/favorable condition prevailed, but intense rainfall occurred ,which could be due to local convection due to increase in evaporation.

Surface Evaporation (EP) (from Geovanni-Merra, 0.5 x 0.667 deg) at Goa (Lat 15.4-16.3, Lon 73.8-74.5 deg) indicates enhanced evaporation in between the intense rain spells (Figure 5) on most of the times. Although negative wind anomalies reduce moisture transport, terrestrial evapo-transpiration over the coast might be playing a role in increasing moisture and convection resulting in intense rainfall. As shown in SFigure 5, time series of area averaged total column water vapor (precipitable water) in 2011 over Goa (Lon 73.25-74.1; Lat 15-18 deg) during June-Sep remains mostly constant 50±2 kg m^{-2} as obtained from Geovanni Atmospheric InfraRed Sounder (AIRS AIRX3STD v006). It has little correlation with rainfall variability. The correlation between in-situ rainfall (at Goa) and OLR as well as geopotential height anomalies (area-averaged as above from Geovanni AIRS) is -0.3. As shown in SFigure 5 most of the rain spells are found to be associated with OLR (over Goa box as above) equal to or less than 200 Wm^{-2} (a value normally used to indicate deep convection by IMD). In July 2013, there were 4 LPS and 1 Depression that clearly indicated the spread of convection from BOB

Table 2. Distribution of Active rain spells over Goa, Offshore trough and Somali jet (wind anomaly) during the summer monsoons of 2011, 2012 and 2013.

Monsoon 2011					
Active rainfall spell	Around June 15, 2011	Around July 15, 2011	**Aug 1-7, 2011**	Sep 1-15, 2011	
OST(-ve GPH anomaly)	NO	YES	NO	YES	
Wind anomaly	+VE	-VE	-VE	+VE	
Monsoon 2012					
Active rainfall spell	**June 15-22, 2012**	July 1-7, 2012	July 15-22, 2012	**Aug 7-15, 2012**	Around Sep 1, 2012
OST(-ve GPH anomaly)	NO	YES	NO	NO	YES
Wind anomaly	-VE	+VE	-VE -Jul 15-18 +VE -Jul 19-22	-VE	+VE

Note: GPH – Geopotential Height at 850 hPa. In 2011 there were no LPS or Depression coincident with the active rain spells at Goa. The four active spells marked BOLD are the ones during which both 'Offshore Trough (OST)' and 'Positive Wind anomalies' were absent. However, the events during Aug 12-14, 2012 and Aug 20-22, 2013 were coincident with LPS and Depression respectively over land. Other active spells were coincident with either OST or Positive Wind anomaly of Somali Jet or both. Thus active rain spells over Goa seem to be mainly influenced by OST and Somali Jet.

to the west coast as seen in OLR anomalies (NOAA/ESRL visualization-- not shown here). Since offshore trough and positive wind anomalies (Figure 5) are also present, it is hardly possible to single out one system as the cause of intense rain spells in July 2013. Although active rain spells are correlated with Offshore trough intensity (R = -0.3), wind anomalies are not consistent with some rainfall spells (June and July) indicating that moisture transport from the Arabian Sea may not be as important as expected. Since the total water vapor is not varying much, the expected decrease in moisture transport (by negative wind anomalies) appears to be compensated by local evapo-transpiration. As shown in Figure 1, wind and air temperature peaks in between intense rainfall events suggests that high temperature and wind result in more evaporation from the land surface leading to intense rainfall after a few days (Figure 5). At smaller spatial scales, local factors (such as air temperature) influence intense rainfall spells more than the large scale factors (Mondal and Mujumdar, 2015). Our results corroborate this fact that local processes also at times contribute much to building up of moisture leading to active rain spells when the synoptic scale environment is unfavorable.

Thus the rainfall over the west coast seems to be mainly affected by Somali jet anomalies and offshore trough intensity and its variability exhibits relatively dominant mode of 3-7 day of monsoon oscillation during intense RF period. Recent study by Karmakar et al., (2015) inferring that the relative strength of Low Frequency Oscillation (LFO) (20–60 day) modes have a significant decreasing trend during the past six decades and this reduction being compensated by a gain in synoptic-scale (3–9 day) variability, corroborates our results. Predictability of seasonal monsoon rainfall increases if the LFO contribution (seasonally persisting component) is significant as it depends on slowly varying boundary conditions and large scale circulations (Krishnamurthy and Shukla, 2000). At smaller spatial scales, local factors (such as air temperature) influence intense rainfall spells more than the large scale factors (Mondal and Mujumdar, 2015). Our study confirms that high frequency mode (3-7 day) associated with semi-permanent systems over the Arabian Sea plays a significant role in rainfall variability over the west coast.

CONCLUSION

Variability of the summer monsoon rainfall over the west coast is dominated by 3-7 day mode as compared to 10-20 day and 30-60 day modes. Unlike the monsoon rainfall over core region, which is dominated by strong 10-20 day mode during the active monsoon period, the rainfall over west coast of India is dominated by an intense phase of 3-7 day mode during active spells of rainfall. Similarly, the 3-7 day and 10-20 day modes are in opposite phase over the west coast, especially during July and August while the 10-20 day and 30-60 day modes are in opposite phase over the monsoon core region. Intense phase of the 3-7 day mode over the west coast is observed to be mostly governed by active 'offshore trough', Somali jet positive wind anomalies and local surface evaporation while some low pressure systes/depressions in Bay of Bengal also contribute to the convection over the west

coast. Rainfall and wind are in opposite phase in terms of relative contribution of 3-7 day mode of oscillation to total variance when the 'offshore trough' is active while they are in phase when the influence of lows/depressions in Bay of Bengal is relatively dominant over the west coast. Thus monsoon rainfall oscillatory modes associated with active rainfall spells over the west coast are unique and different to that observed over monsoon core region. This is mainly due to different degrees of influence by synoptic and semi-permanent systems.

ACKNOWLEDGEMENT

Authors hereby acknowledge with thanks NOAA/ESRL for providing 'online visualization' of meteorological parameters. We are thankful to Geovanni v4.17.1 for providing geopotential height, OLR, precipitable water, latent heat flux, surface evaporation, etc. that have been used in this manuscript for analysis. We would like to thank Prof. T.N. Krishnamurti, Dr. M. Rajeevan and Dr. R. Kriplani for valuable suggestions and comments. We also thank Dr. Onkari Prasad, Dr. Omvir Singh and Dr. M.R.K. Prabhakara Rao for their valuable suggestions that helped us improve the analysis. We are thankful to Prof. B.N. Goswami and IITM for funding the 'Field observational program' at Saligao, Goa. Thanks are due to the Department of Fisheries and Department of Science and Technology, Goa state for providing their 'Tower' and ground support during the experiment. We also thank India Meteorological Department, Pune for providing rainfall data and annual monsoon reports.Thanks are due to Chief Editor for his support and final editing.

Compliance with Ethical Standards

The authors declare that they have no conflict of interest and adhere to copyright norms.

REFERENCES

Bhatla, R., Mohanty, U.C., Raju, P.V.S., and Madan, O.P., 2004. A study on dynamic and thermodynamic aspects of breaks in the summer monsoon over India, International Journal of Climatology, v.24, pp: 341-360.

De, U.S., and Mukhopdhyay, R.K., 2002. Breaks in monsoon and related precursors, Mausam, v.53, pp: 309-318.

Ferranti, L., Slingo, J.M., Palmer, T.N., and Hoskins, B.J., 1997. Relations between interannual and intraseasonal monsoon variability as diagnosed from AMIP integrations, Quart J Roy Meteorol Soc, v.123, pp: 1323-1357.

Foufoula-Georgiou, E., and Kumar, P., 1995. Wavelets in Geophysics. Accademic Press, pp: 210-222.

Francis, P.A., and Gadgil, S., 2006. Intense rainfall events over the west coast of India, Meteor. Atmos. Phys., v.94, pp: 27-42.

Gadgil, S., and Joseph, P.V., 2003. On breaks of the Indian monsoon. Indian Academy of Sciences, Earth and Planetary Sciences, v.112, pp: 529-558.

George, P.A., 1956. Effect of offshore vortices on rainfall along the west coast of India, Ind J Meteorol Geophys, v.7, pp: 235-240.

Goswami, B.N., and Mohan, R.S.A., 2001. Intraseasonal Oscillations and Interannual Variability of the Indian Summer Monsoon, Journal of Climate, v.14, pp: 1180-1198.

Grossman, R.L., and Durran, D.R., 1984. Interaction of Low-Level Flow with the Western Ghat Mountains and Offshore Convection in the Summer Monsoon, Monthly Weather Review, v.112, pp: 652-672.

Joseph, P.V., and Sijikumar, S., 2004. Intraseasonal Variability of the Low-Level Jet Stream of the Asian Summer Monsoon, Journal of Climate, v.17, pp: 1449-1458.

Karmarkar, N., Chakraborty, A., and Nanjundiah, R.S., 2015. Decreasing intensity of monsoon low-frequency intraseasonal variability over India, Environmental Research Letters, v.10, pp: 54018.

Krishnamurthy, V., and Shukla, J., 2000. Intraseasonal and Interannual Variability of Rainfall over India, Journal of Climate, v.13, pp: 4366-4377.

Krishnamurthy, V., and Shukla, J., 2005. Intraseasonal and seasonally persisting patterns of Indian monsoon rainfall. COLA Technical Report, CTR 188.

Krishnamurti, T.N., Chakraborty, D.R., Cubukcu, N., Stefanova, L., and Vijaya Kumar, T.S.V., 2003. A mechanism of the Madden–Julian Oscillation based on interactions in the frequency domain, Quarterly Journal of the Royal Meteorological Society, v.129, pp: 2559-2590.

Krishnamurti, T.N., and Sanjay, J., 2003. A new approach to the cumulus parameterization issue, Tellus, Series A: Dynamic Meteorology and Oceanography, v.55, pp: 257-300.

Krishnan, R., Zhang, C., and Sugi, M., 2000. Dynamics of Breaks in the Indian Summer Monsoon, Journal of the Atmospheric Sciences, v.57, pp: 1354-1372.

Kulkarni, A., Kripalani, R., Sabade, S., and Rajeevan, M., 2011. Role of intra-seasonal oscillations in modulating Indian summer monsoon rainfall, Climate Dynamics, v.36, pp: 1005-1021.

Lawrence, D.M., and Webster, P.J., 2001. Interannual Variations of the Intraseasonal Oscillation in the South Asian Summer Monsoon Region, Journal of Climate, v.14, pp: 2910-2922.

Madden, R.A., and Julian, P.R., 1972. Description of Global-Scale Circulation Cells in the Tropics with a 40–50 Day Period, Journal of the Atmospheric Sciences, v.29, pp: 1109-1123.

Mondal, A., and Mujumdar, P.P., 2015. Modeling non-stationarity in intensity, duration and frequency of extreme rainfall over India, Journal of Hydrology, v.521, pp: 217-231.

Ogura, Y., and Yoshizaki, M., 1988. Numerical Study of OrograPhic-Convective Precipitation over the Eastern Arabian Sea and the Ghat Mountains during the Summer Monsoon, Journal of the Atmospheric Sciences, v.45, pp: 2097-2122.

Sheng, J., and Hayashi, Y., 1990a. Estimation of Atmospheric Energetics in the Frequency Domain during the FGGE Year, Journal of the Atmospheric Sciences, v.47, pp: 1255-1268.

Sheng, J., and Hayashi, Y., 1990b. Observed and Simulated Energy Cycles in the Frequency Domain, Journal of the Atmospheric Sciences, v.47, pp: 1243-1254.

Sikka, D.R., 2003. Evaluation of monitoring and forecasting of summer monsoon over India and a review of monsoon drought of 2002, Proceedings of the Indian Academy of Sciences - Earth and Planetary Sciences A, pp: 479-504.

Singh, H., and Singh, O.P., 2013. Satellite derived precipitation estimates over Indian region during southwest monsoons, J. Ind. Geophys. Union, v.17, pp: 65-74.

Torrence, C., and Compo, G.P., 1998. A Practical Guide to Wavelet Analysis, Bulletin of the American Meteorological Society, v.79, pp: 61-78.

Tyagi, A., Asnani, G.C., Hatwar, H.R., Mazumdar, A.B., Joseph, P.V., Pattanaik, D.R., Rajeevan, M., Francis, P.A., and Gadgil, S., 2012, Monsoon Monograph, IMD., v.2.

Received on: 11.2.17; Revised on: 6.4.17; Accepted on:11.4.17

Mysterious Intraseasonal Oscillations in Monsoons

India's summer monsoon is a major event, single-handedly supplying water for agriculture across all of southern Asia. Because of its widespread effect on the region's environmental and socioeconomic health, the monsoon has long been studied by meteorologists, climatologists, and oceanographers hoping to understand and forecast its behaviour. One phenomenon in particular, the monsoon intraseasonal oscillations (MISOs), has captured scientists' interest. MISOs are alternating periods of heavy and minimal rainfall, each lasting for about a month or so and tending to follow a cyclical, northward shifting pattern from the equator to southern Asia. Although they were once believed to be a function of the tropical atmosphere, more recent studies have suggested that MISOs come from some kind of powerful atmosphere-ocean interaction.

For one such study, researchers examined the pathways of MISOs traveling across the Bay of Bengal, a region where the monsoon undergoes changes in intensity and frequency.

The same team has previously examined the role of ocean salinity stratification (layering of seawater with different salt contents) in variations in sea surface temperature and the atmospheric processes that produce rainfall. Here, however, they addressed the contribution from two other variables: the depth of the mixed layer, which lies just below the sea surface, and the thickness of the barrier layer, which forms the bottom of the mixed layer.Using an ocean model with data from 2000 to 2014, the researchers investigated how these upper ocean processes affect sea surface temperature (and how variations in sea surface temperature, in turn, affect rain formation in the MISOs). An influx of freshwater from the monsoon, the researchers found, creates a shallow mixed layer and a thick barrier layer, causing dramatic fluctuations in sea surface temperature over the course of the season. What's more, these air-sea interactions lead to the highly irregular rainfall patterns seen as the MISOs reach Asia.

Using advanced models and checking them against satellite data allowed the researchers to pinpoint these driving forces behind MISOs with more precision than in previous studies. Their efforts promise to improve the accuracy of future simulations and forecasts of the MISOs that occur during India's summer monsoon. (**Source**: Li et al, 2017,*Jou of Geophy Res: Oceans*, https://doi.org/10.1002/2017JC012692, 2017)

J. Ind. Geophys. Union (July 2017)
v.21, no.4, pp: 309-318

Forecasting El Nino events for the region Nino 3.4

Vinod Kumar*[1], K. S. Hosalikar[2] and M. Satya Kumar[3]

[1]Shyam Bhawan, Road No.11, Ashok Nagar, Kankarbagh Colony, Patna-800020
[2]Regional Meteorological centre, India Meteorological Department, Colaba, Mumbai-400005
[3]H. No. 6-3-565, Flat No. 301, Akshaya Apartment, Somajiguda, Hyderabad-500082
*Corresponding Author: vinodmanjusingh@gmail.com

ABSTRACT

Meteorologists have observed that northern hemisphere (NH) is warmer than southern hemisphere (SH). It is well known that extra tropical low pressure system tends to move equator ward and eastward. Cold air coming from 40°S or from South of 40°S is restricted by persistent lows (negative anomalies of geo potential height at 850 hPa: extra tropical lows) located between 140°E - 080°W/30°S- 40°S during El Nino years. Coverage area of lows may be found to be more in the northern latitudes. Prominent low features may be observed from January-February onwards when three months average value of the Ocean Nino Index (ONI) starts increasing from lower to higher value during certain years. Presence of low is also reflected by associated circulation/trough observed at 850 hPa vector wind between 140°E - 080°W/30°S-40°S. Westerly component of wind can be observed prominently between 160°E - 080°W and 40°S - equator depending upon the position of lows. Subtropical highs (positive anomalies of geo potential height at 850 hPa) at 850 hPa, located between 140°E - 080°W/ 30°S - 40°S weaken and shift southwards, and extra tropical low pressure systems, located south of 40°S shift northwards from their position during El Nino years. The contrast feature is observed during La Nina years and many non El Nino years in the form of prominent highs, which are observed between 140°E-080°W/30°S-40°S and the coverage area may be found to be more in the northern latitudes. Similar feature can be observed in the form of anti cyclone or ridge at 850 vector winds. Easterly component of wind can be observed prominently between 160°E - 080°W and 40°S - equator depending upon the position of highs.

Nino 3.4 is 5°N-5°S/170°W-120°W

Key words: Geo potential height anomalies at 850 hPa, low, high, ONI, El-Nino and La Nina years.

INTRODUCTION

Rise in ONI values (ONI is based on SST departures from average in the Nino 3.4 region) for Nov-Dec-Jan from previous three months average Oct-Nov-Dec sets the panic alarm among the meteorologists all over the globe from January-February onwards. It was widely reported in Indian News Media in the last week of January 2017 (as quoted by private weather forecaster "Skymet"), "El Nino could resurface this year, affecting rainfall in the country. The current prediction indicates a rise in SST and if the trend sustains it could lead to a weak monsoon this year". As per ENSO bulletin issued by NOAA dated 6th February 2017, ONI value for Nov-Dec-Jan (NDJ) 2017 has increased to -0.7 from -0.8 from previous months (OND 2016) ONI value. A weaker than normal Indian monsoon has profound impacts on food production, energy supply and the economy of India. As has been widely reported recently, a weak monsoon could push up food prices and with it inflation testing the present Government's ability to promote economic growth (Slingo et al., 2014). A close observation of monsoon rainfall during El Nino and non El Nino years exhibits a rather unpredictable monsoon rainfall pattern, detailed below: 1) The available recorded information indicates that normal monsoon rainfall occurred over India during El- Nino years: 1953, 1957, 1958, 1963, 1969, 1976, 1977, 1994, 1997 and 2006 (1958 and 1994 have been considered as El Nino years as ONI value reached ≥ 0.5°C from SON). 2) In comparison deficient rainfall occurred over India during non-El-Nino years 1966 and 1974. 3) In contrast deficient rainfall occurred during El-Nino years: 1951, 1965, 1972, 1979, 1982, 1986, 1987, 1991, 2002, 2004, 2009 and 2015 (1979 has been considered as El Nino year because ONI value reached ≥0.5°C from SON). {P.S: El Nino years, in which ONI value reached ≥0.5 from OND (1968, 2014) and started decreasing from DJF and onwards (1983, 1992 and 1998), have not been included in El-Nino years}.

As the details given above clearly exhibit a quixotic monsoon rainfall pattern during El Nino and non El Nino years an attempt has been made, in the present study, to examine the possibility of forecasting EL-Nino events a few months before the onset of Indian summer monsoon in June or at least in the first week of June.

Shortly after Christmas each year a warm ocean current flows south along the coasts of Ecuador and Peru. Not every year, but occasionally, that current is stronger; it flows further south and is very warm. The result is extra

heavy rain, which the coastal inhabitants of those countries have always welcomed for abundance of crops that it brings, and hence the name El Nino (the Christ child), for gifts of plenty that it bestows. Normally there is a large area of high pressure sitting over the eastern edge of the Pacific Ocean, just off the South American coast. From this high pressure zone the southern trade winds blow towards a large area of low pressure that is settled over Indonesia, on the other side of the ocean. These steady winds are strong and they drag the cool water that lies off South America westwards with them, so that it warms by contact with the atmosphere and by the heat of the Sun while travelling vast distances. The result is thick layer of warm water over the Western Pacific (around 40 cm higher than next to South American coast), and a mild deeper current that flows towards the east, known as counter current, which gently brings the warm water back, to cool, rise up off South America and start again. In the sky above, meanwhile, this body of warm water evaporates and moist air rises, adding to rains such as the monsoon. Further aloft and now drier, the air is carried by the fast moving upper-level winds to the east, where it cools and descends, adding to high pressure zone off South America where the cycle began. This, in essence, is the Walker circulation, and this is 'normality' (Lynch 2002). El Nino is a band of warm Ocean water temperatures that periodically develops off the Pacific coast of South America. El Nino is defined by prolonged warming in the Pacific Ocean sea surface temperatures when compared with the average value. The accepted definition is a warming of at least 0.5°C (0.9°F) averaged over the east central tropical Pacific Ocean. Typically, this anomaly happens at irregular intervals of two to seven years and lasts nine months to two years. The average period length is five years. When the warming occurs for only seven to nine months it is classified as El Nino conditions; when it occurs for more than that period it is called El Nino "episodes". Similarly La Nina conditions and episodes are defined for cooling. There is a phase of 'El Nino-Southern Oscillation' (ENSO), which refers to variations in the temperature of the surface of the tropical eastern Pacific Ocean and in air surface pressure in the tropical western Pacific. The two variations are coupled: warm oceanic phase, El Nino, accompanies high air surface pressure in the western Pacific, while the cold phase 'La-Nina' accompanies low air surface pressure in the western Pacific. The Southern Oscillation is the atmospheric component of El Nino. This component is an oscillation in surface air pressure between the tropical eastern and the western Pacific Ocean waters. The strength of the Southern Oscillation is measured by the Southern Oscillation Index (SOI). The SOI is computed from fluctuations in the surface air pressure difference between Tahiti and Darwin, Australia. El Nino episodes are associated with negative values of SOI, meaning there is below normal pressure over Tahiti and above normal pressure off Darwin. Low atmospheric pressure tends to occur over warm water and high pressure over cold water in part because of deep convection over the warm water (Reddy and Reddy 2014). The El Nino–Southern Oscillation is a single climate phenomenon that periodically fluctuates between 3 phases: Neutral, La Nina or El Nino. If the temperature variation from climatology is within 0.5°C (0.9°F), ENSO conditions are described as neutral. Neutral conditions are the transition between warm and cold phases of ENSO. Ocean temperatures (by definition), tropical precipitation, and wind patterns are near average conditions during this phase. Close to half of all years are within neutral periods. During El Nino years the cold water weakens or disappears completely as the water in the Central and Eastern Pacific becomes as warm as the Western Pacific (Wikipedia).

The onset of El Nino takes place during the northern hemispheric winter. At the time of onset of El Nino, weakening of the Southeast Pacific surface anticyclone and associated southeast trade winds, appearance of positive SST anomalies between 10°S and 30°S extending across much of the Southeast Pacific have been observed (Asnani, 2005). It has been observed that SST-anomalies in Eastern Pacific are directly and visibly connected to anomalies in the position and intensity of low-level subtropical anticyclones. It is also known that these low-level subtropical anticyclones in the eastern pacific form a chain of low-level subtropical anticyclones throughout the global subtropics; if one anticyclone has anomalous position or intensity, the whole global chain of low-level subtropical anticyclones manifests anomalies in position and intensity (Asnani and Verma 2007). Two types of El Nino episodes have been identified over Nino 3.4 area: (i) Spring (SP) type in which SST anomaly (SSTA) first increased to > 0.5°C in April or May and (ii) Summer (SU) type in which SSTA became >0.5°C in July-August. Composites of SSTA'S for these two types showed the following characteristics: (a) SP type generally shows stronger warm episode and also longer period episode than SU type event in terms of SSTA'S>0.5°C. (b) For the SP type events, equatorial westerly wind anomaly extends to International Date Line by January of EL Nino year; for SU type events, the westerly wind anomaly extends to International Date Line by May of the El Nino year, (Xu and Chan 2001). The inverse relationship between El Nino and ISMR is statistically significant only during and at the end of the monsoon season (Rajeevan and McPhaden, 2004). Most of the severe droughts over India are associated with El Nino. However, only less than half of El Nino events are associated with deficient rainfall over India. In other El Nino years, ISMR was either normal or excess. A recent study suggested that El Nino with warmest SST anomalies in the Central Pacific are more effective in focusing drought producing subsidence over India than events with the warmest SST

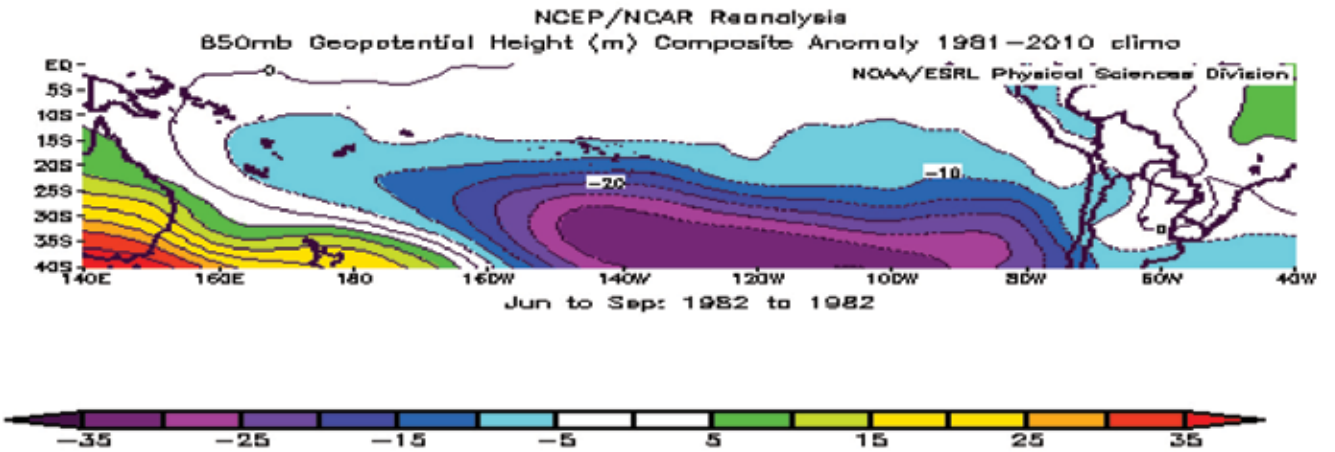

Figure 1. Anomaly of 850 hPa geo potential height for Jun-Sep 1982.

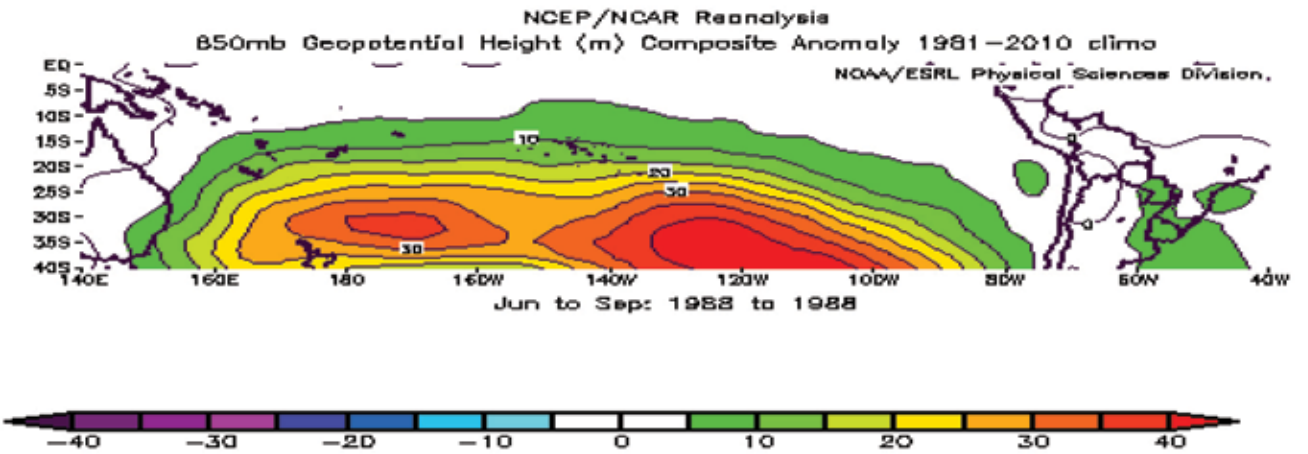

Figure 2. Anomaly of 850 hpa geo potential height for Jun-Sept 1988.

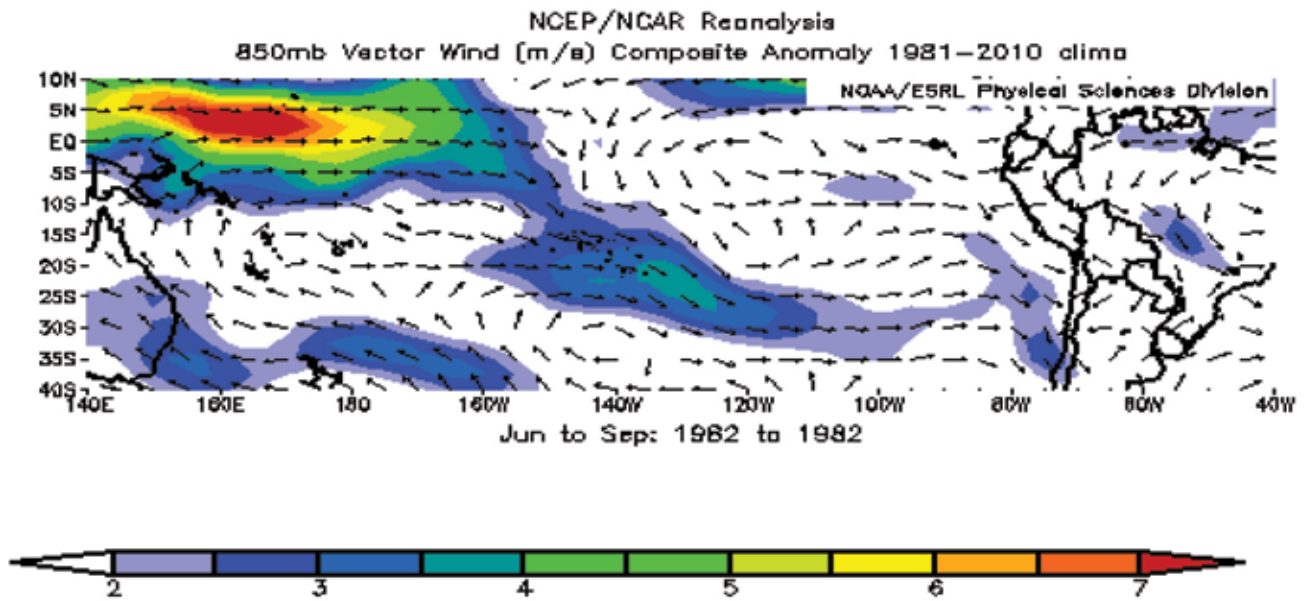

Figure 3. Anomaly of 850 hPa vector wind for June-September 1982.

anomalies in the eastern equatorial Pacific (Rajeevan and Pai, 2007). In the year 2014 Australian Weather Bureau declared an El Nino alert, saying there was at least a 70% chance of occurrence of the weather pattern that is also linked to weak monsoons in India, but some climatic models predicted that it could set in as early as July 2014. The alert was later withdrawn by the end of July. There was consensus among international weather agencies that an El Nino would occur in 2014 but its timing and intensity remained uncertain, as per the then existing scenario as on 30th July (Reddy and Reddy, 2014). For 2014, going by forecasts of IMD and Skymet, it appeared that El-Nino may hit Indian monsoon in the second half of monsoon period. At the time of prediction it was not clear and certain whether it would cause a drought or not. NOAA pegged the probability of El Nino developments intensifying by summer at 70%. Both the Indian weather agencies were forecasting a sub-normal rainfall (IMD forecast at 93% of LPA and Skymet at 94% of LPA but not a drought yet: Saini and Gulati 2014). The forecasts from the Met office (UK) seasonal prediction system from June for July, August and September showed substantial changes in the tropics-wide rainfall with notable decreases in the Indian monsoon. The risk of a poor monsoon was 2-3 times greater in 2014 than normal (Slingo et al., 2014). In reality; the intra monsoon rainfall pattern was rather fluctuating and unclear from region to region leading to considerable hardship to farming community. From this experience it has become clear that weather experts cannot come to any conclusion based on a limited data of local to regional nature, covering a narrow window of time. Keeping this in view we have made use of a large set of data covering a large span of time and viewed closely intricate variations from time to time to have a better synoptic view of weather pattern during El Nino and La Nina years.

At least one pair of high (+ anomaly) and low (- anomaly) combination (high- low or high- low- high or high- low- low or low- high- low- high etc.) is required at 850 hPa, for normal monsoon rainfall over India (% of long period average; rainfall range: 96-104), 97% with an error of ± 6%, during summer monsoon season, north of 40°S/ 30°S between 040°W -120°E. Deficient rainfall (% of long period average; rainfall range: < 90), 88% with an error of ±6%, can be forecast if only low, as was the case in 1968 and 2002, or high (as in 2012) or low-high combination (as in 1982, 1987 and 2009) is observed (Kumar et al., 2016). The fact that the NH is warmer than the SH is potentially linked to the fact that the ITCZ is in the NH (Kang et al., 2008).

DATA

Anomalies of 850 hPa level geo potential height, vector wind, air temperature and SST from 1982 from January onwards for (i) El Nino years: 1951, 1953, 1957, 1958, 1963, 1965, 1969, 1972, 1976, 1977, 1979, 1982, 1986, 1987, 1991, 1994, 1997, 2002, 2004, 2006, 2009 and 2015: 22years, (ii) La Nina years: 1950, 1954, 1955, 1964, 1970, 1973, 1975, 1988, 1995, 1998, 1999, 2007, 2010 and 2011: 14 years and (iii) other significant Indian summer monsoon years: 1956, 1966, 1974, 1983, 1990, 2003, 2014 and 2016: 8 years have been prepared by using NOAA Earth System Laboratory (U.S.A) website. El Nino and La Nina episodes table, based on ONI (NOAA), from 1950 to 2016 has been used. All India monsoon rainfall data for all these years have been used from IMD website.

Analysis and Forecast

The features in anomaly of 850 hPa geo potential height and vector winds for El Nino and La Nina Years from June-September have been studied in relation to El Nino and La Nina events. It has been observed in excess of 80% cases that low/lows (negative anomaly) occupy maximum area in terms of horizontal width between 140°E-080°W/30°S-40°S (Figure 1) during El Nino years and during La Nina years high/highs (positive anomaly) occupy maximum area between the considered longitudinal and latitudinal width (Figure 2). Low/high at 850 hPa geo potential height remains associated with circulation/trough or anticyclone/ ridge respectively at 850 hPa vector winds with minor changes in their cover region, Figure 3 and Figure 4. In 1982 (Figure 3), westerly component of wind has been dominating between 170°W-080°W from 35°S-05°S.

Prominent ridge can be seen in Figure 4 between 140°E - 080°W/35°S. Easterly component of wind is seen from 30°S to north of equator between 160°E-080°W. It has been observed that when ONI value starts increasing from lower to higher value, e.g. -0.8°C (NDJ) to -0.6°C (DJF) or 0.3°C (DJF) to 0.4°C (FMA), prominent low (larger area) with circulation/trough can be observed from January-February onwards. Year wise observation of dominant negative anomalies in different months between Jan to May has been given for the following El Nino years: 1951: Mar (JFM: -0.6), Apr and May, 1953: **Jan** (NDJ: 0.3) and May, 1957: Jan (NDJ: -0.4), Apr and May, 1963: Apr (FMA: 0.1) and May, 1965: Feb (DJF: -0.5), Mar, Apr and May, 1969: Apr (ONI value started decreasing from FMA: 0.9 to JJA: 0.4 and started increasing from JAS: 0.5) and May, 1972: Jan (NDJ: -0.8), Feb, Apr and May, 1979: Apr (FMA: 0.2) and May, 1982: Apr (FMA: 0.2) and May, 1986: Apr (FMA: -0.3) and May, 1997: **Mar** (JFM: -0.4), Apr, and May, 2002: Feb (DJF: -0.2), Mar and May, 2006: Apr (FMA: -0.4) and May, 2009: Apr (FMA: -0.4) and May, 2015: **Mar** (JFM: 0.5), Apr and May. In all the months between Jan and May low may not be found dominating in a month or two. But the reliable synoptic feature can be considered for forecasting El Nino events for the area Nino

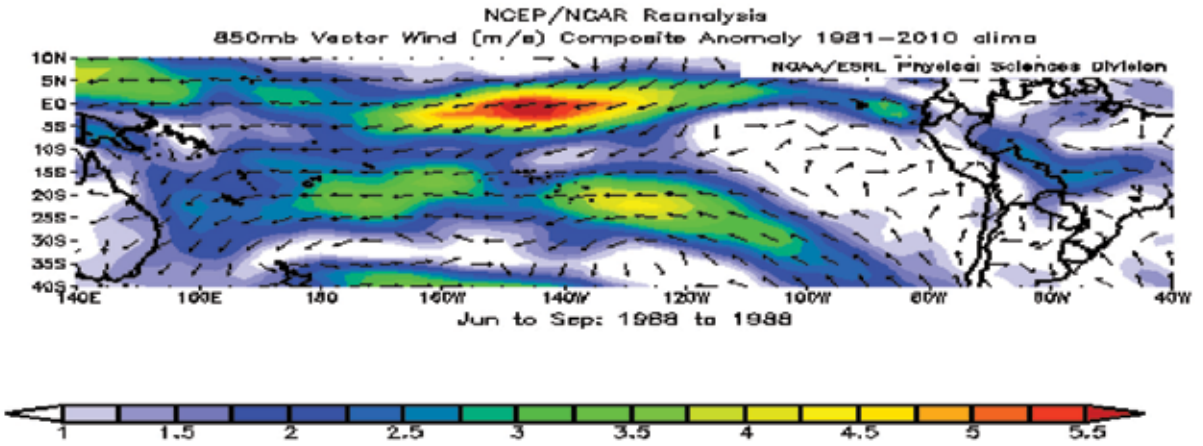

Figure 4. Anomaly of 850 hPa vector wind for Jun-Sep 1988.

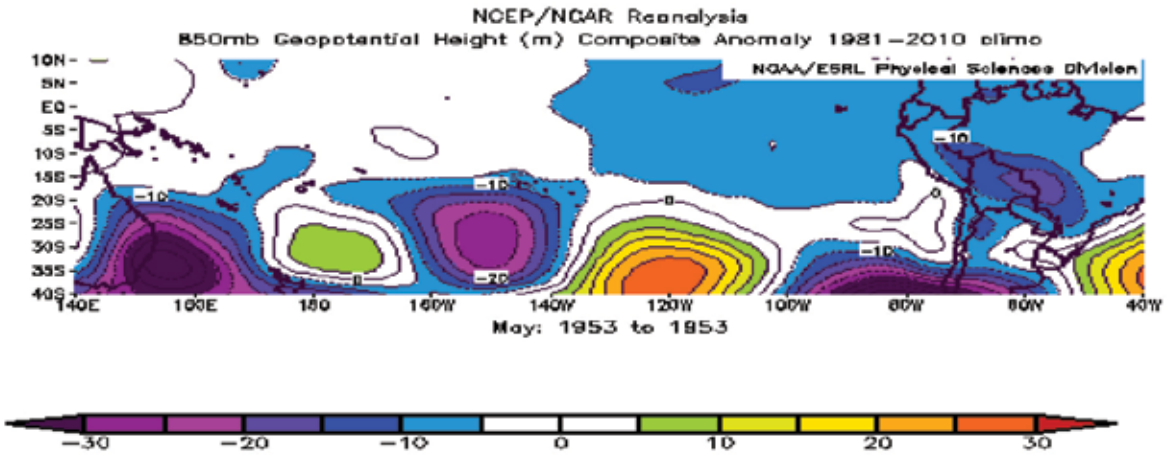

Figure 5. Anomaly of 850 hPa geo potential height for May 1953.

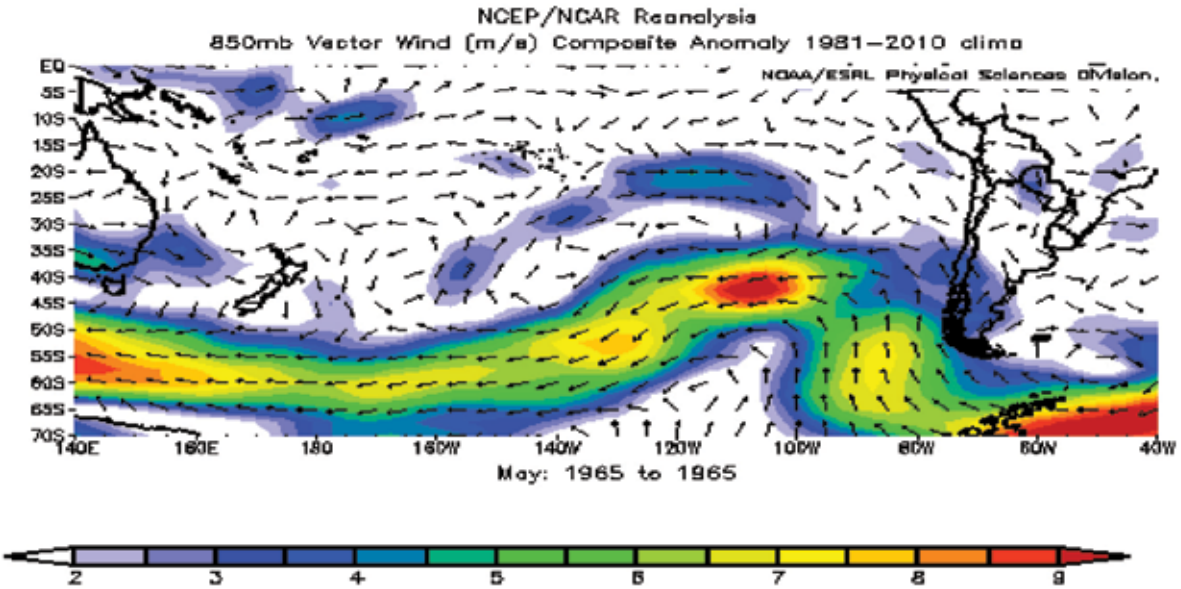

Figure 6. Anomaly of 850 hPa vector wind for May 1965.

3.4 (5°N-5°S/170°W-120°W) in almost all cases (21 years) in the first week of June when global data become available for May during the onset period of Indian Summer Monsoon. ONI value has reached ≥0.5°C for three months average during 1958: SON (0.5), 1976: ASO (0.5), 1977: (ASO: 0.5), 1991: (MJJ: 0.6), 1994: (SON: 0.6) and 2004: (JJA: 0.5) and El Nino events during these years can be forecast only from May data. When three months average ONI values were observed as -0.6, -0.5, **-0**.4, -0.3, 0.1, 0.2 and 0.3 El Nino features have been also observed in different years. Prominent low with circulation, covering maximum longitudinal width between 140°E-080°W/30°S-40°S, have been observed for the month of May for forecasting El Nino events for the following years when anomaly of geo potential height and vector wind were considered: 1951, 1953, 1957, 1958, 1963, 1965, 1969, 1972, 1976, 1977, 1979, 1982, 1986, 1991, 1994, 1997, 2002, 2004, 2006, 2009 and 2015 (21 years). In 1953, low-high-low-high-low composition has been observed with maximum coverage area by lows and last low was located along west coast of South America (Figure 5). Dominant circulation area was also observed at 850 hPa of vector winds.

In other years (except 2004) continuous low can be easily identified. In May 1965, dominant trough at 850 hPa can be seen south of 40°S with dominant circulations along the trough (Figure 6). Westerly component of wind can be seen from 40°S to 15°S between 160°W - 080°W (Figure 6). ISMR during 1965 from Jun-Sep has been observed as -18.2% from normal value, however there is no one to one relationship with El Nino and ISMR.

In May 1972, continuous low is seen from 170°E - 080°W along 40°S and centre of anti cyclone has shifted south of 60°S. However, dominant trough and circulation can be seen above it and north of 40°S (Figure 7) Westerly component of wind can be seen north of 40°S to 20°S between 160°W - 080°W. In 1972, ISMR from Jun-Sep have been found as -23.9% from normal value, which has been observed as the worst till date.

Anomaly of 850 geo potential height for May 2002 shows one low is located from 150°E-125°W and another low near west coast of South America along 080°W/40°S and a feeble high between 120°W-100°W slightly above 40°S. Westerly component of wind can be seen much prominent over the areas of low (Figure 8).

In 2009, ISMR from Jun-Sep has been found as -21.8% from normal value. Dominant low at 850 hPa can be seen along 40°S and has shifted northwards and high has shifted southwards during May 2009 (Figure 9). Anomaly of vector wind at 850 hPa for June shows strong circulations south of 10°S between 140°E-080°W. Feature of a partly occluded extra tropical low pressure system can be seen centred just south of 30°S and 100°W connected with a circulation west of 160°E (Figure 10). Westerly component of wind can be seen dominating from 30°S. All India monsoon rainfall during June 2009 has been observed as -47.2% from normal value.

Dominant low has been found for February and March 1987 between 140°E-080°W along 40°S which confirms that El Nino conditions are getting stronger. But when ONI value started decreasing from Feb-Mar-Apr (1.1 from 1.2) to Apr-May-Jun (0.9), the synoptic features for continuation of strong El Nino events have weakened. A small low is seen from 120°W-140°W between two highs (160°E-150°W and 110°W-080°W) north of 40°S in anomaly of 850 hPa geo potential height for May 1987 (Figure 11). But in the extended chart up to 60°S, a strong low is seen centred south of 40°S between two highs. A circulation is seen prominently in the anomaly at 850 hPa vector wind in association with the low in the extended chart. Another circulation is seen between 30°S-20°S along the west coast of South America. It appears from the climatological studies that the extra tropical low may move equator ward. The picture becomes clear as anomaly of 850 geo potential height from 22 Jun-28 Jun shows strong low from 140°E - 100°W along 40°S. ONI value started increasing from May-Jun-Jul (1.1). So the forecast may be modified in the beginning of July 1987. In 2004, ONI value remained constant as 0.3 up to Jan-Feb-Mar and anomaly of 850 geo potential height showed dominant low for February and March 2004 along 40°S. But when ONI value decreased during Feb-Mar-Apr and Mar-April-May high dominated feature had been observed for April 2004.

In May coverage area for low has been found around 070° (140°E-170°W and 125°W-105°W) and high is restricted to 045° (165°W-135°W and 95°W-80°W) along 40°S. So El Nino is expected during 2004. During 1958 when ONI value started decreasing from Jan-Feb-March (1.5 from 1.7) and the trend continued till Aug-Sep-Oct (0.4), low dominated feature has been observed for May 1958 and ONI value again increased (0.5 to 0.6) from Sep-Oct-Nov onwards. In 1966 and 1974 low dominated features have been observed during May between 140°E-080°W. So, synoptic features had not been found favourable in Nino 3.4 region for good summer rainfall over India during these two years. Warning for deficient rainfall over India has been issued by UK, USA and Australia weather offices from July onwards during 2014 but high dominated features have been observed for April and May 2014 (Figure 12). For the country as a whole, rainfall for the season (June-September) was 88% of its long period average (2014 South West monsoon, End of Season Report, IMD). However, actual rainfall during July (90%), August (90%) and September (108%), has not been observed as deficient. Below normal rainfall occurred in July and August and above normal in September. Anomaly of geo potential height for May 2016 shows dominant low along 40°S but anomaly from 1st - 5th June 2016 shows dominant high from 150°E-080°W.

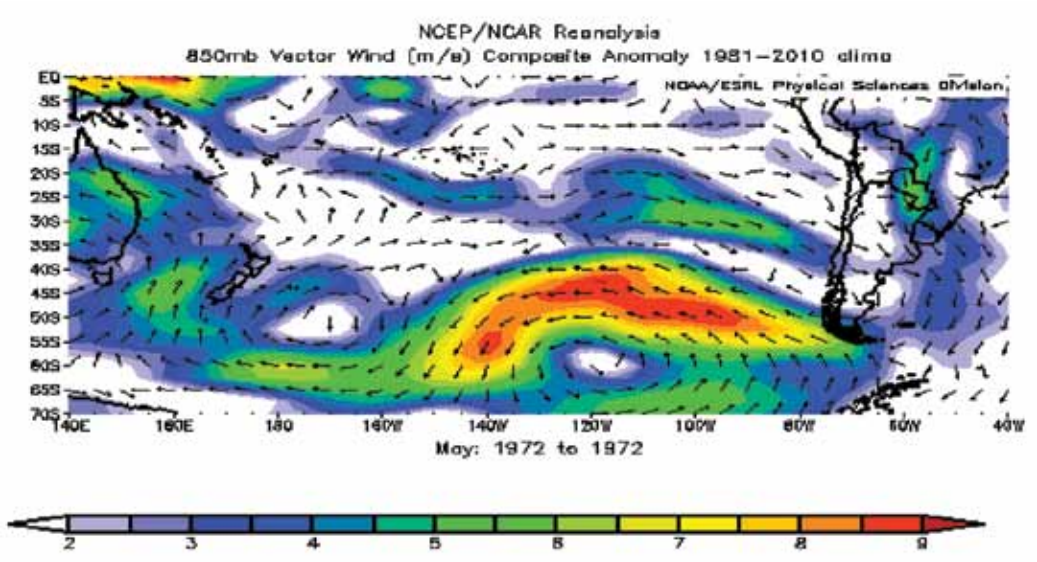

Figure 7. Anomaly of 850 hPa vector wind for May 1972.

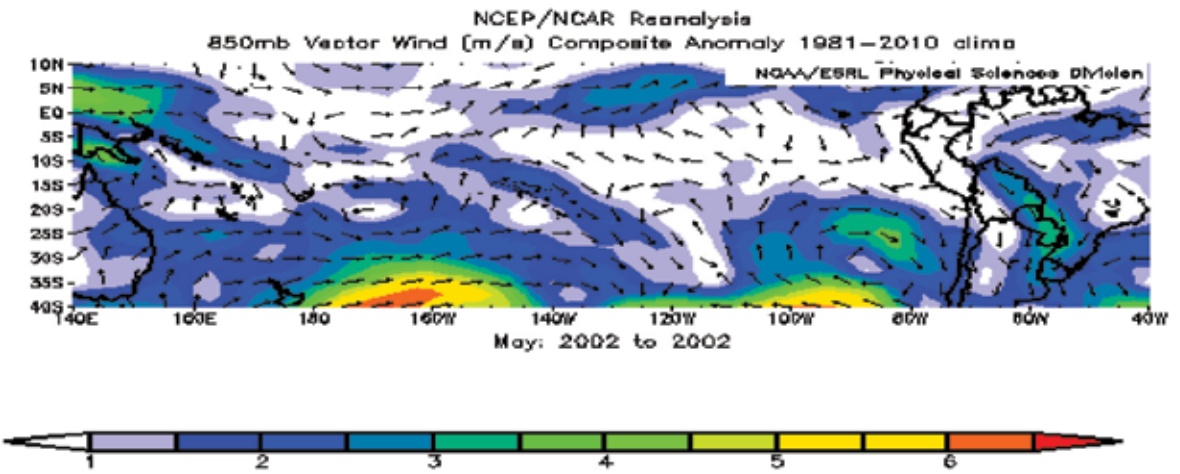

Figure 8. Anomaly of 850 hpa vector wind for May 2002.

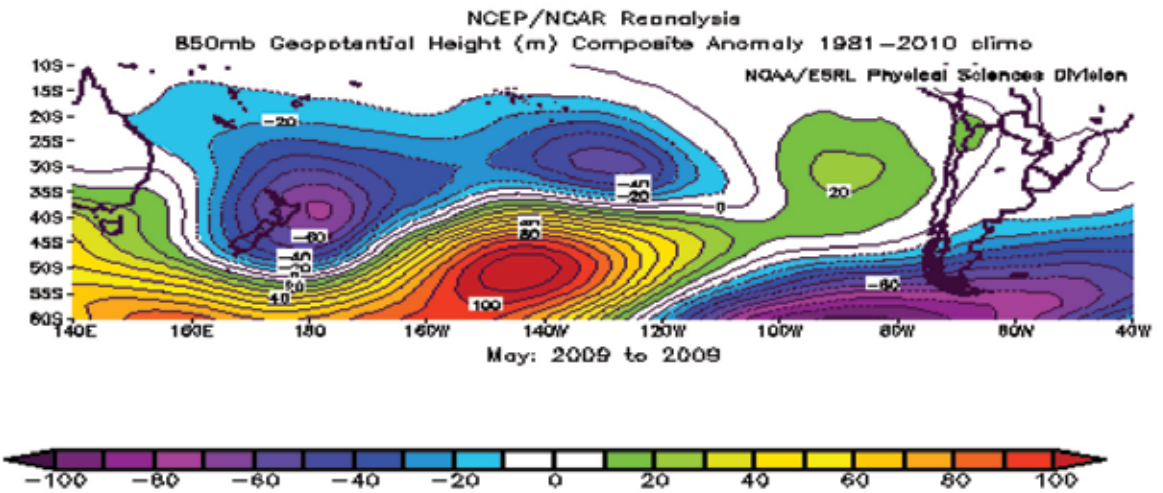

Figure 9. Anomaly of 850 hPa geo potential height of May 2009.

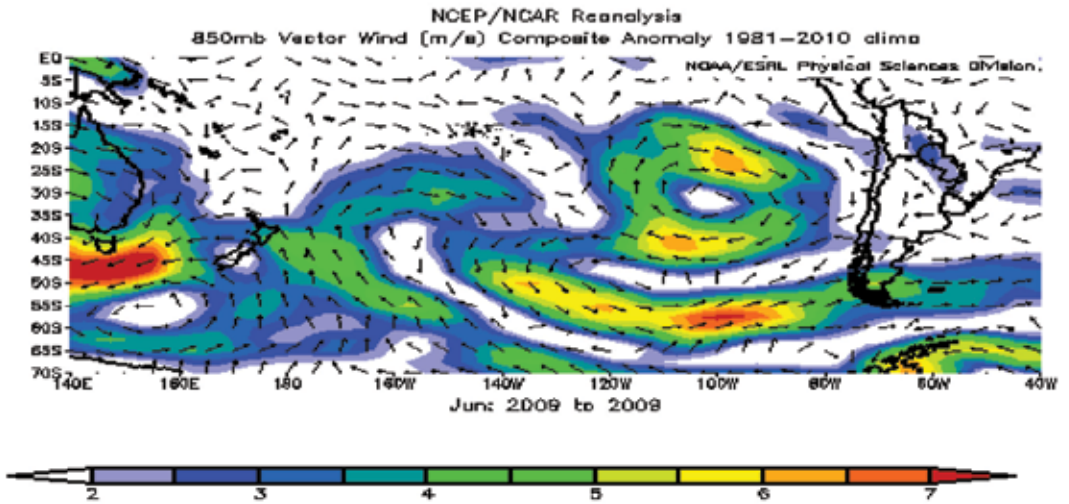

Figure 10. Anomaly of 850 hPa vector wind for Jun 2009.

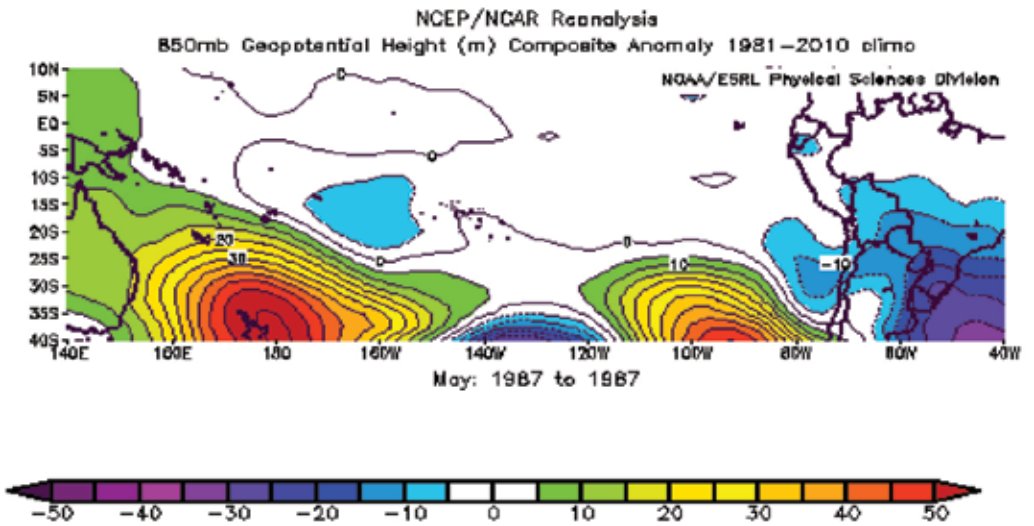

Figure 11. Anomaly of 850 hPa geo potential height for May. 1987.

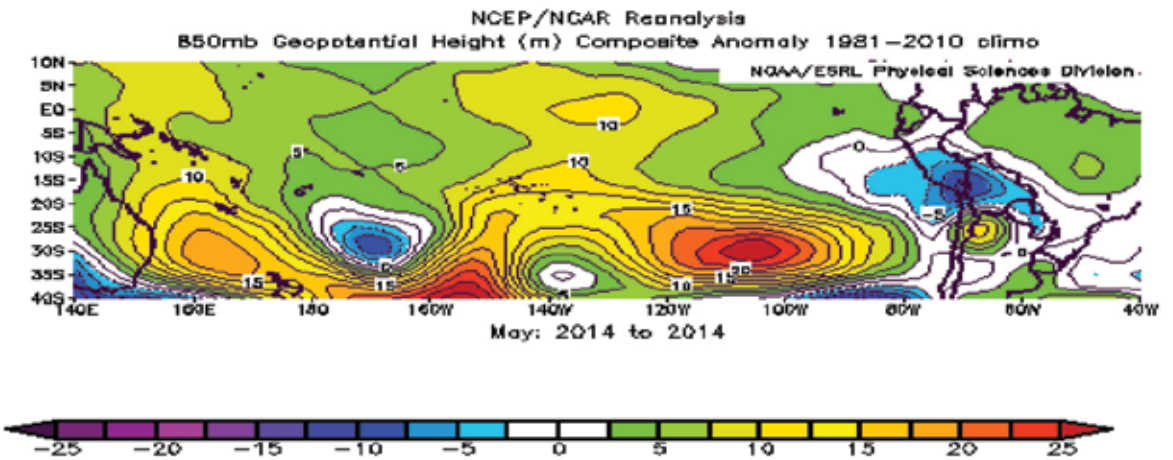

Figure 12. Anomaly of 850 geo potential height for May 2014.

High dominated features have been observed during different months of the following La Nina years (within bracket: months): 1950 (Feb, Mar and May), 1954 (Mar and May), 1955 (Feb, Mar and Apr) 1964(Mar and May), 1970 (Feb and May), 1973 (Feb, Mar and Jun), 1975 (May: vector wind dominant), 1988 (Jan, Mar, Apr and May) 1995 (May), 1998 (Feb, Apr and Jun), 1999 (May), 2007 (Feb, Mar, Apr and May) 2010 (Mar, Apr and May) and 2011 (May). Three months average ONI values have been found ≥ 0.5°C during the following years: 1964 (JFM: 0.6), 1970 (DJF: 0.6), 1973 (DJF: 1.7), 1988 (NDJ: 1.1), 1998 (DJF: 2.1), 2007 (DJF: 0.7) and 2010 (JFM: 1.2), even then La Nina features have been observed during Mar 1964, Feb 1970, Feb 1973, Jan 1988, Feb 1998, Feb 2007 and Mar 2010 respectively. In addition to these years high dominated features have been observed during 1956 (113.6%), 1983 (113%), 1990 (106.2%) and 2003 (102.3%) when above 100% rainfall have been observed over India during summer monsoon season. Study of anomalies of 850 geo potential air temperature and SST did not give any significant result for forecasting EL-Nino events.

CONCLUSIONS

i. Dominant feature of negative anomaly of 850 hPa geo potential height (low) has been observed between 140°E-080°W/30°S-40°S during El Nino years. Associated cyclonic circulation/trough can be observed in anomaly of 850 hPa vector wind. As a result westerly component of wind is found dominant north of 40°S. Dominant negative anomalies have been also observed when three months average ONI values have been reported between -0.8° to 0.3°C.

ii. Dominant contrast feature of positive anomaly of 850 geo potential height (high) has been observed between 140°E-080°W/30°S-40°S during La Nina years. Associated anti cyclone/ ridge can be observed in anomaly of 850 hPa vector wind. As a result easterly component of wind is found dominant north of 40°S. The contrast feature in the month of May has been found correct in 11 years out of 14 La Nina years (78.57%). Dominant positive anomalies have been also observed when three months average ONI values have been reported between 0.4°C and 2.1°C.

iii. Out of 22 years, El Nino events have been forecast correctly for 21 years (95.45%), except 1987, on the basis of May synoptic features. For 1987, modified forecast can be issued in the first July of 1987 as dominant low feature was observed in the last week of July. In 2016, changes have been reflected in 1st - 5th June data. Checking of first week data is needed to rectify El Nino events forecast during certain years.

iv. In 15 years out of 21 years El Nino events have been forecast on the synoptic features of May, when ONI values have been observed <0.5°C.

v. From synoptic features of May, El Nino events have been forecast, when ONI values reached ≥0.5°C during JJA (1951, 1963, 2004 and 2009), ASO (1976, 1977 and 2006) and SON (1979 and 1994).

vi. Persistence of extra tropical lows/circulations/troughs restricts the movement of cold air from 40°S or from south of 40°S to northern latitudes during El Nino years.

vii. Subtropical highs located between 140°E-080°W/30°S-40°S weaken and shift southwards (south of 40°S/45°S/50°S) and extra tropical lows located south of 40°S shift northwards from their position during El Nino years.

viii. Longitudinal width from 140°E-080°W/30°S-40°S has been found significant for forecasting El Nino events.

ix. In 1966 and 1974 conditions were not favourable for ISMR between 140°E-080°W/40°S.

x. Anomaly of 850 hPa air temperatures and SST did not suggest any significant feature for forecasting El Nino events.

ACKNOWLEDGEMENTS

Authors are thankful to NOAA Earth System Laboratory (U.S.A.) for using their website for the preparation of anomalies of geo- potential height at 850 hPa, vector wind, air temperatures and SST for 44 years period and to NOAA Climate Prediction Centre/ NCEP for using ONI data. Authors are thankful to Google website for using their reports (Wikipedia). The authors are thankful to India Meteorological Department for using their web site for monthly and seasonal rainfall data for summer monsoon season for 67 years period and meteorological reports. Authors express sincere thanks to the reviewers Dr. Onkari Prasad and Shri. A.K. Jaswal for their critical comments. We are indebted to Chief Editor for continued support and encouragement. He helped in reframing critical parts of the text during final editing that helped in overall quality enhancement of our study.

Compliance with Ethical Standards

The authors declare that they have no conflict of interest and adhere to copyright norms.

REFERENCES

Asnani, G.C., 2005, Tropical Meteorology (revised edition), v.2, pp: 5-91.

Asnani, G.C., and Mahesh Verma, 2007. A slightly new look at El-Nino/ La-Nina phenomenon, Vayu Mandal, v.33, no.1-4, pp: 37

Kang, S.M., Held, I.M., Frierson, D.M.W., and Zhao, M., 2008. "The response of the ITCZ to extra tropical thermal forcing: Idealized Slab Ocean experiments with a GCM", Journal of Climate, v.21, no.14, pp: 3521-3532

Kumar Vinod, Chand Ramesh, Kumar, Satya, M., and Narayan R.B.S., 2016. "Forecasting rainfall trend over India during summer monsoon" J. Ind. Geophys Union, v.20, no.4, pp: 427.

Lynch John, 2002. "The Southern Oscillation", "The Weather", Fire Fly Books, pp: 100-102.

Rajeevan, M., and McPhaden, M.J., 2004. "Tropical Pacific upper Ocean heat content variations and Indian summer monsoon rainfall", Geophys., Res., Lett., L 18203, doi: 10.1029/2004 GL 020 631., v.31.

Rajeevan, M., and Pai, D.S., 2007. "On the El Nino- Indian monsoon predictive relationship", Geophys., Res., Lett., L 04704, doi: 10. 1029/2006GL028916., v.34.

Reddy, P.R., and Reddy D. Venkat, 2014. "El Nino Effect", International Journal of Earth Science and Engineering, v.7, no.4, pp: 2-6.

Saini Shweta and Gulati Ashok 2014. "El Nino and Indian Droughts – A Scoping Exercise" Working Paper 276, pp: 7.

Slingo Julia, Scaife Adam, Ineson Sarah and Brookshaw Anca, 2014. "Is an El Nino on the way and what might's its impact be", Met Office, pp: 20.

Xu, J.J., and Chan, J.C.L., 2001. "The role of Asian Australian monsoon system in the onset time of El Nino events", J. Climate v.14, pp: 418-433.

Received on: 27.2.17; Revised on: 11.4.17; Accepted on: 23.4.17

*The impact of environmental warming on ice drainage basins of Antarctica

The environment of Antarctica is unique in many ways, one being that the continent is covered almost entirely by a vast sheet of ice, stretching from the towering plateau of East Antarctica to the chain of mountainous islands (interconnected by ice) that form West Antarctica. If Earth's oceans and atmosphere continue to warm at the rates projected by most climate models, over the next few hundred years, the Antarctic ice sheets could melt enough to cause a sea level rise of several meters. Most likely, the severity of ice loss will vary geographically because of physical differences across the continent, such as ice thickness and bedrock topography. The eastern side of the ice sheet is much larger and has slow-flowing glaciers, and its bedrock is a rocky terrain of deep basins and high mountain ranges buried beneath the ice. Recent studies have already shown warm ocean water flowing southward from areas of the East Antarctic Ice Sheet, suggesting that the region could be affected by further warming. To find out more, Golledge et al. used an ice sheet model to simulate the flow of water from melting ice sheets, ice shelves, and ice streams over thousands of years. They also examined data on the average long-term rates of ice loss for each ice drainage basin, or catchment, to determine which catchments are most sensitive to various conditions associated with climate change.Comparing the results of their models to other simulations and observations and given a projected ocean temperature rise of about 36°F, the researchers found that the majority of East Antarctica's future ice loss will most likely come from a catchment in the eastern Weddell Sea called Recovery.The researchers predict that how soon and how much the ice sheet in this region melts will determine the degree to which East Antarctica will contribute to future sea level rise. In turn, this could amplify surface temperatures, producing an even greater global impact. (**Source**: Golledge et al, 2017,Geophysical Research Letters, https://doi.org/10.1002/2016GL072422, 2017).

J. Ind. Geophys. Union (July 2017)
v.21, no.4, pp: 319-326

Atmospheric reactive nitrogen fluxes and scavenging through wet deposition Over Mathura (India)

Mudita Chaturvedi, Reema Tiwari and Umesh Kulshrestha*
School of Environmental Sciences, Jawaharlal University, New Delhi 110067, India
*Corresponding Author: umeshkulshrestha@gmail.com

ABSTRACT
In the era of excessive use of fertilizer and combustion of fossil fuel, the atmospheric deposition of reactive nitrogen species has led to the problem of acidification and eutrophication of the ecosystem. This study has been carried out for estimating the concentrations and wet deposition fluxes of N_r species in rain water along with their scavenging behaviour at a typical residential site under semiarid tropical region. For this purpose, sequential sampling of a rain event was performed for determining N_r levels during monsoon 2015 period. Samples were analysed for their cationic and anionic content using an ion chromatograph. The results showed a relative abundance of NH_4^+ (62.3 ± 2.3 μeql^{-1}) over NO_3^- (46.8 ± 40.1 μ eql^{-1}) in the rain water samples, subsequently creating a higher wet deposition flux of NH_4^+-N (3.6 kg $ha^{-1}y^{-1}$) in comparison to NO_3^- -N (2.1 kg $ha^{-1}y^{-1}$). This clearly indicated that the Nr deposition had very significant contribution over the study area. Scavenging patterns confirmed the presence of NH_4NO_3 showing co-variations along with the rainfall intensity. A strong correlation (0.92) of NH_4 and NO_3 also supported such observations, thereby, confirming the dominant forms in which these Nr species are being deposited over the study area.

Nr: It represents NH_4^+ and NO_3^- in this paper

Key words: Reactive nitrogen, wet scavenging, rainfall intensity, neutralization capacity.

INTRODUCTION

With the growing demand of food and energy production across the globe, the footprints of alteration in the N cycling are becoming significant in the ecosystem responses. This is evident from the tenfold rise in the transformation rates of inert N into reactive nitrogen compounds (Nr) creating cascade of environmental problems along their biogeochemical pathway (Galloway et al., 2004). Expanding sectors of industrial and agricultural activities along with the fossil fuel combustion processes has inadvertently increased their availability as NO_3^- and NH_4^+ in the environment (Galloway et al., 2008; Kulshrestha et al., 2014a). Their direct emission pathways have eventually resulted in these inorganic Nr species becoming the key driver of atmospheric chemistry and climate change (Dentener et al., 2006). However, with the changing dynamics of their atmosphere – biosphere interactions, there has been an exceedance in the Nr deposition fluxes beyond its critical threshold values leading to air pollution, acidification and eutrophication of the ecosystem (Reis et al., 2009; Vet et al., 2014).

Chemical characterization of deposition pathways, in this regard, has provided signatures for spatio temporal evolution of Nr emissions and their consequent interaction with the atmospheric transport dynamics and removal processes. Thus, depending on the Nr solubility and amount of precipitation received in the region, the wet as well as dry deposition processes are becoming detrimental to its fate by controlling the concentration of its gaseous and particulate species in the troposphere (Wallace and Hobbes, 2006). Amongst them, the mechanism of pollutant scavenging through precipitation has been more effective as an atmospheric purging process with more than 90% removal efficiency of their total atmospheric loading (Gromping et al., 1997). With the changing Nr emission scenarios over the past few decades, their precipitation weighted mean concentration has shown a rising trend over Africa (+19%) and Asia (+ 13.6%) but a declining trend over Europe (-2.7%) and North America (-4.3%) (Torseth et al., 2012; Singh et al., 2017). Introduction of NO_X emission reduction strategies has simultaneously resulted in the growing dominance of N reduced (NH_4^+) contribution to the total N wet deposition especially over the agricultural intensive areas. However, a few NO_x dominated emission areas in the eastern and western regions of U.S. has given more than 60% contribution of N oxidized (NO_3^-) to their total N wet deposition fluxes (Vet et al., 2014).

Hence, the chemical composition of rain varying through time and space could be used for deciphering the Nr scavenging patterns based on its source of influence and precipitation amount. A number of studies have already shown the alkaline nature of rain water in India due to the high dust loading of soil derived particles in its atmosphere (Parashar et al., 1996; Kulshrestha et al., 1996; Jain et al., 2000; Norman et al., 2001; Bhaskar and

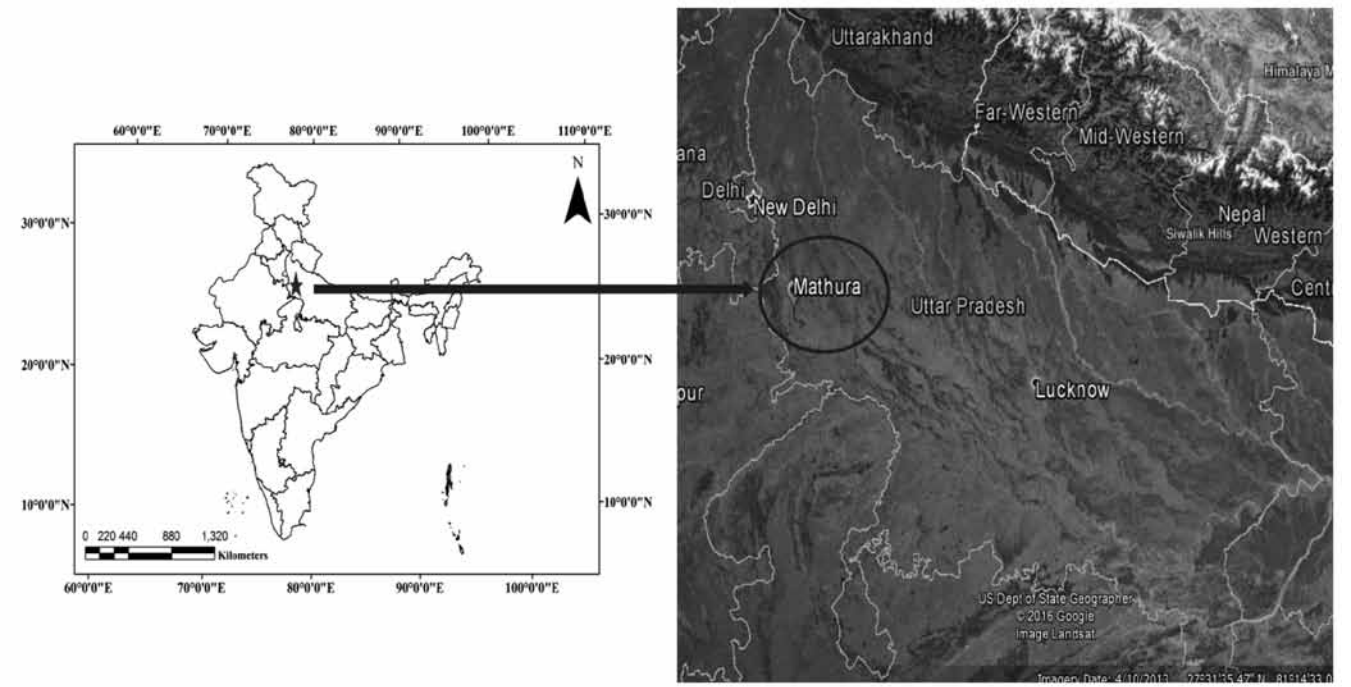

Figure 1. Map showing the sampling site.

Rao, 2016; Kulshrestha et al., 2005; Kulshrestha, 2013). Their below cloud scavenging during precipitation events can, therefore, result in the buffering of NO_3- acidity in rain water through following reaction

$CaCO_3$ (s) + $2HNO_3$ (g) —> $Ca(NO_3)_2$ (s) + H_2O (aq) + CO_2 (g) (below cloud scavenging)

Reduced Nr species like ammonia (NH_3), on the other hand, are involved in the removal of NO_3^- and SO_4^{2-} acidity from the troposphere through their secondary aerosol formation and in- cloud scavenging. As ammonia is the only common base present that is highly soluble in water, it is considered to be primary removal mechanisms of NO_y and SO_x from the troposphere by the way of its following neutralization reaction (Bauer et al., 2007).

NH_3 (g) + HNO_3 (g) <—> NH_4NO_3 (s)

NH_3 (g) + H_2SO_4 (g) —> $(NH_4)_2SO_4$(s)

(in cloud scavenging)

Considering the lack of comprehensive data for Nr deposition fluxes in the western Uttar Pradesh (U.P), restricted by the three month monsoon period (June – September) over the Indian region, the present study has been carried out to determine the levels of NH_4^+ and NO_3^- along with their wet deposition fluxes in Mathura, which is one of the highly polluted cities of U.P characterized by its rapid urbanization. Chemical composition of rain was analyzed for major water soluble ions. Nr scavenging pattern were established based on the rainfall intensity. Neutralization ratios were calculated for ascertaining the source of influence in the chemistry of wet scavenging. Such estimates could further be used for not only substantiating our current understanding of rain water chemistry but also in correlating the changes in the aquatic ecosystem arising from its deposition pathways.

METHOD

Sampling location

Mathura is located at 27.45°N 77.67°E in U.P state of India. Lying on the western side of river Yamuna at 140Km south east of Delhi and 60km North West of Agra, it is a suitable representation of typical urban site characterized by rapid population growth and unplanned urban sprawl. Being a major tourist hub, it is also known for hosting a number of tourist activities resulting in frequent traffic congestions from the vehicular movement throughout the year. Presence of Mathura oil refineries near the city premises has further added to its worsening air quality. The temperature averages at 25.6°C, which becomes highest during June (34.7°C) and lowest during January (14.7°C). The city receives an average precipitation of 707 mm, with a minimum during April (2 mm) and maximum during August (271 mm).

Sample collection:

Rain water samples were collected using a manual set up of polypropylene funnel with a 14cm diameter and bottle of 1 litre capacity. Prewashed assemble of funnel and bottle was fixed with paraffin and were kept at a 13m height for rain

Table 1. Duration of collection of each rain event along with one set of sequential sampling during 7th event.

Event no.	Date of sampling	Time in	Time out	Duration	pH	Volume
1.	04/07	16:05	17:00	55min	6.57	250
2.	09/07	16:25	17:24	60min	6.47	450
3.	02/08	11:50	13:48	118min	6.18	125
4.	09/08	11:30	14:39	189min	6.38	340
5.	10/08	15:15	15:45	30min	5.68	125
6.	14/08	19:27	21:50	143min	5.9	60
7.(I)	15/08	13:55	14:10	15 min	6.12	220
(II)	15/08	14:10	14:25	15 min	6.13	260
(III)	15/08	14:25	14:40	15 min	6.27	45
(IV)	15/08	14:40	18:36	236 min	6.15	36

water collection. Sample collector was withdrawn after each single rain event and the amount collected was determined using measuring cylinder before storing the sample in 125ml polypropylene bottles with thymol. A total of 7 rain events based sampling has been carried out, of which the last event involved collection of 4 sequential samples with varying time period according to the intensity and amount of precipitation. This was done for the purpose of obtaining representative samples during different rain events, to demonstrate the wet scavenging process. The total volume of samples collected was 1911ml during monsoon period of June, July and August.

Sample analysis:

Physical parameters viz. volume, pH and conductance were measured immediately after collection of samples. Chemical composition of rain water, on the other hand, were analyzed for its major cations (K^+, NH_4^+, Na^+, Ca^{2+}, Mg^{2+}) and anions (F^-,Cl^-,NO_3^-, SO_4^{2-}) with the help of ion chromatography (Metrohm–883 basic plus model). Metrosep A SUPP 4, 250/4.0 column and an eluent of 1.8 mmol/L Na_2CO_3 and 1.7 mmol/L $NaHCO_3$ at a flow rate of 1.0ml/min with Metrohm suppressor technique were used for determination of anions. The cation separation was achieved with the metrosep C4-100/4.0 and an eluent of 1.7 mmol/L Nitric acid and 0.7 mmol/L dipicolinic acid at a flow rate of 0.9 ml/min without suppressor. Calibration of the method and quantification of components were carried out using MERCK reference standards (CertiPUR) of 1, 2, 5 ppm for anions and 2, 5, 10 ppm for cations.

Data quality assessment:

The quality of data was checked with the help of ion balance assuming the accountability of major cations (K^+, NH_4^+, Na^+, Ca^{2+}, Mg^{2+}) and anions (F^-,Cl^-,NO_3^-, SO_4^{2-}) for most of the ions in the sample. Based on the principle of electro- neutrality, the cationic equivalents of the rain water sample should be equal to its anionic equivalents (Ayers, 1995; WMO, 1994). The average sum of equivalent cations ($\sum C$) and anions ($\sum A$) was observed to be $\sum C = 270.8$ μeq/l and $\sum A = 180.5$ μeq/l. The relative ion difference was calculated to be 0.2 using the following formula:

$$\text{Relative ion balance} = (\sum C - \sum A) / (\sum C + \sum A)$$

Total percent ion difference was found to be well within the acceptable range with slight deviation arising from the unanalyzed HCO_3^- (Kulshrestha et al., 2003).

RESULTS AND DISCUSSION

Ionic composition of rain water

Equivalent concentration of all the major cations and anions in the rain events is given in Table 2. The average values showed the dominance of Ca^{2+} in the rain water composition due to its strong crustal source of influence over the Indian atmosphere (Kulshrestha et al., 1998, 2003). Strong neutralization affinity of Ca^{2+} with SO_4^{2-}, on the other hand, has inadvertently resulted in the dominance of SO_4^{2-} amongst the major anions (Kulshrestha et al., 2003; 2014b). This has also been evident from our sequential sampling of 15th August single rain event where a decreasing trend in the SO_4^{2-} concentrations clearly indicated scavenging by Ca^{2+} at every interval. The order of its average ionic concentration in the rain water sample was, therefore, observed to be as: **$Ca^{2+} > SO_4^{2-} > Cl^- > NH_4^+ > NO_3^- > Na^+ > Mg^{2+} > K^+ > F^-$**

Changing dynamics of the ionic contribution with the sequential progression of rainfall events were analysed for its cationic and anionic fractions (Figure 2). The observations showed a decline in the contribution of anionic fraction for the samples that were collected during the consecutive period of rainfall events. Absence of active sources of NO_3^- and Cl^- has furthermore provided a sharp decline in their percent contribution to the total ionic composition as

Table 2. Concentration of major ions in rain samples (μeq l^{-1}).

Sample	Cl^-	NO_3^-	SO_4^{2-}	F^-	Na^+	NH_4^+	K^+	Ca^{2+}	Mg^{2+}
04-Jul	180.9	78.5	160.6	4.0	43.1	60.1	60.2	2.2	64.4
09-Jul	22.9	24.8	35.6	1.7	48.8	63.2	7.3	73.6	13.3
02-Aug	305.9	145.2	170.8	1.1	38.2	56.7	91.6	119.4	117.0
09-Aug	70.1	66.7	78.6	2.0	46.2	61.0	25.2	129.2	19.2
10-Aug	74.0	0.9	73.0	4.0	47.2	62.5	26.8	61.4	75.2
14-Aug	27.5	28.2	16.0	0.8	48.6	63.1	9.4	96.4	22.6
15-Aug (I)	48.5	40.6	132.9	0.6	46.3	62.9	19.8	131.8	37.0
15-Aug(II)	20.4	19.2	52.4	1.7	47.6	63.3	9.3	86.8	18.1
15 – Aug (III)	13.9	18.3	36.1	1.7	51.8	65.8	4.7	99.2	15.9
15 Aug (IV)	15.1	45.6	25.2	1.7	48.0	62.5	3.4	116.5	23.0
Average	**77.9**	**46.8**	**78.1**	**1.9**	**46.6**	**62.3**	**25.8**	**91.6**	**40.6**
Min.	**13.9**	**0.9**	**16.0**	**0.6**	**38.2**	**56.7**	**3.4**	**61.4**	**13.3**
Max.	**305.9**	**145.2**	**170.8**	**4.0**	**51.8**	**65.8**	**91.6**	**131.8**	**117.0**
S.D.	**87.33**	**40.14**	**49.15**	**0.92**	**3.47**	**2.32**	**25.96**	**23.26**	**33.22**

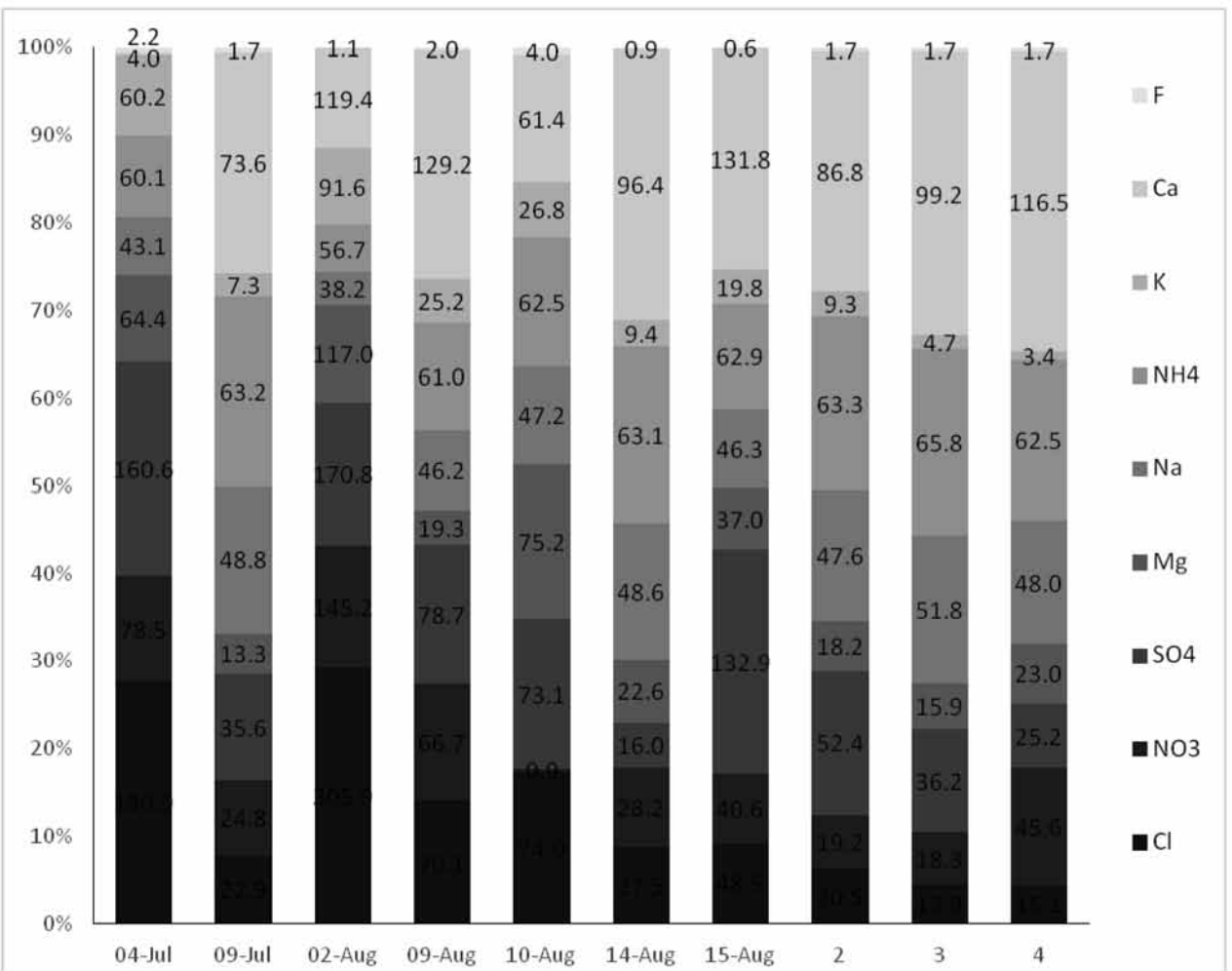

Figure 2. Percentage contribution of major cations and anions for rain event samples.

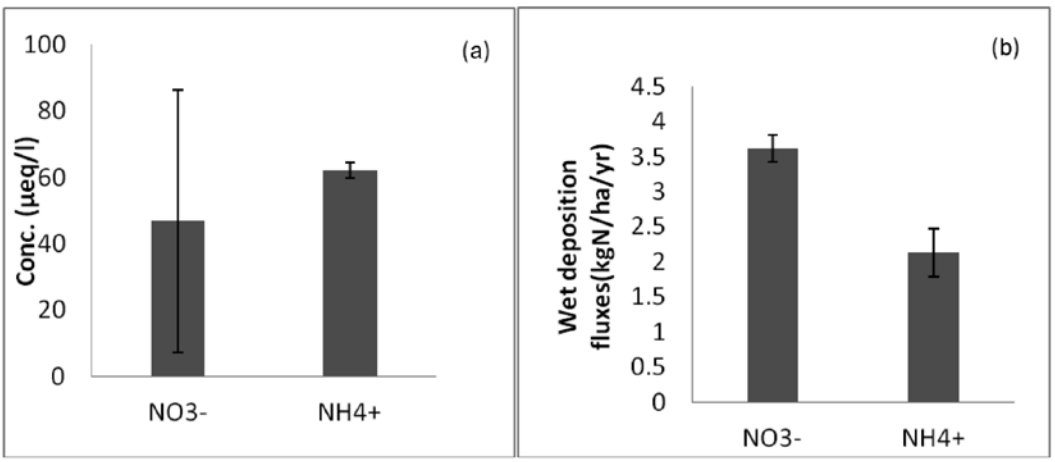

Figure 3. Mean values of NH_4^+ and NO_3^- showing (a) relative abundances in rain water samples (μ eq l^{-1}) and (b) wet deposition fluxes (kgN ha^{-1} y^{-1}) over Mathura.

evident from their 9th and 10th August sequential samples. Similar pattern of ionic contribution has also been observed for the intermittently collected samples from the single rain event of 15th Aug due to its continuous scavenging process for the acidic anionic fractions.

Wet deposition fluxes of Nr:

Relative abundance of reduced (NH_4^+) as well as oxidized (NO_3^-) species of Nr in rain water is shown in Figure 3 (a). While NH_4^+ exhibited minimum variability in its equivalent concentration values ranging from 56.7 to 65.8 μeq l^{-1} with an average of 62.3 ± 2.32 μeq l^{-1}, NO_3- showed a range of 0.9 - 145.2 μeq l^{-1} at an average concentration of 46.8 ± 40.14 μeq l^{-1}. Such variability could be attributed to the progression of monsoon providing active source of NH_4^+ through organic matter decomposition on one hand and continuous scavenging of acidic NO_3^- during consecutive rainfall events on the other.

The resulting wet deposition fluxes of Nr were calculated from their abundances in the rain water sample using the following formula (Du and Liu, 2014).

$$R_i = \Sigma\, C_i \times P_i \times 0.01$$

Where R_i (kg $ha^{-1}y^{-1}$) is annual wet deposition flux, C_i (mg/l) is the concentration of Nr for each precipitation event and P_i is the depth of precipitation (mm).

In synchronization with their relative abundances, the wet deposition fluxes of NH_4^+-N (3.62 kg $ha^{-1}y^{-1}$) were also observed to be higher than NO_3^- - N (2.13 kg $ha^{-1}y^{-1}$) as shown in Figure 3 (b). Such a pattern clearly reflected the growing influence of ammonium source and their active emissions from agriculture and sewage contributing towards their increased scavenged values during monsoon. Lack of active sources of NO_3^- resulting from the low solubility of their precursor gases (NO_X) in the rain water samples and its continuous wet scavenging through buffering reaction has consequently lowered the wet deposition fluxes of NO_3^- - N over the study area. These values might be underestimated values for entire year due to non - inclusion of pre and post monsoonal rain events in the sampling schedule.

Scavenging pattern of Nr:

Variability in the concentration of NH_4^+ and NO_3^- in rain water samples was evaluated with the changing rainfall intensity as shown in Figure 4. NO_3^- being acidic in nature showed higher concentrations during initial period of sampling, thereby, indicating towards their dominant removal through below cloud scavenging reactions. However, with the gradual monsoon progression, a declining trend in NO_3^- concentration from the high rainfall intensities was observed especially for consecutive rain fall events. Such a trend was further established in the sequential sampling of 15th Aug single rain event showing a decline in the NO_3^- concentrations after each intermittent sampling due to its continuous scavenging. NH_4^+ being basic in nature showed variability irrespective of the rain fall intensities. This indicates the dominant removal through in-cloud scavenging process.

In order to find out the scavenging neutralization reactions of Nr, regressions of NO_3^- were plotted with NH_4^+ and Ca^{2+} for ascertaining their wet scavenging mechanism (Figure 5). The results showed the ionic concentrations of NO_3^- and NH_4^+ following a similar pattern with a strong correlation of 0.92 possibly arising from their coexistence in the atmosphere. This, in turn is indicative of their dominant removal through in cloud scavenging process via NH_4NO_3 formation. Also with NH_4^+ and NO_3^- showing systematic variations with rain intensities, the removal of

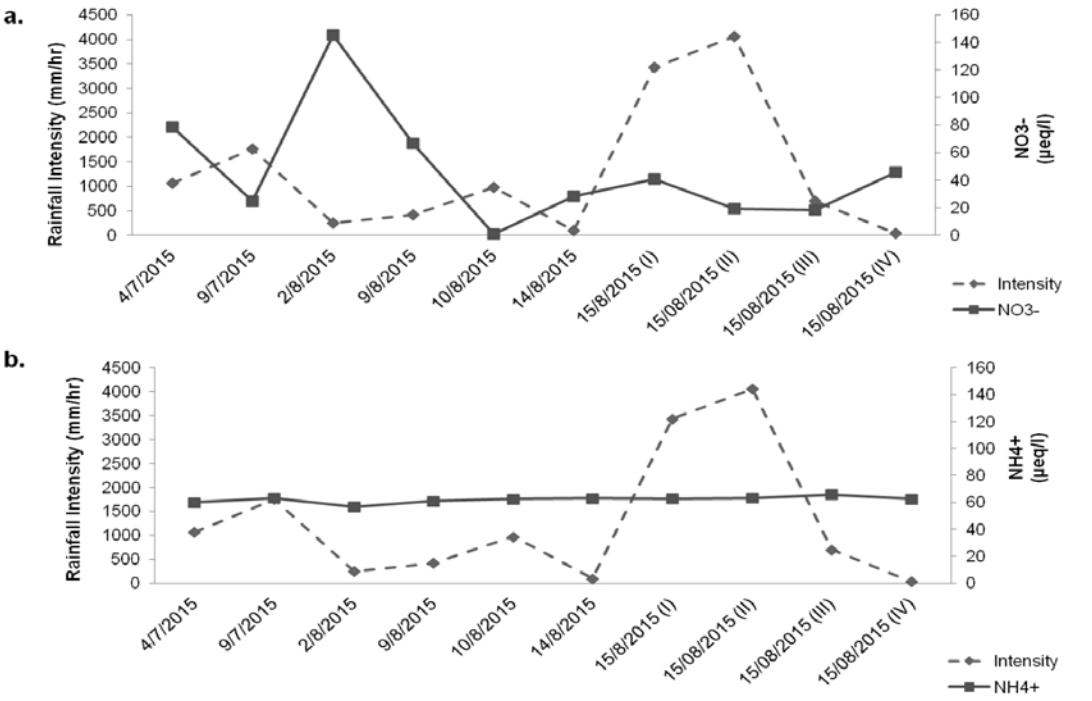

Figure 4. Nr variability with rainfall intensity for a) NH_4^+ and b) NO_3^-.

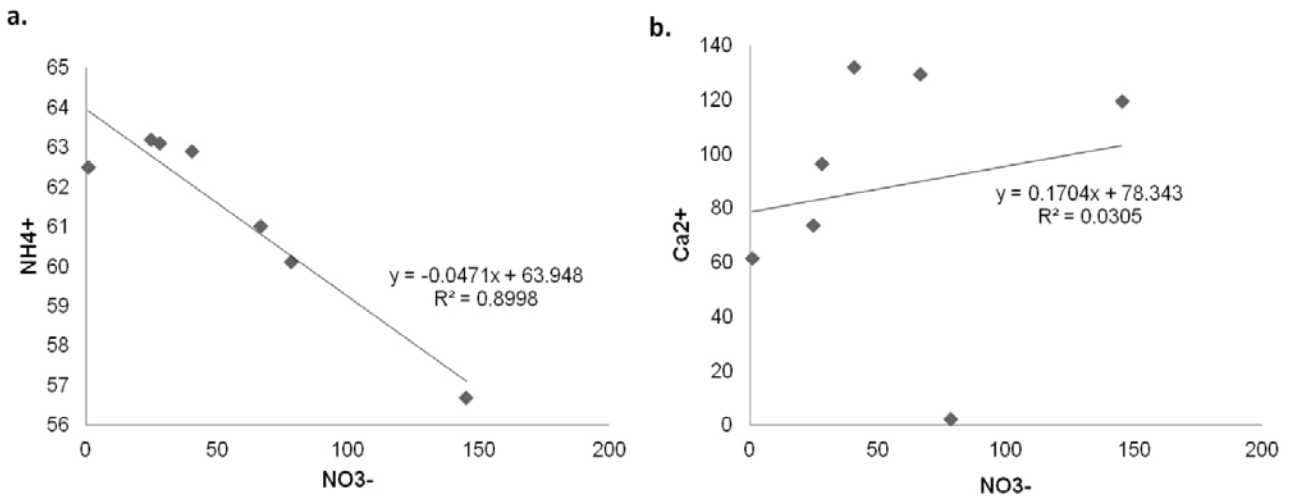

Figure 5. Regression plots of NO_3^- with a) NH_4^+ and b) Ca^{2+} in μeq l^{-1}.

NH_4NO_3 could, therefore, be rendered more effective under low intensity rain through small droplets.

Neutralization capacity of the wet deposition:

Neutralization capacity of the rain water samples was calculated for further substantiating the observed pattern of Nr scavenging (Table 3). It is defined by the relative abundance of sulphate plus nitrate in comparison with calcium and ammonium in rain water samples using the following formula (Alastuey et al., 2001):

$$\text{Neutralizing capacity} = \frac{SO_4^{2-} + NO_3^-}{Ca^{2+} + NH_4^+}$$

Neutralization capacity of the rain water samples was observed to be lowest for the first few initial period of sampling due to the presence of heavy loading of neutralizing agent (Ca^{2+} and NH_4^+) predominantly from their crustal sources in the atmosphere. Subsequent progression of

Table 3. Neutralization capacity of rain water on event basis.

Event	Neutralization capacity
04-Jul	0.38
09-Jul	0.44
02-Aug	1.79
09-Aug	0.76
10-Aug	0.6
14-Aug	0.28
15-Aug (I)	0.89
15 – Aug (II)	0.48
15 – Aug (III)	0.33
15 – Aug (IV)	0.40

the monsoon, on the other hand, provided increasing neutralization capacity from their continuous scavenging of acidic components (NO_3^- and SO_4^{2-}). Nevertheless, their values were observed to be <1 for most of the samples. This suggests the exceedance of major cations against the major anions, especially during consecutive rain events. Sequential sampling of the single rain event of 15th Aug showed similar pattern of neutralization capacity having lowest values during first 15 minutes of rain. With the results showing a 45% decline for the initial 15 minutes followed by 31% decline during the next 15 minute change in its neutralization capacities, a faster scavenging of coarse mode particle of Ca^{2+} associated with SO_4^{2-} and NO_3^- in comparison to their fine mode fraction could be established.

CONCLUSION

The expanding industrial and agricultural sectors significantly contribute to the atmospheric Nr, which are eventually removed by rainfall. The observations showed an abundance of NH_4^+ (62.3 ± 2.3 μeql^{-1}) over NO_3^- (46.8 ± 40.1 μeql^{-1}) in the rain water samples eventually creating a significant contribution of wet deposition fluxes of NH_4^+ - N (3.6 kg ha^{-1} y^{-1}) in comparison to the NO_3^- - N (2.1 kg ha^{-1} y^{-1}) at Mathura. Scavenging patterns confirmed the presence of NH_4NO_3, showing variations along with the rainfall intensity. Correlation of 0.92 between NH_4 and NO_3 also supported these graphical observations, thereby, confirming the dominant forms in which these Nr species are being deposited over the study area. Their scavenging pattern confirmed initial period of rain events are dominated by the below cloud scavenging process. The subsequent monsoonal advancement reveals that the below cloud scavenging remains less effective, especially during consecutive rain events. Neutralization capacities of the rain water samples further substantiated such patterns in the Nr scavenging, thereby, confirming its effective removal through NH_4NO_3 formation by small droplets of rain during low intensity rainfall.

ACKNOWLEDGMENTS

We sincerely thank the financial support received from DST PURSE and UGC to conduct this research work. Thanks are due to Dr. Saumya Singh for proper evaluation of the manuscript and useful suggestions. We sincerely thank Chief Editor for continued support and editing of the manuscript.

Compliance with Ethical Standards

The authors declare that they have no conflict of interest and adhere to copyright norms.

REFERENCES

Alastuey, A., Querol, X., Chaves, A., Lopez - Soler, A., and Ruiz, C.R., 2001. Wet only sequential deposition in a rural area in north eastern Spain. Tellus B, v.53, no.1, pp: 40-52.

Ayers, G.P., 1995. (November). Some practical aspects of acid deposition measurement. In Presentation to the Third Expert Meeting on Acid Deposition Monitoring Network in East Asia Japan: Niigata Prefecture. pp: 14-16.

Bauer, S.E., Koch, D., Unger, N., Metzger, S.M., Shindell, D.T., and Streets, D.G., 2007. Nitrate aerosols today and in 2030: a global simulation including aerosols and tropospheric ozone. Atmospheric Chemistry and Physics, v.7, no.19, pp: 5043-5059.

Bhaskar, V.V., and Rao, P.S.P., 2016. Annual and decadal variation in chemical composition of rain water at all the ten GAW stations in India. Journal of Atmospheric Chemistry, pp: 1-31.

Dentener, F., Drevet, J., Lamarque, J.F., Bey, I., Eickhout, B., Fiore, A.M., Hauglustaine, D., Horowitz, L.W., Krol, M., Kulshrestha, U.C., and Lawrence, M., 2006. Nitrogen and sulfur deposition on regional and global scales: a multimodel evaluation. Global biogeochemical cycles, v.20, no.4, pp: 1-21.

Du, E., and Liu, X., 2014. High rates of wet nitrogen deposition in China: A synthesis. In Nitrogen Deposition, Critical Loads and Biodiversity Springer Netherlands., pp: 49-56.

Galloway, J.N., Dentener, F.J., Capone, D.G., Boyer, E.W., Howarth, R.W., Seitzinger, S.P., Asner, G.P., Cleveland, C.C., Green, P.A., Holland, E.A., and Karl, D.M., 2004. Nitrogen cycles: past, present, and future. Biogeochemistry, v.70, no.2, pp: 153-226.

Galloway, J.N., Townsend, A.R., Erisman, J.W., Bekunda, M., Cai, Z., Freney, J.R., Martinelli, L.A., Seitzinger, S.P., and Sutton, M.A., 2008. Transformation of the nitrogen cycle: recent trends, questions, and potential solutions. Science, v.320, no.5878, pp: 889-892.

Grömping, A.H.J., Ostapczuk, P., and Emons, H., 1997. Wet deposition in Germany: long-term trends and the contribution of heavy metals. Chemosphere, v.34, no.9-10, pp: 2227-2236.

Jain, M., Kulshrestha, U.C., Sarkar, A.K., and Parashar, D.C., 2000. Influence of crustal aerosols on wet deposition at urban and rural sites in India. Atmospheric Environment, v.34, no.29, pp: 5129-5137.

Kulshrestha, U.C., 2013. Encyclopedia of Environmental Management. v.6, no.7, pp: 8.

Kulshrestha, U.C., Sarkar, A.K., Srivastava, S.S., and Parashar, D.C., 1996. Investigation into atmospheric deposition through precipitation studies at New Delhi (India). Atmospheric Environment, v.30, no.24, pp: 4149-4154.

Kulshrestha, U.C., Saxena, A., Kumar, N., Kumari, K.M., and Srivastava, S.S., 1998. Chemical composition and association of size-differentiated aerosols at a suburban site in a semi-arid tract of India. Journal of Atmospheric Chemistry, v.29, no.2, pp: 109-118.

Kulshrestha, U.C., Kulshrestha, M.J., Sekar, R., Sastry, G.S.R., and Vairamani, M., 2003. Chemical characteristics of rainwater at an urban site of south-central India. Atmospheric Environment, v.37, no.21, pp: 3019-3026.

Kulshrestha, U.C., Granat, L., Engardt, M., and Rodhe, H., 2005. Review of precipitation monitoring studies in India—a search for regional patterns. Atmospheric Environment, v.39, no.38, pp: 7403-7419.

Kulshrestha, U.C., Kulshrestha, M.J., Satyanarayana, J., and Reddy, L.A.K., 2014a. Atmospheric deposition of reactive nitrogen in India. In Nitrogen Deposition, Critical Loads and Biodiversity. Springer Netherlands, pp: 75-82.

Kulshrestha, M.J., Singh, R., Duarah, R., and Rao, P.G., 2014b. Influence of crustal aerosols on wet deposition at a rural site of North-East India. International Journal of Environmental Studies, v.71, no.4, pp: 510-525.

Norman, M., Das, S.N., Pillai, A.G., Granat, L., and Rodhe, H., 2001. Influence of air mass trajectories on the chemical composition of precipitation in India. Atmospheric Environment, v.35, no.25, pp: 4223-4235.

Parashar, D.C., Granat, L., Kulshreshta, U.C., Pillai, A.G., Naik, M.S., Momin, G.A., Rao, P.P., Safai, P.D., Khemani, L.T., Naqvi, S.W.A., and Narvekar, P.V., 1996. Chemical composition of precipitation in India and Nepal: a preliminary report on an Indo-Swedish project on atmospheric chemistry. Department of Meteorology; Stockholm University; Stockholm; Sweden.

Reis, S., Pinder, R.W., Zhang, M., Lijie, G., and Sutton, M.A., 2009. Reactive nitrogen in atmospheric emission inventories. Atmospheric Chemistry and Physics, v.9, no.19, pp: 7657-7677.

Singh S., Kumar B., Sharma A., and Kulshrestha U.C., 2017. Wet deposition fluxes of atmospheric inorganic reactive nitrogen at an urban and rural site in the IndoGangetic Plain. Atmospheric Pollution Research, http://dx.doi.org/10.1016/j.apr.2016.12.021.

Tørseth, K., Aas, W., Breivik, K., Fjæraa, A.M., Fiebig, M., Hjellbrekke, A.G., Lund Myhre, C., Solberg, S. and Yttri, K.E., 2012. Introduction to the European Monitoring and Evaluation Programme (EMEP) and observed atmospheric composition change during 1972–2009. Atmospheric Chemistry and Physics, v.12, no.12, pp: 5447-5481.

Vet, R., Artz, R.S., Carou, S., Shaw, M., Ro, C.U., Aas, W., Baker, A., Bowersox, V.C., Dentener, F., Galy-Lacaux, C., and Hou, A., 2014. A global assessment of precipitation chemistry and deposition of sulfur, nitrogen, sea salt, base cations, organic acids, acidity and pH, and phosphorus. Atmospheric Environment, v.93, pp: 3-100.

Wallace, J.M., and Hobbs, P.V., 2006. Atmospheric science: an introductory survey. Academic press, v.92.

WMO (World Meteorological Organization) 1994. Report of the Workshop on Precipitation Chemistry Laboratory Techniques, WMO TD., v.658, pp: 14-15.

Received on: 6.3.17; Revised on: 16.4.17; Accepted on: 18.4.17

NEWS AT A GLANCE

Forthcoming Events:

1) SEGH 2016 — 32nd International conference of Society for Environmental Geochemistry and Health
04 Jul 2017 - 08 Jul 2017,
Brussels, Belgium
Topics: Environmental Chemistry and Geochemistry
Event website: http://segh-brussels.sciencesconf.org/

2) Exoplanet science in the coming decade: The bright and nearby future
26 Jun 2017
Prague, Czech Republic
Topics: Astronomy, Astrophysics and Cosmology
Event website: http://eas.unige.ch/EWASS2017/session.jsp?id=S1

3) IGARSS 2018 - 2018 IEEE International Geosciences and Remote Sensing Symposium
22 Jul 2018 - 27 Jul 2018
Valencia, Spain
Topics: Geography, Global Positioning System, Earth Observation
Event website: http://www.igarss2018.org

4) Conference on Classical and Geophysical Fluid Dynamics: Modeling, Reduction, and Simulation
26 Jun 2017 - 28 Jun 2017
Virginia Tech, Blacksburg, Virginia, United States
Topics: Applied Mathematics (in general), Thermodynamics, Fluid Dynamics and Statistical Physics
Event website: http://www.math.vt.edu/GFD_conference2017/index.html

Awards and Recognition

*Shanti Swarup Bhatnagar Prize for 2016

Dr.Sunil Kumar Singh has been awarded for Earth, Atmosphere, Ocean and Planetary Sciences 2016

*American Meteorological Society has awarded The Roberte Horton Lecture in HYDROLOGY for 2017 to Hoshin V. Gupta for research into calibration and optimization of hydrological models, and for fundamental contributions towards quantifying uncertainty in hydrologic model predictions

* Dr.N.Purnachandra Rao, Chief Scientist of NGRI has been selected as the Director of National Centre for Earth Science Studies (NCESS), Thiruvanathapuram, under the Ministry of Earth Sciences, Govt. of India

Science and Technology News

Since Kyoto conference, nearly two decades back, a large number of international conferences were held in different parts of the globe to take measures to lessen greenhouse gas emissions that are responsible for global warming resultant climate change. It is unfortunate that nothing substantial has been achieved in these meetings/ conferences as reduction of fossil fuel emissions would have significant impact globally on the socio economic structures of developing and developed countries. As something tangible seems to have been achieved during the recent interaction in Paris conference, strong opposition to such fossil fuel reductions by USA in the last couple of months by the new government of USA has in general dampened the spirits of the environmental protagonists. While none can unequivocally quantify the role of natural and manmade causes for climate change, none can argue that global warming has not created significant changes to our environment and thereby to the overall wellbeing of Man, Flora and Fauna. Debates still continue to know explicitly the cause and outcome….Global warming led to climate change or climate change led to global warming. Since it is essential to know some important aspects of global warming in the last one decade I have given below results of some useful studies in the recent past so that young researchers can take measures to address global warming resultant ill effects. These studies also tell us the varied nature of the opinions expressed by the knowledgeable scientists and technological innovators, who in spite of their invaluable expertise could not specifically focus on aspects that could help Man (human race as a whole belonging to one colony-Earth), to lessen the negative impacts due to global warming. I feel sad to agree with intelligent industrial and business lobbies that scientists have become self centred and blinkered in defending their findings, instead of making a concerted focused co-operative effort to solve the climate change and global warming issues. Let us look at the significant studies carried out by scientists belonging to different branches and sub branches of earth system sciences and try to develop one powerful lobby of the scientists to overcome many hurdles in saving life on Earth.

***The Proof of Our Science Lies in the Telling**

Scientists conduct scientific research. It's what they can do. Researchers identify a question and apply all the techniques they can to obtain a solution. Then they publish their results for others to build upon and advance the science and our understanding of the earth, its environment, and the geophysical processes involved. It's a beautiful thing.

Meanwhile, back in the "real" world, the broader public can be left behind, and along with them, the policy community, congress, and the federal agencies. How can this be? Is this merely an expected consequence of the increasing specialization throughout modern society? Or is it an avoidable result of an operationally sequestered scientific community that has stayed in its ivory tower and eschewed contact with policy-makers?

This issue came to the fore at the recent conference on the National Council for Science and the Environment (NCSE), whose theme in 2016 was the Food-Energy-Water Nexus. While numerous technical sessions explored the many aspects of the interaction between food, energy, and water, some focused more broadly on the ways that the scientific community can more effectively provide data, analysis, and advice to the world at large. Though in one keynote lecture, Paul Lussier explained that merely explaining the facts of our science is not enough to inspire the public to alter their behavior to avoid impending social and environmental problems.

Consider the issue of the societal impacts of climate change. Sea level is rising twice as fast in the 21st century as it did in the 20th century because ice is melting and oceans are warming faster in response to radiative forcing. The public does not respond to descriptions of global data sets, measures of Arctic ice, or maps of sea surface temperature–a number like 3 mm/yr does not invoke a public response to alter behavior. They respond more immediately to their home washing away in a storm or to the threat of damage to things to which they are emotionally or financially connected. Emissions reductions and land use planning for sea level rise mitigation, water and energy use for resource conservation, and food production and diet for enhanced human health are only a few examples of areas around which behaviors could be altered for the public good. Yet behaviors are not changing because the knowledge generated by scientific inquiry is not disseminated in terms that the public understands or appreciates. It is our mindset as much as the words we use.

For example, scientists seek to be accurate and objective, while policy-makers want to be realistic and popular, the media needs to be dramatic and persuasive, and businesses must be accountable and visionary. These communities have very different goals, means, and measures of success, as well as contrasting and often conflicting operational languages. In order for the scientific community to help each of these communities to achieve their goals, including the ones they may have in common (such as leaving a planet for their grandchildren that can support them comfortably by providing a sufficient and sustainable flux of environmental goods and services), we must each couch our discussion in terms that have meaning for the communities we are engaging. Only then can our science be put to use for the benefit of society, and subsequently be appreciated, supported, and sustained. (**Source:** https://eos.org/editors-vox/the-proof-of-our-science-lies-in-the-telling)

***Better Tools to Build Better Climate Models**

Developing, maintaining, and enhancing a predictive climate model demand enormous human and computing resources. Decades' worth of observational data must be compiled, vetted, and integrated into a database. Parameters and variables must be identified and built into algorithms that simulate physical processes. Massive calculations can then convert past observations into predictions of the future. To determine the accuracy of predictions, results are validated by comparing them to present-day observations. As new data are fed to the model and scientific understanding of climate systems evolves, new information gets built into the model, and the testing and validation continue. One of the most resource-intensive aspects of climate modeling is the creation of a system for calibrating climate models, where model simulations are used to validate model output against observational data sets that span the globe. It is called a "climate model test bed." Such test bed environments typically evaluate each component of the model in isolation, using a skeleton framework that makes the module behave as if it were functioning within the larger program. To calibrate the model against regional observational data sets, uncertainty quantification techniques assess the accuracy of predictions, given the limitations inherent in the input information. If model developers could compare test bed output to observational measurements as the output was being generated, the comparison could facilitate aligning the model with the observed data. This capability could eliminate some of the more tedious activities associated with model development and evaluation.

If successful, the capability could accelerate the development of climate sub-model components, such as atmosphere, land, ocean, and sea ice. Researchers from five Department of Energy (DOE) laboratories of USA are developing this real-time comparison capability. If successful, the capability could accelerate the development of climate sub-model components, such as atmosphere, land, ocean, and sea ice. It could also improve the process by which the sub-models are integrated with each other to form the resulting coupled Earth system climate model.

For this effort, which began in mid-2011, the test bed developers fed representative observational data sets—for example, satellite data from NASA's Atmospheric Infrared Sounder (AIRS) and Earth Radiation Budget Experiment (ERBE)—into the specialized model testing and verification platform that they developed. This prototype platform allows for the rapid evaluation of model components and algorithms. To build the test bed prototype, the Climate Science for a Sustainable Energy Future (CSSEF) team has employed DOE's high-performance computing resources to make use of several open-source software projects that are steadily gaining recognition and usage in their respective research communities. The team has unveiled a unique and flexible prototype that they hope will accelerate the development of future climate models. The tools and experiences resulting from these DOE-sponsored projects provide the foundation for the prototype test bed's infrastructure. Now, through the integration of existing technologies, open standards, and community expertise, the CSSEF team has unveiled a unique and flexible prototype that they hope will accelerate the development of future climate models.

The prototype test bed team is now under the banner of the newly formed Accelerated Climate Modeling for Energy (ACME) project. Under ACME, the team will continue its efforts to deliver an advanced model development, testing, and execution workflow and data infrastructure production test bed for DOE climate and energy research needs. (**Source:** https://eos.org/project-updates/better-tools-to-build-better-climate-models)

***Himalayan Climate Change Affects Regional, Global Environments**

The high-elevation region that includes the Tibetan Plateau and its surrounding mountain ranges has been dubbed the "Third Pole." This region encompasses approximately 5 million square kms of unforgiving terrain, with an average elevation of more than 4000 meters above sea level, and it straddles tense geopolitical borders. The Third Pole includes an estimated 100,000 square kms of glaciers.

The annual variability of snow in the Third Pole region affects drinking and irrigation water that sustains roughly 1.5 billion people downstream. Cumulatively, this region holds the planet's largest concentrated stock of ice outside the Arctic and Antarctic. The annual variability of snow extent affects global atmospheric circulation patterns, monsoon variability, and, more important, drinking and irrigation water that sustains roughly 1.5 billion people in India, Nepal, China, and Bangladesh.

Scientists from around the globe gathered in May 2016 at the Byrd Polar and Climate Research Center at Ohio State University to address climate issues facing the Tibetan Plateau and surrounding mountain ranges. Climate records from low and middle latitudes are crucial to understanding Earth's changing climate. "It has to do with water resources," said Lonnie Thompson, a renowned

glaciologist and senior researcher at Ohio State. He added, "It has to do with the atmospheric processes that drive the monsoon system in that part of the world."

The workshop included sessions on glacial fluctuations, the Asian monsoon, hydrology, geohazards, and climate change in the Third Pole. Participants also focused on research related to the Third Pole biosphere and anthroposphere. The TPE program and its workshops provide an invaluable opportunity for data, resource, and methods sharing. The new Center for Tibetan Plateau Research aims to serve as a hub for strengthening global cooperation, for example, by assisting with young scientist training programs. In addition to this new center, the TPE program opened its Kathmandu center in 2013 and is planning to open a European center in the near future.

(Citation: Joswiak, M., D. Joswiak, and T. Yao (2017), Himalayan climate change affects regional, global environments, *Eos, 98,* https://doi.org/10.1029/2017EO069289).

***Earth's orbital variations, sea ice synch glacial periods**

New research shows how sea ice growth in the Southern Hemisphere during certain orbital periods could control the pace of ice ages on Earth. The Southern Hemisphere has a higher capacity to grow sea ice than the Northern Hemisphere, where continents block growth. New research shows that the expansion of Southern Hemisphere sea ice during certain periods in Earth's orbital cycles can control the pace of the planet's ice ages. Earth is currently in an interglacial period, a warm pulse between long, cold ice ages when glaciers dominate our planet's higher latitudes. For the past million years, these glacial-interglacial cycles have repeated roughly on a 100,000-year cycle. Now a team of researchers has a new explanation for that timing and why the cycle was different before a million years ago. According to researchers` models, it has to do with the fact that the planet has been generally cooler over the past million years than it was prior to that. The models show that, when Earth was generally warmer than today, precession-related sea ice expansion in the Southern Hemisphere is less likely to occur. That allows the obliquity cycle to dominate the global temperature signature. After a million years ago, when Earth became a bit cooler on average, the obliquity signal starts to take a back seat to the precession/eccentricity signal. Researchers believe their models present a strong new explanation for the history of Earth's glacial cycle -- explaining both the more recent pace and the puzzling transition a million years ago. As for the future of the glacial cycle, that remains unclear state the scientists. It's difficult at this point to predict how human contributions to Earth's greenhouse gas concentrations might alter the future of Earth's ice ages. (**Source:** Jung-Eun Lee et al; Hemispheric sea ice distribution sets the glacial tempo**.** *Geophysical Research Letters*, 2017; DOI: 10.1002/2016GL071307).

***Understanding How Climate Engineering Can Offset Climate Change**

Participants at a meeting in Oslo, Norway, presented new developments in modeling and simulating climate engineering approaches, including stratospheric aerosols, marine cloud brightening, cirrus thinning, and land and ocean brightening.

Climate intervention, also called geoengineering or climate engineering, is an emerging, important area of climate science research. This research focuses on deliberate climate modification to offset some of the effects of anthropogenic greenhouse gas emissions. The Geoengineering Model Inter-comparison Project (GeoMIP) was formed to better understand climate intervention through simulations conducted by multiple climate models.

GeoMIP held its sixth annual meeting at the University of Oslo in Oslo, Norway, in June 2016. The meeting was held in conjunction with the Norwegian project Exploring the Potential and Side Effects of Climate Engineering (EXPECT), which seeks to understand the implications of climate intervention and to stimulate interdisciplinary collaboration among scientists in the natural and social sciences. Participants from a variety of natural science backgrounds presented modeling results from multiple climate intervention methods, including stratospheric aerosols, marine cloud brightening, cirrus thinning, and land and ocean brightening. The first results from multi-model sea spray climate intervention simulations showed strong features of commonality among the responses of different models.

Descriptions of these new areas of research are being added to the GeoMIP website, which is the most up-to-date source of information on past, present, and future simulation designs. Also on the site are a timeline of start dates for the new simulations for Coupled Model and a current list of Testbed experiments. After the conclusion of the 1.5-day GeoMIP meeting, EXPECT held an open forum in which natural and social science experts on climate intervention presented to the general public the current thinking of the research community. In the future, GeoMIP will continue its mission of providing knowledge about key uncertainties in climate intervention research, particularly as an officially endorsed project under CMIP6. As new important areas of research emerge in this field, GeoMIP will continue to provide a scientific focus for addressing important unknowns and a forum for consideration of the full range of approaches to climate intervention. (**Source:** Kravitz,B et al (2017), Understanding how climate engineering can offset climate change, *Eos, 98,* doi:10.1029/2016EO005279).

***Good Night Sunshine: Geoengineering Solutions to Climate Change?**

The goal of 2016 Paris Agreement to limit global warming to 2°C, if not 1.5°C, are admirable, but it's unlikely that this inspirational goal can be reached with voluntary greenhouse gas emission reductions alone. Already, we are nearing the 1.5°C global warming level, with predictions for reaching 2°C not far into the future. The implications of global warming are recognized widely, both in short-term events like coastal inundation and extreme weather, and long-term in the form of permanently shifting climate zones and higher sea level. The range of our actions, however, is not limited to greenhouse gas generation only. Climate engineering takes two approaches: (1) Carbon dioxide removal (CDR), and (2) solar radiation management (SRM). CDR addresses the cause of climate warming by removing greenhouse gas from the atmosphere ("treat the illness"). SRM offsets the warming effects of greenhouse gases by allowing Earth to absorb less solar radiation ("treat the symptoms"). Reduction of greenhouse gas emissions, as proposed in the Paris Agreement, is desirable, but is not a prerequisite for climate engineering. Among the range of techniques, SRM is the main source of professional and public anxiety and has mostly remained taboo. There are concerns about unintended consequences, local applications with global consequences, runaway effects, and even climate warfare.

Given that climate engineering remains highly controversial, a set of thoughtful research papers and scientific commentaries have been published on this topic in AGU's open-access

journal *Earth's Future*. The contributions highlight our much improved understanding of the environmental, political, and societal risks and benefits of climate engineering, but they also recognize that the current state of our knowledge is insufficient for reliable deployment. Computer modeling and integrated assessments have advanced the positive and negative aspects of various techniques, allowing for an informed public debate and eventual decision-making. Some nations are advancing this understanding and are considering some implementation. However, more extensive scientific efforts and social study that includes real-world, outdoor experimentation will be needed to adequately assess near-term deployments and their impact.

Climate engineering has unquestionable potential to limit global warming when coupled with currently available technologies, but the scientific, social and ethical dimensions of implementation are not sufficiently examined. Given the worldwide impact of most deployment approaches, planning should occur on a global scale, involving all nations, both rich and poor, and not be limited to a few technologically advanced, wealthy stakeholders. Judging by the resilience of today's human society to global environmental change, ignoring the potential of climate engineering solutions does not seem prudent and realistic. (**Source**: http://www.climate-engineering.eu/single/eos-editors-vox-good-night-sunshine-geoengineering-solutions-to-climate-change.html).

Details given above clearly indicate the openness in projecting importance and limitations of data, data based modelling. The lack of proper interaction between various scientific groups to build a strong platform from which scientists can leap forward to receive the support of common man and policy makers has been realised in principle. While there is a positive stride in the last couple of years the significant negative impact of US President Trump`s opposition to climate change research and support to fossil fuel usage has negated the positive strides. For us in India we need to initiate various measures to reduce all types of pollution, the negative factor that is hampering our economic growth and affecting quality of life.

Outstanding Contribution in Re-Vitalising CSIR

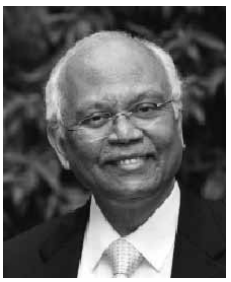

Raghunath Anant Mashelkar (born on 1st January, 1943) is an Indian chemical engineer and a former Director General of the Council of Scientific & Industrial Research (CSIR).

Life and work

Mashelkar studied at the University of Bombay (now the Institute of Chemical Technology, Mumbai) and obtained a Bachelor's degree in Chemical engineering in 1966, and a PhD degree in 1969. Mashelkar is presently the President of Global Research Alliance, a network of publicly funded research and development institutes from Asia-Pacific, South Africa, Europe and USA with over 60,000 scientists. He is the Chairperson of India's National Innovation Foundation. He has been appointed as the first Chairperson of Academy of Scientific and Innovative Research (AcSIR).

Positions held: • Director General, Council of Scientific & Industrial Research, New Delhi, INDIA, (1995-2006) • Director, National Chemical Laboratory, Pune, INDIA (1989-1995) Different Grades of scientist including Director's Grade, National Chemical Laboratory, Pune, INDIA (1976-1989) • Lecturer in Chemical Engineering, University of Salford, UK (1970-1976) • Leverhume Research Fellow,University of Salford (1969-1970).

Honorary Doctorates in Science and Engineering: • Symbiosis International University (2010) • Mahatma Gandhi Kashi Vidyapith, Varanasi (2009) • University of Goa (2009) • Lucknow University, Lucknow (2007) • Deendayal Upadhyay Gorakhpur University, Gorakhpur (2007) • Sri Venkateswara University, Tirupati (2006) • Visva Bharati, Santiniketan (2006) D.Lit. (Desikottama) • Mohanlal Sukhadia University, Udaipur (2006) • Guru Nanak Dev University, Amritsar (2005) • Maharishi Dayanand University, Rohtak (2005) • Govind Ballabh Pant University of Agriculture & Technology, Pantnagar (2004) • Narendra Deva University of Agriculture & Technology, Faizabad (2004) 2 • University of Kalyani, Kalyani (WB) (2004) • M.S. University of Baroda, Varodara (2003) • University of Allahabad, Allahabad (2002) • University of Wisconsin, USA (2002) • Banaras Hindu University, Varanasi (2002) • Tilak Maharashtra Vidyapeeth, Pune (2002) • University of London, UK (2001) • Pretoria University, Pretoria, South Africa (2000) • Anna University, Chennai (2000) • Guwahati University, Assam (2000) • Bundelkhand University, Jhansi (2000) • University of Delhi, Delhi (1998) • Indian School of Mines, Dhanbad (1997) • University of Roorkee, Roorkee (1997) • University of Kanpur, Kanpur (1995) • University of Salford, UK (1993).

Civilian Honours by President of India: • Padmashri (1991) • Padmabhushan (2000)

Election to Prestigious Academies and Scientific Bodies (India and Abroad): • Foreign Fellow, Australian Academy of Technological Sciences and Engineering (ATSE) (2008) • Fellow, Royal Society of Chemistry, Cambridge, UK (2006) • Foreign Associate, US National Academy of Sciences, USA (2005) • Fellow, Indian Association for the Cultivation of Science, Kolkata (2005) • President, Indian National Science Academy (2005-2007) • President, Materials Research Society of India (2004-06) • President, Institution of Chemicals Engineers, UK (2007-08) • Foreign Associate, National Academy of Engineering, USA (2003) • Fellow, Royal Society (FRS), London (1998) • General President, Indian Science Congress (1999-2000) • Fellow, World Academy of Art & Science, USA (2000) • Fellow, The Institute of Physics, London (1998) • Fellow, Institute of Electronics and Telecommunication Engineers (IETE) (1998) • Foreign Member, Royal Academy of Engineering, UK (1996) 3 • Fellow, UK Institute of Chemical Engineering (1996) • Fellow, Third World Academy of Sciences (1994) • Fellow, Indian National Science Academy (1984) • Fellow, Indian Academy of Sciences (1983) • Fellow, Maharashtra Academy of Sciences (1985) • Fellow, National Academy of Engineering (1987) • Fellow, National Academy of Sciences (1989) • Fellow, Indian Institute of Chemical Engineers (1992) • President, Physical Sciences, National Academy of Sciences (1991) • President, Maharashtra Academy of Sciences (1991-94) • President, Society for Polymer Science in India (1986-92) • President, Indian Society of Rheology (1986-93) • Vice-President, Materials Research Society of India (1993-95) • Vice-President, Indian Academy of Sciences (1995-2000) • Foreign Fellow, Australian Academy of Technological Sciences and Engineering (ATSE) (April 2008).

Awards:

He received number of awards, for A) Scientific Research; B) Technology & Industrial Research; C) Leadership; and D) All Round Excellence: Out of more than 100 awards selected are listed below**.**

• Asutosh Mookherjee Memorial Award (2005) by Indian Science Congress Association; • The TWAS medal (2005) by TWAS, the Academy of Sciences for the Developing World; • Life Time Achievement Award (2004) by Indian Science Congress Association; • Hari Om Ashram Prerit Senior Scientist Award (2002) by Physical Research Laboratory, Ahmedabad; • Shanti Swarup Bhatnagar Medal (2001) by Indian National Science Academy, New Delhi; • Shanti Swarup Bhatnagar Award (2001) by Indian Science Congress Association, Calcutta; • Material Scientist of the Year Award (2000), by Materials Research Society of India; • GD Birla Award for Scientific Research (1993); • Shanti Swarup Bhatnagar Prize (1982) for engineering sciences by CSIR, New Delhi; • World Federation of Engineering Organisations (WFEO) Medal of Engineering Excellence (2003) by WEFO, Paris; • Dr. M. Visvesvaraya Memorial Award (2002) by Engineers Foundation, Kolhapur; • H.K. Firodia Award (2000) by H.K. Firodia Foundation, Pune; • Durga Prasad Khaitan Memorial Gold Medal (1996) by Asiatic Society, Calcutta; • National Research Development Corporation (NRDC) Republic Day Award (1995); • OP Bhasin award (1991) by Bhasin Foundation, Delhi; • Pandit Jawaharlal Nehru National Award in Engineering & Technology (1991) by Govt. of Madhya Pradesh; • Vishwakarma medal (1988) by Indian National Science Academy; • Federation of Indian Chamber of Commerce and Industry Award (1987) in physical and mathematical sciences; • IIFA Ben Gurion Award (2009) for contributions in Science & Technology • Rajiv Gandhi Life Time Achievement Award (2007) by Rajiv Rural Development Foundation, Tirupati; • Lakshmipat Singhania – IIML National Leadership Award (2004) by Indian Institute of Management, Lucknow • **IMC Juran Quality Medal (2002)** by Indian Merchants Chamber ***for leadership and continuous involvement as a role model for improvement of quality in CSIR;*** • **JRD Tata Award** for Corporate Leadership (1998) by All India Management Association ***for exemplary leadership provided to CSIR***. • Inaugural BP Lecture, Judge Business School, University of Cambridge (2010); • ETH Presidential Lecture at French Academy of Sciences, (2007) Zurich; • Star of Asia Award (2005) of Business Week (USA); • Shiromani Award (2002) for outstanding achievements in the field of science and commitment to national progress and human welfare; • Lifetime Achievement Award (2001) by Chemtech Foundation for all time lifetime achievement .

Professorships (Honorary & others) :

• Visiting Professor at Laboratory of Nanomedicine, Harvard University, Boston (2010); • Sir Louis Matheson Distinguished Visiting Professor, Monash University, Australia (2007 to 2010); • Visiting Professor at the Harvard/MIT, Boston (2007, 2008); • Fellow, University of Salford, UK (1992-93); • Visiting Professor, University of Delaware, USA (1975-76 & 1988); • Visiting Professor, Technical University of Denmark, Lyngby (1982).

Chairmanship/Membership of National Level High-Powered Committees/Bodies:

• Member, World Economic Forum's Global Agenda Council on Emerging Technologies (2009-) • Chairman, Thermax Innovation Council (2008-) • Chairman, Reliance Innovation Council (2007-) • Chairman, National Innovation Foundation (2000-) • Chairman, Marico Innovation Foundation (2005-) • Member, Scientific Advisory Board, VTT, Finland (2007-09) • Chairman, Scientific Advisory Committee on Hydrocarbons, Ministry of Petroleum & Natural Gas (2002) • Member, Governing Body, Indian Council for Research on International Economic Relations (2001-) • Member, Prime Minister's Knowledge Task Force (2000) • Member, Science Advisory Council to the Prime Minister (1988-90), (2004-2006).

International Bodies/Committees:

• I-20 Global Innovation Leaders, San Francisco, USA (2009) • Member, External Research Advisory Board, Microsoft, USA. (2007-) • Chairman, CSIR (South Africa) International Review Committee (2003) • Member of the Committee of Third World Academy of Sciences (TWAS) in Engineering Science and Technologies (2003) • Member, Research Advisory Committee, Department of Chemistry, Imperial College of Science & Technology, UK (2003) • Member, Review of Chemistry Research in UK Universities (2002) • Chairman, Innovation in Developing World Committee, Third World Academy of Sciences, Trieste (2000) • Member, Advisory Board, World Wide Academy (WIPO), Geneva (1999-) • Chairman, Standing Committee on Information Technology (WIPO), Geneva (1998).

Original contributions to Scientific and Industrial Research

Mashelkar has made some path-breaking contributions in transport phenomena in and thermodynamics of swelling, superswelling and shrinking polymers, modelling of polymerisation reactors, and engineering analysis of non-Newtonian flows. ***His exceptional leadership has transformed CSIR, world's largest chain of national laboratories engaged in industrial R&D.*** In post-liberalised India, Mashelkar has been the dominant force in shaping the direction of S&T in India. His contribution to the interpretation of the phenomenon of unusual retardation and enhancement in polymer dissolution is pathbreaking. In addition he was known for significant contributions in Engineering Analysis of Non-Newtonian Flows, Role of energetic networks in non-Newtonian Flows and Modelling of Industrial Polymerisation Reactors.

Leadership in Science and Technology

As Director General of CSIR (38 laboratories and 22,000 employees), which is the largest chain of industrial R & D labs, conceived & successfully led the process of transformation of CSIR. His white paper "CSIR 2001: Vision & Strategy" set up a new agenda. The story of the transformation of CSIR has been internationally acknowledged. Its appreciation by the Indian business world, has been captured as a cover page story by Business India in 1998 and also in 'World Class in India', a book brought out by Penguin, which has ranked CSIR among the top twelve organisations, who have managed the radical change the best in post-1991 India. [www.csir.res.in].

P.R.Reddy

Climate Change and Global Warming Quotations by Scientists, Heads of Govt., Politicians and Famous Dignitaries

Climate change due to Man's intervention	Climate change – A natural phenomenon
"Saving our planet, lifting people out of poverty, advancing economic growth... these are one and the same fight. We must connect the dots between climate change, water scarcity, energy shortages, global health, food security and women's empowerment. Solutions to one problem must be solutions for all." - *Ban Ki-moon (1944--) Secretary General, United Nations* *** "The time is past when humankind thought it could selfishly draw on exhaustible resources. We know now the world is not a commodity." – *Francois Hollande (1954--) Former President of the French Republic*	"I had the privilege of being fired by Al Gore, since I refused to go along with his alarmism....I have spent a long research career studying physics that is closely related to the greenhouse effect....Fears about man-made global warming are unwarranted and are not based on good science. The earth's climate is changing now, as it always has. There is no evidence that the changes differ in any qualitative way from those of the past." - *Will Harper, (1939--) an American physicist specialised in the study of atomic physics, optics and spectroscopy* "Unfortunately, the IPCC climate change documents do not provide an objective assessment of the earth's temperature trends and associated climate change….As one of the invited expert reviewers for the 2007 IPCC documents, I have pointed out the flawed review process used by the IPCC scientists in one of my letters. I have also pointed out in my letter that an increasing number of scientists are now questioning the hypothesis of Greenhouse gas induced warming of the earth's surface and suggesting a stronger impact of solar variability and large-scale atmospheric circulation patterns on the observed temperature increase than previously believed." - *Madhav L. Khandekar, Former UN scientist* *** "US shouldn't waste "financial resources" on climate change and should instead use them to ensure the world has clean water, eliminate diseases like malaria, increase food production, or develop alternative energy sources."- *Donald Trump (1946--) President of U.S.A*
"The clear and present danger of climate change means we cannot burn our way to prosperity. We already rely too heavily on fossil fuels. We need to find a new, sustainable path to the future we want. We need a clean industrial revolution."- *Ban Ki-moon (1944--) Secretary General, United Nations* *** "The saddest fact of climate change - and the chief reason we should be concerned about finding a proper response - is that the countries it will hit hardest are already among the poorest and most long-suffering. *Bjorn Lomborg (1965--) is a Danish author and adjunct professor at the Copenhagen Business School* *** "Just as Mars - a desert planet - gives us insights into global climate change on Earth, the promise awaits for bringing back to life portions of the Red Planet through the application of Earth Science to its similar chemistry, possibly reawakening its life-bearing potential." - *Buzz Aldrin (1930--) an American engineer, former astronaut and second person to walk on Moon*	
"We must now agree on a binding review mechanism under international law, so that this century can credibly be called a century of decarbonisation." – *Angela Merkel(1954--) Chancellor of Germany*	"The atmosphere has periodic warming and cooling cycles. The sun is the primary source of energy impacting the earth's surface. That energy heats the land and the seas, which then warm the air above them. Water vapor and other gases in the atmosphere also affect temperature....Oceans are the main repository for CO_2. They release CO_2 as their temperature rises - just like your beer. This strongly suggests that warming oceans - heated by the sun - are a major contributor to CO_2 in the atmosphere." - *John Takeuchi, Meteorologist*
"If we do not change our negative habits toward climate change, we can count on worldwide disruptions in food production, resulting in mass migration, refugee crises and increased conflict over scarce natural resources like water and farm land. This is a recipe for major security problems." - *Michael Franti (1966--) an American rapper, musician, spoken word artist and singer-songwriter.* *** "I play fictitious characters often solving fictitious problems. I believe mankind has looked at climate change in the same way, as if it were a fiction."- *Leonardo DiCaprio* (1974--) *an American actor and film producer.* *** "We have a single mission: to protect and hand on the planet to the next generation." – *Francois Hollande (1954--) Former President of France* *** "There's one issue that will define the contours of this century more dramatically than any other, and that is the urgent threat of a changing climate."- *Barack Obama (1961--) Former President of USA*	"There is now a near consensus that global air temperatures are increasing, however, there is no consensus on how this has affected the temperature of the world's oceans, and in particular in the Atlantic Ocean, or how much of the recent warming trend is attributable to man's activities....For the layman, there is sometimes a tendency to regard every new 'discovery' or scientific finding from the latest published paper as an inviolate fact....In reality, rarely is there ever a last and final word in studies of complex systems such as earth's environment. Rather, science is a dynamic process based on the scientific method in which researchers test hypotheses leading to new discoveries, but also reexamine earlier theories and try to improve, build upon, or extend them."- *Peter Dailey (1950--) Director of Atmospheric Science , AIR Worldwide, Boston, U.S.A*
"Being told about the effects of climate change is an appeal to our reason and to our desire to bring about change. But to see that Africans are the hardest hit by climate change, even though they generate almost no greenhouse gas, is a glaring injustice, which also triggers anger and outrage over those who seek to ignore it."- *Sigmar Gabriel* (1959--) *a German politician who currently serves as Minister for Foreign Affairs and Vice Chancellor of Germany* *** "Clean air and a healthy climate benefit all of us, but it will take a diverse coalition to step up to the threat posed by unchecked climate change." - *Keith Ellison* (1963--) *Deputy Chair of the Democratic National Committee since 2017*	"The suppression of scientific evidence that contradicts the causal link between human-generated CO_2 and climate has been of great concern to ethical scientists both here in Australia and around the world....The eco-hysteria that leads the Greens, as well as the left-leaning media, to attack any person who attempts to publish science that contradicts their beliefs is a gross example of the dangerous doctrine that the end justifies the means."- *Art Raiche, Former Chief Research Scienti st of CSIRO, Australia*

Department of Earth Sciences, IIT Roorkee

IITR- IGU STUDENT CHAPTER REPORT

The Department of Earth Sciences, IIT, Roorkee, recently has established IGU student chapter. Under its aegis, as the first event of the chapter,the prestigious L.N. Kailasam Memorial Lecture of IGU was delivered by Shri. S. Mahapatra, Director (E&P), Oil India Limited, Noida on 5th April, 2017. The topic was "E&P Landscape in India-A peep into the future".The lecture was well received by the student community. The speaker touched upon various facets of the oil industry and its volatile nature. At the end of the lecture Shri S. Mahapatra was felicitated by Prof. Shailesh Nayak with a medal and a plaque.

This was followed by a poster-cum-interaction session for students. In his Presidential address Prof. Shailesh Nayak, President of IGU briefed about the importance of establishing IGU chapter at IIT, Roorkee. Dr. Kalachand Sain, Hon. Secretary of IGU has presented a brief review of IGU`s activities since its establishment in 1963.

The L.N. Kailasam Memorial lecture was followed by a poster presentation session. There were 45 poster presentations by students on different fields of geophysics and geology. The event was successfully organized. As a part of this important event an informal interaction of the students with the guests helped the students to get exposed to important facets of research in earth sciences.

All the participants enjoyed the programme.

Shri S. Mahapatra(Director, Oil India Limited) delivering the L.N. Kailasam Memorial Lecture

Prof. Shailesh Nayak (President, IGU) & Dr. Kalachand Sain (Secretary, IGU) honoring Shri S. Mahapatra

Newly formed IIT Roorkee IGU Student chapter team with the IGU team

Prof. ShaileshNayak and Shri S. Mahapatra interacting with a final year student during poster session

ANNOUNCEMENT

54th Annual Convention of Indian Geophysical Union (IGU)

will be held at CSIR-NGRI, Hyderabad

During December 4-7, 2017

on

"RECENT ADVANCES IN GEOPHYSICS: SPECIAL REFERENCE TO EARTHQUAKES"

Hon. Secretary
Indian Geophysical Union
CSIR-NGRI Campus, Uppal Road
Hyderabad- 500 007, India
Email: igu123@gmail.com

NOTIFICATION FOR IGU AWARD/PRIZE - 2017

In connection with the 54th Annual Convention of IGU during December 4-7, 2017 at CSIR-National Geophysical Research Institute (NGRI), Hyderabad. Nominations (both hard and soft copies) for the following Award/Prize are invited on or before 31-8-2017.

IGU - Hari Narain Lifetime Achievement Award to an eminent Senior Scientist for exceptional contribution to the causes of Indian Earth Sciences. Nominator should be past recipients, fellows and EC members of IGU, and any distinguished Earth Scientist/Professor (must be a member of IGU).

Anni Talwani Memorial Prize to meritorious Scientist (below 60 yrs as on 31-01-2017) for outstanding contribution to Earth Sciences covering land and/or offshore of India. Nominator should be a distinguished Earth Scientist/Professor.

For details of Award/Prize, please visit the website: **www.igu.in**

Nomination Proforma for IGU-Hari Narain Lifetime Achievement Award

1. Name of the Award
2. Full name, age and address of the nominee
3. Academic qualifications (bachelor's degree onwards)
4. Position held (in chronological order)
5. Brief statement on significant contribution for citation (within 200 words)
6. Professional achievements
   (a) Awards/Honours/Fellowships
   (b) Memberships in Academics/Societies/Professional bodies
7. Name and Address of Nominator

Nomination for Anni Talwani Memorial Prize is restricted to 2 pages of candidate's CV along with no more than 2 pages each of 3 supporting letters. Nominator may kindly note that exceeding the limits is not permitted.

The Hon. Secretary,
Indian Geophysical Union
NGRI Campus, Uppal Road
Hyderabad- 500 007
Email: igu123@gmail.com

Note:

Send only one nomination

Nominations will be rejected, if they are not in format and within restricted words limit

NOTIFICATION FOR IGU MEDAL/AWARD - 2017

In connection with the 54th Annual Convention of IGU during December 4-7, 2017 at CSIR-National Geophysical Research Institute (NGRI), Hyderabad, Nominations (both hard and soft copies) for the following medal/award in the prescribed proforma are invited from the past recipients or fellows or EC members of IGU or any distinguished Earth Scientist/Professor (must be a member of IGU) on or before 31-8-2017.

Krishnan Medal to Young Scientist (below 40 yrs as on 31-01-2017) for significant contribution to Indian Earth Sciences.

Decennial Award to Senior Scientist for outstanding contribution in establishing a school of Earth Sciences in India.

For details of Medal/Award, please visit the website: **www.igu.in**

Nomination Proforma

1. Name of the Award
2. Full name, age (DoB) and address along with contact number of the nominee
3. Academic qualifications (bachelor's degree onwards)
4. Position held (in chronological order)
5. Brief statement on significant contribution for citation (within 200 words)
6. Professional achievements
   (i) List of publications. Attach reprints of only 5 important publications
   (ii) Awards/Honours
   (iii) Memberships in Academics/Societies/Professional bodies
   (iv) Impact of scientific contribution (within 500 words)
7. Remarks of nominator
8. Name and Address of Nominator

The Hon. Secretary,
Indian Geophysical Union
NGRI Campus, Uppal Road
Hyderabad- 500 007
Email: igu123@gmail.com

Note:
1. Send only one nomination
2. Enclose attested copy of one of the following: Birth certificate/ SSLC/HSC/CBSE marks card for Krishnan medal Nominee
3. Nominations will be rejected, if they are not in format and within restricted words limit

GUIDE LINES TO AUTHORS

The Journal of Indian Geophysical Union (J-IGU), published quarterly by the Indian Geophysical Union (IGU), is an interdisciplinary journal from India that publishes high-quality research in earth sciences with special emphasis on the topics pertaining to the Indian subcontinent and the surrounding Indian Ocean region. The journal covers several disciplines of earth sciences such as the Geosphere, its watery and gaseous envelopes (the Hydrosphere, the Cryosphere and the Atmosphere), and life (the Biosphere). It also publishes articles on Space and Planetary sciences. J-IGU welcomes contributions under the following categories:

- Research papers reporting new findings, results, etc.
- Review articles providing comprehensive overview of a significant research field related to earth sciences

In addition, J-IGU also welcomes short communications on opinion and report on scientific activity, personal information, book reviews, news and views, etc.

The manuscript should be submitted electronically as a single pdf file including the main text, figures, tables, and any other supplementary information along with the signed "Declaration Letter". The manuscript should be submitted by email (jigu1963@gmail.com) to the Editor.

After acceptance of the manuscript the corresponding author would be required to submit all source files (text and Tables in word format) and figures in high resolution standard (*.jpg, *.tiff, *.bmp) format. These files may be submitted to the Editor as a single *.zip file along with the "Copyright Transfer Statement".

IMPORTANT INFORMATION

Ethics in publishing
J-IGU is committed to ensuring ethics in publication and takes a serious view of plagiarism including self-plagiarism in manuscripts submitted to the journal. Authors are advised to ensure ethical values by submitting only their original work and due acknowledgement to the work of others in case used the manuscript. Authors must also refrain from submitting the same manuscript to more than one journal concurrently or publish the same piece of research work in more than one journal which is unethical and unacceptable. Editor of J-IGU is committed to make every reasonable effort to investigate any allegations of plagiarism brought to his attention, as well as instances that come up during the peer review process and has full authority to retract any plagiarized publication from the journal and take appropriate action against such authors if it is proven that such a misconduct was intentional.

Similarly, Editor and Reviewers are also expected to follow ethical norms of publishing by ensuring that they don't use any unpublished information, communicated to them for editorial or review purpose, in their own research without the explicit written consent of the author. They are also expected to keep manuscript/ data/ observations/ any other information related to the peer review confidential to protect the interest of the authors. Reviewers should refrain from reviewing the manuscripts in which they have conflicts of interest resulting from competitive, collaborative, or other relationships or connections with any of the authors, companies, or institutions connected to the manuscript.

Conflict of interest
All authors are requested to disclose any actual or potential conflict of interest including any financial, personal or other relationships with other people or organizations within three years of beginning the submitted work that could inappropriately influence, or be perceived to influence, their work.

Submission declaration
Submission of a manuscript implies that the work has not been published previously and it is not under consideration for publication elsewhere, and that if accepted it will not be published elsewhere in the same or any other form, in English or in any other language, without the written consent of the publisher. It also implies that the authors have taken necessary approval from the competent authority of the institute/organization where the work was carried out.

Copyright
After acceptance of the manuscript the corresponding author would be required to sign and submit the "Copyright Transfer Statement".

MANUSCRIPT PREPARATION

The corresponding author should be identified (include E-mail address, Phone/Mobile number). Full affiliation and postal address must be given for all co-authors.

Abstract:
An abstract of not more than 300 words must be included.

Text:
The manuscript should be structured to include a front page containing the title, Author(s) name, affiliation and address of the institute where the work was carried out, a short title, and 5-to-6 index terms/Key words. Author(s) present address, if different from the above mentioned address, may be given in the footnote. The corresponding author should be identified with an asterisk and his/her email ID should be provided. This page should be followed by the main text consisting of Abstract, Introduction, Methods/ Techniques/ Area description, Results, Discussion, Conclusions, Acknowledgements, and References. Tables and Figures with captions should be inserted in the main text of the manuscript at appropriate places.

Figures/ Illustrations:
All figures should be provided in camera-ready form, suitable for reproduction (which may include reduction) without retouching. Figures in high-resolution (at least 300 dpi) standard formats (*.jpg, *.tiff, *.bmp) are acceptable. Figures should be numbered according to their sequence in the text. References should be made in the text to each figure. Each figure should have a suitable caption.

Tables:
Authors should take note of the limitations set by the size and layout of the journal. Table should not exceed the printed area of the page. They should be typed on separate sheets and details about the tables should be given in the text. Heading should be brief. Large tables should be avoided and may be provided as supplementary information, if required.

Equations:
Equations should be numbered sequentially with Arabic numerals and cited in the text. Subscripts and Superscripts should be set off clearly. Equation writing software that presents each equation as an object in MS Word will be accepted. Style and convention adopted for the equations should be uniform throughout the paper.

References:
All references to publications cited in the main text should be presented as a list of references following the text and all references in the list must be cited in the text. References should be arranged chronologically, in the text. The list of references should be arranged alphabetically at the end of the paper.

References should be given in the following form:
Kaila, K.L., Reddy P.R., Mall D.M., Venkateswarlu, N., Krishna V.G. and Prasad, A.S.S.S.R.S., 1992. Crustal structure of the west Bengal Basin from deep seismic sounding investigations, Geophys. J. Int., v.111,no., pp:45-66.

REVIEW PROCESS:

All manuscripts submitted to the journal are peer-reviewed. It is advisable to send the contact details of **4 potential reviewers** along with the manuscript to expedite the review process. Editor has the option to select reviewers from the list or choose different reviewers. The review process usually takes about 3 months. All enquiries regarding the manuscript may be addressed to the Editor.

GALLEY PROOF:
Technical editing of manuscripts is performed by the editorial board. The author is asked to check the galley proof for typographical errors and to answer queries from the editor. Authors are requested to return the corrected proof **within two days** of its receipt to ensure uninterrupted processing. The editor will not accept new material in proof unless permission from the editorial board has been obtained for the addition of a "note added in proof". Authors are liable for the cost of excessive alterations to galley proof.

PUBLICATION CHARGES:

There are no page charges for publication and printing charges for b/w figures. However, in view of substantial cost involved in printing of color figures, author will be charged for printing of pages containing color figures @ Rs. 2,500/- per page. The charges may be revised at any time based on cost of printing and production. Author will receive an estimate/ invoice of the color figures reproduction cost along with the galley proof. It is the responsibility of the author to remit the color figures reproduction cost **within one month** of the receipt of the estimate/invoice.
The corresponding author will receive a soft copy (pdf format) of his/her published article. Should the author desire to purchase reprints of his/her publication, he/she must send the duly signed Reprint Order Form (accompanies the galley proof and contains price details) along with the corrected galley proof to the Editor. The reprint charges must be paid **within one month** of sending the Reprint Order Form.
Any payment related to printing of color figures and/or purchase of reprints should be made in the form of a Demand Draft in the name of **Treasurer, Indian Geophysical Union**, payable at **Hyderabad**.

You may download the pdf file here: Guide for Authors